Universitat Politècnica de Catalunya

Programa de Doctorat:

Automàtica, Robòtica i Visió

Tesis Doctoral

Integration Techniques of Fault Detection and Isolation using Interval Observers

Jordi Meseguer Amela

Directors: Vicenç Puig i Teresa Escobet

Març 2009

TABLE OF CONTENTS

Abstract

An interval observer has been illustrated to be a suitable approach to detect and isolate faults affecting complex dynamical industrial systems. Concerning fault detection, interval observation is an appropriate passive robust strategy to generate an adaptive threshold to be used in residual evaluation when model uncertainty is located in parameters (interval model). In such approach, the observer gain is a key parameter since it determines the time evolution of the residual sensitivity to a fault and the minimum detectable fault. This thesis illustrates that the whole fault detection process is ruled by the dynamics of the fault residual sensitivity functions and by the time evolution of the adaptive threshold related to the interval observer. Besides, it must be taken into account that these two observer fault detection properties depend on the used observer gain. As a consequence, the observer gain becomes a tuning parameter which allows enhancing the observer fault detection performance while avoiding some drawbacks related to the analytical models, as the wrapping effect. In this thesis, the effect of the observer gain on fault detection and how this parameter can avoid some observer drawbacks (*i.e.* wrapping effect) are deeply analyzed. One of the results of this analysis is the determination of the minimum detectable fault function related to a given fault type. This function allows introducing a fault classification according to the fault detectability time evolution: ***permanently (strongly) detected, non-permanently (weakly) detected or just non-detected***. In this fault detection part of this thesis, two examples have been used to illustrate the derived results: a mineral grinding-classification process and an industrial servo actuator.

Concerning the interface between fault detection and fault isolation, this thesis shows that both modules can not be considered separately since the fault detection process has an important influence on the fault isolation result. This influence is not only due to the time evolution of the fault signals generated by the fault detection module but also to the fact that the fault residual sensitivity functions determines the faults which are affecting a given fault signal and the dynamics of this fault signal for each fault. This thesis illustrates this point suggesting that the interface between fault detection and fault isolation must consider a set of fault signals properties: binary property, sign property, fault residual sensitivity property, occurrence order property and occurrence time instant property. Moreover, as a result of the influence of the observer gain on the fault detection stage and on the fault residual sensitivity functions, this thesis demonstrates that the observer gain has also a key role in the fault isolation module which might allow enhancing its performance when this parameter is tuned properly (*i.e.* fault distinguishability may be increased). As a last point, this thesis analyzes the timed discrete-event nature of the fault signals generated by the fault detection module. As a consequence, it suggests using timed discrete-event models to model the fault isolation module. This thesis illustrates that this kind of models allow enhancing the fault isolation result. Moreover, as the monitored system is modelled using an interval observer, this thesis shows as this qualitative fault isolation model can be built up on the grounds of this system analytical model. Finally, the proposed fault isolation method is applied to detect and isolate faults of the Barcelona's urban sewer system limnimeters.

Keywords: Fault Detection, Fault Diagnosis, Robustness, Observers, Intervals, Discrete-event Systems.

Resumen

En la presente tesis se demuestra que el uso de observadores intervalares para detectar y aislar fallos en sistemas dinámicos complejos constituye una estrategia apropiada. En la etapa de detección del fallo, dicha estrategia permite determinar el umbral adaptativo usado en la evaluación del residuo (*robustez pasiva*). Dicha metodología, responde a la consideración de modelos con parámetros inciertos (*modelos intervalares*). En dicho enfoque, la ganancia del observador es un parámetro clave que permite determinar la evolución temporal de la sensibilidad del residuo a un fallo y el mínimo fallo detectable para un tipo de fallo determinado. Esta tesis establece que todo el proceso de detección de fallos viene determinado por la dinámica de las funciones sensibilidad del residuo a los diferentes fallos considerados y por la evolución temporal del umbral adaptativo asociado al observador intervalar. Además, se debe tener en cuenta que estas dos propiedades del observador respecto la detección de fallos dependen de la ganancia del observador. En consecuencia, la ganancia del observador se convierte en el parámetro de diseño que permite mejorar las prestaciones de dicho modelo respecto la detección de fallos mientras que permite evitar algunos defectos asociados al uso de modelos intervalares, como el efecto wrapping. Uno de los resultados obtenidos es la determinación de la función fallo mínimo detectable para un tipo de fallo dado. Esta función permite introducir una clasificación de los fallos en función de la evolución temporal de su detectabilidad: *fallos permanentemente detectados*, *fallos no permanentemente detectados* y *fallos no detectados*. En la primera parte de la tesis centrada en la detección de fallos se utilizan dos ejemplos para ilustrar los resultados obtenidos: un proceso de trituración y separación de minerales y un servoactuador industrial.

Respecto a la interfaz entre la etapa de detección de fallos y el proceso de aislamiento, esta tesis muestra que ambos módulos no pueden considerarse separadamente dado que el proceso de detección tiene una importante influencia en el resultado de la etapa de aislamiento. Esta influencia no es debida sólo a la evolución temporal de las señales de fallo generados por el módulo de detección sino también porque las funciones sensibilidad del residuo a los diferentes posibles fallos determinan los fallos que afectan a un determinado señal de fallo y la dinámica de éste para cada uno de los fallos. Esta tesis ilustra este punto sugiriendo que el interfaz entre detección y aislamiento del fallo debe considerar un conjunto de propiedades de dichos señales: propiedad binaria, propiedad del signo, propiedad de la sensibilidad del residuo a un fallo dado, propiedad del orden de aparición de las señales causados por los fallos y la propiedad del tiempo de aparición de estos. Además, como resultado de la influencia de la ganancia del observador en la etapa de detección y en las funciones sensibilidad asociadas a los residuos, esta tesis ilustra que la ganancia del observador tiene también un papel crucial en el módulo de aislamiento, el cual podría permitir mejorar el comportamiento de dicho módulo diseñando éste parámetro del observador de forma adecuada (*Ej. Incrementar la distinción de los fallos para su mejor aislamiento*). Como último punto, esta tesis analiza la naturaleza temporal de eventos discretos asociada a las señales de fallo generados por el módulo de detección. A consecuencia, se sugiere usar modelos de eventos discretos temporales para modelizar el módulo de aislamiento del fallo. Esta tesis muestra que este tipo de modelos permite mejorar el resultado de aislamiento del fallo. Además, dado que el sistema monitorizado es modelado usando un observador intervalar, esta tesis muestra como este modelo cualitativo de aislamiento puede ser construido usando dicho modelo analítico del sistema. Finalmente, el método propuesto de aislamiento del fallo es aplicado para detectar y aislar fallos en los limnimetros del sistema de alcantarillado de Barcelona.

Palabras clave: Detección de Fallos, Diagnosis de Fallos, Robusteza, Observadores, Intervalos, Sistemas de Eventos Discretos.

Acknowledgement

This PhD thesis must be considered as a collection of planned results of the research line in fault detection and fault isolation in complex industrial systems carried out in the Advanced Control Systems (SAC) Group at the Automatic Control Department (ESAII) of the Technical University of Catalonia (UPC). Thereby, I would like to thank to all the people of this group because without their effort it would have not been possible to obtain the results presented in this PhD thesis. Moreover, I would also like to thank to those people of other research groups that they have directly or indirectly contributed to this thesis giving me good advices or a key inspiration to carry out my commitment.

In special, I must show gratitude to Dr. Vicenç Puig and Dr. Teresa Escobet because they have introduce me in the research field illustrating me the direction to follow and encouraging me when it was needed. I would also like to thank them the additional effort they have done due to the time limitations imposed by my employment in the private company. Without their effort and understanding, this PhD thesis would have not been possible.

Besides, I must give thanks to my family and close friends for their understanding and their support. They have suffered the negative consequences of this PhD thesis when I could not join them because of my duties in it. They have given me courage to carry out this commitment what has helped me to end it.

Jordi Meseguer Amela

Barcelona, March 2009

Notation

Concerning the notation used in this PhD thesis, as a general rule, scalars are annotated with cursive lower case letters (e.g. *a*, *b*, …), vectors with cursive bold lower case letters (e.g., $\boldsymbol{y}$, $\boldsymbol{x}$, . . .) and, matrices with cursive bold upper case letters (e.g., $\boldsymbol{A}$, $\boldsymbol{B}$, . . .). Regarding vectors, if not otherwise noted, they are column vectors. Besides, throughout this thesis document, the relation between vectors or matrices must be understood component by component.

ϕ	set of fault signal
$\boldsymbol{x}$	system state vector
$\boldsymbol{u}$	measured system input vector
$\boldsymbol{y}$	measured system output vector
$\boldsymbol{u_0}$	system input vector
$\boldsymbol{y_0}$	system output vector
$\boldsymbol{f_y}$	output sensor fault vector
$\boldsymbol{f_u}$	input sensor fault vector
$\boldsymbol{f_a}$	actuator fault vector
$\boldsymbol{f}$	set of faults
$\rightarrow$	mapping
$\hat{\boldsymbol{y}}$	predicted system output vector
$\hat{\boldsymbol{x}}$	predicted system state vector
$\boldsymbol{r}$	residual vector
$\boldsymbol{r_0}$	value of the residual vector when just the model uncertainty is considered neglecting the existence of faults, unknown inputs and noises. This value determines the adaptive threshold used to indicate or not the existence of a fault
r_i^o	nomimal value of the i^{th}-component of the residual $\boldsymbol{r}$
k	discrete time instant
q^{-1}	shift operator
$\boldsymbol{V}$	transfer function matrix related to the residual computational form
$\boldsymbol{O}$	transfer function matrix related to the residual computational form
$\boldsymbol{M}$	system transfer function matrix
$\boldsymbol{\delta}$	vector indicating the difference between the measured system output and the system output
$\boldsymbol{A}$	model state matrix
$\boldsymbol{A}_+$	matrix built up using those positive elements of matrix $\boldsymbol{A}$
$\boldsymbol{A}_-$	matrix built up using those negative elements of matrix $\boldsymbol{A}$
$\boldsymbol{B}$	model input matrix

$\boldsymbol{C}$	model output matrix
$\boldsymbol{D}$	system direct transmission matrix
$\boldsymbol{L}$	observer gain matrix
$\boldsymbol{L}_-$	matrix whose elements determine the observation gain values needed to force the isotonicity of matrix $\boldsymbol{A_0}$
$\boldsymbol{L}_+$	matrix whose elements can be chosen freely to enhance the observer fault detection performance and to guarantee the observer stability
$(\boldsymbol{L})_{ij}$	component of matrix $\boldsymbol{L}$ placed in the i^{th}-row and the j^{th}-column
$\boldsymbol{F_y}$	matrix related to the output sensor fault vector
$\boldsymbol{F_u}$	matrix related to the input sensor fault vector
$\boldsymbol{F_a}$	matrix related to the actuator fault vector
$\boldsymbol{I}$	identity matrix
$\Re^{ny}$	system output vector space
$\Re^{nu}$	system input vector space
$\Re^{nx}$	system state vector space
$\boldsymbol{L_p}$	observer gain matrix value which places all the observer eigenvalues at the origin
$\boldsymbol{G}$	transfer function matrix that determines the influence of the measured system input vector on the predicted system output
$\boldsymbol{H}$	transfer function matrix that determines the influence of the measured system output vector on the predicted system output
$\boldsymbol{G}_{fy}$	transfer function matrix that determines the influence of the output sensor fault vector on the measured system output vector
$\boldsymbol{G}_{fa}$	transfer function matrix that determines the influence of the actuator fault vector on the measured system output vector
$\boldsymbol{G}_{fu}$	transfer function matrix that determines the influence of the input actuator fault vector on the predicted system output
$\lvert\ \rvert$	absolute value operator. When applied to a vector or a matrix, it must be understood element by element
$<$, $\leq$, $>$ and $\geq$	comparative operator. When applied to a vector or a matrix, it must be understood element by element
$\hat{\boldsymbol{y}}(k)_{\boldsymbol{L=0}}$	value of predicted system output vector at time instant k when $\boldsymbol{L=0}$
$\boldsymbol{H}_r$	transfer function matrix which determines the influence of the residual vector on the predicted system output vector
$\boldsymbol{r}(k)_{\boldsymbol{L=0}}$	value of the residual vector at time instant k when $\boldsymbol{L=0}$
$[\hat{\boldsymbol{y}}(k)]$	interval at time instant k associated with the predicted system output vector due to the model uncertainty. It must be understood component by component
$[\boldsymbol{r}(k)]$	interval at time instant k related to the residual as a consequence of the model uncertainty

$\boldsymbol{y}(k) \in [\hat{\boldsymbol{y}}(k)]$	relation showing that the value of the measured system output vector at time instant k belongs to the interval related to the predicted system output vector at this time instant. This relation must be understood component by component
$\tilde{\boldsymbol{\theta}}$	system vector parameter
$\boldsymbol{\theta}$	time-invariant model interval parameter vector
θ_i	model interval parameter vector component placed in the i^{th}-row
$\boldsymbol{A}(\boldsymbol{\theta})$	interval system state matrix whose components depend on the interval parameter vector $\boldsymbol{\theta}$
$\boldsymbol{X}$	set of all the system states
$\boldsymbol{x_0}$	intial value of the system state vector
$\boldsymbol{A_o}$	observer state matrix whose expression is $\boldsymbol{A}_o(\boldsymbol{\theta}) = \boldsymbol{A}(\boldsymbol{\theta}) - \boldsymbol{LC}(\boldsymbol{\theta})$
κ	condition number of $\boldsymbol{A_o}$ whose value is determined by the result of the following matrix product: $\|\|\boldsymbol{A_o}\|\|.\|\|\boldsymbol{A_o}^{-1}\|\|$
$\boldsymbol{B_o}$	observer input matrix whose expression is $\boldsymbol{B}_o(\boldsymbol{\theta}) = [\boldsymbol{B}(\boldsymbol{\theta}) \quad \boldsymbol{L}]$
$\boldsymbol{u}_*$	observer input vector given by $\boldsymbol{u}_*(k) = [\boldsymbol{u}(k) \quad \boldsymbol{y}(k)]^T$
$\boldsymbol{\Theta}$	interval set bounding the interval parameter vector, $\boldsymbol{\theta} \in \boldsymbol{\Theta}$
$\Re^{n\theta}$	model parameter vector space
$\square\, \hat{\boldsymbol{X}}(k)$	interval hull of the predicted system state set
$\|\ \|_\infty$	infinte norm of a vector or a matrix
$\rho(\boldsymbol{A})$	spectral radius of matrix $\boldsymbol{A}$ given by maximum absolute value of all the eigenvalues associated with this matrix
$\hat{\boldsymbol{x}}_c(k)$	mid-point of the interval related to the predicted system state vector $[\hat{\boldsymbol{x}}(k)]$
$\hat{\boldsymbol{\theta}}$	mid-point of the interval model parameter vector $[\boldsymbol{\theta}]$
max	operator that allows to obtaing the maximum value of a given interval
min	operator that allows to obtaing the minimum value of a given interval
$\overline{\hat{\boldsymbol{x}}}(k)$	upper bound of the interval related to the predicted system state vector at time instant k
$\underline{\hat{\boldsymbol{x}}}(k)$	lower bound of the interval related to the predicted system state vector at time instant k
λ	length of the sliding time window measured in number of samples used to compute a certain trajectory of the predicted system output vector / state vector or order of a predictor equivalent to a given observer
FSM	theoretical fault signature matrix
n_f	dimension of the fault set $\boldsymbol{f}$
n_ϕ	dimension of the fault signal set ϕ
FIS	fault information system
DGN	set of fault hypothesis $\boldsymbol{f_j}$ which are consistent with the observed fault signals
$\boldsymbol{S_f}$	residual sensitivity matrix to a fault $\boldsymbol{f}$
$\boldsymbol{S_{fy}}$	residual sensitivity matrix to an output sensor fault $\boldsymbol{f_y}$
$\boldsymbol{S_{fu}}$	residual sensitivity matrix to an output sensor fault $\boldsymbol{f_u}$

$\boldsymbol{S}_{fa}$	residual sensitivity matrix to an output sensor fault $\boldsymbol{f}_a$
$\boldsymbol{d}_f$	residual disturbance vector caused by a fault $\boldsymbol{f}$
$\boldsymbol{d}_f^{\min}$	minimum residual disturbance caused by a fault $\boldsymbol{f}$ so that this fault can be indicated by the system model
$\boldsymbol{f}_f^{min}$	minimum detectable fault of the type $\boldsymbol{f}$ required by the system model so that this fault can be detected
$\boldsymbol{S}_f^+$	left pseudo-inverse matrix of $\boldsymbol{S}_f$
$\boldsymbol{f}_{fy}^{\min}$	minimum detectable output sensor fault vector
$\boldsymbol{f}_{fu}^{\min}$	minimum detectable input sensor fault vector
$\boldsymbol{f}_{fa}^{\min}$	minimum detectable actuator fault vector
t_0	time instant at which the fault occurs
T_w	waiting time calculated from the largest transient time response from non-faulty situation to any faulty situation
***FSM**01*	theoretical fault signature matrix related to the fault signal binary property
***FSM**sign*	theoretical fault signature matrix related to the fault signal sign property
***FSM**sensit*	theoretical fault signature matrix related to the fault residual sensitivity property of a fault signal
***FSM**order*	theoretical fault signature matrix related to the fault signal occurrence order property
***FSM**time*	theoretical fault signature matrix related to the fault signal occurrence time instant property
***factor**01*$_j$	occurrence probability of the fault hypothesis f_j regarding the binary property of the observed fault signals
***factor**sign*$_j$	occurrence probability of the fault hypothesis f_j regarding the sign property of the observed fault signals
***factor**sensit*$_j$	occurrence probability of the fault hypothesis f_j regarding the fault residual sensitivity property of the observed fault signals
***factor**order*$_j$	occurrence probability of the fault hypothesis f_j regarding the occurrence order property of the observed fault signals
***factor**time*$_j$	occurrence probability of the fault hypothesis f_j regarding the occurrence time instant property of the observed fault signals
d_j	occurrence probability of the fault hypothesis f_j
DES	discrete event system
TDES	timed discrete event system
TLTS	timed labelled transition system

List of Tables

List of Figures

CHAPTER 1

PhD thesis introduction

1.1 Introduction

This chapter corresponds to the introduction of this PhD thesis document in which all the work carried out to achieve the planned objectives is detailed. Thereby, the aim of this chapter is to describe the main motivations (*Section 1.2*) which have inspired this PhD thesis. As a consequence, the general thesis objectives (*Section 1.3*) will be introduced, although they will be more detailed in *Chapter 2* as a result of an analysis of the state of art. Finally, in *Section 1.4*, an outline of the structure of the document is depicted providing an abstract of every chapter.

1.2 Motivation

Modern control systems are becoming more and more complex and control algorithms more and more sophisticated. Consequently, the issues of availability, cost efficiency, reliability, operating safety and environmental protection are of major importance. These issues are important to, not only normally accepted safety-critical systems such as nuclear reactors, chemical plants and aircrafts, but also other advanced systems employed in cars, rapid transits trains, etc. For safety-critical systems, the consequences of faults can be extremely serious in terms of human mortality, environmental impact and economic loss. Therefore, there is a growing need for on-line supervision and fault diagnosis to increase the reliability of such safety-critical systems. For systems which are not safety-critical, on-line fault diagnosis techniques can be used to improve plant efficiency, maintainability, availability and reliability. In short, nowadays it is very important to detect and isolate faults in the shorter possible time for avoiding the faults propagation in the whole process, or in order to adapt the control system so that the process can satisfy its purpose even in the presence of faults.

Being conscious of the importance of fault detection and fault isolation in complex industrial systems, the Advanced Control Systems (SAC) Group at the Automatic Control Department (ESAII) of the Technical University of Catalonia (UPC) is carrying out a research line in this field which has already provided successful and significant results in previous PhD theses, conference and journal papers. In this sense, this PhD thesis is performed into the trend established by this research line contributing in some planned aspects. The starting point of these contributions is determined by some drawbacks of the present methods and by some non-considered aspects, as it will be illustrated in detail in *Chapter 2*. As a consequence, the obtained results can be considered as a novelty into the field of the fault detection and isolation.

Thus, the scope of this thesis is focused on *fault detection and isolation based on interval observers applied to dynamical industrial systems* (*Chapter 2*). In these days, the most of the existent contributions in fault detection and isolation field using analytical interval models are based either on the *simulation approach* or on the *prediction approach* (*Chapter 2*). On the other hand, as it will be pointed out in the next chapter, it is demonstrated that

analytical models are affected by some problems which can seriously worsen the performance of the fault detection and isolation module leading to wrong fault diagnosis results. In general, these drawbacks related to analytical models are tackled using a complementary strategy since these analytical models do not have any tuning freedom degrees. Nonetheless, the accurateness of this complementary strategy, in general, is only valid for a certain particular cases.

On the other hand, what, in general, is not taken into account is that the simulation and prediction approaches are just two specific cases of the *observer approach* for two concrete values of the *observer gain* (*Chapter 2*). Concerning the observer approach, this analytical model has a set of tuning freedom degrees which may be used to tackle the mentioned problems and to enhance the whole fault diagnosis performance. These aspects will be analysed in this PhD thesis resulting in its main general objective.

Concerning those residual properties that determine the performance regarding fault detection and isolation, in general, the existing methods do not consider their dynamics (*i.e.* fault residual sensitivity property (see Gertler, 1998)). Conversely, they just consider the steady-state value of these properties. This fact may lead to inaccurate fault detection and fault isolation predictions resulting in a poor fault diagnosis performance of the considered approach. This PhD thesis demonstrates that this residual fault diagnosis properties (mainly, *residual sensitivity to a fault*, *minimum detectable fault* and *adaptive threshold* (*Chapter 2*)) have a time evolution and when it is considered, it will be possible to predict exactly when a fault will be detected or not by the observer model according to its tuning configuration: this is the time evolution of the fault signals generated by the fault detection module. Concerning fault isolation, when the dynamics of these properties are considered, it is illustrated that the fault isolation module performance is enhanced increasing its related fault distinguishability.

As a last aspect, this PhD thesis analyses the kind of model that should be applied to model the fault isolation module. In general, the present approaches model this module according to the nature of the monitored system model: when an analytical model is used, then, the fault isolation module is modelled using analytical techniques while when the nature is qualitative, then, fault isolation uses a qualitative approach. This thesis analyse the nature of the fault signals generated by the fault detection module concluding its timed discrete-event character. As a consequence, it is proposed to model this module using a timed discrete-event approach, in spite the monitored system has been modelled analytically. This fact allows enhancing the fault isolation performance reducing the probability of giving wrong fault diagnosis results.

Although it is not the main objective of this thesis, it will be proposed a new fault detection and isolation approach which takes into account all the results provided by the previous mentioned analyses.

1.3 General objectives

As a result of the previous section, the general objectives of this PhD Thesis are enumerated in the following. It must be noticed that it is in *Chapter 2* where they are explained in detail as a result of the analysis of the state of the art. Thus, the main objectives are to analyse:

(a) The influence of the observer gain on the fault detection module performance.
(b) The influence of the observer gain on the fault isolation module performance.
(c) The influence of the observer gain on the interface between the fault detection and isolation modules.
(d) The influence of the dynamics of the model fault diagnosis properties on the fault diagnosis process.
(e) The most suitable fault isolation model type according to the nature of the fault signals generated by the fault detection module.

1.4 Thesis structure

In this section, the structure of this PhD thesis document is described detailing its different parts and chapters. Thereby, for each chapter, a brief abstract and its related published papers are provided.

Apart from the *Chapter 2* where a state of the art in fault detection and isolation is described, this PhD thesis document is formed by one part related to all the planned objectives associated with the fault detection module and by another one related to the interface between fault detection and fault isolation, and to the fault isolation module itself. Thus, the *Part I* whose title is "*Robust fault detection using linear interval observers and predictors*" is formed by the following chapters:

- *Chapter 3: Observer gain effect in linear interval observer-based fault detection.*
- *Chapter 4: Designing fault detection linear interval observers to avoid the wrapping effect.*
- *Chapter 5: Approximating fault detection linear interval observers using λ-order interval predictors.*

Concerning the *Part II* whose title is "*Fault diagnosis using interval observers*", its associated chapters are:

- *Chapter 6: On the integration of fault detection and isolation in model based fault diagnosis.*
- *Chapter 7: Towards a better integration of passive robust interval-based FDI algorithms.*
- *Chapter 8: Fault isolation using linear interval observers: influence of the observer gain.*
- *Chapter 9: Fault diagnosis using linear interval observers: obtaining **FSM** matrices.*
- *Chapter 10: Fault diagnosis using a timed discrete event approach based on interval observers.*

In the following subsections, for every chapter, a brief abstract and the related published papers are provided.

1.4.1 Chapter 3: Observer gain effect in linear interval observer-based fault detection

In this chapter, an interval observer is illustrated to be a suitable passive robust strategy to generate an adaptive threshold to be used in residual evaluation when model uncertainty is located in parameters (interval model). In such approach, the observer gain plays an important role since it determines the minimum detectable fault for a given type of fault and allows enhancing the observer fault detection properties. The aim of this chapter is to analyze the influence of the observer gain on the time evolution of the residual sensitivity to a fault. Thereby, as a result of this sensitivity study, the minimum detectable fault time evolution for a given type of fault and the interval observer fault detection performance could be determined. In particular, three types of faults according their detectability time evolution are introduced: ***permanently (strongly) detected, non-permanently (weakly) detected or just non-detected***. An example based on a mineral grinding-classification process is used to illustrate the results derived.

This chapter is based on the following published papers:

- *Meseguer, J., Puig, V., Escobet, T. (2006a) "Observer gain effect in linear observer-based fault detection" IFAC SAFEPROCESS'06.*
- *Meseguer, J., Puig, V., Escobet, T. (2007b). "Observer Gain Effect in Linear Interval Observer-based Fault Detection" CDC'07 . New Orleans. USA.*
- *Meseguer, J., Puig, V., Escobet, T. (2008c). "Observer Gain Effect in Linear Interval Observer-based Fault Detection" Journal of Process Control (JPROCONT-D-07-00232).*

1.4.2 Chapter 4: Designing fault detection linear interval observers to avoid the wrapping effect

As illustrated in *Chapter 3*, in model based fault detection is very important to analyze how the effect of model uncertainty is considered when determining the optimal threshold to be used in residual evaluation. In case of model uncertainty is located in parameters (interval model), an interval observer is shown in that chapter to be a suitable strategy to generate this adaptive threshold. However, interval observers can be affected by the wrapping effect when low computational algorithms, such as region-based approaches coming from the interval community, are used to determine the predicted output interval. *Chapter 4* shows that the wrapping effect might be avoided forcing the observer gain to satisfy the isotonicity condition. Then, the effect of this observer condition on the time evolution of the residual sensitivity to a fault and the minimum detectable fault, which were introduced in *Chaper 3*, is analyzed in order to see whether the fault detection performance is enhanced or not. Finally, an example based on an industrial servo actuator will be used to illustrate the derived results.

Regarding the related published papers, they are:

- *Meseguer, J., Puig, V., Escobet, T. (2006b) "Observer gain effect in linear interval observer-based fault detection" IFAC SAFEPROCESS'06.*
- *Meseguer, J., Puig, V., Escobet, T. (2008a) "Robust Fault Detection Linear Interval Observers Avoiding the Wrapping Effect". IFAC World Congress 2008, Seul, Korea.*

1.4.3 Chapter 5: Approximating fault detection linear interval observers using λ-order interval predictors

Interval observers can be described by an ARMA model while λ-order interval predictors by a MA model. Since an ARMA model can be approximated by a MA model, this allows establishing the equivalence between interval observers and interval predictors. *Chapter 5* deals with the fault detection application and focuses on the equivalence between the *λ-order* **predictor and the interval observer** with the same fault detection performance. The predictor approach is developed to obviate the wrapping effect commonly encountered with interval observer approaches. Given a particular linear interval observer, a λ-order interval predictor can be found such that its behaviour is equivalent regarding fault detection and besides, it does not suffer from the wrapping effect. Thus, if the interval observer fulfils the isotonicity property, this λ-order interval predictor can be computed using two point-wise trajectories corresponding to the upper and lower bound of each uncertain parameter. Finally, an example based on an industrial servo actuator will be used to illustrate the derived results.

This paper is based on the following published paper:

- *Meseguer, J., Puig, V., Escobet, T., Tornil, S. (2007c) "Approximating Fault Detection Linear Interval Observers Using l-Order Interval Predictors" Proceedings of European Control Conference 2007 (ECC'07). Kos, Greece.*

1.4.4 Chapter 6: On the integration of fault detection and isolation in model based fault diagnosis

This chapter based on (Puig et al, 2004c) motivates the work which is carried out in the following chapters regarding the interface between fault detection and fault isolation. Thereby, in this chapter it is pointed out that model-based fault diagnosis can be divided in two subtasks: fault detection and fault isolation. Fault detection is based on checking the consistency between the modelled and observed behaviours while fault isolation tries to isolate the component that is affected by the fault. Since these two tasks can be executed in parallel, an interface between them should be considered. Typically, the result of the fault detection tests represented as a binary vector is used as the input to be analysed by the fault isolation module. However, when the result of each of these tests is codified applying a binary approach, some information is lost. In this chapter, the drawbacks of this classical approach are pinpointed suggesting some possible improvements.

1.4.5 Chapter 7: Towards a better integration of passive robust interval-based FDI algorithms

In this chapter, a new interval model-based fault diagnosis method which improves the integration between fault detection and fault isolation modules is proposed. This method is based on the proposed one in (Puig et al, 2005b) and applies a new interface between both stages taking into account the information about the degree of fault signal activation and the dynamics associated with each fault signal. The fault isolation process uses a combination of four theoretical fault signature matrices. They store the knowledge about the faulty system behaviour which is determined by the properties of the fault signals caused by the considered fault set: binary property, sign property, fault residual sensitivity property and occurrence order property. Finally, the proposed method is applied to detect and isolate faults of the Barcelona's urban sewer system limnimeters.

This paper is based on the following published paper:

- *Puig, V., Quevedo, J., Escobet, T., Meseguer, J. (2006b). "Toward a better integration of passive robust interval-based FDI algorithms". IFAC SAFEPROCESS'06. Beijing. China.*

1.4.6 Chapter 8: Fault isolation using linear interval observers: influence of the observer gain

In fault diagnosis, the integration between model-based fault detection and fault isolation plays a significant role in the final result given by the fault diagnoser. The reason for this importance is because model-based fault detection methods have inherent problems as lack of fault indication persistence, noise sensitivity or model errors and as a result, fault detection performance is not as good as it might be required in order to give a reliable fault diagnosis result. In addition, this fact might also confuse the fault isolation module when a set of fault signals must be observed so that the right fault diagnosis result can be derived.

As demonstrated in *Chapter 3*, when using interval observers in fault detection, the observer gain has a key influence on the quality of the fault indication. As a consequence, this chapter shows the observer gain has also an important influence on the fault isolation result since it does depend on the time evolution of the fault signals which can only be observed (detected) by the fault detection module.

This paper is based on the following published paper:

- *Meseguer, J., Puig, V., Escobet, T., Quevedo (2006c)"Observer gain effect in linear interval observer-based fault isolation". International Workshop on Principles of Diagnosis (DX 06).*

1.4.7 Chapter 9: Fault diagnosis using linear interval observers: obtaining FSM matrices

This chapter is based on the interval model-based fault diagnosis method described in *Chapter 8* which improves the integration between fault detection and fault isolation considering the degree of fault signal activation and using a combination of several *theoretical fault signature matrices* which store the theoretical properties of fault signals caused by the occurrence of a certain fault. This chapter focuses on how to obtain those matrices, when an interval observer is considered in the fault detection stage, using a procedure based on the fault residual sensitivity concept. This issue allows studying the influence of the fault detection module on the fault isolation stage. Regarding the fault isolation method proposed in *Chapter 8*, a new fault signal property is considered: the fault signal occurrence time instant which let derive a new theoretical fault signature matrix: ***FSM****time*. Moreover, this chapter considers the time evolution of the fault signal dynamical properties. Finally, the proposed fault diagnosis approach is applied to detect and isolate faults of the Barcelona's urban sewer system limnimeters (level meter sensors).

This paper is based on the following published paper:

- *Meseguer, J., Puig, V., Escobet, T., Quevedo, J. (2007a) "Sensor Fault Diagnosis using Linear Interval Observers" Workshop on Principles of Diagnosis DX'07. Nashville, TN, USA.*

1.4.8 Chapter 10: Fault diagnosis using a timed discrete event approach based on interval observers

This chapter proposes a fault diagnosis method using a *timed discrete-event approach* based on interval observers which improves the integration of fault detection and isolation modules. The interface between fault detection and fault isolation considers the degree of fault signal activation and the occurrence time instants of the fault signals using a combination of several theoretical fault signature matrices which store the knowledge of the relationship between fault signals and faults. This chapter proposes to implement the fault isolation module using a timed discrete event approach. In this way, the diagnosis result will be enhanced since the occurrence of a fault generates a unique sequence of observable events (fault signals) that will be recognized by the isolation module implemented as a *timed discrete event system*. The states and transitions that characterize such a system can be inferred directly from the relation between fault signals and faults. The proposed fault diagnosis approach is applied to detect and isolate faults of the Barcelona's urban sewer system limnimeters (level meter sensors).

This paper is based on the following published paper:

- *Meseguer, J., Puig, V., Escobet, T. (2008b) "Fault Diagnosis using a Timed Discrete Event Approach based on Interval Observers". IFAC World Congress 2008, Seul, Korea.*
- *Meseguer, J., Puig, V., Escobet, T. (2008d) "Fault Diagnosis using a Timed Discrete-Event Approach based on Interval Observers". Submitted to IEEE SMC Transactions - Part A.*
- *Meseguer, J., Puig, V., Escobet, T. (2009) "Fault Isolation Module Implementation using a Timed Discrete-Event Approach". IFAC SAFEPROCESS 2009, Barcelona, Spain.*

CHAPTER 2

State of the Art and Objectives

2.1 Introduction

Since the beginning of 1970s, research in fault diagnosis has been gaining increasing consideration world-wide in both theory and application (Reiter, 1987; Patton et al., 1998; Frank et al., 1997; Gertler, 1998; Blanke et al., 2003; Kościelny et al., 2004; Cordier et al., 2004; Rinner et al., 2004; Isermann, 2006). This development is still mainly stimulated by the trend of automation towards more complexity and the growing demand for higher availability and safety of control systems. However, a strong impetus also comes from the side of modern control theory that has brought forth powerful techniques of mathematical modelling, state estimation and parameter identification that have been made feasible by the spectacular progresses of computer technology.

A '***fault***' is to be understood as an unexpected change of the system function although it may not represent physical failure or breakdown. Such a fault disturbs the normal operation of an automatic system, thus causing an unacceptable deterioration of the performance of the system or even leading to dangerous situations. A monitoring system which is used to detect faults and diagnose their location and significance in a system is called a '***fault diagnosis system***'. Such a system normally consists of the following tasks:

- ***Fault detection***: to make a binary decision – either that something has gone wrong or that everything is fine. It is the identification of the fault appearance and the determination of the moment of its detection
- ***Fault isolation****:* to determine the location of the fault*, e.g., which sensor or actuator has become faulty?* It consists in determining the kind, place and time of the appearance of the fault; it follows the detection of that fault.
- ***Fault identification****:* to estimate the size and type or nature of the fault. It determines the fault size and its changeability in time; it follows the isolation of that fault.

Fault detection is an absolute must for any practical system and isolation is almost equally important while fault identification, on the other hand, may not be essential if no reconfiguration action is involved. Hence, fault diagnosis is very often considered as ***fault detection and isolation***, abbreviated ***FDI***, in the literature.

In practice, the most frequently used diagnosis method is to monitor the level, or trend, of a particular signal, and taking action when the signal reaches a given threshold. A traditional approach to fault diagnosis in the wider application context is based on '***hardware redundancy***' methods which use multiple lanes of sensors, actuators, computers and software to measure and/or control a particular variable. Typically, a voting scheme is applied to the hardware redundant system to decide if and when a fault has occurred and its likely location amongst redundant system components (Favre, 1994). The major problems of this approach are the extra equipment and maintenance cost and, furthermore, the additional space required accommodating the equipment.

In view of the conflict between the reliability and the cost of adding more hardware, it is sensible to attempt to use the dissimilar measured values together to cross check each other, rather than replicating each hardware individually; this is the concept of '***analytical redundancy***'.

In analytical redundancy schemes, the resulting difference generated from the consistency checking of different variables is called as a '***residual signal***'. The residual should be zero-valued when the system is normal, and should diverge from zero when a fault occurs in the system. Analytical redundancy makes use of a mathematical model of the monitored process and is therefore often referred to as the '***model-based approach***' to fault diagnosis. This consistency checking in analytical redundancy is normally achieved through a comparison between a measured signal and its estimation. The estimation is generated by the mathematical model of the system being considered. Consequently, the residual becomes a fault indicator which reflects the faulty situation of the monitored system.

In general, *model-based diagnosis* methods has been developed for many model domains, *e.g.* models from the *AI-field* which are often logic based (Hamscher et al., 1992), or from *Discrete Event Dynamic Systems* for which automata descriptions are common (Larsson, 1999; Sampath et al., 1995, 1996). A third model domain that is commonly considered are models typically found in the field of signals and systems, *e.g.* models involving continuous variables in continuous or discrete time whose typical model formulations are differential / difference equations, transfer functions, and/or static relations. This last model domain based on analytical models is typically used in ***Model-based FDI methods*** applying the already mentioned concept of '***analytical redundancy***'.

The major advantage of the model-based approach is that no additional hardware components are needed in order to realize a fault diagnosis algorithm. This algorithm can be implemented in software on the process control computer.

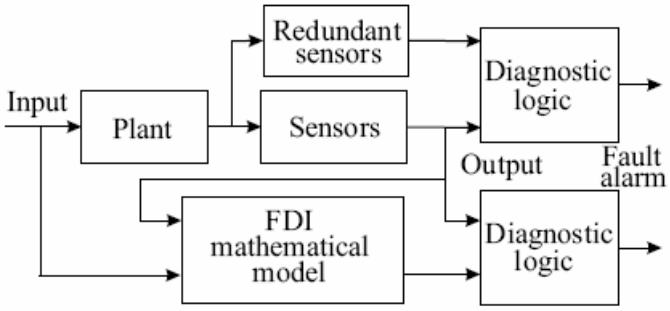

Fig. 2.1 Comparison between hardware and analytical redundancy schemes

As pointed out previously, *Model-based FDI methods* makes used of the mathematical model of the monitored system. However, a perfectly accurate and complete model of a physical system is never available because the presence of model uncertainty, unknown disturbances and noises. Hence, there is always a mismatch between the actual process and its mathematical model even if there are no process faults. These discrepancies constitute a source of false and missed alarms which can corrupt the FDI system performance. The effect of modelling uncertainties is therefore the most crucial point in the model-based FDI concept, and the solution of this problem is the key for its practical applicability (Frank, 1991; Patton et al., 1996; Patton et al., 1997). An FDI scheme designed to provide satisfactory sensitivity to faults, associated with the necessary robustness with respect to modelling uncertainty, is called a '***robust FDI***' scheme. A number of methods have been proposed to tackle this problem, for example, the unknown input observer, eigenstructure assignment, optimally robust parity relation methods (Chen et al., 1999). However, the research is still under the way to develop the practically applicable methods.

Regarding the structure of the *Chapter 2* remainder, a scope of fault detection and fault isolation is given in *Section 2.2*. Then, *Section 2.3* focuses on the state of art of fault detection using system models while *Section 2.4* does on the state of art of model-based fault isolation. Both *Section 2.3* and *Section 2.4* point out the weaknesses and drawbacks of the current approaches describing briefly how they will be tackled by this thesis. Thereby, the goals of this thesis are established in these sections through the analysis of the current methods. Finally, in *Section 2.5*, all the objectives

will be enumerated introducing the fault diagnosis method proposed by this thesis which will be developed in the following chapters.

2.2 Scope of fault detection and fault isolation

As it was mentioned in the introduction, fault detection is the process of generating fault signals (ϕ) on the grounds of the process variables ($\boldsymbol{x}$) in order to detect faults . Thereby, detection algorithms should generate fault signals which ought to contain information about faults. The mapping of the space of process variables into the space of fault signals as well as the evaluation of these signals in order to detect and indicate the fault takes place during the detection stage. Besides, it should be taken into account that in the diagnostics of processes, fault detection is automatically performed by a diagnosing computer.

On the other hand, fault isolation is carried out on the basis of fault signals generated by the detection module. The result of isolation is a diagnosis showing the faults or states of the system. The knowledge of the relationship that exists between the fault signals and the faults or the technical states of the system is necessary in order to perform the fault isolation. Thus, a completely reliable and unequivocal presentation of the existing faults or the definition of the diagnosed system state is not always possible due to incomplete and uncertain knowledge of the system, limited distinguishability of faults or states, uncertainty of fault signals, etc.

In general, fault detection and isolation methods may be classified into two major groups (Venkatasubrarnanian et al., 2003a): those which do not utilize the model of the plant or the process to express the knowledge about its physics and those which do . Regarding the last group, there are two mainly approaches: the analytical one where the process or plant understanding is expressed in terms of mathematical functional relationships between the inputs and outputs of the system and the qualitative one where these relationships are expressed in terms of qualitative functions. The analytical approach is mainly used by the known ***FDI*** methodology which is based on engineering disciplines as control theory and statistics. Conversely, another important methodology is the known as ***DX*** which is based on the fields of computer science and artificial intelligence applying, typically, qualitative models. Nonetheless, this thesis is not focused on comparing the ***FDI*** and ***DX*** methodologies. The techniques analyzed in this thesis are just classified according to its application (fault detection or fault isolation).

Although this thesis is devoted to the model-based methods, the model-free techniques will be briefly reviewed in the following.

2.2.1 Model-free methods

In this approach, the fault detection and isolation methods do not use a model of the plant and they range from physical redundancy and special sensors through limit-checking and spectrum analysis to logical reasoning.

- ***Physical redundancy***. In this approach, multiple sensors are installed to measure the same physical quantity. Any serious discrepancy between the measurements indicates a sensor fault. With only two parallel sensors, fault isolation is not possible. With three sensors, a voting scheme can be built which allows to isolating the faulty sensor. Physical redundancy involves extra hardware cost and extra weight, the latter representing a serious concern, for example, in aerospace applications.
- ***Special sensors*** may be installed explicitly for detection and isolation. A sort of these sensors are the known as *limit sensors* (measuring *e.g.*, temperature or pressure), which perform limit checking using additional hardware.

Other special sensors may measure some fault-indicating physical quantity, such as sound, vibration, elongation, etc.

- ***Limit checking.*** In this approach, plant measurements are compared by computer to preset limits. Exceeding the threshold indicates a fault situation.
- ***Spectrum analysis*** of plant measurements may also be used for detection and isolation. Most plant variables exhibit a typical frequency spectrum under normal operating conditions; any deviation from this is an indication of abnormality. Certain types of faults may even have their characteristic signature in the spectrum, facilitating fault isolation.
- ***Logic reasoning*** techniques form a broad class which is complementary to the methods outlined above, in that they are aimed at evaluating the fault signals obtained by the detection hardware or software. The simplest techniques consist of trees of logical rules of the "IF - fault signal ϕ_i - AND - fault signal ϕ_j - THEN – conclusion" type. Each conclusion can, in turn, serve as a fault signal in the next rule, until the final conclusion is reached.

2.2.2 Model-based methods

Fig. 2.2 shows the general fault diagnosis scheme using systems models. The general idea of fault diagnosis model-based methods is to compare the available measurements of the monitored system with their corresponding predictions obtained using a system model, either analytical or qualitative (Venkatasubrarnanian et al., 2003a). If they differ significantly, then it may be concluded that a fault has occurred. Nonetheless, the problem with this approach is that a precise description of a system that takes the effects of faults into account is usually impossible, and even if such a description exists, the dependence that characterises particular faults cannot be defined on the grounds of it. Therefore, different kinds of simplified models are used in fault detection and isolation.

When classifying models applied to the diagnostics of processes (systems), it is possible to distinguish models of systems applied to fault detection and models used for fault isolation. Models used for fault detection describe relationships existing within the system between the input ($\boldsymbol{u}$) and output ($\boldsymbol{y}$) signals, and allow detecting changes (fault signals ϕ) caused by faults. Models used for fault isolation define the existing relationship between fault signals ϕ and faults $\boldsymbol{f}$, which will be represented by ($\phi \rightarrow \boldsymbol{f}$).

Analytical models as well as fuzzy and neural ones are applied to fault detection. These models usually describe the system in the normal state what allow to calculate residuals reflecting divergences that may exist between the observed operation of the system and the normal operation defined by the model through the computed system predictions ($\hat{\boldsymbol{y}}$). These residuals are most often calculated as differences between the measured and the modelled output signals. In a non-faulty state, residual values should oscillate around zero. In consequence, residual values different than zero denote fault signals which should allow to detect and isolate the fault.

Conversely, residual values are rarely used for fault isolation. The binary or multi-value evaluation of residual values is usually applied, and an inference about faults is carried out on the basis of fault signals which were converted in such a way. Consequently, a classifier is needed for the conversion of residual continuous signals ($\boldsymbol{r}$) into quality fault signals (ϕ) ($\boldsymbol{r} \rightarrow \phi$).

Models applied to fault isolation should map the space of fault signals into the space of faults (f) ($\phi \rightarrow f$).Thereby, and such as it was for the fault detection case, these relationships can be defined on the basis of analytical/qualitative modelling, taking into account the effect of faults, training or using an expert's knowledge.

As it was pointed out previously, there are two mainly approaches in model-based fault detection and isolation: the analytical model-based approach which just uses analytical models and the qualitative model-based approach which just applies qualitative models of the system plant.

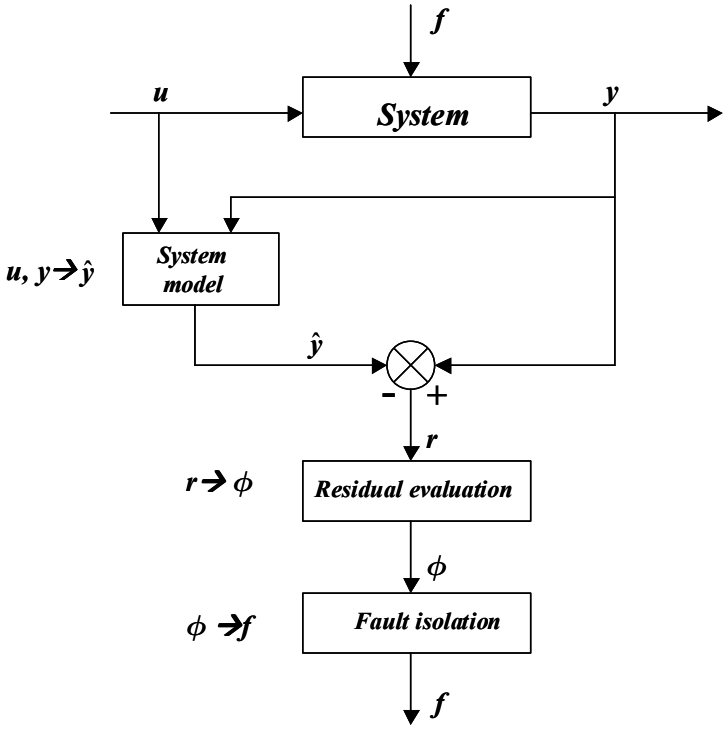

Fig. 2.2 Fault diagnosis diagram using system models

2.2.2.1 Analytical model-based methods

The ***analytical redundancy*** (Isermann, 2005) of the monitored system measurements exists when an additional value of a process variable is calculated on the grounds of a mathematical model that connects the estimated variable with other measured signals. Mathematical models are applied to the calculation of process variable values instead of the application of redundant measuring devices in the system structure. Thereby, analytical redundancy is used both for fault detection and for fault isolation. The analytical model of the diagnosed system contains all relationships existing among process variables what allow to obtain all physical redundant relationships needed to detect and isolate faults.

2.2.2.2 Qualitative model-based methods

These methods can be applied both for fault detection and for fault isolation and mainly they are used because it may often be difficult and time consuming to develop a good mathematical model. As a consequence of this issue, there have been many attempts to use cruder descriptions (Reiter, 1987; Lunze, 1994; Frank 1996; Cordier et al., 2004) as pointed out in (Venkatasubrarnanian et al., 2003b). The model is usually developed based on some fundamental understanding of the physics of the process. In quantitative models this understanding is expressed in terms of mathematical functional relationships between the inputs and outputs of the system. In contrast, in qualitative models

these relationships are expressed in terms of qualitative functions centered around different units in a process. The qualitative approach to fault diagnosis can be motivated by the following circumstances:

- Faults can not be reasonably described by analytical models.
- The on-line information available is not given by quantitative measurements of the system output but by qualitative assessments of the current operation conditions.
- If the system structure or parameters are not precisely known and diagnosis has to be based primarily on heuristic information no quantitative model can be set up.

2.2.3 Type of faults and disturbances

In this section, what is meant by faults will be described and the tasks of fault detection and isolation will be mentioned. According to (Gertler, 1998), ***faults*** are performance deteriorations, malfunctions or breakdowns in the monitored plant or in its instrumentations which may be represented as unknown extra inputs acting on the system (***additive faults***) or as changes of some plant parameters (***multiplicative faults***). While in many cases the classification of a particular fault as additive or multiplicative follows naturally from its nature, sometimes it may also be arbitrary. In general, the faults of interest belong to one of the following categories:

- ***Additive process faults***. These are unknown inputs acting on the plant, which are normally zero and which cause a change in the plant outputs independent of the known inputs. Such faults best describe plant leaks, loads, etc.
- ***Multiplicative process faults***. These are changes (abrupt or gradual) in some plant parameters. They cause changes in the plant outputs, which depend also on the magnitude of the known inputs.
- ***Sensor faults***. These are discrepancies between the measured and actual values of individual plant variables. These faults are usually considered additive (independent of the measured magnitude).
- ***Actuator faults***. These are discrepancies between the input command of an actuator and its actual output. Actuator faults are usually handled as additive.

A ***disturbance*** is also an unknown extra input acting on the plant. Thus, physically there is no difference between a disturbance and certain faults. The distinctions is, indeed, subjective; we consider as faults those extra inputs the presence of which we wish to detect while we consider as disturbances those which we want to ignore and be unaffected by (Gertler, 1998). Some authors refer to the disturbances as ‘nuisance variables’.

Faults and disturbances will be handled as unspecified deterministic functions of time while noises are unknown extra inputs, just like the additive disturbances, but they are assumed to exhibit random behaviour. They are also assumed to have zero mean; any nonzero mean can be handled as a separate disturbance. The noises are also nuisance variables the effect of which needs to be suppressed.

Modelling errors are errors or uncertainties in the parameters of the monitored system. Just like the multiplicative faults, they are discrepancies between the true system and the model but they represent an undesirable interference with fault diagnosis. Thus modelling errors can be considered as multiplicative disturbances. Note that in general it is difficult to distinguish parametric faults from certain modelling errors though their long-term behaviour may provide some clue: parametric faults develop in the course of system operation while some model errors may have been there from the beginning.

Usually, the fault detection and isolation activity takes place on-line, in real time. The two tasks, detection and isolation, may be performed in parallel or sequentially. In some diagnostic systems, a single decision conveys not only the fact that a fault is present but also its location. In other systems, the detection task is running permanently while the isolation task is triggered only upon the detection of the presence of a fault. Particularly, in fault detection and isolation, the following conventions are usually adopted:

- It is assumed that faults are not present initially in the systems but arrive at some later time instant. The faults are generally described by deterministic time-functions which are unknown.
- Faults are those unknown inputs which we wish to detect and isolate while disturbances are nuisances which we wish to ignore.
- Any noise, originating from the plant or from the sensors and actuators, is considered random with zero mean (any nonzero mean is handled as a fault or disturbance).
- Modelling errors are discrepancies between the model (model parameters) and the true system. They may be present ever since the origins of the system or may arise due to operating-point changes. Model errors are nuisances the effect of which we want to suppress. They may be considered as multiplicative disturbances, in contrast to multiplicative faults which are also discrepancies between the model and the true system, but which we wish to detect.

On the other hand, the detection performance of the diagnostic technique is characterized by a number of important and quantifiable benchmarks, namely:

- ***Fault sensitivity***, that is, the ability of the technique to detect faults of reasonably small size;
- ***Reaction speed***, that is, the ability of the technique to detect faults with reasonably small delay after their arrival;
- ***Robustness***, that is, the ability of the technique to operate in the presence of noise, disturbances and modelling errors, with few false alarms.

Those benchmarks arise from the interaction between faults on the one hand and noise, disturbances and model errors on the other hand, and are affected by the detection algorithm.

Regarding the isolation performance, its ability to distinguish faults depends on the physical properties of the plant, on the size of faults, noise, disturbances and model errors and on the design of the algorithm. Multiple simultaneous faults are, in general, more difficult to isolate than single faults. Also, the interplay between faults and disturbances, noise and model errors may lead to uncertain or incorrect isolation decisions. Further, some faults may be non-isolable from one another because they act on the physical plant in an undistinguishable way.

2.3 Fault detection using system models

2.3.1 Model-based fault detection using residuals

In general, model-based fault detection methods use system (process) models in order to generate residuals (Himmelblau, 1978; Gertler, 1998). Thus, *Fig. 2.3* illustrates the general and conceptual structure of a model-based fault detection module which consists in two main parts: the residual generation stage and the residual value stage. This two-stage structure was first suggested by (Chow and Willsky, 1980) and now is widely accepted by the fault diagnosis community. The main purposes of these two main stages are described as follows:

- ***Residual Generation*:** Its purpose is to generate a fault-indicating signal-residual, using available input and output information from the monitored system. This auxiliary signal is designed to reflect the onset of a possible fault in the analyzed system. The residual should be normally zero or close to zero when no fault is present, but should be distinguishably different from zero when a fault occurs. This means that the residual is characteristically independent of system inputs and outputs, in ideal conditions. The algorithm used to generate residuals is called a ***residual generator***. Residual generation is thus a procedure for extracting ***fault signals*** (ϕ) from the system, with the fault signal represented by the ***residual signal*** (***r***). The residual should ideally carry

only fault information and to ensure reliable fault detection, the loss of fault information in residual generation should be as small as possible.

- ***Residual value evaluation*:** Every fault detection algorithm that makes use of an analytical, fuzzy or neural model contains the *decision-making part*, in which the evaluation of the residual value takes place. In this stage, the decision about the existence of a fault is made together with a possible indication of this event generating the corresponding fault signal. This signal should carry information about the effect of the fault on the residual set so that the fault isolation module can isolate this fault. A decision process may consist in a simple threshold test on the instantaneous values or moving averages of the residuals (Puig et al., 1999; Ploix et al., 2000), or it may consist of methods of statistical decision theory, *e.g.*, generalized likelihood ratio (*GLR*) testing or sequential probability ratio testing (*SPRT*) (Willsky et al, 1976; Basseville et al, 1988; Tzafestas and Watanabe, 1990; Basseville and Nikiforov, 1993). On the other hand, this residual evaluation can also be carried out with the use of fuzzy or neural logic (Korbicz et al., 1999) or qualitative methods (Kuipers, 1994; Leicht et al., 1994). The residual evaluation related to these approaches allow taking into account the uncertainty of fault signal values caused by disturbances in the system, measurement noise, modelling errors, and difficulties with the definition of threshold values.

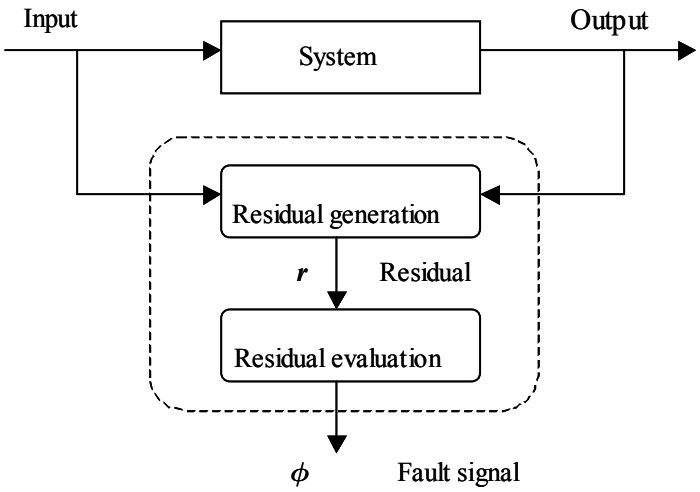

Fig. 2.3 Conceptual structure of model-based fault detection using residuals

Model-based fault detection is concerned mainly with two important properties:

- ***On-line fault diagnosis*** in which the diagnosis is carried out during system operation. This is because the system input-output information required by model-based fault detection module is only available when the system is in operation.
- ***Robustness*** against disturbances, noise and modelling uncertainty that arises from incomplete knowledge and understanding of the monitored processes. Consequently, the residual generated to indicate faults may also react to the presence of noise, disturbances and model errors. Desensitizing the residuals to these sources is a most important aspect in the design of the detection and diagnosis algorithm. In particular:
  - To deal with the effects of noise, the residuals may be filtered and statistical techniques may be applied to their evaluation.
  - Disturbance decoupling may be built into the design of the residual generator, but it competes with isolation enhancement for the available design freedom.

- Robustness in the face of modelling errors is the most fundamental problem in model-based fault detection and isolation. Several methods are available which usually rely on some sort of optimization: the known techniques are effective only under limited circumstances.

In model-based fault detection, the generation of residuals needs to be followed by residual evaluation, in order to arrive at detection and isolation decisions. Because of the presence of noise and model errors, the residuals are never zero, even if there is no fault. Therefore, the residual evaluation requires testing the residuals against thresholds, obtained empirically or by theoretical considerations. As it was already mentioned, another approach to achieve residual evaluation robustness would be the use of a fuzzy or neural logic.

On the other hand, to facilitate fault isolation, the residual generators are usually designed (*enhanced residuals*) exhibiting structural or directional properties. The isolation decisions then can be obtained in a structural (Boolean) or directional (geometric) framework, with or without the inclusion of statistical elements.

Concerning residual generation methods in model-based fault detection and isolation, four main approaches can be considered within the group of analytical methods applied to fault detection. In the next lines, few ideas about those methods are given:

- **Diagnostic Observers**. The basic idea behind the diagnostic observer approaches is to estimate the outputs of the system from the measurements (or a subset of measurements) by using either *Luenberger* observers in a deterministic setting (Beard, 1971; Jones, 1973) or *Kalman filters* in a stochastic setting (Mehra and Peschon, 1971; Willsky, 1976 and 1986; Basseville, 1986). Then, the weighted output estimation error is used as a residual. Thereby, while the flexibility in selecting the observer gains is used to minimize the noise effect on the fault detection result in the *Kalman approach*, this freedom is applied to enhance the residual fault detection and isolation properties in the *Luenberger approach*. As a result, the dynamics of the fault response can be controlled, within certain limits, by placing the poles of the observer. This trend was followed by a long line of researchers, including (Frank and Keller, 1980), (Frank and Wünnenberg, 1989), (Viswanadham and Srichander, 1987), (Patton and Kangethe, 1989), (Chen et al., 1999), (Puig et al., 2003a), etc.
- **Parity (consistency) relations**. Parity relations are rearranged direct input-output model equations, subjected to a linear dynamic transformation. The transformed residuals serve for detection and isolation. The residual sequence is coloured, just like in the case of observers. The design freedom provided by the transformation can be used for disturbance decoupling and fault isolation enhancement. Also, the dynamics of the response can be assigned, within the limits posed by the requirements of casualty and stability. The parity relation approach to generate the residual, based upon consistency checking on system input and output data over a time window, was originally proposed by (Mironovski, 1979 and 1980). The approach was later proposed by (Chow and Willsky, 1984), and has been expressed in several different versions: (Gertler, 1988), (Chen and Zhang, 1990). The latest development regarding parity relation approaches can be found in (Gertler, 1997), (Gertler, 1998), (Chen et al., 1999), (Ploix et al., 2006), etc.
- **Parameter estimation.** Another ***FDI*** approach is the use of parameter estimation which is based directly on system identification techniques. In 1984, Isermann illustrated that process fault detection and isolation can be achieved using the estimation of non-measurable process parameters and/or state variables in his survey paper (Isermann, 1984). Parameter estimation is a natural approach to the detection and isolation of parametric (multiplicative) faults. A reference model is obtained by first identifying the plant in fault-free situation. Then, the parameters are repeatedly re-identified on-line. Deviations from the reference model serve as a basis for detection and isolation. Parameter estimation may be more reliable than the analytical redundancy methods, but it is also more demanding in terms of on-line computation and input excitation requirements and consequently,

this approach will not be considered in the thesis. The latest development and applications can be found in (Isermann, 1997), (Isermann, 2005), (Puig et al., 2005d), (Ingimundarson et al, 2005) .

As it has been realized recently, there is a fundamental equivalence between parity relation and observer based designs (Gertler, 1997). In consequence, the two techniques produce identical residuals if the generators have been designed for the same specification. A relationship, though weaker, has been found between parity relations and parameter estimation.

Within the group of qualitative methods applied to fault detection, the main residual generation approach is based on the use of neural and fuzzy models (Korbicz et al., 1999; Ayoubi, 1994). Neural and fuzzy models allow estimating the values of system variable. Then, residual is generated as a difference between the measurement of the system output and its estimation given by the neural or fuzzy model. A vital advantage of fuzzy and neural techniques is the possibility of non-linear system modelling. Models of systems in the state of complete efficiency are obtained on the grounds of experimental data with the use of different training techniques. This is especially important when analytical models of the system are not known. Such models reflect well system operation within the signal changes range on the grounds of which they are trained.

The advantage of fuzzy and neural networks is the possibility to connect expert's knowledge with the available measurement data. The expert's knowledge is used to define the structure and initial values of the model parameters. The model is a set of rules that can be interpreted and verified by the expert. The number of rules in fuzzy models grows rapidly with the growth of the number of inputs and the number of fuzzy sets for particular inputs. This limits their application to relatively simple systems.

2.3.2 Analytical model-based fault detection techniques

In this thesis, only the analytical model-based fault detection approach will be considered. As pointed out in *Section 2.2.2*, this approach uses a mathematical model of the monitored system in order to estimate the system outputs. Comparing these estimations $\hat{\boldsymbol{y}}(k)$ with the real system outputs ***y(k)*** (***Residual generation stage***), a set of residuals ***r(k)*** is obtained. Then, analyzing this residual set, a decision about the existence of a fault ***f(k)*** is made (***Residual value evaluation stage***) generating the corresponding fault signals $\phi(k)$ in case the residual evaluation determines a fault is affecting the monitored system.

2.3.2.1 Residual generation and evaluation

As mentioned above, analytical model-based fault detection is based on generating a residual comparing the measurements of physical variables $\boldsymbol{y}(k)$ of the process with their estimation $\hat{\boldsymbol{y}}(k)$ provided by the associated system model:

$$\boldsymbol{r}(k) = \boldsymbol{y}(k) - \hat{\boldsymbol{y}}(k) \tag{2.1}$$

Thereby, residuals ***r(k)*** will be generated at every time instant *k* by the ***residual generator***. According to (Gertler, 1998), a residual generator is a linear discrete dynamic algorithm (a computational "system") operating on the plant observables, that is, on the command values of the controlled inputs and on the measured values of the measured inputs and outputs. Its generic form is

$$\boldsymbol{r}(k) = \boldsymbol{V}(q^{-1})\boldsymbol{u}(k) + \boldsymbol{O}(q^{-1})\boldsymbol{y}(k) \tag{2.2}$$

where: ***r(k)*** is the vector of residuals, $\boldsymbol{V}(q^{-1})$ and $\boldsymbol{O}(q^{-1})$ are transfer function matrices. However, this equation is not necessarily a residual generator; it has to return zero-valued residuals when there are no faults, no nuisance inputs

and no modelling errors. Thereby, considering a linear discrete dynamic system, its nominal input-output relationship (without faults, disturbances and noise) is set by

$$\boldsymbol{y}(k) = \boldsymbol{M}(q^{-1})\boldsymbol{u}(k) \tag{2.3}$$

Then, when there are no faults, no nuisance inputs and no modelling errors, the Eq. (2.3) must be satisfied and a proper residual generator must return zero-valued residuals. In consequence,

$$\boldsymbol{V}(q^{-1})\boldsymbol{u}(k) + \boldsymbol{O}(q^{-1})\boldsymbol{M}(q^{-1})\boldsymbol{u}(k) = \boldsymbol{0} \tag{2.4}$$

has to be fulfilled for all $\boldsymbol{u(k)}$, requiring

$$\boldsymbol{V}(q^{-1}) = -\boldsymbol{O}(q^{-1})\boldsymbol{M}(q^{-1}) \tag{2.5}$$

As a result, the generic residual generator (Eq. (2.2)) can be also written as

$$\boldsymbol{r}(k) = \boldsymbol{O}(q^{-1})\left[\boldsymbol{y}(k) - \boldsymbol{M}(q^{-1})\boldsymbol{u}(k)\right] \tag{2.6}$$

Both Eq. (2.2)) and Eq. (2.6) are known as the ***computational form*** of the generic residual generator (Gertler, 1998).

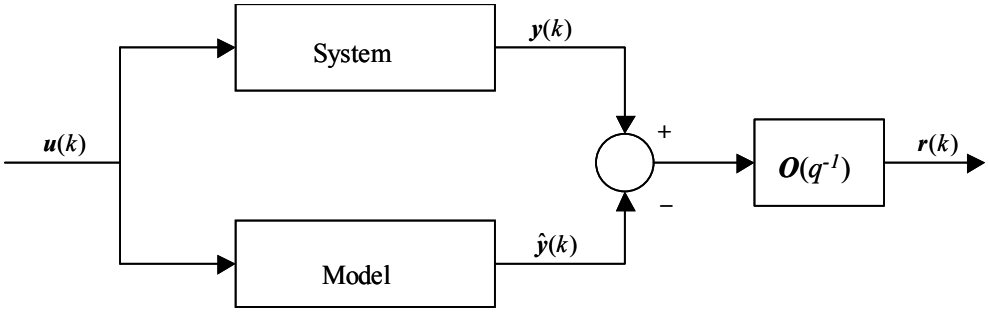

Fig. 2.4 Generic residual generator: computational form

Conversely, it should be noticed that the term

$$\boldsymbol{\delta}(k) = \boldsymbol{y}(k) - \boldsymbol{M}(q^{-1})\boldsymbol{u}(k) \tag{2.7}$$

of Eq. (2.6) is due to the effect of faults and nuisance inputs. In consequence, the generic form of the residual generator can be also written in terms of these effects resulting in its ***internal*** or ***unknown-input-effect*** form (Gertler, 1998):

$$\boldsymbol{r}(k) = \boldsymbol{O}(q^{-1})\boldsymbol{\delta}(k) \tag{2.8}$$

In an ideal situation, where the monitored system may only be affected by known faults and the estimations of the model have no errors regarding the behaviour of the system in a non-faulty scenario, the ***residual value evaluation stage*** will be able to indicate a fault affecting to the monitored system while the residual generator computes non-zero-valued residuals at every time instant. In short, while

$$\boldsymbol{r}(k) = \boldsymbol{0}, \tag{2.9}$$

a fault will not be indicated. Otherwise, the residual value evaluation stage will generate the corresponding fault signals ($\phi(k)$) so that the fault isolation module can diagnose the detected fault.

Being more realistic, the residual $\boldsymbol{r(k)}$ will never be zero-valued since the monitored system is affected by nuisance inputs which can not be either controlled or avoided and furthermore, the system model does have errors regarding the system performance. Consequently, if condition (2.9) were used to determine the existence of a fault, the fault detection module could indicate faults which do not actually exist.

In fault detection and isolation, robust residual generators must be used which do only react in presence of faults and do not in presence of nuisance inputs or because of modelling errors affecting to the considered model. At the

moment, residual generator robustness is the most important aspect when designing a fault detection and isolation algorithm and it is still an open investigation field. This issue will be introduced in *Section 2.3.2.3*.

As it can be inferred from Eq. (2.1), the residual generation stage does depend on the model type used to estimate the system output since this stage requires this estimation so that the residual can be generated. In general, different model types will provide different estimations at every time instant *k*. In consequence, the residual value evaluation stage is also affected by the model type. The reason is that this stage is based on checking if Eq. (2.9) holds or not, assuming an ideal situation. As a result of the two previous statements, it is concluded that the whole fault detection performance of the fault diagnostic system does depend on the type of analytical model used to estimate the system output.

Conversely, as indicated by the residual computational form given by Eq. (2.6), the time evolution of the computed residual does strongly depend on the transfer function $\boldsymbol{O}(q^{-1})$ and consequently, if this function were properly designed, the fault detection performance could be improved in order to achieve a better fault indication and to generate a sequence of fault signals $\phi(k)$ which allow to isolate the fault easily. Moreover, it must be taken into account that $\boldsymbol{O}(q^{-1})$ has an influence on the residual generator structure and therefore, on the fault signals which can be observed when a given fault occurs. In this way, a proper design of this function can add more fault distinguishability in order to improve the reliability of the result given by the diagnostic system. In the following, it will be shown that this function is determined by the used system model.

2.3.2.2 Residual generation using observers

In general, in model-based fault detection, the system model can be used in three different approaches, in simulation, in prediction and in observation:

- ***Simulation approach***. This is an open loop approach and the real measurements are not used to correct the estimation given by the model.
- ***Prediction approach***. This is a closed loop approach and the system output measurement $\boldsymbol{y}(k)$ will be used to correct the estimation given by the model.
- ***Observation approach***. This is a semi-closed loop where the system output $\boldsymbol{y}(k)$ will be partially used in order to correct the estimation given by the model in simulation.

According to (Gertler, 1997), the simulation and prediction approaches (***parity equation approach***) can be seen as two particular cases of the ***observation approach*** for two specific values of the observer gain. Thus, in this thesis, the observer approach will be considered. Moreover, concerning the *residual generation stage*, (Gertler, 1998) shows the equivalence between the observer approach and the parity equations (simulation and prediction approach) in relation to the structure of the obtained residual generator and consequently, a fault detection analysis of the observer performance will also allow to obtain information about the performance of predictors and simulators when particularizing the observation gain matrix for the two values used for these two approaches.

Assuming that the system is completely observable, the general expression of a linear discrete-time observer in its state-space form is given by

$$\begin{aligned} \hat{\boldsymbol{x}}(k+1) &= \boldsymbol{A}\hat{\boldsymbol{x}}(k) + \boldsymbol{B}\boldsymbol{u}(k) + \boldsymbol{L}(\boldsymbol{y}(k) - \hat{\boldsymbol{y}}(k)) \\ \hat{\boldsymbol{y}}(k) &= \boldsymbol{C}\hat{\boldsymbol{x}}(k) \end{aligned} \tag{2.10}$$

where $\boldsymbol{y}(k) \in \Re^{ny}$, $\boldsymbol{u}(k) \in \Re^{nu}$, $\boldsymbol{x}(k) \in \Re^{nx}$ are the system output, input and the state-space vectors respectively; $\hat{\boldsymbol{y}}(k) \in \Re^{ny}$ and $\hat{\boldsymbol{x}}(k) \in \Re^{nx}$ are the estimated system output and state-space vectors respectively; $\boldsymbol{A}$, $\boldsymbol{B}$ and $\boldsymbol{C}$ are the

state, the input and the output matrices respectively; $\boldsymbol{L}$ is the observer gain matrix designed to stabilise the observer and to guarantee a desired performance regarding fault detection. It must be noticed that two extreme cases can be considered in the observer definition. First, the observer becomes a ***simulator*** using $\boldsymbol{L=0}$ and as a consequence, its eigenvalues are equal to the ones of the considered system ($\boldsymbol{L=0}$) (Chow et al, 1984) , but it can only be used when the system is stable. Second, the observer becomes a ***predictor*** (Chow et al, 1984) when the observer gain ($\boldsymbol{L} = \boldsymbol{L}_p$) is selected such that all the observer eigenvalues are at the origin ("***deadbeat observer***") (Patton et al, 1991). Moreover, the observer model has the capability of placing its eigenvalues between these two extreme cases using a set of observation gains ($\boldsymbol{L}=\boldsymbol{L}_o$) which are different from the ones mentioned previously. Regarding the simulation and prediction cases, (Gertler, 1997) sets that they correspond to the well-known ***parity equations*** and they are embedded in the observer equation (2.10).

In the following, the goal is to obtain the expression of the residual computational form (Eq. (2.6)) when an observer model is used in order to obtain the transfer function $\boldsymbol{O}(q^{-1})$ since, as mentioned above, this function rules the most of the fault detection and isolation properties of the considered fault diagnosis model. Thereby, in order to obtain this result some transformations of the interval observer state-space form must be done.

Thus, considering the residual expression given by Eq. (2.1) and taking into account that the residual $\boldsymbol{r(k)}$ can be seen as an extra model input, the observer state-space form can be rearranged as

$$\begin{aligned} \hat{\boldsymbol{x}}(k+1) &= \boldsymbol{A}\hat{\boldsymbol{x}}(k) + \begin{bmatrix} \boldsymbol{B} & \boldsymbol{L} \end{bmatrix} \begin{bmatrix} \boldsymbol{u}(k) \\ \boldsymbol{r}(k) \end{bmatrix} \\ \hat{\boldsymbol{y}}(k) &= \boldsymbol{C}\hat{\boldsymbol{x}}(k) \end{aligned} \tag{2.11}$$

Then, assuming zero initial conditions, the input-output form of the observer using the q-transform is

$$\hat{\boldsymbol{y}}(k) = \boldsymbol{C}\left(q\boldsymbol{I} - \boldsymbol{A}\right)^{-1}\boldsymbol{B}\boldsymbol{u}(k) + \boldsymbol{C}\left(q\boldsymbol{I} - \boldsymbol{A}\right)^{-1}\boldsymbol{L}\boldsymbol{r}(k) \tag{2.12}$$

Thus, defining $\hat{\boldsymbol{y}}(k)_{\boldsymbol{L=0}}$ as the value of $\hat{\boldsymbol{y}}(k)$ when $\boldsymbol{L=0}$ (simulation value) and $\boldsymbol{H}_r(q^{-1},\boldsymbol{\theta})$ as

$$\boldsymbol{H}_r(q^{-1}) = \boldsymbol{C}(q\boldsymbol{I} - \boldsymbol{A})^{-1}\boldsymbol{L} \tag{2.13}$$

the interval observer input-output form can be written as the sum of the estimation given by the simulation approach ($\boldsymbol{L=0}$) and a term which depends on the residual $\boldsymbol{r(k)}$:

$$\hat{\boldsymbol{y}}(k) = \hat{\boldsymbol{y}}(k)_{\boldsymbol{L=0}} + \boldsymbol{H}_r(q^{-1})\boldsymbol{r}(k) \tag{2.14}$$

Thus, it must be noticed that the norm of the steady-sate value of $\boldsymbol{H}_r(q^{-1})$ is proportional to the norm of the observation gain $\boldsymbol{L}$.

Conversely, taking into account that the general expression of the residual is given by Eq. (2.1) and using the observer output estimation given by Eq. (2.14), the residual can be re-written as

$$\boldsymbol{r}(k) = \boldsymbol{y}(k) - \hat{\boldsymbol{y}}(k) = \boldsymbol{y}(k) - \hat{\boldsymbol{y}}(k)_{\boldsymbol{L=0}} - \boldsymbol{H}_r(q^{-1})\boldsymbol{r}(k) \tag{2.15}$$

Then, grouping the terms associated with the residual to the left side of the equation,

$$\left(\boldsymbol{I} + \boldsymbol{H}_r(q^{-1})\right)\boldsymbol{r}(k) = \boldsymbol{y}(k) - \hat{\boldsymbol{y}}(k)_{\boldsymbol{L=0}} \tag{2.16}$$

Examining the right-sided term of this equation and considering the definition of the residual (Eq. (2.1)), it must be seen that this term corresponds to the residual generated by the simulation approach which can be written down as $\boldsymbol{r}(k)_{\boldsymbol{L=0}}$. Thus, taking into account that $\boldsymbol{H}_r(q^{-1})$ is a square matrix and considering $\left(\boldsymbol{I} + \boldsymbol{H}_r(q^{-1},\boldsymbol{\theta})\right)$ has a inverse matrix, this equation can be expressed as

$$\boldsymbol{r}(k) = \left(\boldsymbol{I} + \boldsymbol{H}_r(q^{-1})\right)^{-1}\boldsymbol{r}(k)_{\boldsymbol{L=0}} \tag{2.17}$$

This equation sets the relation between the residual related to the simulation approach and the residual generated by an observer. As seen, this relation is ruled by a transfer function which depends on the observer gain $\boldsymbol{L}$. As a consequence, it can be said that the fault detection and isolation properties of the considered analytical model are determined by $\boldsymbol{L}$. Conversely, this equation such as shown above and all the derived conclusions regarding the influence of the observer gain on the observer fault detection performance can be considered as a novelty presented in this thesis and they will be analyzed in *Chapter 3*.

Comparing the residual computational form given by Eq. (2.6) with the residual form Eq.(2.17), the expression of the transfer function $\boldsymbol{O}(q^{-1})$ for the general case of an observer can be derived:

$$\boldsymbol{O}(q^{-1}) = \left(\boldsymbol{I} + \boldsymbol{H}_r(q^{-1})\right)^{-1} = \left(\boldsymbol{I} + \boldsymbol{C}(q\boldsymbol{I} - \boldsymbol{A})^{-1}\boldsymbol{L}\right)^{-1} \tag{2.18}$$

taking into account the next equality

$$\boldsymbol{y}(k) - \boldsymbol{M}(q^{-1})\boldsymbol{u}(k) = \boldsymbol{r}(k)_{\boldsymbol{L}=\boldsymbol{0}} = \boldsymbol{y}(k) - \hat{\boldsymbol{y}}(k)_{\boldsymbol{L}=\boldsymbol{0}} = \boldsymbol{y}(k) - \boldsymbol{C}\left(q\boldsymbol{I} - \boldsymbol{A}\right)^{-1}\boldsymbol{B}\boldsymbol{u}(k) \tag{2.19}$$

Then, considering the simulation approach ($\boldsymbol{L}=\boldsymbol{0}$), the computational form of the residual is

$$\boldsymbol{r}(k)_{\boldsymbol{L}=\boldsymbol{0}} = \boldsymbol{y}(k) - \boldsymbol{C}\left(q\boldsymbol{I} - \boldsymbol{A}\right)^{-1}\boldsymbol{B}\boldsymbol{u}(k) \tag{2.20}$$

If the prediction approach ($\boldsymbol{L}=\boldsymbol{L}_p$) is used,

$$\boldsymbol{r}(k)_{\boldsymbol{L}=\boldsymbol{L}_p} = \left(\boldsymbol{I} + \boldsymbol{C}\left(q\boldsymbol{I} - \boldsymbol{A}\right)^{-1}\boldsymbol{L}_p\right)^{-1}\left[\boldsymbol{y}(k) - \boldsymbol{C}(q\boldsymbol{I} - \boldsymbol{A})^{-1}\boldsymbol{B}\boldsymbol{u}(k)\right] \tag{2.21}$$

Lastly, for the observer case ($\boldsymbol{L}=\boldsymbol{L}_o$) approach,

$$\boldsymbol{r}(k)_{\boldsymbol{L}=\boldsymbol{L}_o} = \left(\boldsymbol{I} + \boldsymbol{C}\left(q\boldsymbol{I} - \boldsymbol{A}\right)^{-1}\boldsymbol{L}_o\right)^{-1}\left[\boldsymbol{y}(k) - \boldsymbol{C}\left(q\boldsymbol{I} - \boldsymbol{A}\right)^{-1}\boldsymbol{B}\boldsymbol{u}(k)\right] \tag{2.22}$$

Such as it can be seen in equations (2.20) and (2.21), when considering the simulation or prediction approach, the structure of the residual generator is fully established and as a result, so does its fault detection and isolation performance. Thus, using these methods there is nothing it can be done to try to enhance this performance and to avoid some fault diagnosis problems (*lack of fault indication*, *wrapping effect*, *noise effect*, *etc*) which will be pointed out in the following section. On the other hand, when using the observer approach, the structure of its residual generator is not determined since it depends on the value of the observer gain matrix $\boldsymbol{L}_o$ which can be chosen to place the observer eigenvalues between the origin ($\boldsymbol{L}=\boldsymbol{L}_p$) and the ones related to the monitored system ($\boldsymbol{L}=\boldsymbol{0}$). In consequence, this matrix could be designed to try to improve the observer fault detection and isolation performance and to try to avoid some of the fault diagnosis problems. In this line, the ***Kalman filter approach*** designs the observation gain to minimize the noise effect. In consequence, thinking about designing $\boldsymbol{L}$ to minimize the effect of some fault diagnosis drawbacks does not seem to be an unreality. At the same time, a proper design of $\boldsymbol{L}$ could improve some fault diagnosis properties like adding more fault distinguishability or more fault indication persistence. In this way, one of the goals of this thesis is analyzing the effect of the observation gain on the observer fault detection and isolation performance.

2.3.2.3 Robustness issues

As it was mentioned in *Section 2.3.2.1*, when building a model of a complex system to monitor its behaviour, there is always a mismatch between the modelled and real behaviour since some effects are neglected, some parameters have tolerance, some errors in parameters or in the structure of the model are introduced in the calibration process, etc. Many times, these modelling errors could be bounded and included in the fault detection model. There are several ways of modelling the ***uncertainty*** associated with the model. For instance, an approach providing a nominal model plus the uncertainty on every parameter bounded by intervals determines what is known as ***interval model*** approach

(or ***worst case model*** approach). In the ***FDI*** and automatic control community, this type of uncertainty is called ***structured*** because it is assumed that the structure of the model is known but not the model parameters, in opposition to a more general type of uncertainty which considers the structure of the model is not completely known but only bounded. This type of uncertainty is known as ***unstructured***. In ***FDI*** community a fault detection algorithm able to handle uncertainty is called robust. The ***robustness*** of fault detection algorithm is the degree of sensitivity to faults compared to the degree of sensitivity to uncertainty (Patton et al, 1994).

Research on robust fault detection methods has been very active in the ***FDI*** community these last years (Chen et al, 1999). One family of approaches, called ***active***, is based on generating residuals which are insensitive to uncertainty, while at the same time sensitive to faults. This approach has been extensively developed these last years for several researchers using different techniques: unknown input observers, robust parity equations, H_∞, etc. In (Chen and Patton ,1999) there is an excellent survey of the active approach.

On the other hand, there is a second family of approaches, called ***passive***, which enhances the robustness of the fault detection system at the residual value evaluation stage. This approach is still under research. Several techniques have been used, but most of them are based on using an ***adaptive threshold*** at the residual value evaluation stage.

According to (Gertler, 1998), there is no algorithm which is robust under arbitrary model error conditions. To design an algorithm for robustness, rather detailed information is necessary about the nature of errors and uncertainties, and such information is seldom available. But even if it is, what can be achieved is rather limited. Generally ***perfect decoupling*** of the residuals from uncertainties it is only possible in a limited number of model parameters.

Adaptive thresholding techniques were first proposed by (Clark,1989), who suggests an empirical relation between the operation point and the corresponding detection threshold. Further approaches are due to (Emami-Naemi et al, 1988), who develops a theoretical relation between the operation point, the model uncertainty and the detection threshold. This approach is based on H_∞ techniques and it was further explored by (Frank et al, 1991) and (Ding et al, 1991). Another approach for adaptive threshold generation was proposed by (Horak et al, 1988) and it is based on a dynamical optimisation assuming parametric uncertainty.

The passive approach has the advantage over the corresponding active approach that it can achieve robustness in the detection procedure in spite of the number of uncertain parameters in the model, and without using any approximation based on the simplification of the underlying parameter representation.

The passive approach based on adaptive thresholds is based not in avoiding the effect of uncertainty in the residual through perfect decoupling, but in propagating the parameter uncertainty to the residual, and then bounding the residual uncertainty using an interval.

2.3.2.4 Passive robust approach

This thesis focuses on the adaptive thresholding passive robustness approach using ***interval models.*** The use of this type of models has received several names depending on the field of research: in circuit analysis is known as ***worst-case*** or ***tolerance analysis***, in automatic control as ***set-membership, bounding approach*** or ***robust.*** Nowadays, several research groups actually are following this approach. To the best of our knowledge these groups are:

- the group of University of Girona (UdG) (Armengol et al, 2000)
- the group of LAAS-Toulouse (Travé et al, 1997)
- the group of Technical University of Catalonia (UPC) (Puig et al, 1999), (Puig et al, 2000), (Puig et al, 2002a), (Puig et al, 2003a), (Puig et al, 2003b), (Puig et al, 2004a), (Puig et al, 2004b), (Puig et al, 2005a)
- and two groups of CRAN-Nancy (Adrot et al, 2000), (Ploix et al, 2000), (Hamelin et al, 2000), (Ploix et al., 2006)

The problem of adaptive threshold generation in discrete time-domain using interval models can be formulated mathematically as the need of computing at every time instant a system output estimation using an interval $[\hat{\boldsymbol{y}}(k)]$. This interval does only have to wrap the system output when this system is not affected by any fault. Therefore, while the system output interval estimation contains the system output, none fault will be indicated.

$$\boldsymbol{y}(k) \in [\hat{\boldsymbol{y}}(k)] \tag{2.23}$$

In general, this approach compares the system output ***y(k)*** with its interval estimation $[\hat{\boldsymbol{y}}(k)]$, provided by the interval model, computing at every time instant the interval residual [***r***(k)] as

$$[\boldsymbol{r}(k)] = \boldsymbol{y}(k) - [\hat{\boldsymbol{y}}(k)] \tag{2.24}$$

.Then, derived from Eq. (2.23) and Eq. (2.24), the *residual value evaluation stage* does not indicate any fault while

$$\boldsymbol{0} \in [\boldsymbol{r}(k)] \tag{2.25}$$

holds. Thereby, it can be said that the fault detection test is based on propagating the model uncertainty to the residual set (Puig et al 2002) and checking the value of the resultant interval residual according to Eq. (2.25). While the interval residual satisfies Eq. (2.25), no fault can be indicated since the residual value can be due to the model uncertainty. Of course, this approach has the drawback that those faults producing a residual deviation smaller than the residual uncertainty will be missed ("***non-detectable faults***").

When considering a discrete linear time-invariant interval model, there are two main approaches to calculate the system output estimation interval at every time instant: the ***set-based approach*** and the ***trajectory-based approach***. In the next section, these two methodologies are described describing different algorithms for each family and pointing out their drawbacks and strengths.

2.3.2.5 Interval observation using set and trajectory-based approaches

As mentioned in the previous section, passive robust fault detection based on intervals observers needs to compute at every time instant a system output estimation interval $[\hat{\boldsymbol{y}}(k)]$ which is used to obtain the residual interval [***r***(k)] (Eq. (2.24)) required by the *residual value evaluation stage* in order to indicate or not the presence of a fault (Eq. (2.25)) and to generate the corresponding fault signals. Thereby, when considering a discrete linear time-invariant interval model like the interval observer given by Eq. (2.10), there are two main approaches to calculate the system output interval estimation at every time instant: the ***set-based*** (or *region-based*) ***approach*** and the ***trajectory-based approach***. In this section, these two methodologies are described showing different algorithms for each family and pointing out the drawbacks and strengths of both approaches.

In general, the exact set produced by an interval observer (Eq. (2.10)) of the characteristics mentioned previously will require a big effort in order to be calculated using a computer (Adrot et al, 2003) and normally, it is approximated by, for example, a box, a polytope or an ellipsoid. Then, this type of ***simulation or state observation*** is known as ***set-membership*** but when the calculated set is the interval hull of the exact set, then, it is called ***interval simulation or state observation*** (Puig et al, 2005c). In the literature, algorithms can be classified according to if they compute the approximate set of estimated states using one step-ahead iteration based on previous approximate sets (***set-based approaches***)(Adrot et al, 2003; El Ghaoui et al, 1999; Puig et al, 2001), or a set of point-wise trajectories generated by selecting particular values of the observer interval parameter vector $\boldsymbol{\theta}$ using heuristics or optimisation (***trajectory-based approaches***) (Puig et al, 2002b; Puig et al, 2003b; Tibken et al, 1993). In the first case, the set of states $\boldsymbol{X}(k)$ is approximated at each iteration and some propagation algorithm is used to produce the approximate set of states $\boldsymbol{X}(k+1)$. This approach is affected by several problems (specially, in case that the approximate set is

the interval hull): ***wrapping effect***, ***range evaluation*** of an interval function (in this case, the state-space function) and the ***uncertain parameter time dependency***. However, in the second case, the interval hull of $\boldsymbol{X}(k)$ is built following real trajectories generated by selecting particular values of $\boldsymbol{\theta}$. Consequently, this approach overcomes the wrapping effect and preserves the uncertain parameter time dependency, but the problem of the interval function (in this case the trajectory function $\boldsymbol{x}(k,\boldsymbol{u},\boldsymbol{y},\boldsymbol{x_o},\boldsymbol{\theta})$) range evaluation still remains. On the other hand, set-based approaches present a lower computationally complexity than trajectory-based approaches do and consequently, they seems to be more suitable for real-time applications.

2.3.2.5.1 Interval observation

According to (Puig et al, 2005a), the ***interval observation problem*** regarding the computation of the system output estimation interval can be established in the same way than the ***interval simulation problem*** presented in (Puig et al 2003b). This can be done since an interval observer can be seen as an interval simulator with two inputs: ***u(k)*** and ***y(k)***. Thus, considering this point of view and the observer Eq. (2.10), the interval observer can be reorganised as:

$$\begin{aligned}\hat{\boldsymbol{x}}(k+1) &= \left(\boldsymbol{A}(\boldsymbol{\theta})-\boldsymbol{L}\boldsymbol{C}(\boldsymbol{\theta})\right)\hat{\boldsymbol{x}}(k)+\begin{bmatrix}\boldsymbol{B}(\boldsymbol{\theta}) & \boldsymbol{L}\end{bmatrix}\begin{bmatrix}\boldsymbol{u}(k)\\ \boldsymbol{y}(k)\end{bmatrix} = \boldsymbol{A}_o(\boldsymbol{\theta})\hat{\boldsymbol{x}}(k)+\boldsymbol{B}_o(\boldsymbol{\theta})\boldsymbol{u}_*(k)\\ \hat{\boldsymbol{y}}(k) &= \boldsymbol{C}(\boldsymbol{\theta})\hat{\boldsymbol{x}}(k)\end{aligned} \tag{2.26}$$

where $\boldsymbol{A}_o(\boldsymbol{\theta})=\boldsymbol{A}(\boldsymbol{\theta})-\boldsymbol{L}\boldsymbol{C}(\boldsymbol{\theta})$ is the state-space observer matrix, $\boldsymbol{B}_o(\boldsymbol{\theta})=\begin{bmatrix}\boldsymbol{B}(\boldsymbol{\theta}) & \boldsymbol{L}\end{bmatrix}$ is the resultant input matrix, $\boldsymbol{u}_*(k)=\begin{bmatrix}\boldsymbol{u}(k) & \boldsymbol{y}(k)\end{bmatrix}^T$, the resultant input and $\boldsymbol{\theta}\in\boldsymbol{\Theta}$ is a set of time-invariant model parameters bounded by an interval set $\boldsymbol{\Theta}=\left\{\boldsymbol{\theta}\in\Re^{n\theta}\middle|\underline{\theta}_i\le\theta_i\le\overline{\theta}_i, i=1,\cdots,n\theta\right\}$ which represents the uncertainty about the exact knowledge of real system parameters. In consequence, derived from the interval observer structure shown by Eq. (2.26), the observer gain matrix $\boldsymbol{L}$ must be designed to stabilise matrix $\boldsymbol{A_o}$ instead of matrix $\boldsymbol{A}$ and to guarantee a desired performance regarding fault detection for all $\boldsymbol{\theta}\in\boldsymbol{\Theta}$, as mentioned previously.

In line with (Puig et al, 2005a), the ***solution set*** of a system which can be described by the interval observer (2.26) for the time interval *[0,N]* consists of $\hat{\boldsymbol{X}}(0,N)=\left\{\hat{\boldsymbol{x}}(k,\boldsymbol{u},\boldsymbol{y},\hat{\boldsymbol{x}}_o,\boldsymbol{\theta}):k\in[0,N],\ \boldsymbol{\theta}\in\boldsymbol{\Theta},\hat{\boldsymbol{x}}_o\in\hat{\boldsymbol{X}}_o\right\}$, where $\hat{\boldsymbol{x}}(k,\boldsymbol{u},\boldsymbol{y},\boldsymbol{\theta},\hat{\boldsymbol{x}}_o)$ denotes the solution of (2.26) at time *k* for some parameter vector $\boldsymbol{\theta}\in\boldsymbol{\Theta}$ and some initial condition $\hat{\boldsymbol{x}}_o\in\hat{\boldsymbol{X}}_o$ at time *k=0*. The set of values for a certain time instant *k* will be referred as the ***reachability* set** and denoted by

$$\hat{\boldsymbol{X}}(k)=\left\{\hat{\boldsymbol{x}}(k,\boldsymbol{u},\boldsymbol{y},\hat{\boldsymbol{x}}_o,\boldsymbol{\theta}):\boldsymbol{\theta}\in\boldsymbol{\Theta},\hat{\boldsymbol{x}}_o\in\hat{\boldsymbol{X}}_o\right\} \tag{2.27}$$

Thus, given the observer gain matrix $\boldsymbol{L}$ guaranties the model stability for all $\boldsymbol{\theta}\in\boldsymbol{\Theta}$, the reachability set $\hat{\boldsymbol{X}}(k)$ will be bounded by region for each $k\in[0,\infty)$.

Then, the interval observation problem consists in computing the interval hull of the reachability set $\hat{\boldsymbol{X}}(k)$, i.e., the smallest interval vector containing it: $\hat{\boldsymbol{X}}(k)\subseteq\square\hat{\boldsymbol{X}}(k)$, where □ is used to denote the ***interval hull*** of $\hat{\boldsymbol{X}}(k)$, for all $k\in[0,N]$. The sequence of interval vectors $\square\hat{\boldsymbol{X}}(k)$ with $k\in[0,N]$ will be called the ***interval solution*** (or *envelopes*) of the interval observer.

2.3.2.5.2 Interval observation drawbacks

When the interval observation approach is used in fault detection and isolation, several drawbacks must be taken into account. In general, they a related to the type of algorithm applied to compute at every time instant the system output

estimation interval and the corresponding residual. In the following, these drawbacks are described analysing how they can be avoided tuning properly the interval observer model.

(a) Wrapping effect

The wrapping problem is related to the use of a crude approximation of the interval observer solution set and its iteration using one-step ahead recursion of the state-space observer function, *i.e*, a ***region based approach***. This problem does not appear when the estimated trajectory function $\hat{\boldsymbol{x}}(k,\boldsymbol{u},\boldsymbol{y},\boldsymbol{\theta})$, *i.e.*, a ***trajectory based approach,*** is used. On the other hand, when using the one-step ahead recursion approach, at each iteration, the true solution set $\hat{\boldsymbol{X}}(k)$ is wrapped into a superset feasible to construct and to represent the real region on a computer (in this paper, its interval hull $\square\,\hat{\boldsymbol{X}}(k)$). Since the overestimation of the wrapped set is proportional to its radius, a spurious growth of the enclosures can result if the composition of wrapping and mapping is iterated (Kühn, 1998). This ***wrapping effect*** can be completely unrelated to the stability characteristics of the observer, and even stable observers could exhibit exponentially fast growing envelopes which are useless for practical purposes. Not all the interval observers are affected by this problem. It has been shown that those that are monotone with respect to states do not present this problem. These kinds of observers (systems) are known as ***isotonic*** (Cugueró et al, 2002) or ***cooperative*** (Gouzé et al, 2000). In case of observers whose state function is a contractive mapping (see *definition 2*), the overestimation of the wrapped set does not increase along the time (Puig et al, 2003a).

Definition 1 ("*isotonicity property*"): *A discrete-time system satisfies the isotonicity property if the variation of the state function respects all the states and parameters is positive* (Cugueró et al, 2002).

Definition 2 ("*contractivity property*"): *A function* $\boldsymbol{f}:\Re^n \longrightarrow \Re^n$ *is a contraction mapping if there is a number s, with 0<s<1, so that for any vectors* $\boldsymbol{x}$ *and* $\boldsymbol{y}$ *it is satisfied that* $d(f(\boldsymbol{x}),f(\boldsymbol{y})) \le sd(\boldsymbol{x},\boldsymbol{y})$ *where d(x,y) is the diameter function and* $\boldsymbol{s}$ *is the contractivity. When linear functions of the type* $\boldsymbol{f=Ax}$ *are considered,* $\|\boldsymbol{A}\|_\infty = s$

According to the isotonicity and contractivity characteristics defined previously, a stable ($\rho(\boldsymbol{A})<1$, where $\rho(\boldsymbol{A})$ is the spectral radius[1]) interval discrete-time system can be classified in 3 categories regarding the wrapping behavior:

- ***Isotonic systems***: When the isotonicity property is achieved or in other words, all $\boldsymbol{A}(\boldsymbol{\theta})$ matrix elements are positive. In this case, region and trajectory based algorithms obtain the same estimation of states.
- ***Non-isotonic but contractive systems***: Although isotonicity is not achieved, the state matrix is a contractive mapping

$$\|\boldsymbol{A}\|_\infty < 1 \tag{2.28}$$

  and consequently, the state estimation suffers from wrapping effect when the region based approach is used but because of the contractivity property, the state overestimation does not increase in time: *stable wrapping effect*.
- ***Non-isotonic and non-contractive systems***: In spite of the system stability, the state estimation when using region based approach is unstable and consequently, a fast growing of the enclosures appears. In this case, trajectory based approach must be used, in spite of its high complexity.

Comparing the enclosures produced by previous systems when using the region-based approach, the next relation is set:

Isotonicity (without wrapping) $\subset$ *Contractivity (with stable wrapping)* $\subset$ *Stability (with instable wrapping).*

[1] The spectral radius of a given matrix is the maximum absolute value of all the eigenvalues of this matrix.

(b) Temporal variance on uncertain parameters

An additional issue should be taken into account when an interval observer is used: uncertain parameter time-invariance is not naturally preserved using one-step ahead recursion algorithms. If one-step recursion scheme is used (ElGhaoui et al, 1999), the system state set $\boldsymbol{X(k+1)}$ is approximated by a set computed using a previous set which is an approximation of the system state region $\boldsymbol{X(k)}$ and using the uncertain parameter set $\boldsymbol{\Theta}$. Then, the relation between parameters and states is not preserved since every parameter contained in the parameter uncertainty region $\boldsymbol{\Theta}$ is combined with every state of the $\boldsymbol{X(k)}$ approximation set when determining the approximation set of $\boldsymbol{X(k+1)}$. Thus, recursive schemes based on one-step are intrinsically time varying. Parameter time-invariance can only be guaranteed if the relation between parameters and states is preserved at every time instant. One possibility to preserve this dependence is to derive a functional relation between states and parameters at every time instant that will transport the system from the initial state to the present state. Then, two approaches about the assumption of the time-variance of the uncertain parameters are possible:

- the ***time-varying approach*** which assumes that uncertain parameters are unknown but bounded in their uncertainty intervals and can vary at each time step since one-step ahead recursion algorithms are used. This is the approach followed by (ElGhaoui et al, 1999) and (Puig et al, 2001), among others.

- the ***time-invariant approach*** which assumes that uncertain parameters are unknown but bounded in their uncertainty intervals and guarantee that they can not vary at each time step since a functional relation between parameters and states is used instead of a one-step ahead recursion. This is the approach followed by (Tibken, 1993), (Horak et al, 1988) and (Puig et al, 1999), among others.

Although the *set-based* (*region-based*) algorithms belong to the *time-varying approach*, the parameter and state relation is preserved at every time instant when monitoring an isotonic system. This statement is guaranteed by the interval arithmetic. Then, if a system is not isotonic, an isotonic observer might be used in order to avoid this problem and thereby, the system output interval estimation could be computed using a set-based approach which has a low computational complexity.

(c) Range evaluation of an interval function

When predicting the behaviour of a dynamic system with an interval observer, the need to evaluate the interval hull of the system state interval estimation at each time step implies the computation of the range of an interval function. Many approaches to interval observation need to evaluate the range of an interval function at every time instant in order to determine the system state interval estimation. One possibility for evaluating this range is to apply directly ***interval arithmetic*** substituting operations between real numbers by operations between intervals (Moore, 1966). But, although the ranges of basic interval arithmetic operations are exactly the ranges of the corresponding real operations, this is not the case if the operations are composed since multi instances of the same variable are not taken into account. For instance: allow to us consider $x \in [-1,1]$, then the interval for $z = x - x$ should be 0, but when applying interval arithmetic it is $[-2,2]$. This phenomenon is termed as ***interval dependence*** or ***multi-incidence problem*** (Moore,1966). One possibility to avoid this problem is to combine the use of interval arithmetic with a branch and bound algorithm (Hansen, 1992). Another possibility to evaluate the range of an interval function is to solve two optimisation problems (a minimisation and a maximisation) using numerical methods. But, classical numerical optimisation algorithms can only guarantee ***local optimums*** since they are gradient based. Global

optimums can only be obtained if the optimisation problems associated with the range evaluation are convex (Bazaraa, 1993). However, in general, to guarantee global optimums in non-convex optimisation problems, global optimisation algorithms based on branch and bound should be used (Puig et al., 1999).

Lastly, derived from the interval arithmetic properties, this problem only has an effect on those *non-isotonic models* which are computed using a *set-based algorithm*. As analyzed above, when computing isotonic models using a set-based approach, the relation between parameters and states is preserved and consequently, this interval function range evaluation problem also vanishes. Then, when the monitored system is not isotonic, the use of an isotonic observer allows avoiding the range evaluation problem in spite of using the set-based approach.

2.3.2.5.3 Set-based approaches to interval observation

One of the first approaches to compute a estimation of the system state region ***X(k+1)*** using a set-based method was set by (Moore, 1966). This algorithm, when applied to a linear discrete-time interval model as (2.26), computes the system state interval estimation $[\hat{\boldsymbol{x}}(k+1)]$ at time instant *k+1* using as initial condition the system state interval estimation $[\hat{\boldsymbol{x}}(k)]$ at time instant *k*. It is based on computing the natural interval extension of the state-space function by replacing each occurrence of $\hat{\boldsymbol{x}}(k)$ and $\boldsymbol{\theta}$ by its corresponding interval and each standard function by its interval evaluation (***absolute algorithm***) (Moore, 1966):

$$[\hat{\boldsymbol{x}}(k+1)] = \boldsymbol{A}_o([\boldsymbol{\theta}])[\hat{\boldsymbol{x}}(k)] + \boldsymbol{B}_o([\boldsymbol{\theta}])\boldsymbol{u}_*(k) \tag{2.29}$$

However, as explained in *Section 2.3.2.5.2,* replacing real numbers in a function by intervals often leads to large overestimations that derive in a system state interval estimation $[\hat{\boldsymbol{x}}(k+1)]$ which always increases its value, even if the true solution contracts. A better approach is to apply the interval ***mean-value theorem*** (Moore, 1966) to equation (2.29) (***relative algorithm***):

$$[\hat{\boldsymbol{x}}(k+1)] = \hat{\boldsymbol{x}}_c(k+1) + \boldsymbol{A}_o([\boldsymbol{\theta}])\left([\hat{\boldsymbol{x}}(k)] - \hat{\boldsymbol{x}}_c(k)\right) \tag{2.30}$$

where

$$\hat{\boldsymbol{x}}_c(k+1) = \boldsymbol{A}_o(\hat{\boldsymbol{\theta}})\hat{\boldsymbol{x}}_c(k) + \boldsymbol{B}_o(\hat{\boldsymbol{\theta}})\boldsymbol{u}_*(k) \tag{2.31}$$

with $\hat{\boldsymbol{x}}_c(k+1)$, $\hat{\boldsymbol{x}}_c(k)$ and $\hat{\boldsymbol{\theta}}$ being the mid-points of the intervals $[\hat{\boldsymbol{x}}(k+1)]$, $[\hat{\boldsymbol{x}}(k)]$ and $[\boldsymbol{\theta}]$, respectively.

However, this method suffers from the wrapping effect when the observer matrix $\boldsymbol{A_o}$ is not isotonic or this matrix is ill-conditioned, as for example, those ones with eigenvalues with very different magnitudes (Nedialkov et al, 2001). Otherwise, when the observer matrix $\boldsymbol{A_o}$ is isotonic, the Moore's absolute algorithm can be used to calculate the system state interval estimation avoiding the mentioned overestimations what results in a very low demanding computational method.

In those cases where Moore's algorithm is ill-conditioned, the set-based approach given by (Lohner, 1987) can be used.. Lohner's algorithm can avoid the wrapping effect in many systems but (Kühn, 1998) has discovered some cases where this approach fails.

2.3.2.5.4 Trajectory-based approaches to interval observation

Concerning the trajectory-based approach used to compute a estimation of the system state region ***X(k+1)***, a suitable method is given by (Puig et al, 2002b). This method sets that the observer state region $\hat{\boldsymbol{X}}(k)$ will be bounded at any time instant *k* by its interval hull $\square\hat{\boldsymbol{X}}(k) = \left[\underline{\hat{\boldsymbol{x}}}(k), \overline{\hat{\boldsymbol{x}}}(k)\right]$ where:

$$\overline{\hat{\boldsymbol{x}}}(k) = max\left[\boldsymbol{A}_o^k(\boldsymbol{\theta})\hat{\boldsymbol{x}}(0) + \sum_{v=0}^{k-1} \boldsymbol{A}_o^{k-1-v}(\boldsymbol{\theta})\boldsymbol{B}_o(\boldsymbol{\theta})\boldsymbol{u}_*(v) \right] \tag{2.32}$$

$$\underline{\hat{\boldsymbol{x}}}(k) = min\left[\boldsymbol{A}_o^k(\boldsymbol{\theta})\hat{\boldsymbol{x}}(0) + \sum_{v=0}^{k-1} \boldsymbol{A}_o^{k-1-v}(\boldsymbol{\theta})\boldsymbol{B}_o(\boldsymbol{\theta})\boldsymbol{u}_*(v) \right] \tag{2.33}$$

subject to $\boldsymbol{\theta} \in \boldsymbol{\Theta}$ and $\hat{\boldsymbol{x}}_o \in \hat{\boldsymbol{X}}_0$ and assuming time-invariant uncertain parameters: this method is known as a ***time-invariant approach***. At the same time that time invariance is preserved, the wrapping effect is avoided due to the fact that uncertainty is not propagated from step to step but from the initial state. This approach yields the accurate time-invariant worst-case observation without any conservatism, assuming that the previous optimisation problems could be solved with infinite precision and the global optimum could be determined. However, in practice it only could be solved with a given precision. On the other hand, one of the main drawbacks of this approach, besides its high computational complexity, is that the objective function is a polynomial with degree increasing by one at each iteration. As a result, the amount of needed computation increases with time being impossible to operate over a large time interval. Consequently, some kind of approximation should be introduced to make the approach more tractable. If the observer given by Eq. (2.26) is asymptotically stable, any transients settle to negligible values in a finite-time, more precisely in t_s/T_s samples, being t_s the observer settling time and T_s the sampling time. This assumption implies that the outputs of the observer at time k depend only on the inputs that occurred during the last t_s/T_s samples. Therefore, for any time k, it is possible to approximate algorithm given by Eq. (2.32) and Eq. (2.33) using a sliding window of length λ determined by the order of the settling time measured in number of samples (Puig et al, 2003b):

$$\overline{\hat{\boldsymbol{x}}}(k) = max\left[\boldsymbol{A}_o^{\lambda}(\boldsymbol{\theta})\hat{\boldsymbol{x}}(k-\lambda) + \sum_{v=k-\lambda}^{k-1} \boldsymbol{A}_o^{k-1-v}(\boldsymbol{\theta})\boldsymbol{B}_o(\boldsymbol{\theta})\boldsymbol{u}_*(v) \right] \tag{2.34}$$

$$\underline{\hat{\boldsymbol{x}}}(k) = min\left[\boldsymbol{A}_o^{\lambda}(\boldsymbol{\theta})\hat{\boldsymbol{x}}(k-\lambda) + \sum_{v=k-\lambda}^{k-1} \boldsymbol{A}_o^{k-1-v}(\boldsymbol{\theta})\boldsymbol{B}_o(\boldsymbol{\theta})\boldsymbol{u}_*(v) \right] \tag{2.35}$$

subject to: $\boldsymbol{\theta} \in \boldsymbol{\Theta}$ and $\hat{\boldsymbol{x}}(k-\lambda) \in \square\hat{\boldsymbol{X}}(k-\lambda)$.

Of course, with this approximation parameter time-invariance is only guaranteed inside the sliding window. This is why this approach is called ***almost time-invariant*** (Puig et al, 2002b).

Another trajectory-based approach is the proposed by (Kolev et al, 1993). This method suggests an algorithm that provides an ***inner solution*** for the interval observation problem by solving the optimisation problems given by Eq. (2.34) and Eq. (2.35) involved in the previous algorithm but subject to: $\boldsymbol{\theta} \in V(\boldsymbol{\Theta})$ and $\hat{\boldsymbol{x}}_o \in V(\hat{\boldsymbol{X}}_o)$ where: $V(\boldsymbol{\Theta})$ and $V(\hat{\boldsymbol{X}}_o)$ denotes the set of vertices of the uncertain parameters and initial states sets, respectively. Thus, this algorithm is also known as a ***vertices algorithm***. According to Nickel (Nickel, 1985), the inner solution coincides with the interval hull of the solution set for some systems: those unaffected by the wrapping effect that verify their state function is ***isotonic*** with respect to all state variables (Cuguero et al, 2002). For such systems, set and trajectory-based approaches will provide the same results.

2.3.2.5.5 Avoiding the wrapping effect using interval observation

According to (Cugueró et al, 2002) and as mentioned in *Section 2.3.2.5.2*, the wrapping effect affects to those interval models which are not isotonic since there are some elements of their model state-space matrix which are negative. Thus, when modelling a non-isotonic interval system using the interval observation approach, an isotonic interval observer (Eq. (2.26)) could be obtained designing the observer gain matrix $\boldsymbol{L}$ so that its state-space matrix $\boldsymbol{A_o}$ becomes isotonic in spite of the non-isotonicity of system state-space matrix $\boldsymbol{A}$.

As a consequence of using an isotonic interval observer, a simple iterative scheme as Moore's algorithm will work providing the same results than Puig's algorithm starting from the initial state (*i.e*, infinite window length). That means, the optimisation problem given by Eq. (2.32) and Eq. (2.33) can be simplified since computations do not have to be referred to the initial state but only to the previous iteration (*i.e*, window length $\lambda=1$). Such equivalence establishes that in case isotonicity condition is fulfilled, set and trajectory-based approaches to interval observation produce the same results, as mentioned above.

Additionally, as stated in *Section 2.3.2.5.2,* considering either a trajectory or set-based approach to interval observation, parameter time-invariance is or is not, respectively, preserved. In (Cugueró et al, 2001), the relation between the observations produced preserving or not preserving the uncertain parameter time-invariance for the same interval observer is presented. In particular, it is established that $IO_{\text{invariant}} \subseteq IO_{\text{varying}}$ where: *IO* means interval observation. This means that an interval observer modelling an uncertain time-invariant system using the parameter time-varying approach can be very conservative. However, in case an isotonic discrete-time observer, a set-based (therefore time-varying) interval observation, based on one-step recursion, and a trajectory based (therefore time-invariant) interval observation, based on the recursion given by Eq. (2.32) and Eq. (2.33) or on a Kolev's algorithm, will provide the same system state interval estimation (Cugueró et al, 2002). Consequently, in this case, not preserving the relation between parameters and states is not important at all.

This thesis will focus on the conditions the observer gain matrix $\boldsymbol{L}$ must fulfil so that the interval observer becomes isotonic and the wrapping effect can be avoided when using a set-based approach (*Moore's algorithm*) whose computational cost is lower than the corresponding one to the trajectory-based approaches. Moreover, in this thesis, the effect of those observer gains conditions on the interval observer fault detection performance will also be analyzed.

2.3.2.6 Fault detection problems using interval observers

As mentioned in *Section 2.3.2.3*, the residual generator (Eq. (2.6)) obtained using an interval observer approach can have appealing fault detection properties if the observer matrix $\boldsymbol{L}$ is designed properly. This fact is due to the influence of $\boldsymbol{L}$ on the transfer function $\boldsymbol{O}(q^{-1})$, such as it is seen in Eq. (2.18), which sets the model fault detection and fault isolation properties, according to (Gertler, 1998). Conversely, when an interval observer is used to detect and isolate faults, it is known that there are some problems which can affect negatively its performance. Those problems related to the computation at every time instant *k* of the system state estimation interval were already exposed in *Section 2.3.2.5*: *wrapping effect*, *temporal variance on uncertain parameters* and *Range evaluation of an interval function*, where the last two problems can be referred as a ***computational complexity problem***. In that section, it was said that designing the observer gain matrix $\boldsymbol{L}$ so that the interval observer becomes isotonic, those problems can be obviated.

Moreover, interval observation, understood as a general approach which contains both prediction and simulation, also suffers from other kind of problems whose nature affects directly to the quality of fault indication given by the observer:

- **Modelling error and initial condition sensitivity.** The simulation approach is very sensitive to the non-modelled dynamics and the unknown initial conditions. As a result, it tends to diverge very easily, especially if the monitored system contains integrators. Nevertheless, observers and predictors avoid this problem using the system output measurement to correct their estimations.

- **Following fault effect.** This problem appears when the model can not persistently indicate a fault and it is due to the use of the system output measurement to correct the model system output estimation. In this case, the model system output estimation tends to follow the system output and consequently, the expressions (2.23) and (2.25) can be satisfied in spite of the fault existence and as a result, the residual value evaluation stage can no longer indicate the fault. This problem is only avoided when using the simulation approach. However, observers can partially control this effect using a proper observer gain matrix $\boldsymbol{L}$. Conversely, predictors are deeply affected because they use the whole system output measurement and its fault indication can only last a number of time instants equal to its order.
- **Noise sensitivity.** The prediction approach is very sensitive to noise because it substitutes the estimation of the system state by its measurement. Conversely, the observation approach is less noise sensitive because its system state estimation is partially corrected using the system output measurement and this correction is controlled by the value of the observer gain matrix $\boldsymbol{L}$. Finally, the simulation approach is the most insensitive of the three approaches to the noise effect because no correction of the estimated state is introduced. To deal with noise, approaches based on statistical tests can be used, as in the case of the classical fault detection methodologies based on numbers instead of intervals. (Basseville, 1993). Another approach to deal with noise can be designing properly the observer gain matrix such as suggested by the ***Kalman filter*** method.

One of the goals of this thesis is to analyze the influence of the observer gain matrix on the observer fault detection performance in order to find out if the influence of these negative problems can be avoided designing properly this matrix or if their influence on the observer fault detection and isolation performance can partially be filtered out. *Table 2.1* shows the effect of those problems on the different fault detection approaches without taking into account the benefits of a proper observer gain matrix design.

Problem	**Simulation**	**Observation**	**Prediction**
Wrapping Effect	Yes	Yes	No
Computational Complexity	High	High	Low
Model Error Sensitivity	High	Medium	Low
Initial Condition Sensitivity	High	Medium	Low
Following Faults	No	Yes	Yes
Noise Sensitivity	Low	Medium	High

Table 2.1 Interval-based fault detection problems and their influence on simulation, observation and prediction

In practice, concerning passive robustness fault detection, the interval observer method is the most used approach since observers are less model error sensitive than simulators and less noise sensitive than predictors. Regarding the fault following effect, observers show a rather better behaviour than predictors. Moreover, observers can avoid partially this effect when using a proper observation gain. In relation to the wrapping effect and the complexity associated with the computation of the system output interval estimation, last years the research of adaptive thresholding algorithms which use interval models for fault detection and isolation has been a very active research area (Puig et al, 2002a). In (Puig et al, 2003a), interval observation applied to robust fault detection was introduced while an interval simulation algorithm based on a optimization approach was proposed in (Puig et al, 2003b) to compute the system output interval estimation. Nevertheless, this algorithm uses a trajectory-based approach resulting in a high computational complexity. A goal of this thesis is to determine those conditions that the observer

gain matrix must fulfil so that the wrapping effect can be avoided and as a result, less computational cost (set-based) approaches as the *Moore's algorithm* could be used. Moreover, the effect of these conditions on the observer fault detection performance will also be analyzed in order to see how it is affected.

2.4 Fault isolation using system models

According to (Venkatasubrarnanian et al., 2003a), model-based fault isolation has been approached over the last two decades from two different scientific communities: Artificial Intelligence, also known as the ***DX approach*** (Hamscher et al, 1992) (Reiter, 1987), and Automatic Control, also known as ***FDI approach*** (Blanke et al, 2003)(Gertler, 1998)(Patton et al, 2000). The *DX approach* relies upon a well-founded and logically based theory for diagnosis of static systems. From a logical point of view, fault detection is performed through a consistency-check and organized around the *conflict concept* (*fault signal*). In this approach, fault localization or isolation is automatically derived from the conflict detection stage, which usually relies upon some kind of dependency-recording. On the other hand, the *FDI approach* considers fault diagnosis as two separate tasks: fault detection and fault isolation based on generating and evaluating a set of analytical redundancy relations obtained off-line from elementary component models of the physical systems.

Fault detection has traditionally been more deeply investigated in the *FDI community* using a broad set of techniques (*parity equations*, *observers* and *parameter estimation*) and looking at the nuisance effects of noise, perturbations and model uncertainty (*robust fault detection*) (Chen et al, 1999). Conversely, *fault isolation* has been more deeply investigated in the *DX community* thanks to the logical diagnosis theory developed by Reiter (Reiter, 1987). However, when this theory has been applied to dynamical systems, some problems have appeared which prevent to use it directly. In fact, the theoretical formalization for fault diagnosis applied to dynamic systems is nowadays an open issue (Kleer et al, 2003). These problems have motivated further research on analysing off-line the set of dependencies which could become conflicts (*fault signals*) as in the *FDI approach* (Pulido et al, 2002), based on the common framework provided by (Cordier et al, 2000).

According to (Kościelny et al., 2004), fault isolation is carried out on the basis of fault signals, ϕ, generated by the detection module. Thus, the result of fault isolation consists in showing the faults affecting to the system, what requires knowing the relationship that exists between the fault signals, ϕ, and the faults, $\boldsymbol{f}$. A completely reliable and unequivocal presentation of the existing faults or the definition of the diagnosed system state is not always possible due to incomplete and uncertain knowledge of the system, limited distinguishability of faults or states, uncertainty of fault signals, etc.

In general, the following kinds of fault signals are applied as input signals of the fault isolation module or the system state recognition process (Kościelny et al., 2004):

- residuals generated using the system models,
- binary or multi-value signals created as a result of residual value evaluation,
- binary or multi-value signals (features) generated with the use of classical and heuristic fault detection methods,
- statistic parameters that describe random signal properties,
- process variables, i.e., measured or calculated values of physical quantities.

2.4.1 Models applied to fault isolation

Models applied to fault isolation or system state recognition should therefore map the space of fault signals ϕ into the discrete space of faults $\boldsymbol{f}$ ($\phi \rightarrow \boldsymbol{f}$)

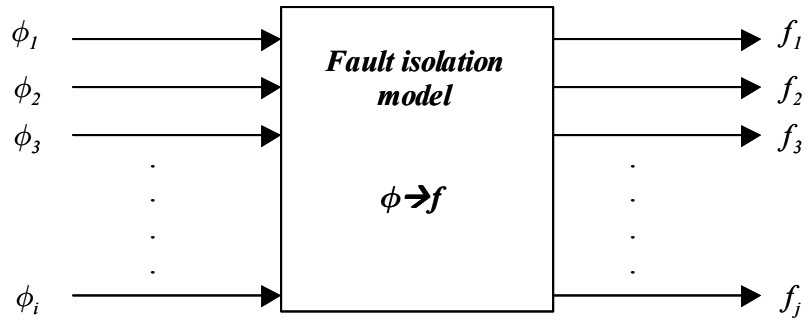

Fig. 2.5 Fault isolation model mapping fault signals and faults

In fault isolation, it is possible to point out the following kind of models (Kościelny et al., 2004):

- models that map the space of binary fault signals into the space of faults,
- models that map the space of multi-value fault signals into the space of faults,
- models that map the space of continuous fault signals into space of faults.

The above models can be defined using different techniques: training, knowledge about the hardware redundant structure, modelling the influence of faults on residual values or the expert's knowledge.

Training data for the state of complete efficiency and for all of the states with faults, or at least a definition of the fault states are necessary in the case of applying the training procedure. However, such data are difficult and often impossible to obtain in the case of the industrial process diagnostics.

Conversely, it is relatively easy to define the relationship that exists between fault signal values when using a hardware redundant structure in the diagnosed system. Nevertheless, such a solution is very rarely applied due to its high costs.

If equations for the generation of residuals that contain the effect of faults are known, then it is possible to define residual value ranges as well as fault signal values that correspond to residuals for the state without faults and for the states with faults. Thereby, sets of fault signal values are obtained for particular faults and for the state of complete efficiency. These sets define specific regions in the space of fault signals. This method requires a mathematical description of the system which must allow deriving the effect of faults on the residuals or fault signals.

Another method consists in using an expert's knowledge. The expert should define fault signal values that correspond to particular faults. As a result, fault signal space regions that correspond to states with single faults and to the non-faulty state are arbitrarily defined.

2.4.1.1 Models mapping the space of binary fault signals into the space of faults

Binary fault signals $\phi_i \in \{0,1\}$ are obtained as a result of a two-value evaluation of residuals or process variable value features. They are also generated as a result of implementing tests which consist in controlling limits or examining the heuristic relationships existing among process variables. In this model group, it is possible to single out the following models:

(a) Binary diagnostic matrix

The model most often applied is a relation defined on the Cartesian product of the sets of faults $\boldsymbol{f} = \{f_j : j = 1,2,....,$ $n_f\}$ and fault signals $\boldsymbol{\phi} = \{\phi_i : i = 1,2,....n_\phi\}$:

$$\boldsymbol{FSM} \subset \boldsymbol{\phi} \; x \; \boldsymbol{f} \tag{2.36}$$

where ***FSM*** is the binary diagnostic matrix (Gertler, 1998; Kościelny, 2001; Cordier et al., 2000) which is also known in the ***FDI*** community as the ***theoretical fault signature matrix*** (Gertler, 1998). This matrix stores the binary influence of a given fault f_j (column of ***FSM***) on a given fault signal ϕ_i (row of ***FSM***). Thereby, if the element $\boldsymbol{FSM}_{ij}$ of this matrix is equal to *'1'*, it means the fault f_j causes the occurrence of the fault signal ϕ_i. Otherwise, when the fault f_j has no effect on the fault signal ϕ_i, the element $\boldsymbol{FSM}_{ij}$ is equal to *'0'*. Such as the ***FSM*** matrix is defined, its j^{th} –column contains the binary effect of fault f_j on the fault signal set ϕ. In consequence, this column is known as the theoretical fault signature of f_j.

This binary diagnostic matrix can be defined on the grounds of the residual equations which take into account the effect of faults.

(b) Diagnostic trees and graphs

The relationship that exists between faults and fault signals can be presented in the form of a binary tree that defines the method of diagnostic inference (Ulerich et al., 1988). The tree vertices correspond to fault signals (tests). Out of each of the vertices come out two branches corresponding to two values of the fault signal: the true and the false result of the test. A fault signal having a value that is analysed as the first one is the root of the tree.

Such a tree can be defined using the theoretical fault signature matrix ***FSM*** (Blanke et al, 2003), or directly on the basis of an expert's knowledge.

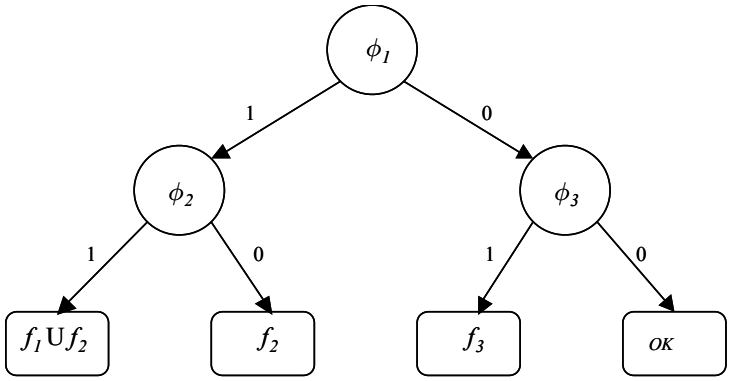

Fig. 2.6 Example of a diagnostic tree

(c) Rules and logic functions

According to (Kościelny et al., 2004), the relationship existing between faults and binary fault signals can be defined in the form of the following types:

$$\textbf{if } (\phi_1 = 0) \text{ and } \cdots \text{ and } (\phi_j = 1) \cdots \text{ and } (\phi_{n\phi} = 1) \textbf{ then fault } f_k \tag{2.37}$$

$$\textbf{if } (\phi_j = 1) \textbf{ then fault } f_\alpha \text{ or } \cdots \text{ or } f_k \text{ or } \cdots \text{ or } f_{nf} \tag{2.38}$$

Every column of the theoretical fault signature matrix ***FSM*** allow obtaining a rule of the type given by Eq. (2.37): this kind of rules is known as parallel reasoning and in general, they are used in the ***FDI*** approaches. Conversely, the rows of ***FSM*** allow defining rules of the type given by Eq. (2.38) which are known as series reasoning and usually they are used in ***DX*** approaches.

The logic function is the simplest possible relationship that exists between fault signals and faults. Binary fault signals act as input, and the result of this function shows the state of a particular fault, *i.e.*, its existence or absence. In a general case, such a function takes the following form:

$$z_{fk} = \left[\phi_a \vee \cdots \vee \phi_b\right] \wedge \left[\phi_i \vee \cdots \vee \phi_j\right] \wedge \cdots \wedge \left[\phi_m \vee \cdots \vee \phi_{n\phi}\right] \tag{2.39}$$

where z_{fk} is a the system binary state which indicates the occurrence of fault f_k: its value is *'1'* when f_k is isolated and *'0'* when it is not.

2.4.1.2 Models mapping the space of multi-value fault signals into the space of faults

Multi-value fault signals appear as a result of residual value or signal feature quantisation. They can also result from process variable limit control with the application of several limiting values. It is assumed that a different set of values $\boldsymbol{w_i}$ can correspond to each one of the fault signals ϕ_i. Thereby, models necessary for fault isolation using multi-value fault signals realise the following mapping (Kościelny et al., 2004):

$$\boldsymbol{\phi} \in \boldsymbol{w}_1 \text{ x} \cdots \text{ x } \boldsymbol{w}_i \text{ x} \cdots \text{ x } \boldsymbol{w}_{n\phi} \Rightarrow \boldsymbol{f} \in \{0,1\}_{nf} \tag{2.40}$$

It is possible to single out the following models belonging to this group: fault information systems, diagnostic trees and graphs, and if-then rules.

(a) Fault information system: FIS

This type of models derives from the information system models used in the set theory developed by (Pawlak, 1983) in the early 1980s. The fault information system models (***FIS***) were first introduced by (Kościelny, 2001) and they can be seen as an extension of binary theoretical fault signature matrix (***FSM***) where the values of its non-null elements are not a binary ones but they belong to the set of values $\boldsymbol{w_{ij}}$ for the fault signal ϕ_i and the fault f_j. This fact allows adding fault distinguishability when using these models in fault isolation.

According to (Kościelny, 2001), a fault information system ***FIS*** is defined as follows:

$$\boldsymbol{FIS} = \left\langle \boldsymbol{f}, \boldsymbol{\phi}, \boldsymbol{w}_\phi, \mu \right\rangle \tag{2.41}$$

where $\boldsymbol{w}_\phi$ is the set of values that contains all the values of the set $\boldsymbol{w_{ij}}$ associated with every couple $\left\langle \phi_i, f_j \right\rangle$:

$$\boldsymbol{w}_\phi = \bigcup_{i=1}^{n_\phi} \bigcup_{j=1}^{n_f} \boldsymbol{w}_{ij} \tag{2.42}$$

Regarding μ, this is a function defined as

$$\mu : \boldsymbol{\phi} \text{ x } \boldsymbol{f} \rightarrow \boldsymbol{w}_\phi \tag{2.43}$$

that determines for every couple $\left\langle \phi_i, f_j \right\rangle$, the corresponding set of values related to ϕ_i:

$$\mu(\phi_i, f_j) = \boldsymbol{w}_{ij} \tag{2.44}$$

Therefore, ***FIS*** is a table that defines fault signal pattern values for particular faults which has the following characteristics regarding the binary ***FSM***:

- an individual set of fault signal values can exist for each one of the fault signals:

- the set of the i^{th}-fault signal values can be a multi-value one;
- any element of the ***FIS*** can contain either one fault signal value or a subset of values.

(b) Other models

Mapping the space of multi-value fault signals into the space of faults or system states can also be represented in the form of a tree or *if-then*-type rules (Venkatasubrarnanian et al., 2003b). These diagnostic trees are a generalisation of the binary ones presented previously where the number of branches coming out of each node that corresponds to a fault signal equals the number of values that each one of the signals can have.
The relation existing between faults and fault signals values can be defined using expressions that normally have the following form:

$$\textbf{if } (\phi_1 \in \boldsymbol{w}_{1k}) \text{ and } \cdots \text{ and } (\phi_j \in \boldsymbol{w}_{jk}) \cdots \text{ and } (\phi_{n\phi} \in \boldsymbol{w}_{n\phi k}) \textbf{ then fault } f_k \tag{2.45}$$

$$\textbf{if } (\phi_j \in \boldsymbol{w}_{jk}) \textbf{ then fault } f_\alpha \text{ or } \cdots \text{ or } f_k \text{ or } \cdots \text{ or } f_{nf} \tag{2.46}$$

Thereby, rules of the form given by Eq, (2.45) can be derived from the columns of the ***FIS*** table, while rules of the form given by Eq. (2.46) correspond to the rows of this table.

2.4.1.3 Models mapping the space of continuous fault signals into the space of faults

Residuals obtained using system models generate continuous fault signals. In this case, models applied to fault isolation consider the following mapping:

$$\boldsymbol{\phi} \in \Re^{n\phi} \Rightarrow \boldsymbol{f} \in \{0,1\}_{nf} \tag{2.47}$$

Thereby, considering the space of continuous fault signals, the effect of a fault f_j on the fault signal set ϕ is defined by a region which should be characteristic of each fault so that a fault can be isolated.
Some methods used to model the mapping defined by Eq. (2.47) are: classic methods of pattern recognition, neural networks, and neural fuzzy networks.

(a) Pattern pictures

The construction of a model for fault isolation consists therefore in defining regions in the space of fault signals which constitute pattern pictures of faults. These regions can be defined in different ways. Thus, it is possible to single out geometrical, polynomial and statistical classifiers (Tadeusiewicz et al, 1991).
Pattern recognition can be obtained during the process of training. In order to achieve this, it is necessary to possess training data for all of faults. However, this is extremely difficult, and for many industrial systems even impossible. The data can be obtained by fault simulation with the use of the system analytical model that takes the effect of faults into account.

(b) Neural networks

Pattern recognition for particular faults can be mapped by a neural network. In early papers (Hoskins et al, 1988; Kramer et al, 1990; Sorsa et al, 1993), neural networks were applied to fault isolation. In this kind of model, residuals generated on the grounds of system models act as network inputs.

(c) Fuzzy neural networks

Fuzzy neural networks applied to fault isolation realise the fuzzy evaluation of residual values as well as diagnostic inference (Syfert et al, 2001). The structure of a fuzzy neural network applied to fault isolation differs from the structures used for system modelling. It contains no layer in which defuzzyfication is carried out. The number of network outputs equals the number of distinguished faults or system states.

2.4.2 Model-based fault isolation techniques

There are a high variety of isolation methods. (Isermann et al, 1996) distinguishes two basic groups: classification methods and automatic concluding methods. According to (Kościelny et al, 2004b), the fault isolation methods can be classified depending on how the knowledge about the relation between fault signals and faults is obtained. In line with this last criterion, (Kościelny et al, 2004b) signals out the following methods:

- Methods in which the diagnostic relation results from the structure of mathematical or qualitative models used for detecting faults. This approach can be divided into those methods that do not model the fault effect and those ones that do model it..
- Methods that require defining the relation between fault signals and faults during the training phase.
- Methods based on an expert's knowledge.
- Methods in which the relation between fault signals and faults results from a redundant hardware structure.

Concerning the relation between fault signals and faults, the following model-based fault isolation methods can be highlighted:

- Methods using different type of graphs (Thoma et at., 2000; Mosterman et al., 1995; Blanke et al, 2003).
- Methods using the binary diagnostic matrix (Gertler, 1998).
- Methods using the fault information system (Kościelny, 2001).
- Methods using fault-attributed regions in the space of fault signals (Gertler, 1998; Patton and Chen, 1991).
- Methods using neural networks (Hoskins et al, 1988; Kramer et al, 1990; Sorsa et al, 1993).
- Methods using fuzzy neural networks (Syfert et al, 2001).

The problems of choosing an adequate set of detection algorithms in order to ensure, among other things, the required distinguishability of faults will be dealt in the successive subsections.

2.4.2.1 General approaches to fault isolation

In this section, general fault isolation methods using the fault isolation models introduced in *Section 2.4.1* will be described.

2.4.2.1.1 Fault isolation based on the binary diagnostic matrix

As mentioned in *Section 2.4.1.1*, the binary diagnostic matrix ***FSM*** presents the relation existing between the values of binary fault signals ϕ and faults $\boldsymbol{f}$. It can be designed using system equations and taking the effect of faults into account or on the basis of an expert's knowledge. Fault isolation inference carried out by means of the binary diagnostic matrix can be realised with the use of classical (Gertler, 1998) or fuzzy logic (Kościelny et al, 2001). The latter approach allows taking fault signal uncertainty into consideration.

The binary diagnostic matrix is used for fault isolation together with different fault detection methods under the specification that the fault signals being the outputs of the fault detection algorithms have to be binary ones.

Such as it was *Section 2.4.1.1*, fault isolation methods using the binary fault isolation matrix can isolate faults comparing the value of the observed fault signals with the information stored in that matrix ***FSM***. Thereby, there are two main groups of fault isolation methods using a binary ***FSM*** matrix depending on how they carry out this comparison: parallel inference approach and series inference approach.

(a) Rules of parallel diagnostic inference on the assumption about single faults

Parallel diagnostic inference based on the binary diagnostic matrix consists in formulating a fault isolation result comparing the observed binary fault signals $\boldsymbol{\phi} = \{\phi_i : i = 1,2,....n_\phi\}$ where $\phi_i \in \{0,1\}$ with the theoretical fault signature associated with all considered fault hypotheses determined by the set $\boldsymbol{f} = \{f_j : j = 1,2,....n_f\}$ (Kościelny et al, 1995) (Gertler, 1998). Thereby, as mentioned in *Section 2.4.1.1*, it must be taken into account that the theoretical fault signature of the fault hypothesis f_j is stored in the j^{th}-column of matrix ***FSM*** where each element of this matrix $\boldsymbol{FSM}_{ij} \in \{0,1\}$.

Assuming that only a single fault exists, fault isolation is carried out using the set of observed fault signals $\boldsymbol{\phi}$. Thereby, the inference procedure consists in comparing the binary fault signals $\phi_i(k)$ computed at every time instant by the fault detection module with the theoretical binary fault signature related to every fault hypothesis f_j of the set $\boldsymbol{f}$ which is stored in the j^{th}-column of the binary matrix ***FSM***. If all fault signals are zero-valued, the fault isolation module shows a lack of faults:

$$\forall \phi_i \in \boldsymbol{\phi} : \ \phi_i = 0 \Rightarrow \boldsymbol{DGN} = \boldsymbol{0} \tag{2.48}$$

where ***DGN*** is the set of fault hypothesis $\boldsymbol{f_j}$ which are consistent with the observed fault signals.
When some fault signal values equal one according to the residual evaluation carried out by the fault detection module, the fault isolation algorithm gives as diagnosis result a subset of the fault hypothesis set $\boldsymbol{f}$ whose signatures are consistent with the observations:

$$\boldsymbol{DGN} = \left\{ f_j \in \boldsymbol{f} : \phi_i = \boldsymbol{FSM}_{ij}, \forall \phi_i \in \boldsymbol{\phi} \right\} \tag{2.49}$$

In case, using a robust fault detection approach based on interval models and according to *Section 2.3.2.3*, the binary value of every fault signal is computed as it follows:

$$\phi_i(k) = \begin{cases} 0 & y_i(k) \in [\hat{y}_i(k)] \\ \\ 1 & y_i(k) \notin [\hat{y}_i(k)] \end{cases} \tag{2.50}$$

Then, a general approach of carrying out the comparison between the observed fault signature $\phi(k)$ and the theoretical one related to every fault hypotheses is calculating the distance between both vectors: $\phi(k)$ and the j^{th}-column of matrix ***FSM*** for the hypothesis f_j, *e.g.* using the Hamming distance measurement. As a result of this comparison, a distance measurement $d_j(k)$ is obtained for every fault hypothesis f_j, being $\boldsymbol{d}(k)$ the vector of all the computed distances at time instant k: $\boldsymbol{d}(k) = \left[d_1(k), \cdots, d_j(k), \cdots, d_{nf}(k) \right]$. If the Hamming distance approach is applied, then

$$d_j(k) = \sum_{i=1}^{n\phi} (\boldsymbol{FSM}_{ij} \oplus \phi_i(k)) \tag{2.51}$$

where ⊕ is the XOR logic operator. Then, the fault hypotheses with the shortest distance regarding the current observed fault signature ϕ are considered as the fault isolation result:

$$\boldsymbol{DGN} = \left\{ f_j \in \boldsymbol{f} : \forall j \text{ where } d_j(k) = \min_{\forall v \in \{1,\cdots,nf\}} \left[d_v(k) \right] \right\} \tag{2.52}$$

This approach gives a simple idea of the fault isolation problem but it has many drawbacks which can lead towards a wrong diagnosis result: *e.g.*, this algorithm always provides a diagnosis result, even when no fault hypothesis exactly matches the current observed fault signature vector. Consequently, this can cause the diagnosis to jump from a fault hypothesis to another fault hypothesis, every time instant when a new symptom appears. Mostly, this fault isolation methods using the binary theoretical fault signature matrix and based on a parallel inference are used by the *FDI* community which uses analytical models to monitor the system. In this community, this method is known as the fault isolation *column view approach*.

In general, the single fault assumption is not always justified. In that case, the states of multiple faults should be taken into account in the diagnostic inference. It is usually sufficient to widen the set of the analyzed states of the system with the states with multiple faults. This can be done by increasing the number of columns of the theoretical fault signature matrix ***FSM*** or equally, increasing the fault set ***f*** grouping single faults. Thereby, there will be a new column for each of the new considered multiple fault states where each of these columns shows the theoretical effect of the related multiple fault state on the residuals, such as it was done for the case of single fault assumption.

(b) Rules of series diagnostic inference on the assumption about single faults

Series diagnostic inference consists in analysing subsequent fault signal values $\phi_i(k)$ and formulating the diagnosis step by step, each time narrowing the set ***f*** of possible faults (Kościelny et al, 1995) (Gertler, 1998). Unlike the parallel diagnostic inference method, this approach is mostly applied by the ***DX*** community. The fault isolation process begins after the first fault signal has been observed ($\phi_{i1}(k)=0 \rightarrow \phi_{i1}(k+1)=1$ where subindex '*i1*' stands for the first observed component of the fault signal vector*)*. Thus, the appearance of this fault signal implies the existence of a fault of the set ***f*** which $\phi_{i1}(k)$ is sensitive to. The subset of fault hypotheses satisfying this condition is shown in the first given fault diagnosis:

$$\boldsymbol{DGN}_1 = \left\{ f_j : \forall_{j:f_j \in \boldsymbol{f}} \left[1 = \boldsymbol{FSM}_{i1\,j} \right] \right\} \tag{2.53}$$

Thereby, this subset $\boldsymbol{DGN}_1$ of ***f*** is the set of possible fault hypotheses which must be considered when the next fault signal will be observed. In consequence, the performance of this method allows narrowing the set of possible fault hypotheses every time a new fault signal occurs. In general, once the series diagnostic inference has been applied *p-1* times and a new fault signal $\phi_{ip}(k)$ has been observed, the result of the new series diagnostic inference can be written as it follows:

$$\boldsymbol{DGN}_p = \boldsymbol{DGN}_{p-1} \cap \left\{ f_j : \forall_{j:f_j \in \boldsymbol{f}} \left[1 = \boldsymbol{FSM}_{ip\,j} \right] \right\} \tag{2.54}$$

In general, the series diagnostic inference only considers those fault hypotheses which can explain all the observed fault signals. If the theoretical fault signature related to a given fault hypothesis f_j contains a null value ($\boldsymbol{FSM}_{ij}=0$) where a fault signal has been observed ($\phi_i(k)=1$), this fault hypothesis will be automatically rejected by this method. Regarding the parallel diagnostic inference method presented previously, this series reasoning avoids the flickering

of the fault diagnosis result mentioned in the parallel diagnostic approach since this series inference method is based on an incremental reasoning and not on an absolute reasoning such as it is used by the column view approach. Therefore, this method is more suitable for those dynamic systems with time delays. On the other hand, the drawback of this incremental reasoning is that every inference process leads to a set of possible faults requiring the observation of all affected fault signals in order to give the final fault isolation result but conversely, the time it requires is unknown by this method because temporal or dynamics aspects of the fault signals are not considered.

As mentioned in the fault parallel diagnostic inference method, this method assumes the single fault hypothesis. However, this method can deals with multiple faults if the number of columns of the ***FSM*** is increased considering an extra column (theoretical fault signature) for each considered multiple fault hypotheses, such as mentioned in the column view approach.

2.4.2.1.2 Diagnosing based on the information system

The information system is a generalisation of the binary diagnostic matrix ***FSM*** as mentioned in *Section 2.4.1.2*. It allows applying a multi-value evaluation of residuals, carried out individually for each fault signal. Thereby, a generalisation of the binary parallel and series inference methods can be distinguished in this approach. Moreover, although this approach is defined in the single fault assumption, it can also deal with multiple fault hypotheses increasing the set ***f*** of fault hypotheses considering the multiple fault case, such as it was described in the fault in the binary diagnostic matrix method explained previously.

(a) Parallel diagnostic inference based on the fault information system

The general shape of a diagnosis based on the fault information system ***FIS*** presented in *Section 2.4.1.2* can be described by the following formula*:*

$$\boldsymbol{DGN} = \left\{ f_j \in \boldsymbol{f} : \phi_i \in \mu(\phi_i, f_j), \forall \phi_i \in \boldsymbol{\phi} \right\} \tag{2.55}$$

The diagnosis shows those faults whose theoretical signatures, which are predetermined by the ***FIS*** function $\mu(\phi_i, f_j)$, are consistent with the obtained values of the observed fault signals $\phi_i(k)$. This consistency means that the value of each fault signal belongs to the subset of pattern values $\mu(\phi_i, f_j)$ defined in the ***FIS***.

Comparing this approach with the binary parallel inference method based on the binary fault diagnostic matrix (*Section 2.4.2.1.1*), the fact of considering the fault information system instead of the binary matrix ***FSM*** adds more fault distinguishability. However, it does not avoid the fault isolation flickering problem which affects the binary approach since this is due to the absolute reasoning process of this method and the fact that the temporal aspects of the fault signals are not taken into account.

(b) Series diagnostic inference based on the fault information system

Series diagnostic inference based on the fault system information is carried out similarly as in the case of the binary diagnostic matrix presented in Section *2.4.2.1.1*. Thus, fault isolation process begins after the first fault signal has been observed ($\phi_{i1}(k)=0 \rightarrow \phi_{i1}(k+1)=1$). Then, the first diagnosis contains all faults detected by this fault signal:

$$\boldsymbol{DGN}_1 = \left\{ f_j : \forall_{j:f_j \in \boldsymbol{f}} \left[\phi_{i1} \in \mu(\phi_{i1}, f_j) \right] \right\} \tag{2.56}$$

As mentioned in the binary case, the performance of this method allows narrowing the set of possible fault hypotheses every time a new fault signal occurs. Then, after applying this inference *p-1* times and observing a new fault signal $\phi_{ip}(k)$, the result of the new series diagnostic inference can be written as it follows:

$$\boldsymbol{DGN}_p = \boldsymbol{DGN}_{p-1} \cap \left\{ f_j : \forall_{j:f_j \in \boldsymbol{f}} \left[\phi_{ip} \in \mu(\phi_{ip}, f_j) \right] \right\} \tag{2.57}$$

The basic advantage of serial inference is the possibility of giving the current diagnosis at every moment of the diagnosis. In order to obtain the final diagnosis, the interpretation of all diagnostic signals usually is not necessary. In consequence, it is possible to obtain a fault diagnosis in a shorter period of time than in the case of parallel inference. That is only possible when all the fault hypotheses are clearly distinguishable from the isolation point of view. Otherwise, all fault signals must be observed in order to give the resultant fault diagnosis being unknown the required time. However, the fact of considering a fault information system (***FIS***) instead of a binary diagnostic matrix (***FSM***) allows adding more fault distinguishability to the fault isolation reasoning being this point the advantage regarding the binary fault diagnostic matrix approach.

2.4.2.1.3 Diagnosing based on the residual space

In the case of fault detection carried out with the use of system models, a set of residuals is generated. The space whose all elements are residuals is called *residual space*, or *parity space* (Patton and Chen, 1991). Thus, the residual set needs to have distinctive properties regarding each considered particular fault so that the fault can be isolated. Residual sets designed with this objective in mind are referred to as enhanced residuals. There are two fundamental residual enhancement approaches:

- ***Directional residuals***. In order to ensure the possibility of isolating faults, the set of residuals is designed in such a way that the occurrence of particular faults characterises the specific (unique for each fault) place of residuals in the parity space. One can therefore assign to each of the faults an individually designed directional vector (Gertler, 1998) (Patton and Chen, 1991).
- ***Structured residuals.*** They are designed so that each residual responds to a different subset of faults and is insensitive to the others. When a particular fault occurs, some of the residuals do respond and others do not. Then, the pattern of the response set, the fault signature, must be characteristic of that fault so that it can be isolated.

In general, those fault isolation methods using these enhanced residuals are based on the binary fault diagnostic matrix approaches explained previously (Gertler, 1998) being affected by the same drawbacks.

2.4.2.1.4 Other methods

Many other fault isolation methods are applied beside the ones presented above. It is possible to distinguish:

- ***Pattern recognition methods.*** The possibility of applying pattern recognition methods in diagnostics results from the assumption that a certain class of system patterns being in a defined technical state are closer to each other than system patterns in other states despite measurement errors, different random factors, etc. (Himmelblau, 1978) (Pau, 1981).
- ***Diagnostic graphs.*** Fault isolation in these methods consists in defining graph paths, which can explain an incorrect operation of the system. Bond graphs form a method of physical system modelling (Thoma et at., 2000) which describe transformation, storage and dissipation of energy within the system, and present these processes in the form of a graph which connects process variables. Thereby, this graph form is built on the

grounds of the physical equations that describe the system. Diagnostics with the application of bond graphs was used by (Mosterman et al., 1995).

- ***Diagnostic inference on the basis of inconsistency.*** This group of methods was initiated by (Reiter at el., 1987). In this approach, diagnosis is formulated on the basis of the analysis of inconsistencies detected in the operation of the system. Inconsistencies are detected as a result of the comparison of the system operation and the model on the basis of measurement data. The detected inconsistencies are the basis for generating the set of conflicts understood as system element sets that contain a faulty element.
- ***Application of stochastic automatons to the diagnostics of dynamical systems*** (Lunze, 2000).

2.4.2.2 Analytical model-based fault isolation techniques

Such as it was mentioned in *Section 2.3.2*, in this thesis the monitored system is modelled using an analytical model given by an interval observer (***FDI*** approach). Traditionally, applying this analytical approach to fault isolation, the relationship between fault signals ϕ and faults $\boldsymbol{f}$ is inferred using the analytical model of the system. In general, this relationship is obtained using the residual equations $\boldsymbol{r}$ (Eq. (2.2)) or the analytical redundant relations (***ARR's***) built on the grounds of the considered system model. Although using accurate system models, the most of the *FDI* fault isolation approaches just consider a binary interface between fault detection and fault isolation modules. These approaches are based, in general, on the binary diagnostic matrix ***FSM*** explained in *Section 2.4.2.2.1* whose architecture can be described by *Figure 2.7*.

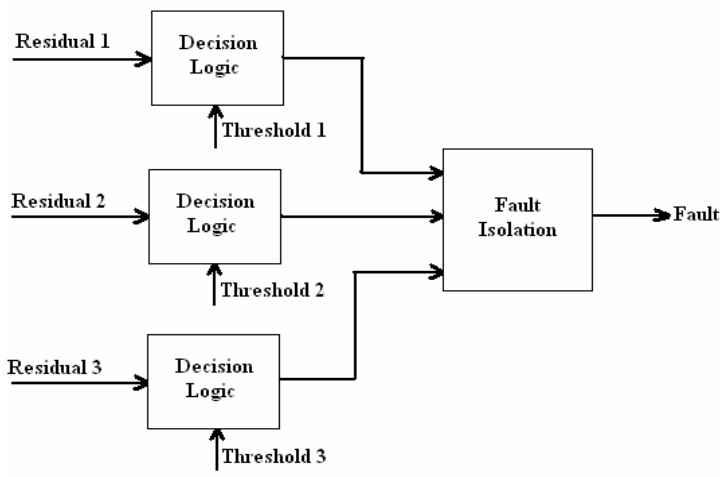

Fig. 2.7 Binary fault detection and fault isolation interface

As a result of this poor interface, these methods are affected by certain drawbacks which can lead to a wrong fault diagnosis result:

- The presence of noise produces chattering using the binary evaluation of the residual.
- All fault signals $\phi_i(k)$ affected by a certain fault $f_j(k)$ according to the structure of the matrix ***FSM*** should be activated at the same time instant and they should be persistently observed during the whole fault isolation process. Otherwise, a wrong fault diagnosis result could be given. Nonetheless, because fault signals have their own dynamics, neither they necessarily have to be activated at the same time nor they are persistently observed.
- Restricting the relation between faults and fault signals to a binary one causes a loss of useful information that can add fault distinguishability and accurateness to the fault isolation algorithm preventing possible wrong fault diagnosis results. The occurrence of a fault causes the apparition of a certain subset of fault signals such that

each of them have characteristic dynamical properties for this fault which can improve the performance of the fault isolation algorithm if they are taken into account.

In general, these drawbacks are caused because the dynamics and the discrete event nature of the fault signals are not considered. Thereby, restricting the interface between fault detection and fault isolation to a binary one causes the loss of crucial information which can enhance the whole fault diagnosis process. A significant fault signal properties that should be considered are:

- The sign of the fault signal.
- The sensitivity of the fault signal regarding to each fault hypothesis.
- The order of the fault signal occurrence.
- The time required for a fault signal to be observed once the fault occurs.

Some of the most important non-binary fault isolation methods that try to tackle some of the drawbacks mentioned previously are:

- ***DMP – Diagnostic Model Processor*** (Petti et al., 1990). In this method, the binary fault indication test (2.50) is replaced by a fuzzy one based on the Kramer function preventing the chattering of the test result. Besides, instead of using a binary diagnostic matrix, ***FSM***, a matrix with the same structure is applied but each element is related to the steady-state value of the fault residual sensitivity property (Gertler, 1998) associated with this element. Regarding the fault isolation, this is still based on a kind of parallel diagnostic inference method, in spite of its mentioned weaknesses: *e.g.*, *DMP*-method is blind for unexpected fault signals and thus, a wrong fault diagnosis can be obtained.
- ***DMA – Deep Model Algorithm*** (Chang et al., 1994). This method improves some weaknesses of the DMP method.
- ***Finite State Automatons*** (Lunze, 1994). This is the first method to deal with time aspects. In this automaton, every state represents a partial or complete diagnosis. During the reasoning process, the automaton switches from an initial state to partial-diagnosis states and in the end to a final diagnosis. Every transition is connected to a condition that depends on time and the upcoming fault signals. Thus, time windows can be defined for every transition and the time dependent fault pattern can be codified. Although this method considers time aspects related to the fault signals, it is still a pure binary method being affected by the already mentioned drawbacks of the binary approaches.
- ***DTS – Dynamic Table of States*** (Kościelny et al., 1995). Its major benefit is that it establishes a fault signal detection time, which describes the maximum time between the occurrence of a certain fault and the observation of a certain fault signal. Those times can be derived from the monitored system model or they are known from the system expert knowledge. Regarding the used fault isolation algorithm, it is based on a parallel diagnostic inference approach and therefore, it suffers from the drawbacks mentioned previously.
- ***BM – Behavioural Modes*** (Nyberg, 1999). In the *BM method*, the monitored system is divided in several components, each of them having different behavioural modes: fault-free mode and different faulty ones. In contrast to many other methods, the *BM method* uses explicit models of every behavioural mode of the components. Thus, this approach compares the real system to those system models. An advantage of this approach is that it is possible to isolate multiple faults thanks to the 'negative' reasoning. Additionally, any fault type can be modelled and many different ones for every component. Besides, the whole dynamic behaviour of a fault is modelled. On the other hand, the size of the fault has to be known in order to get model-based estimations of the faulty system behaviour that exactly correspond to the behaviour of the real system. Thereby,

this method requires a big effort in order to model all the behavioural modes of the system components and to identify the fault is affecting the system.

Considering the drawbacks of all the approaches presented previously, the second part of this thesis is focused on the interface between fault detection and fault isolation proposed by (Puig et al, 2005b). This method can be viewed as an extension of the *binary diagnostic matrix* proposed by (Gertler, 1998) in the sense that considers one diagnostic matrix ***FSM*** for each fault signal property: binary, sign, fault residual sensitivity, fault signal occurrence order and fault signal occurrence time. Thereby, this method, once the fault signal appears, registers all these properties in order to compare their values with the theoretical ones stored in several diagnostic matrices. Moreover, instead of using the binary fault detection test given by Eq. (2.50), this method uses a fuzzy test based on the one proposed by the *DMP*-method. As illustrated in (Puig et al, 2005b) and such as it will be described in *Chapter 7*, this interface has an appealing performance when used in dynamical systems. Nonetheless, it is affected by some weaknesses which are derived from some simplifications:

- Although every fault signal has its own dynamics and consequently, its properties evolve with the time, this method just considers the steady-state value of them.
- This method does not consider interval models and as a result, it uses a fixed fault detection threshold instead of an adaptive one.
- This method just considers a simulation model of the monitored system.

Regarding the fault isolation interface, one of the goals of this thesis will be to tackle the previous weaknesses of this interface using an interval observer model of the system. On the other hand, concerning the fault isolation algorithm, this thesis deals with the fact that a fault affecting the monitored system will generate a unique temporal sequence of fault signals (events) where every fault signal evolves according to its own dynamics. Thereby, observing this sequence and registering its dynamical properties, the fault can be isolated. This fault isolation discrete-event approach built on the grounds of the analytical model of the system can be considered neither as a pure quantitative approach nor as a pure qualitative one but as a hybrid approach.

2.4.2.2.1 Fault isolation based on interval observers

The main idea of using an extension of the fault detection and fault isolation interface proposed by (Puig et al, 2005b) is that these two modules can not be considered separately when a fault diagnosis process is carried out. The reason is that the result of the fault detection module, a temporal sequence of fault signals, has a crucial influence of the whole fault isolation process since:

- When a permanent fault occurs, a fault signal might not be observed permanently as a result of the fault following effect (*Table 2.1*) of the used system model.
- Certain expected fault signals can not be observed because the size of the fault is not big enough so that the related fault detection test (Eq. (2.50)) can indicate the fault according to the corresponding adaptive threshold.
- In general, fault isolation requires the observation of a subset of fault signals in order to determine a result. In consequence, the fact that every fault signal has its own dynamics and some of them can not be observed persistently o simply, they are not observed, can lead to a wrong fault isolation result if the whole fault diagnosis process does not take into account these circumstances.

In general, this influence between fault detection and fault isolation modules is obviated assuming an ideal fault detection result. This approach can lead to inconsistent results which might determine wrong decisions. These negative aspects can be prevented if dynamical properties of fault signals are taken into account by the fault isolation

module such as it is the case of the mentioned extension of the approach proposed by (Puig et al, 2005b) which will be considered in this thesis.

On the other hand, according to (Puig et al., 2005b), the value of a fault signal at a certain time instant is set by the value of its associated residual (Eq. (2.2)) at this time instant, such as it will be illustrated in *Section 7.2.2* of *Chapter 7*. Then, taking into account that the residual dynamics are deeply affected by the observer gain matrix $\boldsymbol{L}$ (Eq. (2.22)), the time evolution of the fault signals will also be affected by this matrix. As a result, it can be said that the influence of the fault detection stage on the result of the fault isolation module may depend on the observer gain $\boldsymbol{L}$. In this thesis, the influence of fault detection on the fault isolation result will be illustrated analyzing the effect of the observer gain. Regarding fault detection, it was mentioned in *Section 2.3.2.5* that an appealing design of the observer gain matrix $\boldsymbol{L}$ might help to prevent those negative drawbacks (*Table 2.1*) (e.g. the following fault effect and the wrapping effect) related to the analytical system model what may also help to improve the fault isolation performance. Conversely, as derived from Eq. (2.22), the dynamical properties of fault signals will be affected by the observer gain and as a result, it may also be possible to design $\boldsymbol{L}$ in order to add more fault distinguishability and to enhance the performance of the fault isolation module.

As viewed in *Section 2.3.2.5*, the structure of the diagnostic matrix $\boldsymbol{FSM}$ determines the fault signals which must be observed when a certain fault occurs and consequently, this aspect has also an important influence on the obtained fault isolation result. Thereby, according to definition of this matrix, $\boldsymbol{FSM}$, its structure derives from the structure of the residual generator (Eq. (2.2)) which depends on the observer gain matrix $\boldsymbol{L}$ as shown in Eq. (2.22). In consequence, a suitable design of $\boldsymbol{L}$ might allow obtaining suitable structures of the matrices $\boldsymbol{FSM}$ which enhance the result of fault isolation. In this thesis, these aspects will also be illustrated.

2.5 Thesis Objectives

In *Section 2.3* and *Section 2.4*, the state of art of the current methods applied to fault detection and fault isolation was described pointing out their weaknesses and drawbacks. As a result of this analysis, in this sections it is briefly described how this thesis tackles this present problems establishing its main objectives. Thus, in *Section 2.5*, these objectives are enumerated grouping them according to the fault diagnosis module which they belong to: *fault detection module*, *fault detection/isolation interface module* and *fault isolation module*. Finally, in this section, the proposed fault diagnosis is also briefly described.

2.5.1 Fault detection objectives

The main aim of this group is to analyze the influence of the observer gain matrix $\boldsymbol{L}$ on the robust fault detection performance for the purpose of:

(a) Obtaining fault detection quality considering the following observer properties:
   1. Observer gain influence on the residual sensitivity to a fault.
   2. Observer gain influence on the minimum detectable fault function.
   3. Observer gain influence on the fault detection persistency.

(b) Avoiding the problems associated with the computation of the system output estimation interval when a set-based approach is used.
   1. Wrapping effect.
   2. Range evaluation of an interval function.
   3. Temporal variance on uncertain parameters.

(c) Illustrating the equivalence between interval observers and interval predictors since:
    1. This equivalence can be used to tackle the problems mentioned in point *(b)*
    2. Interval predictors are not affected by the problems related to the initial state estimation.

2.5.2 Fault isolation objectives

The main objective of this group is to analyze the influence of the observation gain matrix ***L*** on the fault isolation module focusing on:

(d) The influence of the fault detection module on the fault isolation result.

(e) The influence of the observer gain ***L*** on the structure of the fault residual generator.

(f) The event nature of the generated fault signals which allows modelling the fault isolation module using a timed discrete event approach.

The purpose of this analysis is to illustrate that a proper design of matrix ***L*** can enhance the fault isolations performance.

2.5.3 Fault detection/isolation interface objectives

As mentioned in *Section 2.4.2.2*, the objectives of this thesis regarding the interface between fault detection and fault isolation are focused on tackling the weaknesses of the interface presented in (Puig et al, 2005b). Thereby, the interface proposed in this thesis must consider:

- Model uncertainty derived from the proposed passive robust fault detection approach based on interval observers.
- The dynamics related to fault signals and the time evolution of their properties.
- Lack of fault indication because of the fault following effect.
- Fault indication delays once the fault has occurred.
- Influence of the observer gain matrix ***L*** on the fault detection and fault isolation modules.

As a result, a new interface will be proposed which will be described in the following section.

2.5.4 Fault diagnosis proposed approach

This thesis proposes a new fault diagnosis approach that tries to take into account the summarized aspects mentioned in *Section 2.5.1*, *Section 2.5.2* and *Section 2.5.3*. Thereby, this approach applies the architecture presented in *Figure 2.8* whose modules are described briefly in the following:

- ***Fault detection module*** generates a fault signal measuring the system inputs and outputs taking into account model uncertainty. This is carried out using a fault detection interval observer which allows generating an adaptive threshold that evolves along time. Thus, this computed adaptive threshold allows evaluating robustly the consistency between the available measurements and the set of considered residual relations. Regarding the chattering effect produced by noise, it is tackled using a fuzzy evaluation.
- ***Fault detection/isolation interface module*** evaluates fault signals generated by the fault detection module in order to register their dynamical properties which will allow the fault isolation module to isolate the fault among the considered fault hypotheses. These properties are summarized using several indicators which take into account not only the activation value of the fault signal but also its fault sensitivity/sign and its activation time/order.

- ***Fault isolation module*** reasons with the information used to build all the indicators provided by the improved fault detection and isolation interface using a discrete-event fault diagnosis model that can be automatically built from the analytical redundancy relations obtained from the monitored system model equations and the system available measurements.

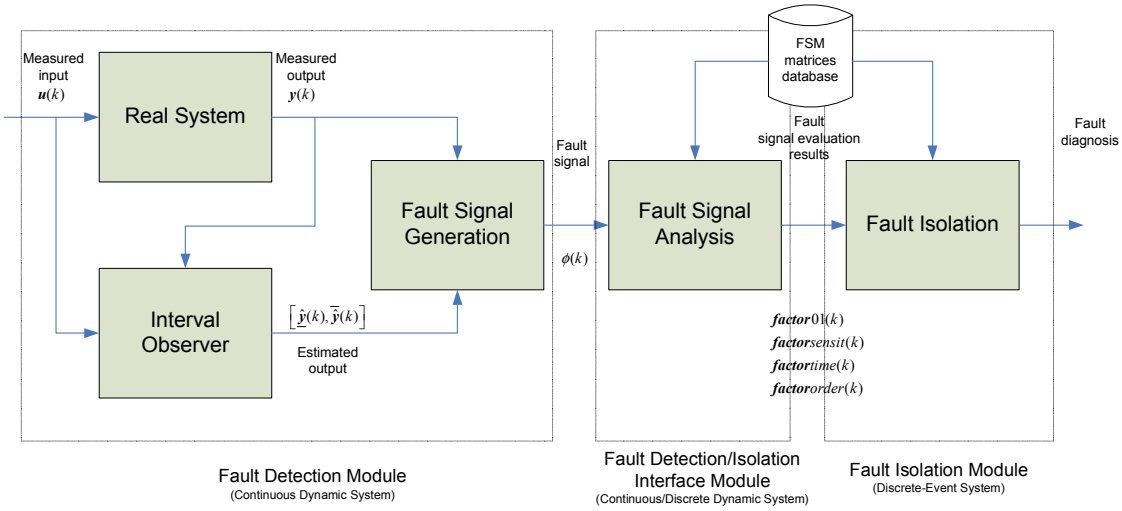

Fig. 2.8 Block diagram of the fault diagnosis system

Part I

Robust fault detection using linear interval observers and predictors

CHAPTER 3

Observer gain effect in linear interval observer-based fault detection

3.1 Introduction

Model-based fault detection of dynamic processes relies on the use of models to check the consistency of observed behaviors. This consistency check is based on computing the difference between the predicted value from the model and the real value measured by the sensors. Then, this difference, known as residual, will be compared with a threshold value (zero in the ideal case). When the residual is bigger than the threshold, it is determined that there is a fault in the system. Otherwise, it is considered that the system is working properly. However, when building a model of a dynamic process to monitor its behavior, there is always a mismatch between the modeled and the real behavior. This is because some effects are neglected in the model, some non-linearities are linearised in order to simplify the model, some parameters have tolerance when they are compared between several units of the same component, some errors in parameters or in the structure of the model are introduced in the model estimation process, etc. These modeling errors introduce uncertainty in the model and interfere with the fault detection. A fault detection algorithm able to handle uncertainty is called robust. Thus, in case of model parameter uncertainty, a model whose parameter values are bounded by intervals, known as an interval model, is usually considered. The robustness of a fault detection system means that it must be only sensitive to faults, even in the presence of model-reality differences (Chen et al, 1999).

Robustness can be achieved at residual generation (active) or evaluation phase (passive). Most of the passive robust residual evaluation methods are based on an adaptive threshold changing in time according to the plant input signal and taking into account model uncertainty either in the time domain (Horak, 1988) or in the frequency domain (Frank et al, 1994) (Hamelin et al, 2000). Recently, several researchers have used interval models in fault detection (Fagarasan et al, 2004) (Ploix et al, 2006) (Sainz et al, 2002). Conversely, interval observers applied to robust fault detection were already introduced in (Puig et al, 2003b) for linear interval systems using an optimization based algorithm. Whereas in (Puig et al, 2006a), the extension to non-linear interval systems was presented. Furthermore, in (Johansson et al, 2006), interval observation is solved using an inequality involving the convolution operator.

In observer-based fault detection methods, the observer gain plays an important role because it determines the time evolution of the residual sensitivity to a fault and therefore the minimum detectable fault at any time instant (Chen at al, 1999). In (Gertler, 1998), for example, the importance of residual sensitivity to a fault is noticed. Based on this concept, the notion of ***"triggering limit"***, which corresponds with the minimum detectable fault because it is a fault that brings a residual to its threshold, is introduced. Therefore, a fault which is slightly smaller than the triggering limit is never detected (***"non-detectable fault"***), while a slightly bigger fault is always detected (***"detectable fault"***). In (Gertler, 1998), the residual sensitivity to a fault is analyzed in steady state, but according to (Gertler, 1988), it is not certain that the maximum fault effect (sensitivity) on the residual occurs in steady state. In fact, this is not, in general, the case.

The aim of this chapter is to generalize the residual fault sensitivity presented in (Gertler, 1988) to the case of interval observers, showing it is a time function and determines the minimum detectable fault at any time instant. This will allow establishing three types of faults according to their detectability time evolution: ***permanently (strongly) detected, non-permanently (weakly) detected or just non-detected***. As a consequence, the problem of how fault detectability evolves with time is opened. In addition, another problem appears when faults are not permanently detected. Thus, the lack of fault indication persistency can confuse the fault isolation module in case that the residual would have to be evaluated jointly with a set of residuals, being necessary that a subset of them are active at the same time instant to isolate a given fault. This problem has been already noticed by (Combastel et al, 2003) who suggests registering the maximum residual value once reached. However, this strategy introduces an additional problem, since then, once the fault is detected, its indication is still active in spite the fault has already vanished. Finally, the effect of the observer gain on the time evolution of the residual sensitivity to a fault and the minimum detectable fault at any time instant will be analyzed.

Regarding the structure of the *Chapter 3* remainder, fault detection concepts using interval observers are introduced in *Section 3.2*. Then, the time evolution of the fault residual sensitivity depending on the observer gain is analyzed (*Section 3.3*). In *Section 3.4*, using the sensitivity studies, the time evolution of the minimum detectable fault and its observer gain dependence is presented using interval observer-based methods. Finally (*Section 3.5*), an example based on a mineral grinding-classification process will be used to illustrate the derived.

3.2 Fault detection using linear interval observers

3.2.1 Interval observer expression

Considering that the system to be monitored can be described by a MIMO linear uncertain dynamic model in discrete-time, its state-space form considering faults is[2]

$$\begin{aligned} \boldsymbol{x}(k+1) &= \boldsymbol{A}(\tilde{\boldsymbol{\theta}})\boldsymbol{x}(k) + \boldsymbol{B}(\tilde{\boldsymbol{\theta}})\boldsymbol{u}_0(k) + \boldsymbol{F}_a(\tilde{\boldsymbol{\theta}})\boldsymbol{f}_a(k) \\ \boldsymbol{y}(k) &= \boldsymbol{C}(\tilde{\boldsymbol{\theta}})\boldsymbol{x}(k) + \boldsymbol{D}(\tilde{\boldsymbol{\theta}})\boldsymbol{u}_0(k) + \boldsymbol{F}_y(\tilde{\boldsymbol{\theta}})\boldsymbol{f}_y(k) \end{aligned} \tag{3.1}$$

where $\boldsymbol{y}(k)\in\Re^{ny}$, $\boldsymbol{u_0}(k)$[3]$\in\Re^{nu}$, $\boldsymbol{x}(k)\in\Re^{nx}$ are the system output, input and the state-space vectors respectively; $\boldsymbol{A}(\tilde{\boldsymbol{\theta}})\in\Re^{nx\times nx}$, $\boldsymbol{B}(\tilde{\boldsymbol{\theta}})\in\Re^{nx\times nu}$, $\boldsymbol{C}(\tilde{\boldsymbol{\theta}})\in\Re^{ny\times nx}$ and $\boldsymbol{D}(\tilde{\boldsymbol{\theta}})\in\Re^{ny\times nu}$ are the state, the input, the output and the direct transmission matrices respectively; $\tilde{\boldsymbol{\theta}}\in\Re^{n\theta}$ is the system parameter vector; $\boldsymbol{f_y}(k)\in\Re^{ny}$ and $\boldsymbol{f_a}(k)\in\Re^{nu}$ represent faults in the system output sensors and actuators respectively being $\boldsymbol{F_y}(\tilde{\boldsymbol{\theta}})\in\Re^{ny\times ny}$ and $\boldsymbol{F_a}(\tilde{\boldsymbol{\theta}})\in\Re^{nx\times nu}$ their associated matrices.

The system in Eq. (3.1) can be expressed in its input-output form using the shift operator q^{-1} and assuming zero initial conditions:

$$\boldsymbol{y}(k) = \boldsymbol{y}_0(k) + \boldsymbol{G}_{fa}(q^{-1},\tilde{\boldsymbol{\theta}})\boldsymbol{f}_a(k) + \boldsymbol{G}_{fy}(q^{-1},\tilde{\boldsymbol{\theta}})\boldsymbol{f}_y(k) \tag{3.2}$$

where

$$\boldsymbol{y}_0(k) = \boldsymbol{M}(q^{-1},\tilde{\boldsymbol{\theta}})\boldsymbol{u}_0(k) \tag{3.3}$$

[2] It is assumed that the system is in open-loop. The study of the effect of the loop is let a further research. Some preliminary results of effect of loop in the fault sensitivity analysis can be found in (Jaques et al., 2003). Concerning the effect caused by disturbances and noises, it is not considered in the scope of this PhD, in spite of its importance, being left as a further work.

[3] It should be noticed that $\boldsymbol{u_0}(k)$ is the real system input and does not have to be equal to the measured system input since the input sensor might be faulty or affected by noise.

corresponds to the system output without faults. $\boldsymbol{M}(q^{-1},\tilde{\boldsymbol{\theta}})$ is the transfer function matrix regarding the system input vector which can be expressed in terms of the system matrices as:

$$\boldsymbol{M}(q^{-1},\tilde{\boldsymbol{\theta}}) = \boldsymbol{C}(\tilde{\boldsymbol{\theta}})(q\boldsymbol{I} - \boldsymbol{A}(\tilde{\boldsymbol{\theta}}))^{-1}\boldsymbol{B}(\tilde{\boldsymbol{\theta}}) + \boldsymbol{D}(\tilde{\boldsymbol{\theta}}) \tag{3.4}$$

$\boldsymbol{G_{fa}}$ and $\boldsymbol{G_{fy}}$ are the system transfer functions regarding the system faults ($\boldsymbol{f_a}$, $\boldsymbol{f_y}$) and can be expressed as follows:

$$\boldsymbol{G}_{fa}(q^{-1},\tilde{\boldsymbol{\theta}}) = \boldsymbol{C}(\tilde{\boldsymbol{\theta}})(q\boldsymbol{I} - \boldsymbol{A}(\tilde{\boldsymbol{\theta}}))^{-1}\boldsymbol{F}_a(\tilde{\boldsymbol{\theta}}) \tag{3.5}$$

$$\boldsymbol{G}_{fy}(q^{-1},\tilde{\boldsymbol{\theta}}) = \boldsymbol{F}_y(\tilde{\boldsymbol{\theta}}) \tag{3.6}$$

In line with *Section 2.3.2.5*, the system described by Eq. (3.1) is monitored using a linear observer with *Luenberger* structure based on an ***interval model***. This type of model considers that model parameters $\boldsymbol{\theta}$ are bounded by an interval set $\boldsymbol{\Theta} = \left\{\boldsymbol{\theta} \in \Re^{n\theta} \middle| \underline{\theta}_i \le \theta_i \le \overline{\theta}_i, i = 1,\cdots,n\theta\right\}$. This set represents the uncertainty about the exact knowledge of real system parameters $\tilde{\boldsymbol{\theta}}$. The interval for uncertain parameters can be inferred from real data using set-membership parameter estimation algorithms (Milanese et al., 1996) (Ploix et al., 1999). The resulting ***interval observer*** assuming the observability of the system (Eq. (3.1)) for all $\tilde{\boldsymbol{\theta}} \in \boldsymbol{\Theta}$ can be written as:

$$\begin{aligned}\hat{\boldsymbol{x}}(k+1,\boldsymbol{\theta}) &= (\boldsymbol{A}(\boldsymbol{\theta}) - \boldsymbol{LC}(\boldsymbol{\theta}))\hat{\boldsymbol{x}}(k) + (\boldsymbol{B}(\boldsymbol{\theta}) - \boldsymbol{LD}(\boldsymbol{\theta}))\boldsymbol{u}(k) + \boldsymbol{Ly}(k) = \boldsymbol{A}_o(\boldsymbol{\theta})\hat{\boldsymbol{x}}(k) + \boldsymbol{B}_o(\boldsymbol{\theta})\boldsymbol{u}(k) + \boldsymbol{Ly}(k)\\ \hat{\boldsymbol{y}}(k,\boldsymbol{\theta}) &= \boldsymbol{C}(\boldsymbol{\theta})\hat{\boldsymbol{x}}(k) + \boldsymbol{D}(\boldsymbol{\theta})\boldsymbol{u}(k)\end{aligned} \tag{3.7}$$

where ***u(k)*** is the measured system input vector, $\hat{\boldsymbol{x}}(k,\boldsymbol{\theta})$ is the estimated system space-state vector and $\hat{\boldsymbol{y}}(k,\boldsymbol{\theta})$ is the estimated system output vector for a given value of $\boldsymbol{\theta} \in \boldsymbol{\Theta}$. Noticing that the relation between the measured system, ***u(k)***, and the real system input, $\boldsymbol{u_0(k)}$, includes the effect of faults in the input sensors and as result, the expression of ***u(k)*** can be written as:

$$\boldsymbol{u}(k) = \boldsymbol{u}_0(k) + \boldsymbol{F}_u(\boldsymbol{\theta})\boldsymbol{f}_u(k) \tag{3.8}$$

where $\boldsymbol{f_u}(k) \in \Re^{nu}$ is the input sensor fault while $\boldsymbol{F_u(\theta)} \in \Re^{nu \times nu}$ is its associated matrix.

The observer gain matrix $\boldsymbol{L} \in \Re^{nx \times ny}$ is designed to stabilise the matrix $\boldsymbol{A}_o(\boldsymbol{\theta})$ and to guarantee a desired performance regarding fault detection for all $\boldsymbol{\theta} \in \boldsymbol{\Theta}$ (Chilali et al., 1996). Thereby, as mentioned in *Section 2.3.2.2*, three cases are embedded in the observer structure according to the chosen observation gain value ***L***. In the first case, the observer eigenvalues are equal to the ones of the monitored systems since $\boldsymbol{L=\theta}$ (***simulation approach***). Then, the case in which all the observer eigenvalues are placed at the origin using $\boldsymbol{L=L_p}$ (***prediction approach***) and finally, the case in which the observer eigenvalues range between the ones associated with the simulation and prediction approaches using $\boldsymbol{L=L_o}$ (***observation approach***).

The effect of the uncertain parameters $\boldsymbol{\theta}$ on the observer temporal response $\hat{\boldsymbol{y}}(k,\boldsymbol{\theta})$ will be bounded using an interval satisfying:

$$y_i(k,\tilde{\boldsymbol{\theta}}) \in [\ \underline{\hat{y}}_i(k), \overline{\hat{y}}_i(k)\ ] \tag{3.9}$$

in a non-faulty case. Such interval is computed independently for each output (neglecting couplings among outputs):

$$\underline{\hat{y}}_i(k) = \min_{\boldsymbol{\theta} \in \boldsymbol{\Theta}}(\hat{y}_i(k,\boldsymbol{\theta})) \text{ and } \overline{\hat{y}}_i(k) = \max_{\boldsymbol{\theta} \in \boldsymbol{\Theta}}(\hat{y}_i(k,\boldsymbol{\theta})) \tag{3.10}.$$

subject to the observer equations given by (3.7). Such interval can be computed using the algorithm based on numerical optimisation presented in (Puig and et al., 2003a).

For simplicity, in the following the uncertain parameter dependency will only be made explicit in the system matrices/transfer functions but not in the signals.

Alternatively, the observer given by Eq. (3.7) can be expressed in input-output form using the *q*-transform and considering zero initial conditions as follows:

$$\begin{aligned}\hat{\boldsymbol{y}}(k) &= \boldsymbol{G}(q^{-1},\boldsymbol{\theta})\boldsymbol{u}(k) + \boldsymbol{H}(q^{-1},\boldsymbol{\theta})\boldsymbol{y}(k) \\ &= \boldsymbol{G}(q^{-1},\boldsymbol{\theta})\boldsymbol{u}_0(k) + \boldsymbol{H}(q^{-1},\boldsymbol{\theta})\boldsymbol{y}(k) + \boldsymbol{G}_{fu}(q^{-1},\boldsymbol{\theta})\boldsymbol{f}_u(k)\end{aligned} \tag{3.11}$$

where

$$\boldsymbol{G}(q^{-1},\boldsymbol{\theta}) = \boldsymbol{C}(\boldsymbol{\theta})(q\boldsymbol{I} - \boldsymbol{A}_o(\boldsymbol{\theta}))^{-1}\boldsymbol{B}_o(\boldsymbol{\theta}) + \boldsymbol{D}(\boldsymbol{\theta}) \tag{3.12}$$

$$\boldsymbol{H}(q^{-1},\boldsymbol{\theta}) = \boldsymbol{C}(\boldsymbol{\theta})(q\boldsymbol{I} - \boldsymbol{A}_o(\boldsymbol{\theta}))^{-1}\boldsymbol{L} \tag{3.13}$$

$$\boldsymbol{G}_{fu}(q^{-1},\boldsymbol{\theta}) = \boldsymbol{G}(q^{-1},\boldsymbol{\theta})\boldsymbol{F}_u(\boldsymbol{\theta}) \tag{3.14}$$

3.2.2 Fault detection using interval observers

Fault detection is based on generating a residual comparing the measurements of physical variables $\boldsymbol{y}(k)$ of the process with their estimation $\hat{\boldsymbol{y}}(k)$ provided by the associated system model:

$$\boldsymbol{r}(k) = \boldsymbol{y}(k) - \hat{\boldsymbol{y}}(k) \tag{3.15}$$

where $\boldsymbol{r}(k) \in \Re^{ny}$ is the residual set. According to (Gertler, 1998), a generic form of a residual generator can be obtained using Eq. (3.11) and written as:

$$\boldsymbol{r}(k,\boldsymbol{\theta}) = \boldsymbol{V}(q^{-1},\boldsymbol{\theta})\boldsymbol{u}(k) + \boldsymbol{O}(q^{-1},\boldsymbol{\theta})\boldsymbol{y}(k) \tag{3.16}$$

where: $\boldsymbol{V}(q^{-1},\boldsymbol{\theta})$ and $\boldsymbol{O}(q^{-1},\boldsymbol{\theta})$ are transfer functions. This residual expression is known as its ***computational form***. The transfer functions $\boldsymbol{V}(q^{-1},\boldsymbol{\theta})$ and $\boldsymbol{O}(q^{-1},\boldsymbol{\theta})$ can be obtained using Eq. (3.15) and Eq. (3.11). Then, it results:

$$\boldsymbol{V}(q^{-1},\boldsymbol{\theta}) = -\boldsymbol{G}(q^{-1},\boldsymbol{\theta}) \tag{3.17}$$

$$\boldsymbol{O}(q^{-1},\boldsymbol{\theta}) = \boldsymbol{I} - \boldsymbol{H}(q^{-1},\boldsymbol{\theta}) \tag{3.18}$$

As a result, using Eq. (3.17) and Eq. (3.18), the computational form of the residual could be written as follows:

$$\boldsymbol{r}(k,\boldsymbol{\theta}) = -\boldsymbol{G}(q^{-1},\boldsymbol{\theta})\boldsymbol{u}(k) + \left(\boldsymbol{I} - \boldsymbol{H}(q^{-1},\boldsymbol{\theta})\right)\boldsymbol{y}(k) \tag{3.19}$$

In addition, the residual given by Eq. (3.19) can be also expressed in terms of the effects caused by faults using its ***internal*** or ***unknown-input-effect form*** (Gertler, 1998). This form, obtained combining Eq. (3.15), Eq. (3.11) and Eq. (3.2), is expressed as

$$\boldsymbol{r}(k,\boldsymbol{\theta}) = \boldsymbol{r}_0(k,\boldsymbol{\theta}) + \left(\boldsymbol{I} - \boldsymbol{H}(q^{-1},\boldsymbol{\theta})\right)\left(\boldsymbol{G}_{fa}(q^{-1},\tilde{\boldsymbol{\theta}})\boldsymbol{f}_a(k) + \boldsymbol{G}_{fy}(q^{-1},\tilde{\boldsymbol{\theta}})\boldsymbol{f}_y(k)\right) - \boldsymbol{G}_{fu}(q^{-1},\boldsymbol{\theta})\boldsymbol{f}_u(k) \tag{3.20}$$

where

$$\boldsymbol{r}_0(k,\boldsymbol{\theta}) = -\boldsymbol{G}(q^{-1},\boldsymbol{\theta})\boldsymbol{u}_0(k) + \left(\boldsymbol{I} - \boldsymbol{H}(q^{-1},\boldsymbol{\theta})\right)\boldsymbol{y}_0(k) \tag{3.21}$$

would be the expression of the non-faulty residual. Comparing Eq. (3.21) and Eq. (3.16), it should be noticed both $\boldsymbol{r}_0(k)$ and $\boldsymbol{r}(k)$ are affected in the same way by the observation gain $\boldsymbol{L}$.

When considering model uncertainty located in parameters, the residual generated by Eq. (3.15) will not be zero even in a non-faulty scenario. Thus, it must be considered that the propagation of the parameter uncertainty to the residual will allow computing a residual interval at every time instant:

$$\left[\boldsymbol{r}(k)\right] = \left[\underline{\boldsymbol{r}}(k), \overline{\boldsymbol{r}}(k)\right] \tag{3.22}$$

where for the residual $r_i(k)$ related to the system output $y_i(k)$[4] (neglecting couplings among outputs):

$$\underline{r}_i(k) = \min_{\boldsymbol{\theta}\in\boldsymbol{\Theta}}(r_i(k)) \text{ and } \overline{r}_i(k) = \max_{\boldsymbol{\theta}\in\boldsymbol{\Theta}}(r_i(k)) \tag{3.23}$$

Notice that according to Eq. (3.9) and Eq. (3.15), $\underline{r}_i(k) < 0$ and $\overline{r}_i(k) > 0$ when the monitored system is not affected by any fault..

Then, the fault detection test is based on propagating the parameter uncertainty to the residual (Puig et al, 2002a) and checking if

$$\boldsymbol{\theta} \in [\boldsymbol{r}(k)] = \boldsymbol{y}(k) - [\hat{\boldsymbol{y}}(k)] \text{ or } \boldsymbol{y}(k) \in [\hat{\boldsymbol{y}}(k)] \tag{3.24}$$

holds or not. In case it does not hold a fault can be indicated.

3.2.3 Effect of the observer gain on the residual interval

Before analyzing the effect of the different types of faults on the residual, it is important to determine the influence of the observer gain $\boldsymbol{L}$ on the residual interval (Eq. (3.22)) since, such as it is derived from Eq. (3.24), it has a decisive influence on the observer fault detection performance. In order to illustrate this influence, the interval observer state-space form is expressed as

$$\begin{aligned} \hat{\boldsymbol{x}}(k+1) &= \boldsymbol{A}(\boldsymbol{\theta})\hat{\boldsymbol{x}}(k) + [\boldsymbol{B}(\boldsymbol{\theta}) \quad \boldsymbol{L}] \begin{bmatrix} \boldsymbol{u}(k) \\ \boldsymbol{r}(k) \end{bmatrix} \\ \hat{\boldsymbol{y}}(k) &= \boldsymbol{C}(\boldsymbol{\theta})\hat{\boldsymbol{x}}(k) + \boldsymbol{D}(\boldsymbol{\theta})\boldsymbol{u}(k) \end{aligned} \tag{3.25}$$

using Eq. (3.7) and Eq.(3.15).

Then, assuming zero initial conditions, the input-output form of the observer using the q-transform is

$$\hat{\boldsymbol{y}}(k) = \left(\boldsymbol{C}(\boldsymbol{\theta})\left(q\boldsymbol{I} - \boldsymbol{A}(\boldsymbol{\theta})\right)^{-1}\boldsymbol{B}(\boldsymbol{\theta}) + \boldsymbol{D}(\boldsymbol{\theta})\right)\boldsymbol{u}(k) + \boldsymbol{C}(\boldsymbol{\theta})\left(q\boldsymbol{I} - \boldsymbol{A}(\boldsymbol{\theta})\right)^{-1}\boldsymbol{L}\boldsymbol{r}(k) \tag{3.26}$$

Thus, defining $\hat{\boldsymbol{y}}(k)_{\boldsymbol{L}=\boldsymbol{0}}$ as the value of $\hat{\boldsymbol{y}}(k)$ when $\boldsymbol{L}=\boldsymbol{0}$ (simulation value) and $\boldsymbol{H}_r(q^{-1},\boldsymbol{\theta})$ as

$$\boldsymbol{H}_r(q^{-1},\boldsymbol{\theta}) = \boldsymbol{C}(\boldsymbol{\theta})\left(q\boldsymbol{I} - \boldsymbol{A}(\boldsymbol{\theta})\right)^{-1}\boldsymbol{L} \tag{3.27}$$

the interval observer input-output form can be written as:

$$\hat{\boldsymbol{y}}(k) = \hat{\boldsymbol{y}}(k)_{\boldsymbol{L}=\boldsymbol{0}} + \boldsymbol{H}_r(q^{-1},\boldsymbol{\theta})\boldsymbol{r}(k) \tag{3.28}$$

Conversely, taking into account that the general expression of the residual is given by Eq. (3.15) and using the observer output estimation given by Eq. (3.28), the residual can be re-written as

$$\boldsymbol{r}(k) = \boldsymbol{y}(k) - \hat{\boldsymbol{y}}(k) = \boldsymbol{y}(k) - \hat{\boldsymbol{y}}(k)_{\boldsymbol{L}=\boldsymbol{0}} - \boldsymbol{H}_r(q^{-1},\boldsymbol{\theta})\boldsymbol{r}(k) \tag{3.29}$$

Then, taking into account that the transfer function $\boldsymbol{H}_r(q^{-1},\boldsymbol{\theta})$ (Eq. (3.27)) is a square matrix and considering that $\left(\boldsymbol{I} + \boldsymbol{H}_r(q^{-1},\boldsymbol{\theta})\right)$ has an inverse matrix, this equation can be expressed as

$$\boldsymbol{r}(k) = \left(\boldsymbol{I} + \boldsymbol{H}_r(q^{-1},\boldsymbol{\theta})\right)^{-1}\boldsymbol{r}(k)_{\boldsymbol{L}=\boldsymbol{0}} = \left(\boldsymbol{I} + \boldsymbol{C}(\boldsymbol{\theta})\left(q\boldsymbol{I} - \boldsymbol{A}(\boldsymbol{\theta})\right)^{-1}\boldsymbol{L}\right)^{-1}\boldsymbol{r}(k)_{\boldsymbol{L}=\boldsymbol{0}} \tag{3.30}$$

for every value of $\boldsymbol{\theta} \in \boldsymbol{\Theta}$ and where $\boldsymbol{r}(k,\boldsymbol{\theta})_{\boldsymbol{L}=\boldsymbol{0}} = \boldsymbol{y}(k) - \hat{\boldsymbol{y}}(k)_{\boldsymbol{L}=\boldsymbol{0}}$ is the residual generated by the simulation approach (Eq. (3.15)). This equation shows that the residual generated by the observer approach for a certain value of $\boldsymbol{\theta} \in \boldsymbol{\Theta}$ depends on the observer gain $\boldsymbol{L}$.

[4] As indicated for the system output estimation interval, the residual interval can be calculated using the algorithm presented in (Puig et al., 2003b).

In the remainder of this chapter it will be assumed that all elements of the matrices $\boldsymbol{A}$ and $\boldsymbol{L}$ are positive[5] ($\boldsymbol{A}\geq\boldsymbol{0}$ and $\boldsymbol{L}\geq\boldsymbol{0}$) . Thus, taking into account this assumption and the observer model definition, it follows: $\boldsymbol{0}\leq\boldsymbol{LC}\leq\boldsymbol{A}$[6]. Note that the extreme case $\boldsymbol{LC}=\boldsymbol{A}$ is just reached by the predictor approach ($\boldsymbol{L}=\boldsymbol{L_p}$) when $\boldsymbol{C}$ has an inverse matrix[7]. Nonetheless, the applied observer gain is assumed to satisfy the following relation: $\boldsymbol{0}\leq\boldsymbol{L_o}\leq\boldsymbol{L_p}$, understood also element by element. Under these conditions, the next relation can be established for whatever time instant $k>0$

$$\left[r_i(k)_{\boldsymbol{L}=\boldsymbol{L_p}}\right]\subseteq\left[r_i(k)_{\boldsymbol{L}=\boldsymbol{L_o}}\right]\subseteq\left[r_i(k)_{\boldsymbol{L}=\boldsymbol{0}}\right]\quad i=1,\cdots,ny \tag{3.31}$$

See the proof in the *Appendix A*.

Concerning the steady-state values of the residuals, relation given by Eq. (3.31) is satisfied when

$$\left\|\lim_{q\to 1}\left(\boldsymbol{I}+\boldsymbol{H}_r(q^{-1},\boldsymbol{\theta})\right)\right\|=\left\|\boldsymbol{I}+\boldsymbol{C}(\boldsymbol{\theta})\left(\boldsymbol{I}-\boldsymbol{A}(\boldsymbol{\theta})\right)^{-1}\boldsymbol{L}\right\|\geq 1 \tag{3.32}$$

as it will be demonstrated in *Appendix B*. It must be noticed that this relation (Eq. (3.32)) does not need $\boldsymbol{A}$ and $\boldsymbol{L}$ to be positive matrices, although this case is out of the scope of this chapter.

Under the same conditions in which Eq. (3.31) is satisfied and taking into account Eq. (3.16) and Eq. (3.21), it must be noticed that this inclusion relation is also satisfied by $\boldsymbol{r_0(k)}$.

$$\left[r_{0_i}(k)_{\boldsymbol{L}=\boldsymbol{L_p}}\right]\subseteq\left[r_{0_i}(k)_{\boldsymbol{L}=\boldsymbol{L_o}}\right]\subseteq\left[r_{0_i}(k)_{\boldsymbol{L}=\boldsymbol{0}}\right]\quad i=1,\cdots,ny \tag{3.33}$$

Conversely, according to the residual definition given by Eq. (3.15), the residual interval could be written as

$$[\boldsymbol{r}(k)]=\boldsymbol{y}(k)-[\hat{\boldsymbol{y}}(k)] \tag{3.34}$$

and consequently, considering the influence of the observer gain $\boldsymbol{L}$ on the residual interval shown by Eq. (3.31), the next relation regarding the influence of the observer gain on the system output estimation interval can be set

$$\left[\hat{y}_i(k)_{\boldsymbol{L}=\boldsymbol{L_p}}\right]\subseteq\left[\hat{y}_i(k)_{\boldsymbol{L}=\boldsymbol{L_o}}\right]\subseteq\left[\hat{y}_i(k)_{\boldsymbol{L}=\boldsymbol{0}}\right]\quad i=1,\cdots,ny \tag{3.35}$$

3.3 Fault sensitivity

3.3.1 Fault sensitivity concept

The ***sensitivity of the residual*** (Gertler, 1998) to a fault is given by

$$\boldsymbol{S_f}=\frac{\partial\boldsymbol{r}}{\partial\boldsymbol{f}} \tag{3.36}$$

which is a transfer function that describes the effect on the residual, $\boldsymbol{r}$, of a given fault $\boldsymbol{f}$. In this section, the effect of the observation gain matrix $\boldsymbol{L}$ on the fault residual sensitivity time evolution is analyzed considering output sensor faults $\boldsymbol{f_y}$, input sensor faults $\boldsymbol{f_u}$ and actuator faults $\boldsymbol{f_a}$. The expressions of these fault residual sensitivity functions are obtained using Eq. (3.36) and the residual ***internal form*** given by Eq. (3.20). Thus, it will be shown these functions have a time evolution which is determined by the observation gain matrix $\boldsymbol{L}$.

---

[5] The case where this condition is not fulfilled has been analysed in *Chapter 4* which is based on (Meseguer et al., 2008a) adapting the results presented in this paper. The mentioned condition $\boldsymbol{A}\geq\boldsymbol{0}$ is a typical assumption when dealing with interval observers since in this case the wrapping effect is avoided (Puig et al, 2002a) and the interval related to the system output estimation trajectories are generated by the vertices of the interval parameters. See for example (Gouzé et al, 2000) (Rapaport et al, 2003).

[6] $0\leq\boldsymbol{LC}\leq\boldsymbol{A}$ should be understood element by element, that is: $0\leq(\boldsymbol{LC})_{ij}\leq a_{ij}$, where $i,j=1,...,nx$.

3.3.2 Sensitivity of the residual to an output sensor fault

Analyzing the residual ***internal form*** given by Eq. (3.20), and considering the fault residual sensitivity definition given by Eq. (3.36), the sensitivity for the case of an output sensor fault $\boldsymbol{f_y}$ is given by a matrix $\boldsymbol{S}_{fy}$ of dimension $ny \times ny$ whose expression is:

$$\boldsymbol{S}_{fy}(q^{-1},\boldsymbol{\theta}) = \left(\boldsymbol{I} - \boldsymbol{H}(q^{-1},\boldsymbol{\theta})\right)\boldsymbol{G}_{fy}(q^{-1},\tilde{\boldsymbol{\theta}}) = \left(\boldsymbol{I} - \boldsymbol{C}(\boldsymbol{\theta})\left(q\boldsymbol{I} - \left(\boldsymbol{A}(\boldsymbol{\theta}) - \boldsymbol{L}\boldsymbol{C}(\boldsymbol{\theta})\right)\right)^{-1}\boldsymbol{L}\right)\boldsymbol{F}_y(\tilde{\boldsymbol{\theta}}) =$$
$$= \begin{pmatrix} S_{fy_{1,1}}(q^{-1},\boldsymbol{\theta}) & \cdots & S_{fy_{1,ny}}(q^{-1},\boldsymbol{\theta}) \\ \vdots & \ddots & \vdots \\ S_{fy_{ny,1}}(q^{-1},\boldsymbol{\theta}) & \cdots & S_{fy_{ny,ny}}(q^{-1},\boldsymbol{\theta}) \end{pmatrix} \tag{3.37}$$

where the element of this matrix located at the i^{th}-row and in the j^{th}-column, noted as $S_{fy_{i,j}}$, describes the sensitivity of the residual $r_i(k)$ related to the output system $y_i(k)$ regarding the fault $f_{y_j}(k)$ affecting the sensor related to the output system $y_j(k)$.

This expression shows the residual sensitivity to an output sensor fault is a time function and how its dynamics and steady-state gain is influenced by the observer gain. Thus, in order to point out this influence, this residual sensitivity can be re-written using the *matrix inversion lemma*[8]:

$$\boldsymbol{S}_{fy}(q^{-1},\boldsymbol{\theta}) = \left(\boldsymbol{I} - \boldsymbol{H}(q^{-1},\boldsymbol{\theta})\right)\boldsymbol{G}_{fy}(q^{-1},\tilde{\boldsymbol{\theta}}) = \left(\boldsymbol{I} + \boldsymbol{H}_r(q^{-1},\boldsymbol{\theta})\right)^{-1}\boldsymbol{F}_y(\tilde{\boldsymbol{\theta}}) =$$
$$= \left(\boldsymbol{I} + \boldsymbol{C}(\boldsymbol{\theta})\left(q\boldsymbol{I} - \boldsymbol{A}(\boldsymbol{\theta})\right)^{-1}\boldsymbol{L}\right)^{-1}\boldsymbol{F}_y(\tilde{\boldsymbol{\theta}}) \tag{3.38}$$

Then, its value at time instant *k=0*, i.e. when an abrupt fault (modelled as a unit-step function) occurs, is

$$\boldsymbol{s}_{fy}(0) = \lim_{q\to\infty}\boldsymbol{S}_{fy}(q^{-1},\boldsymbol{\theta}) = \boldsymbol{F}_y(\tilde{\boldsymbol{\theta}}) \tag{3.39}$$

independently of the observer gain matrix $\boldsymbol{L}$. When $\boldsymbol{F}_y(\tilde{\boldsymbol{\theta}})$ is a diagonal matrix (*i.e. additive output sensor fault case*),

$$\boldsymbol{s}_{fy}(0) = \begin{pmatrix} s_{fy_{1,1}}(0) & \cdots & s_{fy_{1,ny}}(0) \\ \vdots & \ddots & \vdots \\ s_{fy_{1,ny}}(0) & \cdots & s_{fy_{ny,ny}}(0) \end{pmatrix} = \begin{pmatrix} F_{y_1} & & 0 \\ & \ddots & \\ 0 & & F_{y_{ny}} \end{pmatrix} \tag{3.40}$$

where F_{y_i} ($i=1,...,ny$) are the diagonal elements of matrix $\boldsymbol{F}_y(\tilde{\boldsymbol{\theta}})$. It must be taken into account that the expression given by Eq. (3.40) has a meaningful importance regarding fault isolation since it illustrates that when an output sensor fault $f_{y_j}(k)$ occurs at a certain time instant, the only residual $r_i(k)$ that reacts to this faulty situation at this time instant is the one related to the faulty sensor while the other fault signals require more time in order to be observed. This property allows rejecting the rest of possible output sensor fault hypothesis from the fault occurrence time instant.

On the other hand, the steady-state value of Eq. (3.38) for an abrupt fault modelled as a unit-step function (Gertler, 1998) is given by

---

[7] When $\boldsymbol{C}$ has an inverse matrix, $\boldsymbol{\theta} \le \boldsymbol{L}\boldsymbol{C} \le \boldsymbol{A}$ and $\boldsymbol{L_p}\boldsymbol{C}=\boldsymbol{A}$ force the observer gain to satisfy the relation $\boldsymbol{\theta} \le \boldsymbol{L_o} \le \boldsymbol{L_p}$ understood element by element.

[8] Matrix inversion lemma: $(\boldsymbol{A}_x + \boldsymbol{B}_x\boldsymbol{D}_x\boldsymbol{C}_x)^{-1} = \boldsymbol{A}_x^{-1} - \boldsymbol{A}_x^{-1}\boldsymbol{B}_x(\boldsymbol{D}_x^{-1} + \boldsymbol{C}_x\boldsymbol{A}_x^{-1}\boldsymbol{B}_x)^{-1}\boldsymbol{C}_x\boldsymbol{A}_x^{-1}$, being $\boldsymbol{A}_x = \boldsymbol{I}$, $\boldsymbol{B}_x = \boldsymbol{C}(\boldsymbol{\theta})$, $\boldsymbol{D}_x = (q\boldsymbol{I} - \boldsymbol{A}(\boldsymbol{\theta}))^{-1}$ and $\boldsymbol{C}_x = \boldsymbol{L}$.

$$\begin{aligned}\boldsymbol{s}_{f\hat{y}}(\infty) &= \lim_{q\to 1}\boldsymbol{S}_{f\hat{y}}(q^{-1},\boldsymbol{\theta}) = \lim_{q\to 1}\left[\left(\boldsymbol{I}+\boldsymbol{H}_r(q^{-1},\boldsymbol{\theta})\right)^{-1}\boldsymbol{F}_y(\tilde{\boldsymbol{\theta}})\right] \\ &= \left(\boldsymbol{I}+\boldsymbol{C}(\boldsymbol{\theta})(\boldsymbol{I}-\boldsymbol{A}(\boldsymbol{\theta}))^{-1}\boldsymbol{L}\right)^{-1}\boldsymbol{F}_y(\tilde{\boldsymbol{\theta}})\end{aligned} \tag{3.41}$$

In general, Eq. (3.38) demonstrates clearly that the time evolution of residual sensitivity to an output sensor fault is affected by the observer gain matrix $\boldsymbol{L}$ and that this residual property can be tuned adjusting $\boldsymbol{L}$ in order to enhance the fault detection and isolation results.

When the simulation approach is considered ($\boldsymbol{L}=\boldsymbol{0}$), Eq (3.41) is equal to Eq. (3.39) .

$$\boldsymbol{s}_{f\hat{y}}(\infty)_{\boldsymbol{L}=\boldsymbol{0}} = \boldsymbol{F}_y(\tilde{\boldsymbol{\theta}}) \tag{3.42}$$

That means the simulator capability to detect a fault is a constant characteristic along the time. Moreover, it can be noticed that in the case showed in Eq. (3.40), the sensitivity value of the residual $r_i(k)$ to a fault f_{y_j} is zero-valued for all j: $j\neq i$ and is not null when the fault is affecting the output sensor related to $y_i(k)$.

On the other hand, comparing Eq. (3.41) and Eq. (3.42) and taking into account that the considered interval observer satisfies the Eq. (3.32), the following relation is derived regarding the diagonal elements of $\boldsymbol{S}_{f\hat{y}}(q^{-1},\boldsymbol{\theta})$ for every value of $\boldsymbol{\theta}\in\boldsymbol{\Theta}$

$$\left|s_{f\hat{y}_{i,i}}(\infty)\right| \le \left|s_{f\hat{y}_{i,i}}(0)\right| \quad i=1,\cdots,ny \tag{3.43}$$

while the other elements satisfy

$$\left|s_{f\hat{y}_{i,j}}(\infty)\right| \ge \left|s_{f\hat{y}_{i,j}}(0)\right| \quad i=1,\cdots,ny \quad j=1,\cdots,ny \quad i\neq j \tag{3.44}$$

since their initial value is null (Eq.(3.40)). As mentioned, stability is assumed in any case.

That means the observer and predictor capability to detect a fault $f_{y_i}(k)$ affecting the sensor output $y_i(k)$ using the residual $r_i(k)$(Eq. (3.24)) is worsened regarding the initial time instant when the fault occurs while the simulator keeps constant this capability. On the other hand, except in the simulation case, the capability to detect a fault $f_{y_j}(k)$ ($j\neq i$) using the residual $r_i(k)$ is improved along the time.

Evaluating the influence of $\boldsymbol{L}$ on diagonal elements of Eq. (3.41) and taking into account that the considered interval observer satisfies the Eq. (3.32), it can be noticed that the steady-state value of the observer fault residual sensitivity is bigger than the corresponding to the predictor resulting

$$\left|s_{f\hat{y}_{i,i}}(\infty,\boldsymbol{\theta})_{\boldsymbol{L}=\boldsymbol{L}_p}\right| \le \left|s_{f\hat{y}_{i,i}}(\infty,\boldsymbol{\theta})_{\boldsymbol{L}=\boldsymbol{L}_o}\right| \le \left|s_{f\hat{y}_{i,i}}(\infty,\boldsymbol{\theta})_{\boldsymbol{L}=\boldsymbol{0}}\right| \quad i=1,\cdots,ny \tag{3.45}$$

for every value of $\boldsymbol{\theta}\in\boldsymbol{\Theta}$. Otherwise, for the non-diagonal elements ($j\neq i$) the following relation holds

$$\left|s_{f\hat{y}_{i,j}}(\infty,\boldsymbol{\theta})_{\boldsymbol{L}=\boldsymbol{L}_o}\right| \ge \left|s_{f\hat{y}_{i,j}}(\infty,\boldsymbol{\theta})_{\boldsymbol{L}=\boldsymbol{0}}\right| = 0 \quad i=1,\cdots,ny \quad j=1,\cdots,ny \quad i\neq j \tag{3.46}$$

3.3.3 Sensitivity of the residual to an input sensor fault

In this case, considering the residual ***internal form*** given by Eq. (3.20), and the fault residual sensitivity definition given by Eq. (3.36), the residual sensitivity to an input sensor fault $\boldsymbol{f_u}$ is given by a matrix $\boldsymbol{S}_{fu}$ of dimension $ny\times nu$ whose expression is:

$$\boldsymbol{S}_{fu}(q^{-1},\boldsymbol{\theta}) = -\boldsymbol{G}(q^{-1},\boldsymbol{\theta})\boldsymbol{F}_u(\boldsymbol{\theta}) = -\Big(\boldsymbol{C}(\boldsymbol{\theta})\big(q\boldsymbol{I} - \big(\boldsymbol{A}(\boldsymbol{\theta}) - \boldsymbol{L}\boldsymbol{C}(\boldsymbol{\theta})\big)\big)^{-1}\big(\boldsymbol{B}(\boldsymbol{\theta}) - \boldsymbol{L}\boldsymbol{D}(\boldsymbol{\theta})\big) + \boldsymbol{D}(\boldsymbol{\theta})\Big)\boldsymbol{F}_u(\boldsymbol{\theta}) =$$

$$= \begin{pmatrix} S_{fu_{1,1}}(q^{-1},\boldsymbol{\theta}) & \cdots & S_{fu_{1,nu}}(q^{-1},\boldsymbol{\theta}) \\ \vdots & \ddots & \vdots \\ S_{fu_{ny,1}}(q^{-1},\boldsymbol{\theta}) & \cdots & S_{fu_{ny,nu}}(q^{-1},\boldsymbol{\theta}) \end{pmatrix} \tag{3.47}$$

where each row of this matrix is related to one component of the residual vector $\boldsymbol{r} = \{r_i(k): i = 1,2,....ny\}$ (Eq. (3.15) while each column is related to one component of the input sensor fault vector $\boldsymbol{f_u} = \{f_{u_j} : j = 1,2,...,nu\}$. This expression shows the residual sensitivity to an input sensor fault is also a time function whose dynamics and steady-state gain are influenced by the observer gain. Then, its value at time instant $k=0$, *i.e.* when an abrupt fault (modelled as a unit-step function) occurs, is

$$\boldsymbol{s}_{fu}(0) = \lim_{q\to\infty} \boldsymbol{S}_{fu}(q^{-1},\boldsymbol{\theta}) = -\boldsymbol{D}\boldsymbol{F}_u(\boldsymbol{\theta}) \tag{3.48}$$

independently of the observer gain matrix $\boldsymbol{L}$[9]. When $\boldsymbol{D}\approx\boldsymbol{0}$, Eq. (3.48) means that none input fault can be detected at its occurrence time instant.

On the other hand, the steady-state value for an abrupt fault modelled as a unit-step function (Gertler, 1998) is given by

$$\boldsymbol{s}_{fu}(\infty) = \lim_{q\to 1} \boldsymbol{S}_{fu}(q^{-1},\boldsymbol{\theta}) = -(\boldsymbol{C}(\boldsymbol{\theta})(\boldsymbol{I} - \boldsymbol{A}_o(\boldsymbol{\theta}))^{-1}\boldsymbol{B}_o(\boldsymbol{\theta}) + \boldsymbol{D})\boldsymbol{F}_u(\boldsymbol{\theta}) \tag{3.49}$$

Eq. (3.49) shows the steady-state value of this sensitivity depends on the observation gain matrix $\boldsymbol{L}$. Besides, comparing this equation with Eq. (3.48), assuming $\boldsymbol{D}\approx\boldsymbol{0}$,the next relation between them is derived for every value of $\boldsymbol{\theta}\in\boldsymbol{\Theta}$:

$$\left|s_{fu_{i,j}}(\infty)\right| \geq \left|s_{fu_{i,j}}(0)\right| \quad i = 1,\cdots,ny \quad j = 1,\cdots,nu \tag{3.50}$$

Unlike the output fault case, an input sensor fault is likelier to be detected after its occurrence time instant than when the fault just appears. When the simulation approach is considered ($\boldsymbol{L}=\boldsymbol{0}$), Eq. (3.49) can be re-written as follows:

$$\boldsymbol{s}_{fu}(\infty)_{\boldsymbol{L}=\boldsymbol{0}} = -\Big(\boldsymbol{C}(\boldsymbol{\theta})\big(\boldsymbol{I} - \boldsymbol{A}(\boldsymbol{\theta})\big)^{-1}\boldsymbol{B}(\boldsymbol{\theta}) + \boldsymbol{D}(\boldsymbol{\theta})\Big)\boldsymbol{F}_u(\boldsymbol{\theta}) \tag{3.51}$$

Then, considering the predictor case ($\boldsymbol{L}=\boldsymbol{L_p}$), the Eq. (3.49) becomes:

$$\boldsymbol{s}_{fu}(\infty)_{\boldsymbol{L}=\boldsymbol{L_p}} = -\Big(\boldsymbol{C}(\boldsymbol{\theta})\big(\boldsymbol{I} - \big(\boldsymbol{A}(\boldsymbol{\theta}) - \boldsymbol{L_p}\boldsymbol{C}(\boldsymbol{\theta})\big)\big)^{-1}\big(\boldsymbol{B}(\boldsymbol{\theta}) - \boldsymbol{L_p}\boldsymbol{D}(\boldsymbol{\theta})\big) + \boldsymbol{D}(\boldsymbol{\theta})\Big)\boldsymbol{F}_u(\boldsymbol{\theta}) \tag{3.52}$$

According to the influence of matrix $\boldsymbol{L}$ on Eq. (3.49) and neglecting the value of matrix $\boldsymbol{D}$, the following relation is fulfilled both by $\boldsymbol{S}_{fu}$:

$$\left|s_{fu_{i,j}}(\infty,\boldsymbol{\theta})_{\boldsymbol{L}=\boldsymbol{L_p}}\right| \leq \left|s_{fu_{i,j}}(\infty,\boldsymbol{\theta})_{\boldsymbol{L}=\boldsymbol{L_o}}\right| \leq \left|s_{fu_{i,j}}(\infty,\boldsymbol{\theta})_{\boldsymbol{L}=\boldsymbol{0}}\right| \quad i = 1,\cdots,ny \quad j = 1,\cdots,nu \tag{3.53}$$

for every value of $\boldsymbol{\theta}\in\boldsymbol{\Theta}$ and assuming stability.

As demonstrated in *Appendix C*, matrix $\boldsymbol{S}_{fu}$ satisfies relation (3.53) because the considered observer fulfils the relations: $\boldsymbol{0} \leq \boldsymbol{L}\boldsymbol{C} \leq \boldsymbol{A}$ and $\boldsymbol{0} \leq \boldsymbol{L_o} \leq \boldsymbol{L_p}$.

[9] Mostly, the direct transmission matrix $\boldsymbol{D}$ is considered zero-valued and thus, the residual sensitivity to an input sensor fault is null at its occurrence time instant according to Eq. (3.48).

Thus, in general, the absolute value of $s_{fu_{i,j}}$ associated with the simulation approach is bigger than the corresponding one to the observation approach while this is also bigger than the corresponding to the prediction approach.

3.3.4 Sensitivity of the residual to an actuator fault

In this case, considering the residual ***internal form*** given by Eq. (3.20), and the fault residual sensitivity definition given by Eq. (3.36), the residual sensitivity to an actuator fault $\boldsymbol{f_a}$ is given by a matrix $\boldsymbol{S}_{fa}$ of dimension $ny \times nu$ whose expression is:

$$\begin{aligned}
&\boldsymbol{S}_{fa}(q^{-1},\boldsymbol{\theta}) = \left(\boldsymbol{I} - \boldsymbol{H}(q^{-1},\boldsymbol{\theta})\right)\boldsymbol{G}_{fa}(q^{-1},\tilde{\boldsymbol{\theta}}) = \\
&= \left(\boldsymbol{I} - \boldsymbol{C}(\boldsymbol{\theta})\left(q\boldsymbol{I} - \left(\boldsymbol{A}(\boldsymbol{\theta}) - \boldsymbol{L}\boldsymbol{C}(\boldsymbol{\theta})\right)\right)^{-1}\boldsymbol{L}\right)\boldsymbol{C}(\tilde{\boldsymbol{\theta}})\left(q\boldsymbol{I} - \boldsymbol{A}(\tilde{\boldsymbol{\theta}})\right)^{-1}\boldsymbol{F}_a(\tilde{\boldsymbol{\theta}}) = \\
&= \begin{pmatrix} S_{fa_{1,1}}(q^{-1},\boldsymbol{\theta}) & \cdots & S_{fa_{1,nu}}(q^{-1},\boldsymbol{\theta}) \\ \vdots & \ddots & \vdots \\ S_{fa_{ny,1}}(q^{-1},\boldsymbol{\theta}) & \cdots & S_{fa_{ny,nu}}(q^{-1},\boldsymbol{\theta}) \end{pmatrix}
\end{aligned} \tag{3.54}$$

where each row of this matrix is related to one component of the residual vector $\boldsymbol{r} = \{r_i(k): i = 1,2,....ny\}$ (Eq. (3.15)) while each column is related to one component of the actuator fault vector $\boldsymbol{f_a} = \{ f_{a_j} : j = 1,2,....nu \}$. This expression shows the residual sensitivity to an actuator fault is also a time function whose dynamics and steady-state gain are influenced by the observer gain. Furthermore, such as it was done for the output sensor fault residual sensitivity case, in order to point out this influence, Eq. (3.54) is re-written using the *matrix inversion lemma*:

$$\begin{aligned}
&\boldsymbol{S}_{fa}(q^{-1},\boldsymbol{\theta}) = \left(\boldsymbol{I} - \boldsymbol{H}(q^{-1},\boldsymbol{\theta})\right)\boldsymbol{G}_{fa}(q^{-1},\tilde{\boldsymbol{\theta}}) = \left(\boldsymbol{I} + \boldsymbol{H}_r(q^{-1},\boldsymbol{\theta})\right)^{-1}\boldsymbol{G}_{fa}(q^{-1},\tilde{\boldsymbol{\theta}}) = \\
&= \left(\boldsymbol{I} + \boldsymbol{C}(\boldsymbol{\theta})\left(q\boldsymbol{I} - \boldsymbol{A}(\boldsymbol{\theta})\right)^{-1}\boldsymbol{L}\right)^{-1}\boldsymbol{C}(\tilde{\boldsymbol{\theta}})\left(q\boldsymbol{I} - \boldsymbol{A}(\tilde{\boldsymbol{\theta}})\right)^{-1}\boldsymbol{F}_a(\tilde{\boldsymbol{\theta}})
\end{aligned} \tag{3.55}$$

Analyzing this equation and the associated with the output sensor fault residual sensitivity given by Eq. (3.38), it is seen the effect of the observer gain matrix $\boldsymbol{L}$ on both residual sensitivity equations is the same. Then, its value at time instant $k=0$, i.e. when an abrupt fault (modelled as a unit-step function) occurs, is

$$\boldsymbol{s}_{fa}(0) = \lim_{q\to\infty}\boldsymbol{S}_{fa}(q^{-1},\boldsymbol{\theta}) = \boldsymbol{0} \tag{3.56}$$

independently of the observer gain matrix $\boldsymbol{L}$. The residual sensitivity matrix at this time instant is null, such as it is for the input sensor fault assuming the direct transmission matrix $\boldsymbol{D}$ is zero-valued. That means none actuator fault can be detected at this time instant. According to the effect of the observer gain matrix on this residual sensitivity, it might be expected that the residual sensitivity at fault time occurrence were not zero-valued. But, on the other hand, it should be taken into account that the effect of an actuator fault requires a period of time fixed by the system dynamics till it affects to the system output.

The steady-state value for an abrupt fault modelled as a unit-step function (Gertler, 1998) is given by

$$\begin{aligned}
&\boldsymbol{s}_{fa}(\infty) = \lim_{q\to 1}\boldsymbol{S}_{fa}(q^{-1},\boldsymbol{\theta}) = \lim_{q\to 1}\left[\left(\boldsymbol{I} + \boldsymbol{H}_r(q^{-1},\boldsymbol{\theta})\right)^{-1}\boldsymbol{G}_{fa}(q^{-1},\tilde{\boldsymbol{\theta}})\right] \\
&= \left(\boldsymbol{I} + \boldsymbol{C}(\boldsymbol{\theta})\left(\boldsymbol{I} - \boldsymbol{A}(\boldsymbol{\theta})\right)^{-1}\boldsymbol{L}\right)^{-1}\boldsymbol{C}(\tilde{\boldsymbol{\theta}})\left(\boldsymbol{I} - \boldsymbol{A}(\tilde{\boldsymbol{\theta}})\right)^{-1}\boldsymbol{F}_a(\tilde{\boldsymbol{\theta}})
\end{aligned} \tag{3.57}$$

shows the steady-state value of this sensitivity is influenced by the observation gain matrix $\boldsymbol{L}$ such as it was mentioned for the output sensor fault case (*Section 3.3.2*). Comparing this equation with Eq. (3.56), the following relation between them is obtained for every value of $\boldsymbol{\theta} \in \boldsymbol{\Theta}$:

$$\left|s_{fa_{i,j}}(\infty)\right| \geq \left|s_{fa_{i,j}}(0)\right| \quad i = 1,\cdots,ny \quad j = 1,\cdots,nu \tag{3.58}$$

Unlike the output fault case, an actuator fault is likelier to be detected after its occurrence time instant than when the fault just appears, such as it is for the input sensor fault case. When the simulation approach is considered ($\boldsymbol{L}=\boldsymbol{\theta}$), Eq. (3.57) can be re-written as follows:

$$\boldsymbol{s}_{fa}(\infty)_{\boldsymbol{L}=\boldsymbol{\theta}} = \boldsymbol{C}(\tilde{\boldsymbol{\theta}})\left(\boldsymbol{I}-\boldsymbol{A}(\tilde{\boldsymbol{\theta}})\right)^{-1}\boldsymbol{F}_a(\tilde{\boldsymbol{\theta}}) \tag{3.59}$$

Then, considering the predictor case ($\boldsymbol{L}=\boldsymbol{L_p}$), the Eq. (3.57) becomes:

$$\boldsymbol{s}_{fa}(\infty)_{\boldsymbol{L}=\boldsymbol{L}_p} = \left(\boldsymbol{I}+\boldsymbol{C}(\boldsymbol{\theta})\left(\boldsymbol{I}-\boldsymbol{A}(\boldsymbol{\theta})\right)^{-1}\boldsymbol{L}_p\right)^{-1}\boldsymbol{C}(\tilde{\boldsymbol{\theta}})\left(\boldsymbol{I}-\boldsymbol{A}(\tilde{\boldsymbol{\theta}})\right)^{-1}\boldsymbol{F}_a(\tilde{\boldsymbol{\theta}}) \tag{3.60}$$

According to the influence of matrix $\boldsymbol{L}$ on Eq. (3.57), the following relation is fulfilled by $\boldsymbol{S}_{fa}$:

$$\left|s_{fa_{i,j}}(\infty)_{\boldsymbol{L}=\boldsymbol{L}_p}\right| \le \left|s_{fa_{i,j}}(\infty)_{\boldsymbol{L}=\boldsymbol{L}_o}\right| \le \left|s_{fa_{i,j}}(\infty)_{\boldsymbol{L}=\boldsymbol{\theta}}\right| \quad i=1,\cdots,ny \quad j=1,\cdots,nu \tag{3.61}$$

for every value of $\boldsymbol{\theta}\in\boldsymbol{\Theta}$ and assuming stability. It must be noticed that relation (3.61) is satisfied because the interval observer fulfils the condition given by Eq.(3.32).

3.3.5 Residual in terms of fault sensitivity

Finally, it is also important to notice how the fault residual sensitivity concept (see Eq. (3.36)) determines the value of the residual at each time instant when the monitored system is affected by a fault. Thus, considering the residual internal form given by Eq. (3.20), the residual sensitivity to an output sensor fault, $\boldsymbol{S}_{fy}$ (Eq. (3.37)), to an input sensor fault, $\boldsymbol{S}_{fu}$ (Eq. (3.47)), and to an actuator, $\boldsymbol{S}_{fa}$ (Eq. (3.54)), the residual expression can be re-written as follows:

$$\boldsymbol{r}(k,\boldsymbol{\theta}) = \boldsymbol{r}_0(k,\boldsymbol{\theta}) + \boldsymbol{S}_{fa}(q^{-1},\boldsymbol{\theta})\boldsymbol{f}_a(k) + \boldsymbol{S}_{fy}(q^{-1},\boldsymbol{\theta})\boldsymbol{f}_{fy}(k) + \boldsymbol{S}_{fu}(q^{-1},\boldsymbol{\theta})\boldsymbol{f}_{fu}(k) \tag{3.62}$$

As noticed by (Gertler, 1998) and (Chen et al, 1999), this equation let us understand the importance of the fault residual sensitivity to indicate the fault taking into account that a fault is detected while test (3.24) is not satisfied.

3.4 Minimum detectable fault

3.4.1 Minimum fault concept

As it has been already mentioned in the introduction of this paper, the minimum detectable fault ("***triggering limit***") corresponds to a fault that brings a residual to its threshold, provided no other faults and nuisance inputs are present. Nevertheless, as it was mentioned, this model property is obtained by (Gertler, 1998) considering the residual sensitivity to a fault in steady state. However, this is not right according to the results derived from *Section 3.3*. Then, in this section, the minimum detectable fault concept can be adapted to the interval based fault detection methods as the fault, $\boldsymbol{f}_f^{min}(k)$, whose residual disturbance counteracts the interval observer adaptive threshold from its occurrence time instant, as it will be shown in the following.

Considering the system is just affected by one fault $\boldsymbol{f}(k)$ ($\boldsymbol{f_y}(k)$ or $\boldsymbol{f_a}(k)$ or $\boldsymbol{f_u}(k)$) whose occurrence time instant is given by t_0, the residual can be expressed in terms of the fault according to Eq. (3.62) as it follows:

$$\boldsymbol{r}(k,\boldsymbol{\theta}) = \begin{cases} \boldsymbol{r}_0(k,\boldsymbol{\theta}) + \boldsymbol{d}_f(k,\boldsymbol{\theta}) & k \ge t_0 \\ \boldsymbol{r}_0(k,\boldsymbol{\theta}) & k < t_0 \end{cases} \tag{3.63}$$

for every value of $\boldsymbol{\theta}\in\boldsymbol{\Theta}$ and where

$$\boldsymbol{d}_f(k,\boldsymbol{\theta}) = \boldsymbol{S}_f(q^{-1},\boldsymbol{\theta})\boldsymbol{f}(k)q^{-t_0} \tag{3.64}$$

is the residual disturbance caused by the fault $\boldsymbol{f(k)}$, $\boldsymbol{S_f(k)}$ is the residual sensitivity to that fault, and $\boldsymbol{r_0(k)}$, (Eq. (3.21)), is a vector which contains the effect of the model parameter uncertainty on the residual. Thus, in line with the fault detection test given by Eq. (3.24), its limit condition is given when

$$\bar{\boldsymbol{r}}(k) = \boldsymbol{0} \text{ or } \underline{\boldsymbol{r}}(k) = \boldsymbol{0} \tag{3.65}$$

considered componentwise.

The residual disturbance $\boldsymbol{d_f(k)}$ which allow reaching one of the fault detection limit conditions for those values of $\boldsymbol{\theta} \in \boldsymbol{\Theta}$ such that $\boldsymbol{r}(k) = \bar{\boldsymbol{r}}(k)$ or $\boldsymbol{r}(k) = \underline{\boldsymbol{r}}(k)$ will be noted as $\boldsymbol{d}_f^{\min}(k)$:

$$\boldsymbol{d}_f^{\min}(k) = \begin{cases} \boldsymbol{0} & if \quad k < t_0 \\ -\boldsymbol{r}_0(k) & if \quad k \geq t_0 \end{cases} \tag{3.66}$$

where $\boldsymbol{d}_f^{\min}(k)$ is considered zero-valued when $k< t_0$ because the fault has not occurred yet. Regarding the detection border condition given by Eq. (3.66), it can be considered it takes place when the residual disturbance, $\boldsymbol{d}_f^{\min}(k)$, caused by the fault $\boldsymbol{f(k)}$ counteracts the effect of parameter uncertainty on the residual, $\boldsymbol{r_0(k)}$. Therefore, $\boldsymbol{r_0(k)}$ can be understood as an adaptive threshold associated to the interval observer.

Then, according to the minimum detectable fault concept given at the beginning of this section and, considering Eq. (3.66) and the expression of the residual disturbance caused by the fault $\boldsymbol{f(k)}$ given by Eq. (3.64), the minimum detectable fault function $\boldsymbol{f}_f^{min}(k)$ can be written as it follows:

$$\begin{aligned} &\boldsymbol{f}_f^{min}(k - t_0) = -\boldsymbol{S}_f(q^{-1})^{-1}\boldsymbol{r}_0(k) \\ &k \geq t_0 \end{aligned} \tag{3.67}$$

assuming $\boldsymbol{S_f^{-1}}$exists and for those values of $\boldsymbol{\theta} \in \boldsymbol{\Theta}$ such that $\boldsymbol{r}(k) = \bar{\boldsymbol{r}}(k)$ or $\boldsymbol{r}(k) = \underline{\boldsymbol{r}}(k)$. Thus, a fault $\boldsymbol{f(k)}$ producing a residual disturbance ($\boldsymbol{d}_f(k)$) bigger than the associated to $\boldsymbol{f}_f^{min}(k)$ ($\boldsymbol{d}_f^{min}(k)$) is always detected (*strong fault detection*) in concordance with Eq. (3.65) and fault detection test given by Eq. (3.24), while a fault producing a smaller residual disturbance is never detected.

It must be noticed that the procedure given by Eq. (3.67) presents two drawbacks: the non-existence of $\boldsymbol{S_f^{-1}}$ and the non-causalty of some elements of $\boldsymbol{f}_f^{min}(k)$. The first one occurs when the matrix $\boldsymbol{S_f}$ of dimension *ny x nf* is non-square and can be tackled using the left pseudo-inverse[10], $\boldsymbol{S_f^+}$, of $\boldsymbol{S_f}$. Thus, $\boldsymbol{S_f^+}$ will exist if and only if $ny \geq nf$ meaning that the number of residuals associated to the vector $\boldsymbol{r(k)}$ must be greater or equal than the number of faults associated with the vector $\boldsymbol{f(k)}$. Regarding the second drawback, when some elements of $\boldsymbol{f}_f^{min}(k)$ are non-causal, (Peng et al., 1997) proposes multiplying every of these elements by the required number of delays so that each of them satisfies the causalty property.

In the following, for the clearness of the derived results, it is assumed the existence and stability of $\boldsymbol{S_f^{-1}}$ and the causalty of all the components of $\boldsymbol{f}_f^{min}(k)$.

3.4.2 Fault classification

[10] The expression of $\boldsymbol{S_f^+}$ is given by: $\boldsymbol{S}_f^+(q^{-1}) = \left(\boldsymbol{S}_f^T(q^{-1})\boldsymbol{S}_f(q^{-1})\right)^{-1}\boldsymbol{S}_f^T(q^{-1})$

As follows from the previous section, the minimum detectable fault function evolves with time according to Eq. (3.67) , presenting a maximum and a minimum value for a given observation gain. Hence, the next fault classification from detection point of view can be established:

- ***Non-detectable faults*** are never detected for any period of time because its interval residual disturbance $d_f(k)$ given by Eq. (3.64) is always contained in the corresponding one associated with the minimum detectable fault, $\boldsymbol{d}_f^{min}(k)$, given by Eq. (3.66) and consequently, the fault is never detected.

$$\left[\boldsymbol{S}_f(q^{-1},\boldsymbol{\theta})\boldsymbol{f}(k)q^{-t_0}\right] \subset \left[\boldsymbol{d}_f^{\min}(k,\boldsymbol{\theta})\right] \quad \forall\, k \geq t_0 \tag{3.68}$$

- ***Permanently detected faults*** *(strong fault detection)* are always detected from its occurrence time instant. This group of faults satisfies:

$$\left[\boldsymbol{S}_f(q^{-1},\boldsymbol{\theta})\boldsymbol{f}(k)q^{-t_0}\right] \not\subset \left[\boldsymbol{d}_f^{\min}(k,\boldsymbol{\theta})\right] \quad \forall\, k \geq t_0 \tag{3.69}$$

- ***Non-permanently detected faults*** *(weak fault detection)* are only detected for a period of time but detection does not persist while fault does. These faults satisfy:

$$\left[\boldsymbol{S}_f(q^{-1},\boldsymbol{\theta})\boldsymbol{f}(k)q^{-t_0}\right] \not\subset \left[\boldsymbol{d}_f^{\min}(k,\boldsymbol{\theta})\right] \tag{3.70}$$

  for some time instants, $k \geq t_0$.

In addition, because the residual disturbance caused by a fault and the system adaptive threshold can be adjusted through the observer gain, a non-detectable fault for the given observation gain can become non-permanently detected fault, if a suitable observation gain is set. Thereby, the fault detection time could also be adjusted using the observation gain.

3.4.3 Fault detection time: detection persistence

In order to determine the fault detection time, the detection test (3.24) and its derived limit condition (3.65) must be evaluated. Thus, it is concluded the fault is detected while its effect on the residual (residual disturbance) surpasses the effect of the model structured uncertainty on the residual (interval observer threshold). This condition can be expressed using the following equation:

$$\left[-\boldsymbol{d}_f(k,\boldsymbol{\theta})\right] \not\subset \left[\boldsymbol{r}_0(k,\boldsymbol{\theta})\right] \quad k \geq t_0 \tag{3.71}$$

According to the expressions of the residual disturbance caused by the fault (Eq. (3.64)) and the observer threshold (Eq. (3.21)), the observer gain $\boldsymbol{L}$ has an important influence on the relation (3.71) and as a result, on the fault detection time. Thus, the observer gain dependence of $\boldsymbol{d_f(k)}$ is set by the function $\boldsymbol{S_f}$ (*Section 3.3*) while the observer gain dependence of $\boldsymbol{r_0(k)}$ is set by Eq. (3.33) (*Section 3.2*).

3.4.4 Minimum detectable fault analysis

In this section, the minimum detectable fault function $\boldsymbol{f}_f^{min}(k)$ given by Eq. (3.67) is particularized considering output sensor faults $\boldsymbol{f_y}$, input sensor faults $\boldsymbol{f_u}$ and actuator faults $\boldsymbol{f_a}$. The aim of this particularization is to analyze the effect of the observation gain $\boldsymbol{L}$ on the time evolution of this function. It must be noticed that both the minimum fault function $\boldsymbol{f}_f^{min}(k)$ and the adaptive threshold $\boldsymbol{r_0(k)}$ are theoretical concepts which are not required to be calculated on-line to indicate the fault according to the fault indication test (3.24). However, their analyses will be interesting because they provide a goodness index of the used fault diagnosis algorithm to detect faults. Thus, they help to tune it (*i.e.* using

the observer gain $\boldsymbol{L}$) in order to achieve the fault diagnosis requirements of the monitored system. Moreover, it could be thought that both $\boldsymbol{f}_f^{min}(k)$ and $\boldsymbol{r_0(k)}$ are computed in a initial configuration stage of the diagnosis algorithm.

Moreover, it must be noticed that since this analysis is carried out using vectors and matrices ($\boldsymbol{f_y}$ represents the set of all single faults related to the system output sensors, $\boldsymbol{f_u}$ is the set of all single faults related to the system inputs sensors and $\boldsymbol{f_a}$ is the set of all single faults related to the system actuators), the minimum detectable fault vector $\boldsymbol{f}_f^{min}(k)$ related to certain fault type (output sensor, input sensor or actuator) is obtained assuming a multiple fault scenario where all the single faults of this type must be detected. This approach can give valuable information about the goodness of the used method to detect faults but it can present a high complexity. Thereby, in order to prevent this complexity, this analysis can be carried out for every residual assuming a single fault scenario. As a result, for every residual and for every single fault, a minimum detectable fault function is obtained. Then, for a given single fault scenario, the minimum detectable fault which will be indicated by all the residuals is the one of this set whose absolute value is maximum at every time instant. This approach offers also helpful information about the goodness of the used fault diagnosis approach to diagnose faults. Moreover, it prevents some difficulties derived from the existence of the inverse matrix.

3.4.4.1 Minimum detectable output sensor fault

Considering that the output sensor fault residual sensitivity ($\boldsymbol{S_{fy}}$) is given by Eq. (3.37), the minimum detectable fault function given by Eq. (3.67) can be particularized for the output sensor fault as:

$$\begin{aligned}&\boldsymbol{f}_{fy}^{min}(k-t_0)=-\boldsymbol{S}_{fy}(q^{-1},\boldsymbol{\theta})^{-1}\boldsymbol{r}_0(k)=-\boldsymbol{F}_y(\tilde{\boldsymbol{\theta}})^{-1}\left(\boldsymbol{I}+\boldsymbol{C}(\boldsymbol{\theta})\left(q\boldsymbol{I}-\boldsymbol{A}(\boldsymbol{\theta})\right)^{-1}\boldsymbol{L}\right)\boldsymbol{r}_0(k)\\&k\geq t_0\end{aligned} \tag{3.72}$$

At time instant $k=t_0$ when the fault appears, the value of the minimum detectable output sensor fault is given by

$$\boldsymbol{f}_{fy}^{\min}(0)=-\boldsymbol{s}_{fy}(0)^{-1}\boldsymbol{r}_0(t_0)=-\boldsymbol{F}_y(\tilde{\boldsymbol{\theta}})^{-1}\boldsymbol{r}_0(t_0) \tag{3.73}$$

where $\boldsymbol{s_{fy}(0)}$ is given by Eq. (3.39).Considering matrix $\boldsymbol{F_y}$ is equal to the identity, Eq. (3.73) means the fault must be bigger than the absolute value of the observer threshold at time instant t_0 in order to be detected at its occurrence time instant. As a consequence, given $\boldsymbol{r_0(k)}$ depends on the observation gain $\boldsymbol{L}$ such as it is derived from Eq. (3.21), the fault detection at this time instant depends on the observation gain in spite the residual sensitivity to a fault at this time does not depend on $\boldsymbol{L}$ according to Eq. (3.39). In general, given $\boldsymbol{r_0(k)}$ depends on the observation gain $\boldsymbol{L}$ such as it is derived from Eq. (3.33), the next expression is fulfilled for every element of the vector $\boldsymbol{f}_{fy}^{\min}(0)$:

$$\left|\left(\boldsymbol{f}_{fy}^{\min}(0)_{\boldsymbol{L}=\boldsymbol{L}_p}\right)_i\right|<\left|\left(\boldsymbol{f}_{fy}^{\min}(0)_{\boldsymbol{L}=\boldsymbol{0}}\right)_i\right| \quad i=1,\cdots,ny \tag{3.74}$$

where the subindex 'i' indicates a certain component of the vector $\boldsymbol{f}_{fy}^{\min}(0)$. Eq. (3.74) means that the minimum detectable output sensor fault at fault occurrence time instant is bigger when the simulation approach is considered than when the prediction approach is used.

On the other hand, the steady-state value of Eq. (3.72) is given by

$$\boldsymbol{f}_{fy}^{min}(\infty)=-\boldsymbol{s}_{fy}(\infty)^{-1}\boldsymbol{r}_0(\infty)=-\boldsymbol{F}_y(\tilde{\boldsymbol{\theta}})^{-1}\left(\boldsymbol{I}+\boldsymbol{C}(\boldsymbol{\theta})\left(\boldsymbol{I}-\boldsymbol{A}(\boldsymbol{\theta})\right)^{-1}\boldsymbol{L}\right)\boldsymbol{r}_0(\infty) \tag{3.75}$$

where $\boldsymbol{s_{fy}(\infty)}$ is given by Eq. (3.41) and $\boldsymbol{r_0(\infty)}$ is the steady-state of the adaptive threshold given by Eq. (3.21):

$$\begin{aligned}\boldsymbol{r}_0(\infty)&=\lim_{q\to 1}\left(-\boldsymbol{G}(q^{-1},\boldsymbol{\theta})\right)\boldsymbol{u}_0(\infty)+\lim_{q\to 1}\left(\boldsymbol{I}-\boldsymbol{H}(q^{-1},\boldsymbol{\theta})\right)\boldsymbol{y}_0(\infty)\\&=-\boldsymbol{C}(\boldsymbol{\theta})(\boldsymbol{I}-\boldsymbol{A}_o(\boldsymbol{\theta}))^{-1}\boldsymbol{B}(\boldsymbol{\theta})\boldsymbol{u}_0(\infty)+\left(\boldsymbol{I}-\boldsymbol{C}(\boldsymbol{\theta})(q\boldsymbol{I}-\boldsymbol{A}_o(\boldsymbol{\theta}))^{-1}\boldsymbol{L}\right)\boldsymbol{y}_0(\infty)\end{aligned} \tag{3.76}$$

, assuming matrix $\boldsymbol{D}$ is zero-valued. Thus, using Eq. (3.76), the steady-state of the minimum detectable fault given by Eq. (3.75) can be expressed as follows:

$$\boldsymbol{f}_{fy}^{min}(\infty) = -\boldsymbol{F}_y(\tilde{\boldsymbol{\theta}})^{-1}\left(-\boldsymbol{C}(\boldsymbol{\theta})\left(\boldsymbol{I}-\boldsymbol{A}(\boldsymbol{\theta})\right)^{-1}\boldsymbol{B}(\boldsymbol{\theta})\boldsymbol{u}_0(\infty)+\boldsymbol{y}_0(\infty)\right) \tag{3.77}$$

where a matrix product property[11] is used.

Thus, Eq. (3.77) shows the steady-state value of the minimum detectable output fault does not depend on the observer gains and its absolute value is given by the observer threshold steady-state value when all the observer gains are equal to zero. This is because the observer gain effects on the observer threshold and on the residual sensitivity to a fault counteract each other.

3.4.4.2 Minimum detectable input sensor fault

Considering that the input sensor fault residual sensitivity ($\boldsymbol{S}_{fu}$) is given by Eq. (3.47), the minimum detectable fault function given by Eq. (3.67) can be particularized for the input sensor fault as:

$$\begin{aligned}&\boldsymbol{f}_{fu}^{min}(k-t_0) = -\boldsymbol{S}_{fu}(q^{-1},\boldsymbol{\theta})^{-1}\boldsymbol{r}_0(k) = \boldsymbol{F}_u(\boldsymbol{\theta})^{-1}\left(\boldsymbol{C}(\boldsymbol{\theta})(q\boldsymbol{I}-\boldsymbol{A}_o(\boldsymbol{\theta}))^{-1}\boldsymbol{B}(\boldsymbol{\theta})\right)^{-1}\boldsymbol{r}_0(k)\\ &k \geq t_0\end{aligned} \tag{3.78}$$

where matrix $\boldsymbol{D}$ is considered zero-valued.

At time instant $k=t_0$ when the fault appears, the value of the minimum detectable input sensor fault is given by

$$\boldsymbol{f}_{fu}^{\min}(0) = -\boldsymbol{s}_{fu}(0)^{-1}\boldsymbol{r}_0(t_0) = \boldsymbol{\infty} \tag{3.79}$$

where $\boldsymbol{s}_{fu}(0)$ is given by Eq. (3.48). This expression means that an input sensor fault can not be detected at its occurrence time instant t_0 since the residual sensitivity to this type of fault at this time instant is null such as it was already noticed in *Section 3.3.3*.

On the other hand, the steady-state value of Eq. (3.78) is given by

$$\boldsymbol{f}_{fu}^{min}(\infty) = -\boldsymbol{s}_{fu}(\infty)^{-1}\boldsymbol{r}_0(\infty) = -\boldsymbol{F}_u(\boldsymbol{\theta})^{-1}\left(\boldsymbol{u}_0(\infty)+\left(-\boldsymbol{C}(\boldsymbol{\theta})\left(q\boldsymbol{I}-\boldsymbol{A}(\boldsymbol{\theta})\right)^{-1}\boldsymbol{B}(\boldsymbol{\theta})\right)^{-1}\boldsymbol{y}_0(\infty)\right) \tag{3.80}$$

using $\boldsymbol{s}_{fu}(\infty)$ given by Eq (3.49), the steady-state of the adaptive threshold, $\boldsymbol{r}_0(\infty)$, given by Eq. (3.76) and the *matrix product property*.

Eq. (3.80) shows the steady-state value of the minimum detectable input sensor fault does not depend on the observer gains such as it was determined in *Section 3.4.4.1* when the output sensor fault case was considered. This is also because the observer gain effects on the observer threshold and on the residual sensitivity to a fault counteract each other.

Regarding the transient-state values of $\boldsymbol{f}_{fu}^{min}$, the influence of the observer gain matrix $\boldsymbol{L}$ is very similar to the minimum detectable output sensor fault case (*Section 3.4.4.1*). Thus, as a consequence of the dependence of the adaptive threshold $\boldsymbol{r}_0(k)$ (Eq. (3.21)) on $\boldsymbol{L}$ described by Eq. (3.33), it can be set that, in general, the lower the norm of $\boldsymbol{L}$, the bigger the instant value of $\boldsymbol{f}_{fu}^{min}$ is. Then, once this function reaches its steady-state, its value does not depend on $\boldsymbol{L}$ (Eq. (3.80)) such as mentioned above.

3.4.4.3 Minimum detectable actuator fault

[11] Matrix product property: $\left(\boldsymbol{A}_x-\boldsymbol{B}_x\boldsymbol{D}_x^{-1}\boldsymbol{C}_x\right)^{-1}\boldsymbol{B}_x\boldsymbol{D}_x^{-1} = \boldsymbol{A}_x^{-1}\boldsymbol{B}_x\left(\boldsymbol{D}_x-\boldsymbol{C}_x\boldsymbol{A}_x^{-1}\boldsymbol{B}_x\right)^{-1}$ being $\boldsymbol{A}_x=\boldsymbol{I}$, $\boldsymbol{B}_x=\boldsymbol{C}(\boldsymbol{\theta})$, $\boldsymbol{D}_x=(q\boldsymbol{I}-\boldsymbol{A}_O(\boldsymbol{\theta}))$ and $\boldsymbol{C}_x=\boldsymbol{L}$.

Considering that the actuator fault residual sensitivity ($\boldsymbol{S_{fa}}$) is given by Eq. (3.54), the minimum detectable fault function given by Eq. (3.67) can be particularized for the actuator fault as:

$$\begin{aligned} &\boldsymbol{f}_{fa}^{min}(k-t_0) = -\boldsymbol{S}_{fa}(q^{-1},\boldsymbol{\theta})^{-1}\boldsymbol{r}_0(k) = -\boldsymbol{G}_{fa}(q^{-1},\tilde{\boldsymbol{\theta}})^{-1}\left(\boldsymbol{I}+\boldsymbol{C}(\boldsymbol{\theta})\left(q\boldsymbol{I}-\boldsymbol{A}(\boldsymbol{\theta})\right)^{-1}\boldsymbol{L}\right)\boldsymbol{r}_0(k) \\ &k \geq t_0 \end{aligned} \tag{3.81}$$

where $\boldsymbol{G_{fa}}$ is given by Eq. (3.5).

At time instant $k=t_0$ when the fault appears, the value of the minimum detectable actuator fault is given by

$$\boldsymbol{f}_{fa}^{\min}(0) = -\boldsymbol{s}_{fa}(0)^{-1}\boldsymbol{r}_0(t_0) = \boldsymbol{\infty} \tag{3.82}$$

where $\boldsymbol{s_{fa}(0)}$ is given by Eq. (3.56). This expression means that an actuator fault can not be detected at its occurrence time instant t_0 since the residual sensitivity to this type of fault at this time instant is null such as it was mentioned in *Section 3.3.4*

Conversely, the steady-state value of Eq. (3.81) is given by

$$\begin{aligned} &\boldsymbol{f}_{fa}^{min}(\infty) = -\boldsymbol{s}_{fa}(\infty)^{-1}\boldsymbol{r}_0(\infty) \\ &= -\left(\boldsymbol{C}(\tilde{\boldsymbol{\theta}})(\boldsymbol{I}-\boldsymbol{A}(\tilde{\boldsymbol{\theta}}))^{-1}\boldsymbol{F}_a(\tilde{\boldsymbol{\theta}})\right)^{-1}\left(-\boldsymbol{C}(\boldsymbol{\theta})\left(\boldsymbol{I}-\boldsymbol{A}(\boldsymbol{\theta})\right)^{-1}\boldsymbol{B}(\boldsymbol{\theta})\boldsymbol{u}_0(\infty)+\boldsymbol{y}_0(\infty)\right) \end{aligned} \tag{3.83}$$

using $\boldsymbol{s_{fa}(\infty)}$ given by Eq. (3.57), the steady-state of the adaptive threshold given by Eq.(3.76) and the matrix product property.

Eq. (3.83) shows the steady-state value of the minimum detectable input sensor fault does not depend on the observer gains such as it was determined in *Section 3.4.2* when the output sensor fault case was considered. This is also because the observer gain effects on the observer threshold and on the residual sensitivity to a fault counteract each other.

Concerning the influence of the observer gain matrix $\boldsymbol{L}$ on the transient-state values of $\boldsymbol{f}_{fa}^{min}$, the same behaviour can be stated in regard to $\boldsymbol{f}_{fy}^{min}$ (*Section 3.4.4.1*) and $\boldsymbol{f}_{fu}^{min}$ (*Section 3.4.4.2*).

3.5 Application example

3.5.1 Description

The application example proposed to illustrate the obtained results deals with a mineral grinding-classification process used in (Maquin et al., 2000). This process, such as presented in this reference is composed by two grinding machines (B_1 and B_2) and three mineral separators (H_1, H_2 and H_3). Each separator classifies the mineral particles in two types depending on their size. The only input of the process ($u(t)$) is the input mineral flow, while the only output ($y(t)$) is the output mineral flow whose mineral particles have the required size. On the other hand, this reference considers two non-measured states: the output mineral flow of B_2 ($x_2(t)$) and the output mineral flow of B_1 ($x_1(t)$). Besides, the considered process parameters are the time constants of B_1 and B_2 (T_1 = 300 s. and T_2 = 60 s.) and the separation coefficients of H_1, H_2 and H_3 (c_1 = 0.5, c_2 = 0.3 and c_3 = 0.1).

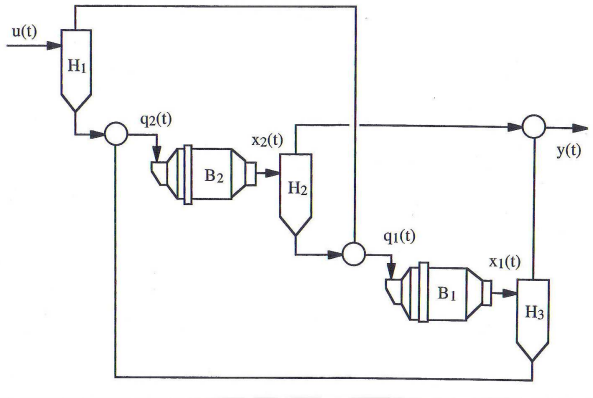

Fig. 3.1 Scheme of the mechanical treatment unity to grind and classify a mineral flow

Nonetheless, in order to show all derived conclusions showed in the previous sections, some adaptations of the application used in (Maquin et al., 2000) are considered in this paper. On one hand, parameter uncertainty is considered in order to illustrate the interval observer case and on the other hand, the system output will not be given by *y(t)* but by the states $x_1(t)$ and $x_2(t)$. As a result, the application used in this section is based on a SIMO system with two outputs instead of a SISO system with one output such as used initially in (Maquin et al., 2000). Thus, in order to build up the related interval observer, it is assumed that both states are measured. Then, the state-space form in discrete time of the linear dynamic process is given by

$$\begin{bmatrix} x_1(k+1) \\ x_2(k+1) \end{bmatrix} = \begin{bmatrix} a_{11} & a_{12} \\ a_{21} & a_{22} \end{bmatrix} \begin{bmatrix} x_1(k) \\ x_2(k) \end{bmatrix} + \begin{bmatrix} b_{11} \\ b_{21} \end{bmatrix} u(k-1)$$
$$\boldsymbol{y}(k) = \begin{bmatrix} y_1(k) \\ y_2(k) \end{bmatrix} = \begin{bmatrix} x_1(k) \\ x_2(k) \end{bmatrix} \tag{3.84}$$
$$a_{11} = 1 - \frac{T_s}{T_1},\ a_{12} = c_2 \frac{T_s}{T_1},\ a_{21} = c_3 \frac{T_s}{T_2},\ a_{22} = 1 - \frac{T_s}{T_2},\ b_{11} = (1-c_1)\frac{T_s}{T_1},\ b_{21} = c_1 \frac{T_s}{T_2}$$

taking into account that ***y(k)*** is the output vector of the adapted application example and where T_s is the sample period, which must be chosen according to the eigenvalues of the state-space matrix (nominal value) in continuous time. According to (Maquin et al., 2000), these eigenvalues are: $\lambda_1 = -3.216\times10^{-3}\,s^{-1}$ and $\lambda_2 = -1.678\times10^{-2}\,s^{-1}$. In this case, T_s=*5.95 s.* is used. The input mineral flow considered in this example is *u(k)=1 Kg/s*. Moreover, the time instant *k=0* is considered as the system start-up time instant and therefore, before that time instant the system was not working. Thus, the monitored system initial conditions are assumed to be zero-valued.

Thereby, the related interval observer expressed in its state-space form (Eq. (3.7)) is

$$\begin{bmatrix} \hat{y}_1(k+1) \\ \hat{y}_2(k+1) \end{bmatrix} = \begin{bmatrix} a_{11} & a_{12} \\ a_{21} & a_{22} \end{bmatrix} \begin{bmatrix} \hat{y}_1(k) \\ \hat{y}_2(k) \end{bmatrix} + \begin{bmatrix} b_{11} \\ b_{21} \end{bmatrix} u(k) + \begin{bmatrix} k_{11} & k_{12} \\ k_{21} & k_{22} \end{bmatrix} \left(\begin{bmatrix} y_1(k) \\ y_2(k) \end{bmatrix} - \begin{bmatrix} \hat{y}_1(k) \\ \hat{y}_2(k) \end{bmatrix} \right) \tag{3.85}$$

where $a_{11} \in [0.9752, 0.9850]$, $a_{12} \in [0.0059, 0.0060]$, $a_{21} \in [0.0099, 0.01]$ and $a_{22} \in [0.8962, 0.9052]$ are the uncertain elements of observer state-space matrix whose nominal values are given by the expressions shown in Eq. (3.84); $b_{11} \in [0.0098, 0.01]$ and $b_{21} \in [0.0492, 0.0501]$ are the uncertain elements of the observer input matrix; k_{11}, k_{12}, k_{21} and k_{22} are the elements of the observer gain matrix.

The input-output form of this interval observer can be written using Eq. (3.11) and Eq. (3.85) can be written as:

$$\hat{\boldsymbol{y}}(k)=\boldsymbol{G}(q^{-1},\boldsymbol{\theta})\boldsymbol{u}(k)+\boldsymbol{H}(q^{-1},\boldsymbol{\theta})\boldsymbol{y}(k)=\begin{bmatrix}\hat{y}_1(k)\\ \hat{y}_2(k)\end{bmatrix}=\begin{bmatrix}\dfrac{b_{11}q^{-1}+\left(a^o_{12}b_{21}-a^o_{22}b_{11}\right)q^{-2}}{1-\left(a^o_{22}+a^o_{11}\right)q^{-1}+\left(a^o_{11}a^o_{22}-a^o_{12}a^o_{21}\right)q^{-2}}\\ \dfrac{b_{21}q^{-1}+\left(a^o_{21}b_{11}-a^o_{11}b_{21}\right)q^{-2}}{1-\left(a^o_{22}+a^o_{11}\right)q^{-1}+\left(a^o_{11}a^o_{22}-a^o_{12}a^o_{21}\right)q^{-2}}\end{bmatrix}u(k)+$$
$$+\begin{bmatrix}\dfrac{k_{11}q^{-1}+\left(a^o_{12}k_{21}-a^o_{22}k_{11}\right)q^{-2}}{1-\left(a^o_{22}+a^o_{11}\right)q^{-1}+\left(a^o_{11}a^o_{22}-a^o_{12}a^o_{21}\right)q^{-2}} & \dfrac{k_{12}q^{-1}+\left(a^o_{12}k_{22}-a^o_{22}k_{12}\right)q^{-2}}{1-\left(a^o_{22}+a^o_{11}\right)q^{-1}+\left(a^o_{11}a^o_{22}-a^o_{12}a^o_{21}\right)q^{-2}}\\ \dfrac{k_{21}q^{-1}+\left(a^o_{21}k_{11}-a^o_{11}k_{21}\right)q^{-2}}{1-\left(a^o_{22}+a^o_{11}\right)q^{-1}+\left(a^o_{11}a^o_{22}-a^o_{12}a^o_{21}\right)q^{-2}} & \dfrac{k_{22}q^{-1}+\left(a^o_{21}k_{12}-a^o_{11}k_{22}\right)q^{-2}}{1-\left(a^o_{22}+a^o_{11}\right)q^{-1}+\left(a^o_{11}a^o_{22}-a^o_{12}a^o_{21}\right)q^{-2}}\end{bmatrix}\begin{bmatrix}y_1(k)\\ y_2(k)\end{bmatrix} \quad (3.86)$$

where $a^o_{11}=a_{11}-k_{11}$, $a^o_{12}=a_{12}-k_{12}$, $a^o_{21}=a_{21}-k_{21}$ and $a^o_{22}=a_{22}-k_{22}$.

In the following, the residual sensitivity to a fault, the interval adaptive threshold and the minimum detectable fault will be evaluated using the model parameters that allow computing $\bar{\hat{\mathbf{y}}}(k)$ which must be obtained applying Eq. (3.10) and using a suitable algorithm as the one presented in (Puig et al., 2006). In the considered application example, according to (Cugueró et al., 2002), $\bar{\hat{\mathbf{y}}}(k)$ is obtained when $\boldsymbol{\theta}=\overline{\boldsymbol{\theta}}$, while $\underline{\hat{\boldsymbol{y}}}(k)$ is when $\boldsymbol{\theta}=\underline{\boldsymbol{\theta}}$ since all the elements of the state-space matrix are positive. This fact is fully irrelevant for the results described in this chapter since it does not focus on the computation of the system output estimation interval but on the fault detection performace related to an interval observer model and on the influence of $\boldsymbol{L}$ on this performance.

In the following, the residual sensitivity to a fault, the interval adaptive threshold and the minimum detectable fault will be evaluated using the model parameters that allow computing $\bar{\hat{y}}(k)$. According to (Cugueró et al., 2002), $\bar{\hat{y}}(k)$ is obtained when $\boldsymbol{\theta}=\overline{\boldsymbol{\theta}}$, while $\underline{\hat{y}}(k)$ is when $\boldsymbol{\theta}=\underline{\boldsymbol{\theta}}$ since all the elements of the state-space matrix are positive.

Regarding the interval observer residual, its expression using the q^{-1} transform is

$$\boldsymbol{r}(k)=-\boldsymbol{G}(q^{-1},\boldsymbol{\theta})\boldsymbol{u}(k)+\left(\boldsymbol{I}-\boldsymbol{H}(q^{-1},\boldsymbol{\theta})\right)\boldsymbol{y}(k)=\begin{bmatrix}r_1(k)\\ r_2(k)\end{bmatrix}=-\begin{bmatrix}\dfrac{b_{11}q^{-1}+\left(a^o_{12}b_{21}-a^o_{22}b_{11}\right)q^{-2}}{1-\left(a^o_{22}+a^o_{11}\right)q^{-1}+\left(a^o_{11}a^o_{22}-a^o_{12}a^o_{21}\right)q^{-2}}\\ \dfrac{b_{21}q^{-1}+\left(a^o_{21}b_{11}-a^o_{11}b_{21}\right)q^{-2}}{1-\left(a^o_{22}+a^o_{11}\right)q^{-1}+\left(a^o_{11}a^o_{22}-a^o_{12}a^o_{21}\right)q^{-2}}\end{bmatrix}u(k)+$$
$$+\begin{bmatrix}\dfrac{1-\left(a^o_{22}+a_{11}\right)q^{-1}+\left(a_{11}a^o_{22}-a^o_{12}a_{21}\right)q^{-2}}{1-\left(a^o_{22}+a^o_{11}\right)q^{-1}+\left(a^o_{11}a^o_{22}-a^o_{12}a^o_{21}\right)q^{-2}} & \dfrac{-k_{12}q^{-1}-\left(a^o_{12}k_{22}-a^o_{22}k_{12}\right)q^{-2}}{1-\left(a^o_{22}+a^o_{11}\right)q^{-1}+\left(a^o_{11}a^o_{22}-a^o_{12}a^o_{21}\right)q^{-2}}\\ \dfrac{-k_{21}q^{-1}-\left(a^o_{21}k_{11}-a^o_{11}k_{21}\right)q^{-2}}{1-\left(a^o_{22}+a^o_{11}\right)q^{-1}+\left(a^o_{11}a^o_{22}-a^o_{12}a^o_{21}\right)q^{-2}} & \dfrac{1-\left(a_{22}+a^o_{11}\right)q^{-1}+\left(a^o_{11}a_{22}-a_{12}a^o_{21}\right)q^{-2}}{1-\left(a^o_{22}+a^o_{11}\right)q^{-1}+\left(a^o_{11}a^o_{22}-a^o_{12}a^o_{21}\right)q^{-2}}\end{bmatrix}\begin{bmatrix}y_1(k)\\ y_2(k)\end{bmatrix} \quad (3.87)$$

where $\boldsymbol{r}(k)=[r_1(k)\ r_2(k)]^T$

3.5.2 Sensitivity of the residual to an output sensor fault

According to *Section 3.3.2,* the sensitivity of the residual to a sensor fault is given by Eq. (3.37). When particularizing this property for the application example case, this function becomes a square matrix of dimension 2×2 whose expression, considering $\boldsymbol{F}_y$ is equal to the identity $\boldsymbol{I}$, is

$$\boldsymbol{S}_{fy}(q^{-1},\boldsymbol{\theta})=\left(\boldsymbol{I}-\boldsymbol{H}(q^{-1},\boldsymbol{\theta})\right)\boldsymbol{G}_{fy}(q^{-1},\tilde{\boldsymbol{\theta}})=\begin{bmatrix} S_{fy_{1,1}} & S_{fy_{1,2}} \\ S_{fy_{2,1}} & S_{fy_{2,2}} \end{bmatrix}=$$

$$=\begin{bmatrix} \dfrac{1-\left(a_{22}^{o}+a_{11}\right)q^{-1}+\left(a_{11}a_{22}^{o}-a_{12}^{o}a_{21}\right)q^{-2}}{1-\left(a_{22}^{o}+a_{11}^{o}\right)q^{-1}+\left(a_{11}^{o}a_{22}^{o}-a_{12}^{o}a_{21}^{o}\right)q^{-2}} & \dfrac{-k_{12}q^{-1}-\left(a_{12}^{o}k_{22}-a_{22}^{o}k_{12}\right)q^{-2}}{1-\left(a_{22}^{o}+a_{11}^{o}\right)q^{-1}+\left(a_{11}^{o}a_{22}^{o}-a_{12}^{o}a_{21}^{o}\right)q^{-2}} \\ \dfrac{-k_{21}q^{-1}-\left(a_{21}^{o}k_{11}-a_{11}^{o}k_{21}\right)q^{-2}}{1-\left(a_{22}^{o}+a_{11}^{o}\right)q^{-1}+\left(a_{11}^{o}a_{22}^{o}-a_{12}^{o}a_{21}^{o}\right)q^{-2}} & \dfrac{1-\left(a_{22}+a_{11}^{o}\right)q^{-1}+\left(a_{11}^{o}a_{22}-a_{12}a_{21}^{o}\right)q^{-2}}{1-\left(a_{22}^{o}+a_{11}^{o}\right)q^{-1}+\left(a_{11}^{o}a_{22}^{o}-a_{12}^{o}a_{21}^{o}\right)q^{-2}} \end{bmatrix} \tag{3.88}$$

where each function $S_{fy_{i,j}}$ is the sensitivity of the residual $r_i(k)$($r_1(k)$ or $r_2(k)$) regarding a fault affecting the sensor related to the output $y_j(k)$ ($y_1(k)$ or $y_2(k)$).

Considering the observer gain parameterization $k_{ij}=la_{ij}$ ($i=1,2$ and $j=1,2$) and assuming an abrupt fault modelled as a unit-step function, the time evolution of $S_{fy_{1,1}}$ and $S_{fy_{2,1}}$ are drawn varying l from simulation (l=0) to prediction (l=1) , being the sweeping interval $\Delta l=0.04$ and where the time unit is set by a sample period.

Fig. 3.2[12] shows the residual sensitivity function $S_{fy_{1,1}}$ does not depend on the observation gain at fault occurrence time instant being equal to one according to Eq. (3.39) when $\boldsymbol{F_y}=\boldsymbol{I}$, while its steady-state value does: it is equal to the initial value for simulators while it is smaller than this value for predictors according to what is derived in *Section 3.3.2* (Eq. (3.45)). Besides, the greater the observation gain is, the faster the dynamics of the residual sensitivity is and consequently, the fault detection of a predictor approach could only last during few time steps unlike observer and simulator approach.

Regarding the time evolution of the residual sensitivity function $S_{fy_{2,1}}$ plotted in *Fig*. 3.3, this function does not depend on the observation gain at fault occurrence time instant either being its value null such as derived from Eq. (3.39). It must be taken into account that the existence of this function is because of the use of the observation gains meaning that $S_{fy_{2,1}}$ is zero-valued for every time instant when the simulation approach is used (*Fig*. 3.2)(Eq. (3.38)). Concerning the steady-state of this function, it presents a maximum for a given value between simulation and prediction which is obtained for $l=0.04$ in *Fig. 3.3* (Eq. (3.46)).

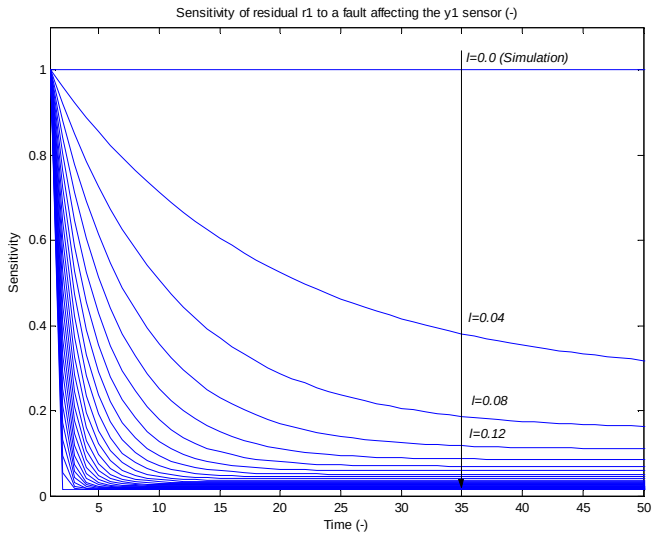

Fig. 3.2 Time evolution of the sensitivity of residual $r_1(k)$ to an abrupt fault affecting the output sensor $y_1(k)$ regarding the observation gain when $\hat{y}(k)=\bar{\hat{y}}(k)$

[12] The arrow direction drawn in the figure sets the direction in which the observer gain increases its value.

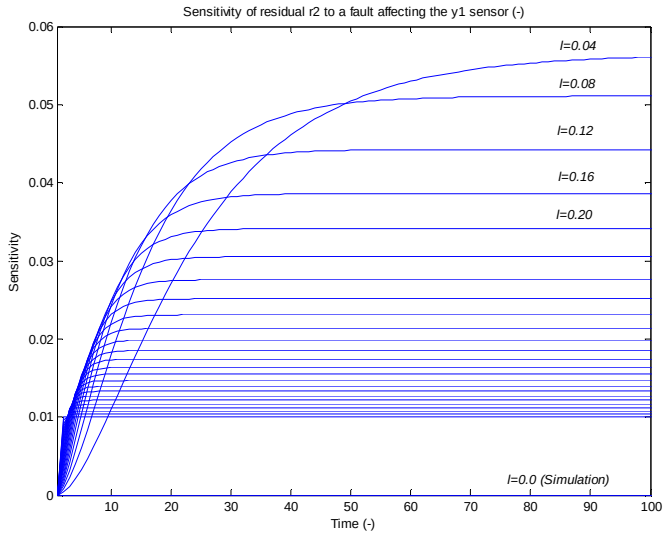

Fig. 3.3 Time evolution of the sensitivity of residual $r_2(k)$ to an abrupt fault affecting the output sensor $y_1(k)$ regarding the observation gain when $\hat{y}(k) = \bar{\hat{y}}(k)$

3.5.3 Sensitivity of the residual to an input sensor fault

The sensitivity of the residual to a sensor fault is given by Eq. (3.47) (see *Section 3.3.3)*. Thereby, considering the application example, this function becomes a matrix of dimension 2×1 whose expression, considering $\boldsymbol{F_u}$ is equal to the identity $\boldsymbol{I}$, is:

$$\boldsymbol{S}_{fu}(q^{-1},\boldsymbol{\theta}) = -\boldsymbol{G}(q^{-1},\boldsymbol{\theta})\boldsymbol{F}_u(\boldsymbol{\theta}) = \begin{bmatrix} S_{fu_{1,1}} \\ S_{fu_{2,1}} \end{bmatrix} = -\begin{bmatrix} \dfrac{b_{11}q^{-1} + \left(a_{12}^o b_{21} - a_{22}^o b_{11}\right)q^{-2}}{1 - \left(a_{22}^o + a_{11}^o\right)q^{-1} + \left(a_{11}^o a_{22}^o - a_{12}^o a_{21}^o\right)q^{-2}} \\ \dfrac{b_{21}q^{-1} + \left(a_{21}^o b_{11} - a_{11}^o b_{21}\right)q^{-2}}{1 - \left(a_{22}^o + a_{11}^o\right)q^{-1} + \left(a_{11}^o a_{22}^o - a_{12}^o a_{21}^o\right)q^{-2}} \end{bmatrix} \tag{3.89}$$

Considering the parameterization $k_{ij}=la_{ij}$ ($i=1,2$ and $j=1,2$), the time evolution of the residual sensitivity function $S_{fu_{1,1}}$ without taking into account the sign of Eq. (3.89) is drawn varying l from simulation ($l=0$) to prediction ($l=1$), being the sweeping interval $\Delta l=0.04$.

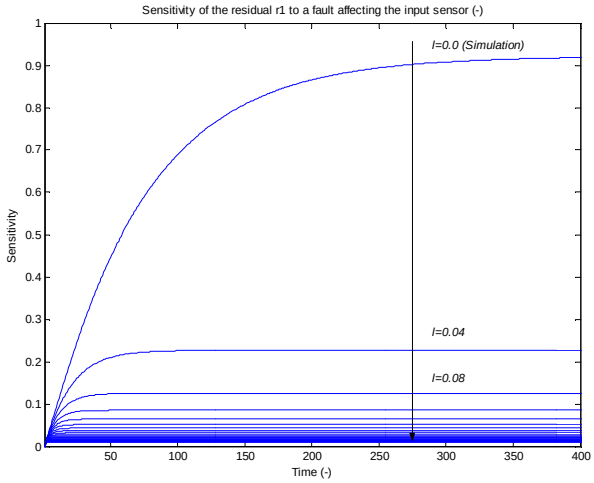

Fig. 3.4 Time evolution of the sensitivity of residual $r_1(k)$ to an abrupt fault affecting the input sensor regarding the observation gain when $\hat{y}(k) = \bar{\hat{y}}(k)$

In *Fig*. 3.4, the residual sensitivity function $S_{fu_{1,1}}$ does not depend on the observation gain at initial time instant either and it is equal to zero according to Eq. (3.48) when matrix $\boldsymbol{D}\approx\boldsymbol{0}$. On the other hand, its dynamics and steady-state value show a similar observation gain dependency to the output sensor fault case. As it can be seen, *Fig. 3.4* is in concordance with results presented in *Section 3.3.3*, specially, the fulfillment of the relation given by Eq. (3.53).

3.5.4 Sensitivity of the residual to an actuator fault

Finally, the sensitivity of the residual to an actuator fault is given by Eq. (3.54)(see *Section* 3.3.4). In the application example case, this function becomes a matrix of dimension 2×1. Regarding $\boldsymbol{G_{fa}}$ (Eq. (3.5)), it is assumed that satisfies the following expression:

$$\boldsymbol{G}_{fa}(q^{-1},\tilde{\boldsymbol{\theta}}) = \boldsymbol{G}(q^{-1},\tilde{\boldsymbol{\theta}})_{\boldsymbol{L=\theta}} = \begin{bmatrix} G_{y1} \\ G_{y2} \end{bmatrix} \tag{3.90}$$

where the value of the function $\boldsymbol{G}$ (Eq. (3.12)) is given by Eq. (3.86) in this application example case. Then, the expression of the residual sensitivity to actuator fault is given by

$$\begin{aligned} \boldsymbol{S}_{fa}(q^{-1},\boldsymbol{\theta}) &= \big(\boldsymbol{I}-\boldsymbol{H}(q^{-1},\boldsymbol{\theta})\big)\boldsymbol{G}_{fa}(q^{-1},\tilde{\boldsymbol{\theta}}) = \begin{bmatrix} S_{fa_{1,1}} \\ S_{fa_{2,1}} \end{bmatrix} = \begin{bmatrix} S_{fy_{1,1}} & S_{fy_{1,2}} \\ S_{fy_{2,1}} & S_{fy_{2,2}} \end{bmatrix} \begin{bmatrix} G_{y_1} \\ G_{y_2} \end{bmatrix} = \\ &= \begin{bmatrix} \dfrac{1-\left(a_{22}^o+a_{11}\right)q^{-1}+\left(a_{11}a_{22}^o-a_{12}^oa_{21}\right)q^{-2}}{1-\left(a_{22}^o+a_{11}^o\right)q^{-1}+\left(a_{11}^oa_{22}^o-a_{12}^oa_{21}^o\right)q^{-2}}G_{y1} + \dfrac{-k_{12}q^{-1}-\left(a_{12}^ok_{22}-a_{22}^ok_{12}\right)q^{-2}}{1-\left(a_{22}^o+a_{11}^o\right)q^{-1}+\left(a_{11}^oa_{22}^o-a_{12}^oa_{21}^o\right)q^{-2}}G_{y2} \\ \dfrac{-k_{21}q^{-1}-\left(a_{21}^ok_{11}-a_{11}^ok_{21}\right)q^{-2}}{1-\left(a_{22}^o+a_{11}^o\right)q^{-1}+\left(a_{11}^oa_{22}^o-a_{12}^oa_{21}^o\right)q^{-2}}G_{y1} + \dfrac{1-\left(a_{22}+a_{11}^o\right)q^{-1}+\left(a_{11}^oa_{22}-a_{12}a_{21}^o\right)q^{-2}}{1-\left(a_{22}^o+a_{11}^o\right)q^{-1}+\left(a_{11}^oa_{22}^o-a_{12}^oa_{21}^o\right)q^{-2}}G_{y2} \end{bmatrix} \end{aligned} \tag{3.91}$$

Then, the time evolution of $S_{fa_{1,1}}$ considering the parameterization $k_{ij}=la_{ij}$ ($i=1,2$ and $j=1,2$) can be drawn varying l from simulation ($l=0$) to prediction ($l=1$). In this case, the resulting figure looks like the one obtained in the input sensor fault case (*Fig. 3.4*).

As it was discussed in *Section 3.3.4*, the residual sensitivity to an actuator fault does not depend on the observation gain at initial time instant either being zero-valued (Eq. (3.56)). On the other hand, its dynamics and its steady-state value show a similar observation gain dependency regarding the input sensor fault case. In short, these results are in line with what was presented in *Section 3.3.4*, highlighting the relation given by Eq. (3.61).

3.5.5 Interval observer adaptive threshold

According to Eq. (3.63), the interval observer adaptive threshold $\boldsymbol{r_0(k)}$ might be obtained from Eq. (3.87) assuming there are no faults and as a result, $\boldsymbol{r_0(k)}$ is a vector of dimension 2×1 ($\boldsymbol{r_0(k)}=[\, r_{01}(k)\ r_{02}(k)]^T$). Thus, the time evolution of the lower bound of $\boldsymbol{r_{01}(k)}$ related to $\hat{y}_1(k)=\overline{\hat{y}}_1(k)$ is drawn varying l ($k_{ij}=la_{ij}$ ($i=1,2$ and $j=1,2$)) from simulation ($l=0$) to prediction ($l=1$) without taking into account the sign of Eq. (3.87) and being the sweeping interval $\Delta l=0.04$.

Fig. 3.5 shows the influence of the observer gains on the threshold dynamics and its steady-state value. In the simulation approach ($l=0$), the parameter uncertainty has the maximum effect on the adaptive threshold and consequently, the maximum residual disturbance caused by the fault is required in order to be detected. This figure illustrates the fulfillment of the interval threshold relation given by Eq. (3.33).

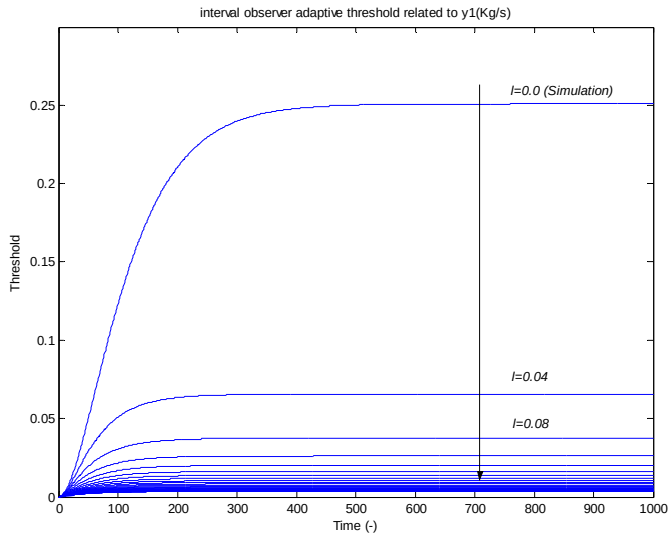

Fig. 3.5 Time evolution of the lower bound of the interval observer adaptive threshold $r_{0l}(k)$ regarding the observation gain considering an abrupt step system input given by $u(k)=1$ *Kg/s*

3.5.6 Minimum detectable output sensor fault function

As mentioned previously, the minimum detectable output sensor fault is given by Eq. (3.67) using the residual sensitivity to an output sensor fault given by Eq. (3.37) and the interval observer adaptive threshold given by Eq. (3.21) .Thereby, when particularizing this expression for the example application case, it becomes a vector of dimension 2×1 which can be obtained using the residual sensitivity to an output sensor fault given by Eq. (3.88) and the interval adaptive threshold obtained using the residual equation (Eq. (3.87)) such as mentioned in the previous section. Thus, its expression is

$$\begin{aligned}
&\boldsymbol{f}_{fy}^{\min}(k-t_0) = -\boldsymbol{S}_{fy}(q^{-1},\boldsymbol{\theta})^{-1}\boldsymbol{r}_0(k) = \begin{bmatrix} f_{fy_1}^{\min}(k-t_0) \\ f_{fy_2}^{\min}(k-t_0) \end{bmatrix} = -\begin{bmatrix} S_{fy_{1,1}} & S_{fy_{1,2}} \\ S_{fy_{2,1}} & S_{fy_{2,2}} \end{bmatrix}^{-1} \begin{bmatrix} r_{01}(k) \\ r_{02}(k) \end{bmatrix} = \\
&= \begin{bmatrix} \dfrac{1-\left(a_{22}+a_{11}^o\right)q^{-1}+\left(a_{22}a_{11}^o-a_{12}a_{21}^o\right)q^{-2}}{1-\left(a_{22}+a_{11}\right)q^{-1}+\left(a_{22}a_{11}-a_{12}a_{21}\right)q^{-2}} r_{01}(k) + \dfrac{k_{12}q^{-1}+\left(k_{22}a_{12}-k_{12}a_{22}\right)q^{-2}}{1-\left(a_{22}+a_{11}\right)q^{-1}+\left(a_{22}a_{11}-a_{12}a_{21}\right)q^{-2}} r_{02}(k) \\ \dfrac{k_{21}q^{-1}+\left(k_{11}a_{21}-k_{21}a_{11}\right)q^{-2}}{1-\left(a_{22}+a_{11}\right)q^{-1}+\left(a_{22}a_{11}-a_{12}a_{21}\right)q^{-2}} r_{01}(k) + \dfrac{1-\left(a_{11}+a_{22}^o\right)q^{-1}+\left(a_{11}a_{22}^o-a_{21}a_{12}^o\right)q^{-2}}{1-\left(a_{22}+a_{11}\right)q^{-1}+\left(a_{22}a_{11}-a_{12}a_{21}\right)q^{-2}} r_{02}(k) \end{bmatrix} \\
&k \geq t_0
\end{aligned} \tag{3.92}$$

where it must be noticed that both $f_{fy_1}^{min}$ and $f_{fy_1}^{min}$ are causal functions. In the following, the time evolution of $f_{fy_1}^{min}$ given by Eq. (3.92) when $\boldsymbol{\theta}=\bar{\boldsymbol{\theta}}$ and t_0= *200* is plotted varying l ($k_{ij}=la_{ij}$ ($i=1,2$ and $j=1,2$)) from simulation ($l=0$) to prediction ($l=1$), being the sweeping interval $\Delta l=0.04$. It must be taken into account that at this fault occurrence time instant (t_0) the system is still at its transient state.

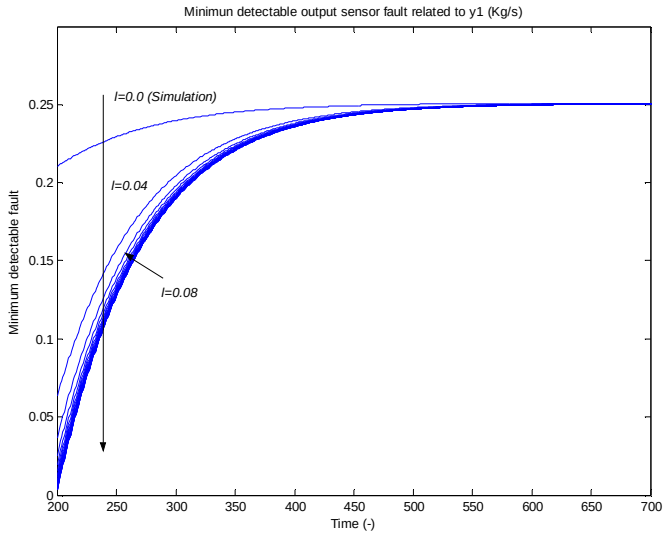

Fig. 3.6 Time evolution of the minimum detectable output sensor fault related to $y_1(k)$ regarding the observation gain when $\boldsymbol{\theta}=\overline{\boldsymbol{\theta}}$ and $t_0=200$.

In *Fig.* 3.6 ($t_0=200$), the observer gain dependence is such as described by Eq. (3.72). At time instant $t_0=200$, when fault occurs, its initial value is just determined by the threshold value at this time instant. This is because the system has not reached its steady state yet. Then, the observer gains have an influence on the threshold dynamics and thus, on the minimum detectable fault transitory state. When that fault reaches its steady state, the observer gains influence disappears because its effect on the threshold and on the residual sensitivity counteracts each other.

On the other hand, when just analyzing a fault affecting to the output sensor related to $y_1(k)$, $f_{y_1}(k)$, assuming the other sensors and actuators are non-faulty, the method showed in *Section 3.4.1* allows obtaining a minimum detectable fault function related to residual $r_1(k)$, $f^{\min}_{fy_{1,1}}$, and another one related to residual $r_2(k)$, $f^{\min}_{fy_{2,1}}$. Thereby, their expressions are

$$f^{\min}_{fy_{1,1}}(k-t_0)=-S_{fy_{1,1}}(q^{-1},\boldsymbol{\theta})^{-1}r_{01}(k)=-\frac{1-\left(a^o_{22}+a^o_{11}\right)q^{-1}+\left(a^o_{11}a^o_{22}-a^o_{12}a^o_{21}\right)q^{-2}}{1-\left(a^o_{22}+a_{11}\right)q^{-1}+\left(a_{11}a^o_{22}-a^o_{12}a_{21}\right)q^{-2}}r_{01}(k) \qquad (3.93)$$

$$k\geq t_0$$

$$f^{\min}_{fy_{2,1}}(k-t_0)=-S_{fy_{2,1}}(q^{-1},\boldsymbol{\theta})^{-1}r_{02}(k)q^{-1}=\frac{1-\left(a^o_{22}+a^o_{11}\right)q^{-1}+\left(a^o_{11}a^o_{22}-a^o_{12}a^o_{21}\right)q^{-2}}{k_{21}+\left(a^o_{21}k_{11}-a^o_{11}k_{21}\right)q^{-1}}r_{02}(k) \qquad (3.94)$$

$$k\geq t_0$$

where according to the procedure given by (Peng et al., 1997), $f^{\min}_{fy_{2,1}}$ is delayed one time instant since the resultant function is not causal. Then, evaluating Eq. (3.93) for $\boldsymbol{\theta}=\overline{\boldsymbol{\theta}}$ ($\hat{y}(k)=\overline{\hat{y}}(k)$) or $\boldsymbol{\theta}=\underline{\boldsymbol{\theta}}$ ($\hat{y}(k)=\underline{\hat{y}}(k)$), this expression sets the minimum detectable output sensor fault related to $y_1(k)$ so that $r_1(k)$ can indicate the fault (Eq. (3.24)). Thus, regarding Eq. (3.94), this expression sets also the minimum detectable output sensor fault related to $y_1(k)$, but this time, so that $r_2(k)$ can indicate the fault (Eq. (3.24)). On the other hand, it must be taken into account that if fault isolation were required, all the residuals affected by the fault should violate the condition given by Eq. (3.24). In this case, the absolute value of the minimum detectable fault related to $y_1(k)$($f^{\min}_{fy_{1,1}}$), which guarantees that both $r_1(k)$ and $r_2(k)$ indicate this fault, is

$$abs\left(f^{\min}_{fy_1}\right)=\max\left(abs\left(f^{\min}_{fy_{1,1}}\right),abs\left(f^{\min}_{fy_{2,1}}\right)\right) \qquad (3.95)$$

3.5.7 Minimum detectable input sensor fault function

As pointed out in *Section 3.4.4.2*, the minimum detectable input sensor fault is given by Eq. (3.78) using the residual sensitivity to an input sensor fault given by Eq. (3.47) and the interval observer adaptive threshold given by Eq. (3.21). Then, evaluating this expression when using the application example, using the input sensor fault residual sensitivity (Eq. (3.89)) and the interval adaptive threshold (Eq. (3.87)), it must be noticed that the procedure determined by Eq. (3.67) can not be applied since matrix $\boldsymbol{S_{fu}}$ (Eq. (3.89)) is not a square matrix. In this case, as mentioned in *Section 3.4.1*, a modified procedure can be used where the left pseudo-inverse matrix of $\boldsymbol{S_{fu}}$, $\boldsymbol{S_{fu}}^{+}$, is considered instead of $\boldsymbol{S_{fu}}^{-1}$. As a result, a minimum detectable input sensor fault vector whose dimension is just 1×1 is determined. This vector can be interpreted as the result of the equation system given by (3.65), formed by 2 equations when considering the application example, such that the quadratic error regarding the exact solution of every equation is minimum. Although this modified procedure allow us validating the goodness of the considered system model from the input sensor fault detection point of view, it seems to be more reasonable to analyze each residual independently in order to obtain the minimum detectable input sensor fault regarding the residual $r_1(k)$, $f_{fu_1}^{\min}$, and the minimum detectable input sensor fault regarding the residual $r_2(k)$, $f_{fu_2}^{\min}$, such as it was done in *Section 3.5.6* to obtain the functions $f_{fy_{1,1}}^{\min}$ (Eq. (3.93)) and $f_{fy_{2,1}}^{\min}$ (Eq. (3.94)). Thereby, the expressions of these functions are

$$f_{fu_1}^{\min}(k-t_0) = -S_{fu_{1,1}}(q^{-1},\boldsymbol{\theta})^{-1} r_{01}(k) q^{-1} = \frac{1-\left(a_{22}^o + a_{11}^o\right)q^{-1} + \left(a_{11}^o a_{22}^o - a_{12}^o a_{21}^o\right)q^{-2}}{b_{11} + \left(a_{12}^o b_{21} - a_{22}^o b_{11}\right)q^{-1}} r_{01}(k) \qquad (3.96)$$

$$k \geq t_0$$

$$f_{fu_2}^{\min}(k-t_0) = -S_{fu_{2,1}}(q^{-1},\boldsymbol{\theta})^{-1} r_{02}(k) q^{-1} = \frac{1-\left(a_{22}^o + a_{11}^o\right)q^{-1} + \left(a_{11}^o a_{22}^o - a_{12}^o a_{21}^o\right)q^{-2}}{b_{21} + \left(a_{21}^o b_{11} - a_{11}^o b_{21}\right)q^{-1}} r_{02}(k) \qquad (3.97)$$

$$k \geq t_0$$

where $S_{fu_{1,1}}$ and $S_{fu_{2,1}}$ are given by Eq. (3.89) and both $f_{fu_1}^{\min}$ and $f_{fu_2}^{\min}$ have been delayed one time instant according to the method given by (Peng et al., 1997) since they were not causal. When evaluating $f_{fu_1}^{\min}$ (Eq. (3.96)) for $\boldsymbol{\theta} = \overline{\boldsymbol{\theta}}$ ($\hat{y}(k) = \overline{\hat{y}}(k)$) or $\boldsymbol{\theta} = \underline{\boldsymbol{\theta}}$ ($\hat{y}(k) = \underline{\hat{y}}(k)$), this function establishes the minimum detectable input sensor fault related to $u(k)$ so that $r_1(k)$ can indicate the fault (Eq. (3.24)). Conversely, $f_{fu_2}^{\min}$ (Eq. (3.97)), this expression sets also the minimum detectable input sensor fault related to $u(k)$,but this time, so that $r_2(k)$ can indicate the fault (Eq. (3.24)). As a result, the minimum detectable input sensor fault, such that both $r_1(k)$ and $r_2(k)$ can indicate the fault according to the fault detection test Eq. (3.24), is given by

$$abs\left(f_{fu}^{\min}\right) = \max\left(abs\left(f_{fu_1}^{\min}\right), abs\left(f_{fu_2}^{\min}\right)\right) \qquad (3.98)$$

In the following, the time evolution of $f_{fu_1}^{\min}$ given by Eq. (3.96) when $\boldsymbol{\theta} = \overline{\boldsymbol{\theta}}$ and $t_0 = 200$ is plotted varying l ($k_{ij} = la_{ij}$ ($i=1,2$ and $j=1,2$)) from simulation ($l=0$) to prediction ($l=1$), being the sweeping interval $\Delta l = 0.04$.

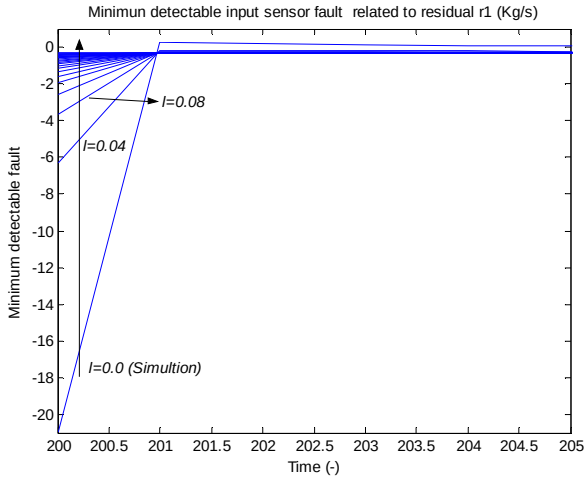

Fig. 3.7 Time evolution of the minimum detectable input sensor fault related to $r_1(k)$ regarding the observation gain when $\boldsymbol{\theta} = \bar{\boldsymbol{\theta}}$ and $t_0 = 200$.

Comparing the influence of the observer gain on the minimum detectable input sensor fault function described in *Section 3.4.4.2* with the time evolution of $f_{fu_1}^{\min}$ (Eq. (3.96)) plotted in *Fig*. 3.7 ($t_0=200$), some differences can be seen in line with the initial value of the function at time instant $k= t_0$ and its steady-state value. These discrepancies respond to the facts that $f_{fu_1}^{\min}$ has been delayed one time instant in order to achieve the causality property and $f_{fu_1}^{\min}$ is the minimum detectable input sensor fault function related just to $r_1(k)$ since the exact procedure shown in *Section 3.4.4.2* could not be applied due to $\boldsymbol{S_{fu}}$ has no inverse matrix. Taking into account these particulars, the transient-state of function $f_{fu_1}^{\min}$ plotted *Fig*. 3.7 is in line with the results of *Section 3.4.4*.2. Concerning the steady-state value of $f_{fu_1}^{\min}$, *Fig*. 3.7 shows this value depends slightly on the observer gain, unlike Eq. (3.80). However, this influence could be assumed negligible in comparison with the dependence observed in the transient-state.

3.5.8 Minimum detectable actuator fault function

In *Section 3.4.4.3*, the influence of the observer gain matrix $\boldsymbol{L}$ on the time evolution of the minimum detectable actuator fault function was analysed. This function is set by Eq. (3.81) using the actuator fault residual sensitivity matrix, $\boldsymbol{S_{fa}}$ (Eq. (3.54)) and the interval observer adaptive threshold given by Eq. (3.21). When particularizing this expression for the application example, matrix $\boldsymbol{S_{fa}}$ is set by Eq. (3.91) while the interval adaptive threshold is set by Eq. (3.87). However, such as mentioned in the minimum detectable input sensor fault case (*Section 3.5.7*), the minimum detectable actuator fault procedure given by Eq. (3.81) can not be applied since $\boldsymbol{S_{fa}}$ has no inverse matrix when particularized for the application example. In this case, the left pseudo-inverse matrix of $\boldsymbol{S_{fa}}$, $\boldsymbol{S_{fa}}^{+}$, could be used allowing to obtain a minimum detectable actuator fault vector whose dimension is just 1×1, such as it was already described in *Section 3.5.7* for the minimum detectable input sensor fault case. Nonetheless, such as pointed out in the previous section, another procedure to obtain the minimum detectable actuator fault consists in analyzing each residual independently in order to obtain the minimum detectable input sensor fault regarding the residual $r_1(k)$, $f_{fa_1}^{\min}$, and the minimum detectable input sensor fault regarding the residual $r_2(k)$, $f_{fa_2}^{\min}$. Then, the expressions of these functions are

$$f_{fa_1}^{\min}(k-t_0) = -S_{fa_{1,1}}(q^{-1},\boldsymbol{\theta})^{-1} r_{01}(k) q^{-1} \qquad k \geq t_0 \tag{3.99}$$

$$f_{fa_2}^{\min}(k-t_0) = -S_{fa_{2,1}}(q^{-1},\boldsymbol{\theta})^{-1} r_{02}(k) q^{-1}$$
$$k \geq t_0 \tag{3.100}$$

where $S_{fa_{1,1}}$ and $S_{fa_{2,1}}$ are given by Eq. (3.91) and both $f_{fa_1}^{\min}$ and $f_{fa_2}^{\min}$ have been delayed one time instant (Peng et al., 1997) since they were not causal. When evaluating $f_{fa_1}^{\min}$ (Eq. (3.99)) for $\boldsymbol{\theta} = \overline{\boldsymbol{\theta}}$ ($\hat{y}(k) = \overline{\hat{y}}(k)$) or $\boldsymbol{\theta} = \underline{\boldsymbol{\theta}}$ ($\hat{y}(k) = \underline{\hat{y}}(k)$), this function establishes the minimum detectable actuator fault related to *u(k)* so that $r_1(k)$ can indicate the fault (Eq. (3.24)). Conversely, $f_{fa_2}^{\min}$ (Eq. (3.100)), this expression sets also the minimum actuator fault related to *u(k),*but this time, so that $r_2(k)$ can indicate the fault (Eq. (3.24)). As a result, the minimum detectable actuator fault, such that both $r_1(k)$ and $r_2(k)$ can indicate the fault according to the fault detection test Eq. (3.24), is given by

$$abs\left(f_{fa}^{\min}\right) = \max\left(abs\left(f_{fa_1}^{\min}\right), abs\left(f_{fa_2}^{\min}\right)\right) \tag{3.101}$$

Next, the time evolution of $f_{fa_1}^{\min}$ given by Eq. (3.99) when $\boldsymbol{\theta} = \overline{\boldsymbol{\theta}}$ and t_0= *200* is plotted varying *l* (k_{ij}=la_{ij} (*i=1,2* and *j=1,2*)) from simulation (*l=0*) to prediction (*l=1*), being the sweeping interval Δl=*0.04*.

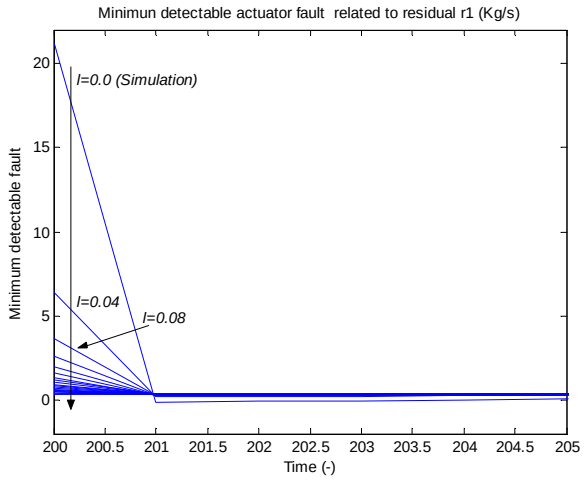

Fig. 3.8 Time evolution of the minimum detectable actuator fault related to $r_1(k)$ regarding the observation gain when $\boldsymbol{\theta} = \overline{\boldsymbol{\theta}}$ and t_0= *200*.

Comparing the influence of the observer gain on the minimum detectable actuator fault function described in *Section 3.4.4.3* with the time evolution of $f_{fa_1}^{\min}$ (Eq. (3.99)) plotted in *Fig.* 3.8 (t_0=*200*), some discrepancies are stated regarding the initial value of the function at time instant *k*= t_0 and its steady-state value, such as mentioned in *Fig. 3.7* where the time evolution of $f_{fu_1}^{\min}$ is plotted. These dissimilarities are due to the facts that $f_{fa_1}^{\min}$ has been delayed one time instant and $f_{fa_1}^{\min}$ is the minimum detectable actuator fault function related just to $r_1(k)$. Concerning the time evolution of function $f_{fa_1}^{\min}$ plotted *Fig. 3.8*, this is in line with the results of *Section 3.4.4.*3 considering the mentioned particulars. Conversely, the steady-state value of $f_{fa_1}^{\min}$ shows a slightly dependence on the observer gain, unlike Eq. (3.83), such as mentioned in the previous section for the input sensor fault case. However, this influence could also be neglected in comparison with the dependence observed in the transient-state.

3.5.9 Fault classification: output sensor fault case

In the following, assuming a fault scenario affecting the output sensor related to $y_1(k)$, different additive output sensor faults are applied to this sensor in order to illustrate the three fault types shown in *Section 3.4.2*. Thus, it is considered that the fault occurrence time instant is t_0=200 and the observers gains are tuned as follows: k_{11}=la_{11} and

$k_{22}=la_{22}$ being $l=0.04$ while $k_{12}=a_{12}$ and $k_{21}=a_{21}$. Firstly, a slightly bigger fault than the minimum detectable one obtained using Eq. (3.95) is applied. In *Fig. 3.9*, the time evolution of the output sensor measurements ($y_1(k)$ and $y_2(k)$) and their interval estimations computed by the interval observer are plotted pointing out that the fault is indicated permanently by both residuals ($r_1(k)$ and $r_2(k)$) (*strong fault detection*) according to detection test given by Eq. (3.24) . Conversely, when a slightly smaller fault than the one established by Eq. (3.93) is applied (*Fig*. 3.10), the fault is not indicated by none residual since the detection test is always fulfilled (see Eq. (3.24)). Finally, in *Fig. 3.11* a constant fault whose value is *0.15 Kg/s* (roughly, 20% of the system output nominal steady-state value) is considered. Then, the fault is indicated during a period of time by $r_1(k)$ since its occurrence time instant, but not by $r_2(k)$. Later on, the fault is not longer indicated since it becomes smaller than the minimum detectable fault required for every residual and consequently, the fault is not persistently indicated (*weak fault detection*).

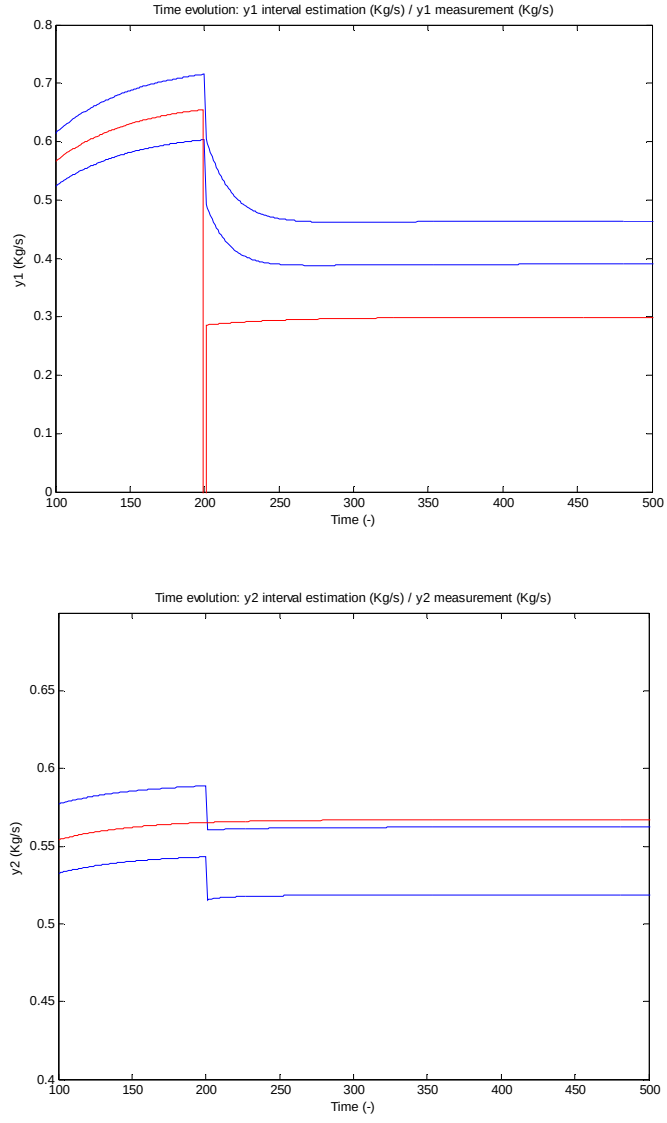

Fig. 3.9 Time evolution of $y_1(k)$ and $y_2(k)$) and their interval estimations assuming a single fault scenario affecting the output sensor related to $y_1(k)$ at time instant $t_0=200$ which is slightly bigger than the required one by both residuals (Eq. (3.95)).

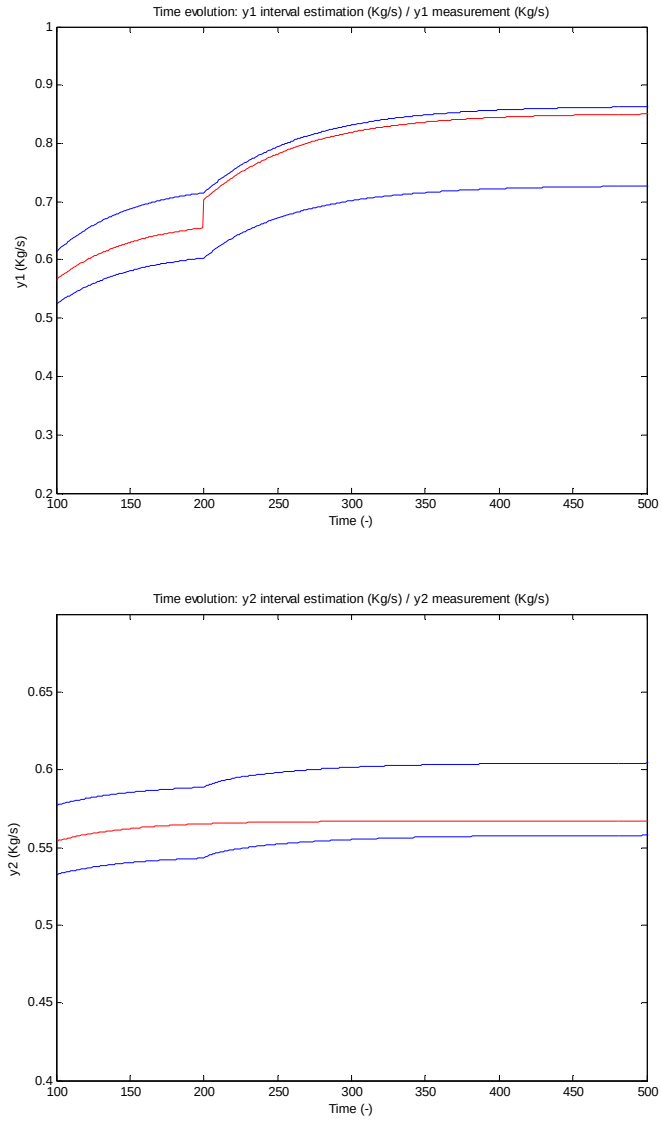

Fig. 3.10 Time evolution of $y_1(k)$ and $y_2(k)$) and their interval estimations assuming a single fault scenario affecting the output sensor related to $y_1(k)$ at time instant $t_0=200$ which is slightly smaller than the required one by $r_1(k)$ (Eq. (3.93)).

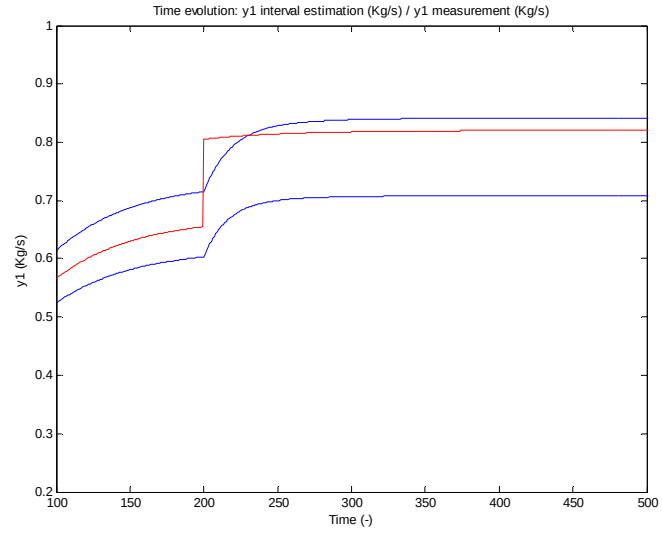

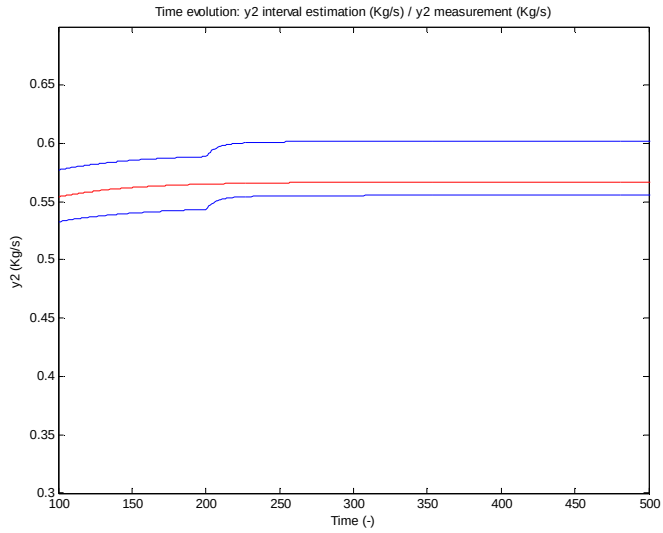

Fig. 3.11 Time evolution of $y_1(k)$ and $y_2(k)$) and their interval estimations assuming a single fault scenario affecting the output sensor related to $y_1(k)$ at time instant $t_0=200$ which has a constant value of *0.15 Kg/s*

3.5.10 Fault classification: input sensor fault case

In this case, a fault scenario affecting the input sensor related to $u(k)$ is assumed applying different additive input sensor faults to illustrate the three fault types shown in *Section 3.4.2*. Concerning the fault occurrence time instant, this is t_0=200. On the other hand, the observer gains are tuned as follows: $k_{11}=la_{11}$ and $k_{22}=la_{22}$ being $l=0.04$ while $k_{12}=a_{12}$ and $k_{21}=a_{21}$. Firstly, a slightly bigger fault than the minimum detectable one obtained using Eq. (3.98) is applied. In *Fig. 3.12*, the time evolution of the output sensor measurements ($y_1(k)$ and $y_2(k)$) and their interval estimations computed by the interval observer are plotted illustrating both residuals ($r_1(k)$ and $r_2(k)$) are indicating permanently the fault (*strong fault detection*)(Eq. (3.24)). Then, when a slightly smaller fault than the one established by Eq. (3.97) is applied (*Fig*. 3.13), the fault is not indicated by none residual since the detection test is always fulfilled (see Eq. (3.24)). Finally, in *Fig. 3.14* a fault which is only indicated during a period of time by $r_2(k)$ since its occurrence time instant, but not by $r_1(k)$ is considered. Later on, the fault is not longer indicated by any residual (Eq. (3.24)) (*weak fault detection*).

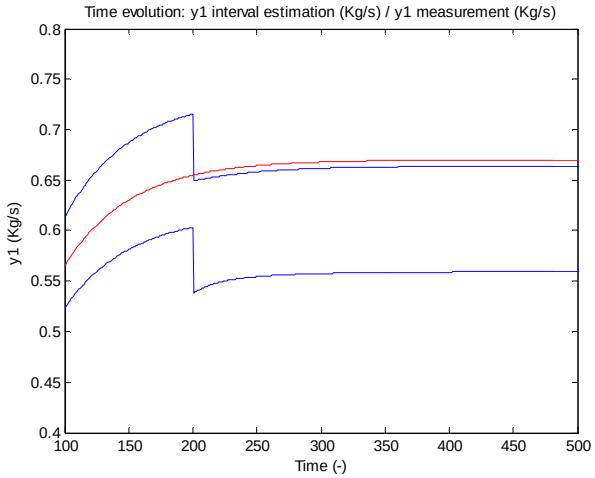

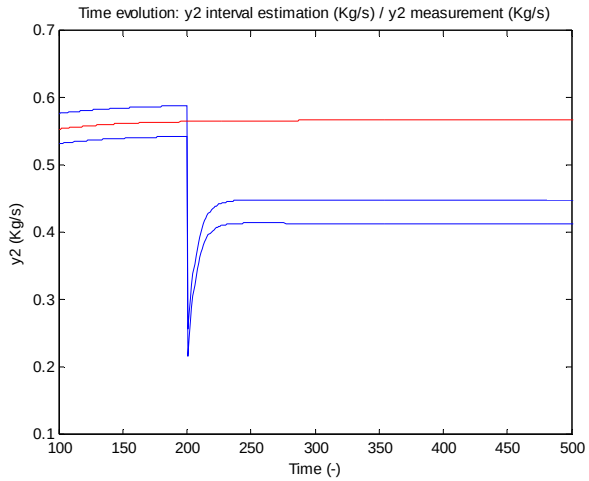

Fig. 3.12 Time evolution of $y_1(k)$ and $y_2(k)$) and their interval estimations assuming a single fault scenario affecting the input sensor related to $u(k)$ at time instant $t_0=200$ which is slightly bigger than the required one by both residuals (Eq. (3.98)).

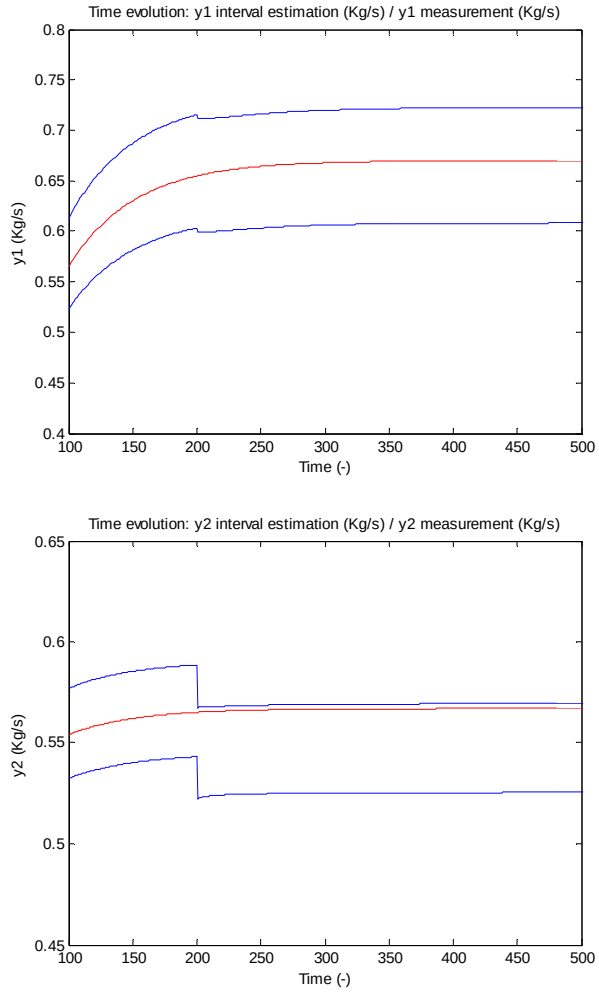

Fig. 3.13 Time evolution of $y_1(k)$ and $y_2(k)$) and their interval estimations assuming a single fault scenario affecting the input sensor related to $u(k)$ at time instant $t_0=200$ which is slightly smaller than the required one by $r_2(k)$ (Eq. (3.97)).

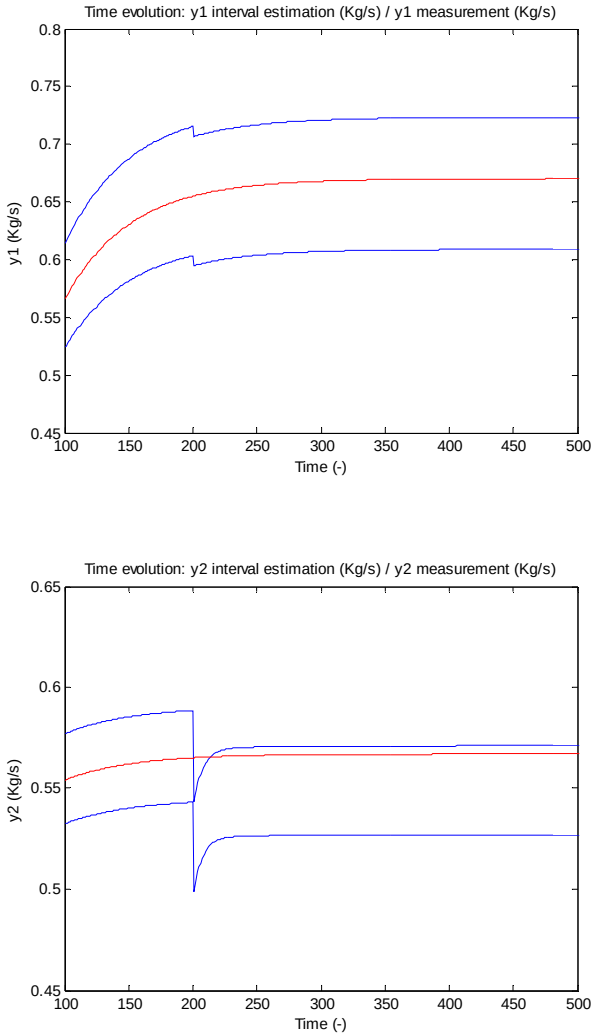

Fig. 3.14 Time evolution of $y_1(k)$ and $y_2(k)$) and their interval estimations assuming a single fault scenario affecting the input sensor related to $u(k)$ at time instant $t_0=200$ which is only detected for few time instants by $r_2(k)$

3.5.11 Fault classification: actuator fault case

In this section, a fault scenario affecting the actuator $u(k)$ is assumed applying different additive actuator faults in order to illustrate the three fault types shown in *Section 3.4.2*. Concerning the fault occurrence time instant and the applied observer gains: t_0=200, $k_{11}=la_{11}$ and $k_{22}=la_{22}$ being $l=0.04$ while $k_{12}=a_{12}$ and $k_{21}=a_{21}$. Firstly, a slightly bigger fault than the minimum detectable one obtained using Eq. (3.101) is applied. In *Fig. 3.15*, the time evolution of the output sensor measurements ($y_1(k)$ and $y_2(k)$) and their interval estimations computed by the interval observer are plotted pointing out both residuals ($r_1(k)$ and $r_2(k)$) are indicating permanently the fault (*strong fault detection*)(Eq. (3.24)). Then, when a smaller fault than the one established by Eq. (3.100) is applied (*Fig*. 3.16), the fault is not indicated by none residual since the detection test is always fulfilled (see Eq. (3.24)). Finally, in *Fig. 3.17* a fault which is only indicated during a period of time by $r_2(k)$ since its occurrence time instant, but not by $r_1(k)$ is considered. Later on, the fault is not longer indicated by any residual (Eq. (3.24)) (*weak fault detection*).

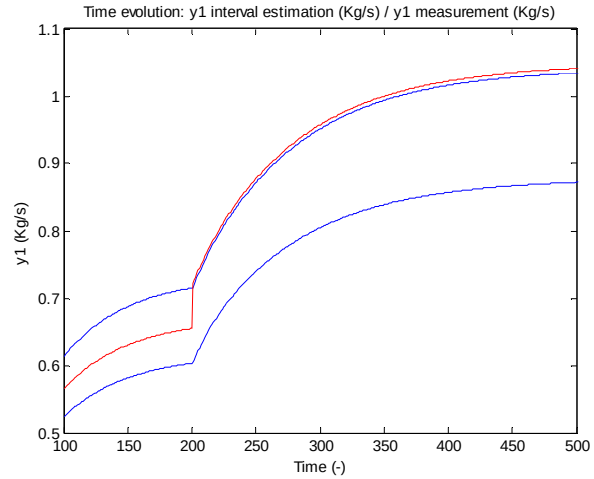

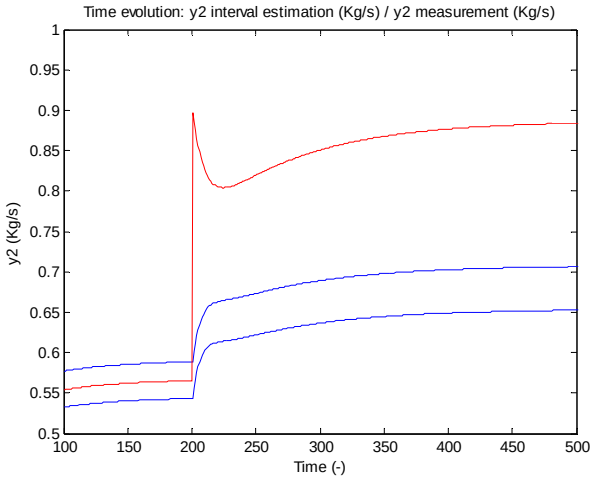

Fig. 3.15 Time evolution of $y_1(k)$ and $y_2(k)$) and their interval estimations assuming a single fault scenario affecting the actuator $u(k)$ at time instant $t_0=200$ which is slightly bigger than the required one by both residuals (Eq. (3.101)).

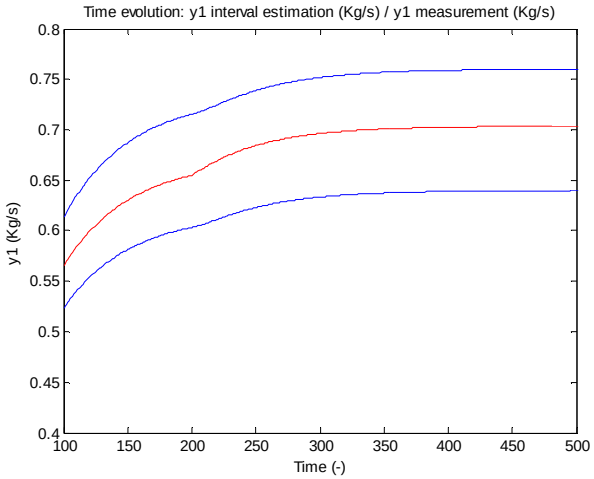

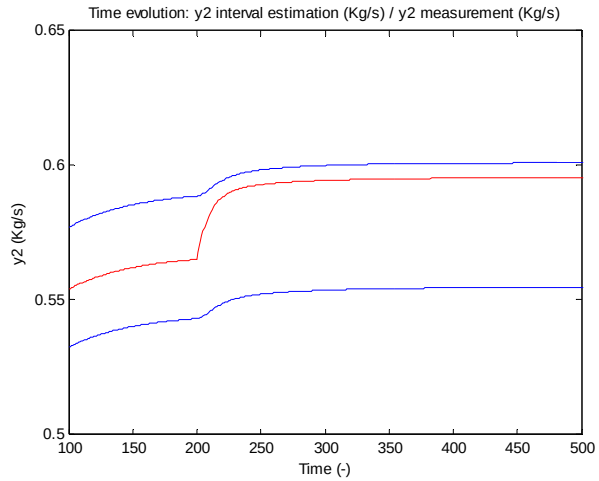

Fig. 3.16 Time evolution of $y_1(k)$ and $y_2(k)$) and their interval estimations assuming a single fault scenario affecting the actuator $u(k)$ at time instant $t_0=200$ which is smaller than the required one by $r_2(k)$ (Eq. (3.100)).

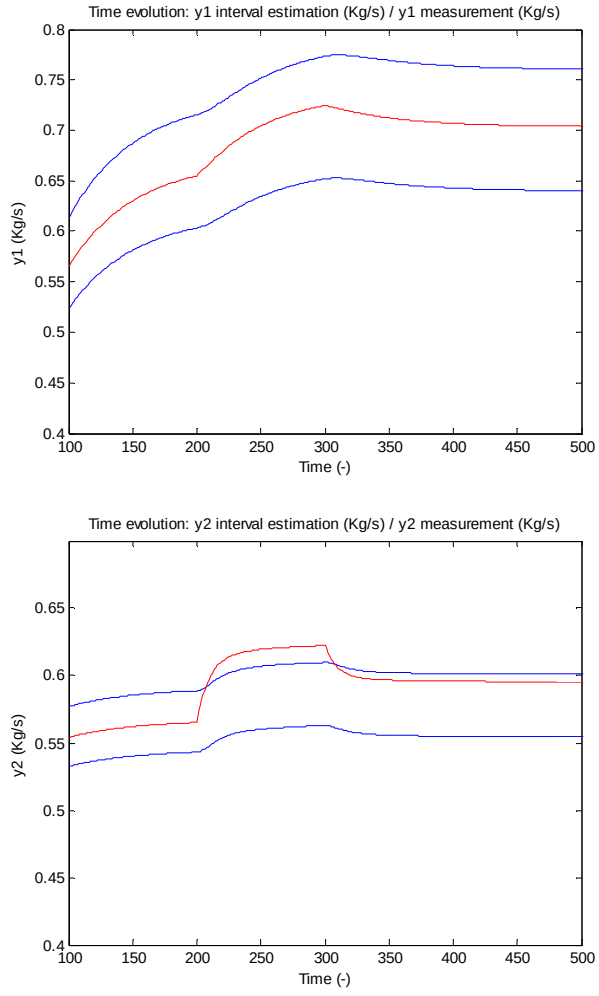

Fig. 3.17 Time evolution of $y_1(k)$ and $y_2(k)$) and their interval estimations assuming a single fault scenario affecting the actuator $u(k)$ at time instant $t_0=200$ which is only detected for few time instants by $r_2(k)$

3.6 Conclusions

This *Chapter* has presented a study that shows how the observer gain affects the fault detection performance of the

interval observer-based methods, according to the fault detection objectives enumerated in *Section 2.5.1*. This analysis, carried out following the seminal ideas proposed by (Gertler, 1998), points out the influence of the observer gain on the time evolution of the residual sensitivity to a fault, considering both sensor and actuator faults. As a novelty, this thesis considers the dynamical properties of the fault residual sensistivity pointing out their importance in the fault diagnosis process. The qualitative results of this analysis regarding the influence of the observation gain on fault residual sensitivy are briefly illustrated in *Table 3.1*. On the other hand, the effect of observer gain on the time evolution of the residual and its associated adaptive threshold is described. Thereby, the residual is expressed in terms of the fault residual sensitivity functions and its adaptive threshold allowing to obtain the minimum detectable fault. As a novelty, the time evolution of the minimum detectable fault for a given type of fault is determined using the residual adaptive threshold and the observer gain. This let us introduce three types of faults according to the time evolution of its residual disturbance: permanently detected (*strong fault detection*), non-permanently detected (*weak fault detection*) or just non-detected. Finally, an example based on a mineral grinding-classification process is used to illustrate the results derived.

	Simulation ***L=0***	***Observation*** ***L= L_o***	***Prediction*** ***L= L_p***
S_{fy}	Constant	Pulse	Deadbeat
S_{fu}	Dynamic response	Dynamic response	Constant
S_{fa}	Dynamic response	Dynamic response	Constant

Table 3.1 Qualitative influence of the observer gain on the time evolution of the fault residual sensitivity functions

CHAPTER 4

Designing fault detection linear interval observers to avoid the wrapping effect

4.1 Introduction

Most of the robust residual evaluation methods are based on an adaptive threshold changing in time according to the plant input signal and taking into account the model uncertainty. These last years the research of adaptive thresholding algorithms that use interval models for FDI has been a very active research area since the seminal work (Horak, 1988): (Armengol et al, 2000), (Puig et al, 2002a), (Fagarasan el al, 2004) and (Ploix et al, 2006). In (Puig et al, 2003a) interval observers applied to robust fault detection have been introduced and in (Puig et al, 2003b), an interval simulation algorithm based on optimization through the set of possible real trajectories contained in the interval model is proposed. However, this trajectory based approach has a very high computational complexity. On the other hand, region (or set) based algorithms coming from the interval analysis (Kühn, 1998) are much less computational demanding but interval observers can suffer from several problems, such as the wrapping effect, if the model matrix does not fulfil the isotonicity property (Cugueró et al, 2002). The aim of this chapter is to show how those problems, mainly the wrapping effect, can be avoided when an interval observer model is considered in spite a low computational algorithm is used to estimate the output interval time evolution. This will only be possible if the observer gain matrix satisfies a key condition. On the other hand, the effect of this condition on the observer fault detection performance is also analyzed to see whether it is enhanced or not. This chapter continues the work developed in *Chapter 3* based on the derived results of reference (Meseguer et al., 2007b) which is focused on fault detection based on intervals observers. It shows the influence of the observer gain on the residual sensitivity to a fault and on the minimum detectable fault (Gertler, 1998) since, such as it was noticed by (Chen et al 1999), the observer gain plays an important role in fault detection because it determines the time evolution of those fault detection properties.

The structure of the *Chapter 4* remainder is the following: in *Section 4.2*, fault detection concepts using interval observers are recalled and besides, the observer gain matrix design to avoid the wrapping effect is discussed. Then, (*Section 4.3*), the influence of avoiding the wrapping effect using the observer gain matrix on the observer fault detection performance is analyzed. In *Section 4.4*, the conclusions obtained in previous sections are exemplified using an application example based on an industrial smart actuator. Finally, *Section 4.5* describes the main conclusions of this chapter.

4.2 Interval observation: adaptive thresholding

The problem of adaptive threshold generation in discrete time-domain using interval observers can be formulated mathematically as the need of determining the predicted output interval $[\underline{\hat{y}}(k), \overline{\hat{y}}(k)]$ at every time-instant using the interval observer given by Eq. (3.7) and according to the expressions given by Eq. (3.10).

In order to determine $[\underline{\hat{y}}(k), \overline{\hat{y}}(k)]$, the observer given by Eq. (3.7) is written as a model with one output and two inputs, assuming the observability of the system (Eq. (3.1)) for all $\tilde{\boldsymbol{\theta}} \in \boldsymbol{\Theta}$:

$$\begin{aligned} \hat{\boldsymbol{x}}(k+1) &= \boldsymbol{A}_o(\boldsymbol{\theta})\hat{\boldsymbol{x}}(k) + \begin{bmatrix} \boldsymbol{B}_o(\boldsymbol{\theta}) & \boldsymbol{L} \end{bmatrix} \begin{bmatrix} \boldsymbol{u}(k) \\ \boldsymbol{y}(k) \end{bmatrix} \\ \hat{\boldsymbol{y}}(k) &= \boldsymbol{C}(\boldsymbol{\theta})\hat{\boldsymbol{x}}(k) + \boldsymbol{D}(\boldsymbol{\theta})\boldsymbol{u}(k) \end{aligned} \tag{4.1}$$

where $\boldsymbol{A}_o(\boldsymbol{\theta}) = \boldsymbol{A}(\boldsymbol{\theta}) - \boldsymbol{LC}(\boldsymbol{\theta})$ and $\boldsymbol{B}_o(\boldsymbol{\theta}) = \boldsymbol{B}(\boldsymbol{\theta}) - \boldsymbol{LD}(\boldsymbol{\theta})$ and taking into account that the matrix and vector dimensions were given in *Section 3.2.1*. Then, interval observation can be formulated as an ***interval simulation*** and the existent algorithms for this methodology can be used (Puig et al, 2003b). As mentioned in *Chapter 2*, *Section 2.3.2.5*, a possible classification of those algorithms can be established according to if they compute the output interval using (Puig et al, 2005a): one step-ahead iteration based on previous approximations of the set of estimated states (***region or set based approaches***), or a set of point-wise trajectories generated by selecting particular values of $\boldsymbol{\theta} \in \boldsymbol{\Theta}$ using heuristics or optimisation (***trajectory based approaches***). But, when the undesired wrapping effect wants to be avoided, (Puig et al, 2005a) shows the trajectory based approach must be used in spite of its high computational cost. In this section, it is demonstrated that region based algorithms can also avoid wrapping effect and others pathologies when the interval observer is not formulated as a simulator but a proper observation gain matrix is used in order to counteract the model matrix elements that cause the appearance of the wrapping effect. Once the unsuitable elements of the model matrix $\boldsymbol{A}(\boldsymbol{\theta})$, which cause the undesired effects**,** are identified, an suitable observation gain matrix $\boldsymbol{L}$ must be set in order to counteract them in the interval observer matrix $\boldsymbol{A}_0(\boldsymbol{\theta})$. Only if the observation gain matrix $\boldsymbol{L}$ satisfies that condition, the low computational cost algorithms can be used in order to evaluate the output interval at every time instant. In contrast to *Chapter 3*, it must be noticed that in this chapter the assumption $\boldsymbol{A>0}$ and $\boldsymbol{L>0}$ is not applied.

4.2.1 Problems to be considered in interval observation

These problems were already introduced in *Chapter 2, Section 2.3.2.5.2*, and consequently, in this section they are just briefly recalled in order to understand how the observation gain matrix can avoid their effects:

4.2.1.1 Wrapping effect problem

As mentioned in *Chapter 2*, the problem of wrapping is due to the use of a crude approximation of the interval observer solution set and its iteration using one-step ahead recursion of the state space observer function, *i.e*, a ***region based approach***. This problem does not appear if instead the estimated trajectory function $\hat{\boldsymbol{x}}(k, \boldsymbol{u}, \boldsymbol{y}, \boldsymbol{\theta})$, *i.e.*, a ***trajectory based approach*** is used. The ***wrapping effect problem*** can be completely unrelated to the stability characteristics of the observer. Thereby, it must be noticed that not all the interval observers are affected by this drawback. According to (Cugueró et al, 2002), those that are monotone with respect to states do not present this problem: these kinds of observers (systems) are known as ***isotonic*** (Cugueró et al, 2002) or ***cooperative*** (Gouzé et al,

2000). In case of observers whose state function is contractive mapping (see *Definition 2* of *Section 2.3.2.5.2*), the overestimation of the wrapped set does not increase along the time (Puig et al, 2003b).

4.2.1.2 Temporal variance on uncertain parameters

As mentioned in *Chapter 2*, an additional issue that should be taken into account is how uncertain parameter time-invariance is assured since a step-ahead algorithm does not preserve it. In the literature two approaches can be found:

- The ***time-varying approach*** which assumes that uncertain parameters are unknown but bounded in their confidence intervals and can vary at each time step (ElGhaoui et al, 1999) (Puig et al ,2001).
- The ***time-invariant approach*** which assumes that uncertain parameters are unknown but bounded in their confidence intervals and they can not vary at each time step (Horak, 1988), (Puig et al, 1999).

Although the region based algorithms belong to the time-varying approach, in the case of isotonic systems, the parameter and state relation is preserved at every time instant because the interval arithmetic guarantees it. If a system is not isotonic, an isotonic observer must be used in order to avoid this problem when using low computational complexity algorithms.

4.2.1.3 Range evaluation of an interval function

Many approaches to interval observation need to evaluate the range of an interval function at every time instant in order to determine the interval for system states. One possibility for evaluating the range of the function is to use interval arithmetic (Moore, 1966). But, although the ranges of basic interval arithmetic operations are exactly the ranges of the corresponding real operations, this is not the case if the operations are composed. This phenomenon is termed as interval dependence or multi-incidence problem (Moore,1966). As mentioned in *Section 2.3.2.5.2,* one possibility to avoid this problem is to combine the use of interval arithmetic with a branch and bound algorithm (Hansen, 1992). Another possibility to evaluate the range of an interval function is to solve two optimization problems (a minimization and a maximization) using numerical methods. On the other way, it is not hard to show that isotonic systems do not suffer this problem and consequently, another way to avoid the multi-incidence problem is using an isotonic observer. At the same time, wrapping effect is also avoided when algorithms that propagate regions are used.

In short, the previous problems appear because of the non-isotonicity property of the system model matrix $\boldsymbol{A}(\boldsymbol{\theta})$ when using the region-based approach. In order to avoid them, non-isotonic models must be turned into isotonic observers using a proper observation gain matrix $\boldsymbol{L}$. That kind of observers allows to use low computational algorithms in fault detection applications.

4.2.2 Designing the observer gain matrix $\boldsymbol{L}$ to avoid the wrapping effect

When an observer is used instead of an interval simulator, the observer matrix, $\boldsymbol{A}_0 = \boldsymbol{A}(\boldsymbol{\theta}) - \boldsymbol{LC}(\boldsymbol{\theta})$, sets the dynamical properties of the observer instead of the system matrix, $\boldsymbol{A}(\boldsymbol{\theta})$ including the appearance of the wrapping effect. If $\boldsymbol{A}_0(\boldsymbol{\theta})$ is isotonic (Cugueró et al, 2002), the interval observer does not suffer from that pathology when using a region-based approach, in spite of the non-isotonicity of $\boldsymbol{A}(\boldsymbol{\theta})$. Therefore, the clue to avoid this undesired problem is to design properly the observation gain matrix $\boldsymbol{L}$ so that $\boldsymbol{A}_0(\boldsymbol{\theta})$ becomes an isotonic matrix.

In this section, a stable interval observer whose matrix $\boldsymbol{A}(\boldsymbol{\theta})$ is neither isotonic nor contractive (see *Definition 2* of *Section 2.3.2.5.2*) is considered. Thus, the non-isotonicity property of matrix $\boldsymbol{A}(\boldsymbol{\theta})$ establishes the existence of at least one state $\hat{x}_i(k)$ of the model state vector $\hat{\boldsymbol{x}}(k)$ whose variation regarding another state $\hat{x}_j(k)$ is negative or, in other words, at least one element of the considered system matrix, $\boldsymbol{A}(\boldsymbol{\theta})$, is negative: $a_{ij} < 0$. Then, the observer matrix $\boldsymbol{A}_o(\boldsymbol{\theta})$ achieves isotonicity only if the corresponding element a_{oij} of this matrix is zero-valued.

$$a_{oij} = a_{ij} - (\boldsymbol{LC})_{ij} = 0 \qquad \forall i, j \text{ where } a_{ij} < 0 \text{ [13]} \tag{4.2}$$

where $(\boldsymbol{LC})_{ij}$ is the element of the resultant matrix $\boldsymbol{LC} \in \Re^{nx \times nx}$ placed in the i^{th}-row and j^{th}-column. Conversely, condition given by Eq. (4.2) can be also expressed as it follows:

$$a_{ij} = \sum_{\alpha=1}^{ny} l_{i\alpha} c_{\alpha j} \qquad \forall i, j \text{ where } a_{ij} < 0 \tag{4.3}$$

where $l_{i\alpha}$ are the i^{th}-row elements of the observation gain matrix $\boldsymbol{L}$ and $c_{\alpha j}$ are the j^{th}-column elements of the output matrix $\boldsymbol{C}(\boldsymbol{\theta})$ related to the observer model. Thereby, while the elements $c_{\alpha j}$ of matrix $\boldsymbol{C}(\boldsymbol{\theta})$ are determined by the observer model structure and they can not be chosen freely in order to force condition (4.3), there are much more freedom degrees in order to force that condition choosing the elements $l_{i\alpha}$ associated with the observation gain matrix $\boldsymbol{L}$.

When forcing condition (4.3), a prediction relation of the state $\hat{x}_i(k)$ regarding $\hat{x}_j(k)$ is established in order to avoid the appearance of the wrapping effect when using the region-based approach. Nevertheless, the rest of the elements $(\boldsymbol{LC})_{mn}\big|_{m \neq i, n \neq j}$ of the resultant matrix $\boldsymbol{LC} \in \Re^{nx \times nx}$ do not have any effect on the isotonicity property of the observer matrix $\boldsymbol{A}_o(\boldsymbol{\theta})$. And consequently, the elements $l_{m\alpha}$ $(1 \leq \alpha \leq ny)$ associated with the observation gain matrix $\boldsymbol{L} \in \Re^{nx \times ny}$ might be chosen freely in order to achieve the desired fault detection performance but it must be taken into account that condition (4.3) can also have an influence on the observer stability and therefore, the values of those observer gains might verify additional restrictions in order to guarantee it.

Condition (4.3) is not necessary to turn an unstable wrapping into a stable one. In this case, $(\boldsymbol{LC})_{ij}$ must fulfil

$$(\boldsymbol{LC})_{ij} \subset \left[0, a_{ij}\right] \tag{4.4}$$

and being $\boldsymbol{A}_0(\boldsymbol{\theta})$ a contractive matrix (see *Definition 2* of *Section 2.3.2.5.2*). Derived from (4.4), the state overestimation using region-based algorithms decreases when the observation relation of $\hat{x}_i(k)$ regarding $\hat{x}_j(k)$ becomes closer to a prediction. Then, isotonicity is achieved and trajectory and region-based approaches obtain the same state estimations (Puig et al, 2005a).

Regarding the observation gain $\boldsymbol{L}$, this matrix can be partitioned in a matrix $\boldsymbol{L}_-$ whose elements determine the observation gain values needed to force the isotonicity condition (4.3) and a matrix $\boldsymbol{L}_+$ whose elements can be chosen freely to enhance the observer fault detection performance and to guarantee the observer stability. Thereby, the observer matrix $\boldsymbol{A}(\boldsymbol{\theta})$ can be seen as the sum of two matrices: $\boldsymbol{A}_+(\boldsymbol{\theta})$ built up using those positive elements of $\boldsymbol{A}(\boldsymbol{\theta})$ and $\boldsymbol{A}_-(\boldsymbol{\theta})$ determined by the negative ones. Then, in line with the definition of those matrices, the next expressions can be set:

$$\boldsymbol{A}(\boldsymbol{\theta}) = \boldsymbol{A}_+(\boldsymbol{\theta}) + \boldsymbol{A}_-(\boldsymbol{\theta}) \tag{4.5}$$

[13] Expressing the system (3.1) in its observable canonical form given its observability for all $\tilde{\boldsymbol{\theta}} \in \boldsymbol{\Theta}$, condition (4.2) can be applied for all the negative elements of matrix $\boldsymbol{A}$. This is also the case when $\boldsymbol{C}$ has a inverse matrix.

$$\boldsymbol{L} = \boldsymbol{L}_{+} + \boldsymbol{L}_{-} \tag{4.6}$$

$$\boldsymbol{A}_o(\boldsymbol{\theta}) = \left(\boldsymbol{A}_{+}(\boldsymbol{\theta}) - \boldsymbol{L}_{+}\boldsymbol{C}(\boldsymbol{\theta})\right) + \left(\boldsymbol{A}_{-}(\boldsymbol{\theta}) - \boldsymbol{L}_{-}\boldsymbol{C}(\boldsymbol{\theta})\right) \tag{4.7}$$

$$\left(\boldsymbol{A}_{+}(\boldsymbol{\theta})\right)_{mn} = \begin{cases} a_{mn} & \forall m \neq i, n \neq j \text{ where } a_{mn} > 0 \\ 0 & \forall m = i, n = j \text{ where } a_{ij} < 0 \end{cases} \tag{4.8}$$

$$\left(\boldsymbol{A}_{-}(\boldsymbol{\theta})\right)_{mn} = \begin{cases} 0 & \forall m \neq i, n \neq j \text{ where } a_{mn} > 0 \\ a_{mn} & \forall m = i, n = j \text{ where } a_{ij} < 0 \end{cases} \tag{4.9}$$

$$\left(\boldsymbol{L}_{+}\boldsymbol{C}(\boldsymbol{\theta})\right)_{mn} = \begin{cases} \sum_{\alpha=1}^{ny} l_{m\alpha} c_{\alpha n} & \forall m \neq i, n \neq j \text{ where } a_{mn} > 0 \\ 0 & \forall m = i, n = j \text{ where } a_{ij} < 0 \end{cases} \tag{4.10}$$

$$\left(\boldsymbol{L}_{-}\boldsymbol{C}(\boldsymbol{\theta})\right)_{mn} = \left(\boldsymbol{A}_{-}(\boldsymbol{\theta})\right)_{mn} \tag{4.11}$$

Thus, the elements of matrix $\boldsymbol{L}_{+}\boldsymbol{C}$ are positive or zero-valued while those elements of matrix $\boldsymbol{L}_{-}\boldsymbol{C}$ are negative or zero-valued. Then, comparing the norm of the observer gain matrix $\boldsymbol{A}_o(\boldsymbol{\theta})$ (Eq. (4.7)) when the isotonicity condition (4.3) (or equivalently, condition (4.11)) is forced or not, the next relation is set

$$\left\| \boldsymbol{A}_o(\boldsymbol{\theta})_{\boldsymbol{L}_{-}\boldsymbol{C}=\boldsymbol{0}} \right\| \geq \left\| \boldsymbol{A}_o(\boldsymbol{\theta})_{\boldsymbol{L}_{-}\boldsymbol{C}=\boldsymbol{A}_{-}} \right\| \tag{4.12}$$

In spite of the previous relation (Eq.(4.12)), it must be taken into account that condition (4.3) forces the negative elements of $\boldsymbol{A}_o(\boldsymbol{\theta})$ to be null what let also establish the next relation:

$$\left\| \boldsymbol{I} - \boldsymbol{A}_o(\boldsymbol{\theta})_{\boldsymbol{L}_{-}\boldsymbol{C}=\boldsymbol{0}} \right\| \geq \left\| \boldsymbol{I} - \boldsymbol{A}_o(\boldsymbol{\theta})_{\boldsymbol{L}_{-}\boldsymbol{C}=\boldsymbol{A}_{-}} \right\| \tag{4.13}$$

Alternatively, analyzing the non-zero-valued elements of matrix $\boldsymbol{L}_{-}$, they must fulfil the relation given by condition (4.3). Thereby, when all non-zero-valued elements of $\boldsymbol{C(\theta)}$ are positive, the non-zero-valued elements of $\boldsymbol{L}_{-}$ must be negative while the non-zero-valued elements of $\boldsymbol{L}_{+}$ must be positive. In general, neither all elements of matrix $\boldsymbol{L}_{-}$ have to be negative nor all elements of matrix $\boldsymbol{L}_{+}$ have to be positive when forcing condition (4.3).

4.3 Influence of the isotonicity condition used to avoid the wrapping effect on the interval observer fault detection performance

The aim of this *s*ection is to show the effect of condition (4.3) used to avoid the wrapping effect on the interval observer fault detection performance. As it was mentioned previously, that condition sets some element values of the resultant matrix $\boldsymbol{LC}$ and consequently, it may also affect to the interval observer fault detection performance as it will be illustrated in this section. First, the effect on the residual sensitivity to a fault studied in *Section 4.3.1* is analyzed. Then, the effect of this condition on the time evolution of the computed interval observer residual and the associated adaptive threshold is illustrated (*Section 4.3.2*). Finally, using the done sensitivity analysis, the effect on the minimum detectable faults (*Section 4.3.3*) and the fault detection time (*Section 4.3.4*) is studied.

4.3.1 Influence of the isotonicity condition on the residual sensitivity to a fault function

The residual sensitivity to a fault is given by Eq. (3.36) as it was presented in *Section 3.3.1* of *Chapter 3*. In this section, the effect of condition (4.3) on the residual sensitivity to a fault is shown when it is particularized to an output sensor fault given by $\boldsymbol{f_y}$, to an input sensor fault given by $\boldsymbol{f_u}$ and to an actuator fault given by $\boldsymbol{f_a}$.

4.3.1.1 Residual sensitivity to an output sensor fault

As it was mentioned in *Section 3.3.2*, the residual sensitivity to an output sensor fault is given by Eq. (3.37) and both its dynamics and its steady-state value are influenced by the observer gain matrix $\boldsymbol{L}$. Then, when condition (4.3) (or equivalently, condition (4.11)) is forced to turn $\boldsymbol{A}_0(\boldsymbol{\theta})$ into a isotonic matrix assigning prediction values to those elements $\boldsymbol{(LC)}_{mn}$ of the resultant matrix $\boldsymbol{LC}$ where the associated element a_{ij} of matrix $\boldsymbol{A}(\boldsymbol{\theta})$ is negative, the residual sensitivity time evolution is deeply affected. The residual sensitivity to a fault at time instant $k=0$, i.e. when an abrupt fault (modelled as a unit-step function) occurs, is

$$\boldsymbol{s}_{fy}(0) = \lim_{q\to\infty} \boldsymbol{S}_{fy}(q^{-1},\boldsymbol{\theta}) = \boldsymbol{F}_y(\tilde{\boldsymbol{\theta}}) \tag{4.14}$$

, independently of the observer gains such as it was shown in Eq. (3.39) and consequently, it is unaffected by condition (4.3) . On the other hand, the steady-state value for an abrupt fault modelled as a unit-step function is given by the Eq. (3.41) analyzed in *Section 3.3.2*. Thereby, taking into account the condition (4.3), this equation can be re-written as it follows:

$$\boldsymbol{s}_{fy}(\infty) = \lim_{q\to 1} \boldsymbol{S}_{fy}(q^{-1},\boldsymbol{\theta}) = \left(\boldsymbol{I} + \boldsymbol{C}(\boldsymbol{\theta})\left(\boldsymbol{I} - \boldsymbol{A}(\boldsymbol{\theta})\right)^{-1}\left(\boldsymbol{L}_+ + \boldsymbol{L}_-\right)\right)^{-1} \boldsymbol{F}_y(\tilde{\boldsymbol{\theta}}) \tag{4.15}$$

Analyzing the non-zero-valued elements of matrix $\boldsymbol{L}_-$, they must fulfil the relation given by the condition (4.11). In this way, assuming all non-zero-valued elements of $\boldsymbol{C(\theta)}$ are positive, the non-zero-valued elements of $\boldsymbol{L}_-$ must be negative while the non-zero-valued elements of $\boldsymbol{L}_+$ must be positive. Consequently, when forcing the isotonicity condition of $\boldsymbol{A}_o(\boldsymbol{\theta})$, the steady-state value of the elements of $\boldsymbol{S}_{fy}(q^{-1},\boldsymbol{\theta})$ for every value of $\boldsymbol{\theta}\in\boldsymbol{\Theta}$ (Eq.(4.15)) may increase its value regarding the case where that condition is not forced.

$$\left|\boldsymbol{s}_{fy_{i,j}}(\infty)_{\boldsymbol{L_-C=\theta}}\right| \le \left|\boldsymbol{s}_{fy_{i,j}}(\infty)_{\boldsymbol{L_-C=A_-}}\right| \quad i=1,\cdots,ny \quad j=1,\cdots,ny \tag{4.16}$$

As derived from the structure of matrix $\boldsymbol{S_{fy}}$ (Eq. (3.38)), relation (4.16) is satisfied when matrices $\boldsymbol{A}$, $\boldsymbol{L}$ and $\boldsymbol{C}$ do not fulfil the condition given by Eq. (3.32). In *Chapter 3*, the assumption of $\boldsymbol{A>0}$ and $\boldsymbol{L>0}$ was made and consequently, according to the observer structure and the stability condition, this condition was always fulfilled. In this chapter, matrix $\boldsymbol{A}$ does not satisfy the isotonicity property and as a result, when avoiding the wrapping effect using condition (4.2), the elements of $\boldsymbol{L}$ may not be positive, as mentioned above, and consequently, condition (3.32) may not be satisfied resulting the relation given by Eq. (4.16).

In this case, this effect caused by the isotonicity condition might be partially counteracted choosing properly values of matrix $\boldsymbol{L}_+$ since they have positive values.

Summarizing in regard to the effect of the isotonicity condition (4.3) on the time evolution of the output sensor fault residual sensitivity function, it is concluded:

1. The interval observer dynamics determined by matrix $\boldsymbol{A}_o(\boldsymbol{\theta})$ are affected because that condition set some elements of matrix $\boldsymbol{LC}$ to their prediction values and as a consequence of that, the eigenvalues of the interval observer matrix are closer to the null value.
2. At time instant when the fault occurs, that condition has no effect on the residual sensitivity function since its value at this time instant does not depend on the observation gain matrix $\boldsymbol{L}$ such as it is indicated by Eq. (4.14).

3. The steady-state value and the gain of the residual sensitivity function is affected by the isotonicity condition such as it is seen in Eq. (4.15) but, because that condition force some elements of matrix $\boldsymbol{LC}$ to their prediction values, it was expected a decreasing of this values such as it was mentioned in *Section 3.3.2* (Meseguer et al., 2007b). Indeed, this is not the case when the isotonicity condition is forced since it sets the use of observation gains whose values are negative (*i.e.* the elements of the output matrix $\boldsymbol{C}$ are positive). Then, the relation (4.16) may be satisfied meaning that the steady-state value increases regarding the case where the isotonicity condition is not forced.

4.3.1.2 Residual sensitivity to an input sensor fault

In this case, the residual sensitivity function is given by Eq. (3.47) (*Section 3.3*.3) and according to its structure , this function is also deeply affected when the interval observer matrix $\boldsymbol{A}_0(\boldsymbol{\theta})$ is forced to satisfy the isotonicity property using the condition (4.3) such as it was mentioned in the output sensor fault case shown in the previous section. Thereby, following the analysis steps used in the previous section, the residual sensitivity to a fault at time instant *k=0*, i.e. when an abrupt fault (modelled as a unit-step function) occurs, is

$$\boldsymbol{s}_{fu}(0) = \lim_{q\to\infty} \boldsymbol{S}_{fu}(q^{-1},\boldsymbol{\theta}) = -\boldsymbol{D}\boldsymbol{F}_u(\boldsymbol{\theta}) \tag{4.17}$$

, independently of the observer gains such as it was shown in Eq. (3.48) and thus, it is not affected by condition (4.3) such as in the output sensor case. Regarding the steady-state value determined in *Section 3.3.3*, this is given by Eq. (3.49) where matrix $\boldsymbol{A}_0(\boldsymbol{\theta})$ can be expressed in terms of matrices $\boldsymbol{L}_+\boldsymbol{C}$ and $\boldsymbol{L}_-\boldsymbol{C}$ (Eq. (4.7)). Thus, this equation can be re-written as it follows:

$$\boldsymbol{s}_{fu}(\infty) = \lim_{q\to 1} \boldsymbol{S}_{fu}(q^{-1},\boldsymbol{\theta}) = -\Big(\boldsymbol{C}(\boldsymbol{\theta})\big(\boldsymbol{I} - \big(\boldsymbol{A}(\boldsymbol{\theta}) - \boldsymbol{L}_+\boldsymbol{C}(\boldsymbol{\theta}) - \boldsymbol{L}_-\boldsymbol{C}(\boldsymbol{\theta})\big)\big)^{-1}\big(\boldsymbol{B}(\boldsymbol{\theta}) - \boldsymbol{L}\boldsymbol{D}(\boldsymbol{\theta})\big) + \boldsymbol{D}\Big)\boldsymbol{F}_u(\boldsymbol{\theta}) \tag{4.18}$$

taking into account that mostly $\boldsymbol{D}\approx\boldsymbol{0}$. As indicated by Eq. (4.13), when forcing the isotonicity condition (4.3), the norm of the matrix $\boldsymbol{I} - \boldsymbol{A}_o(\boldsymbol{\theta})$ decreases regarding the case in which that condition is not forced. Therefore, according to the *contractivity property* (see *Definition 2* in *Section 2.3.2.5.2*) of a linear system,,it is concluded that the steady-state value of the elements of $\boldsymbol{S}_{fu}(q^{-1},\boldsymbol{\theta})$ for every value of $\boldsymbol{\theta}\in\boldsymbol{\Theta}$ (Eq. (4.18)) may also increase its value regarding the case where that condition is not forced such as it was shown in the previous section for the output sensor case.

$$\left|\boldsymbol{s}_{fu_{i,j}}(\infty)_{\boldsymbol{L}_-\boldsymbol{C}=\boldsymbol{\theta}}\right| \le \left|\boldsymbol{s}_{fu_{i,j}}(\infty)_{\boldsymbol{L}_-\boldsymbol{C}=\boldsymbol{A}_-}\right| \quad i=1,\cdots,ny \quad j=1,\cdots,nu \tag{4.19}$$

In regard to the effect of the isotonicity condition on the dynamics of the residual sensitivity to an input sensor fault, the conclusions obtained for the output sensor case are also valid.

4.3.1.3 Residual sensitivity to an actuator fault

Comparing the actuator fault residual sensitivity function given by Eq.(3.54) regarding the residual sensitivity to an output sensor fault given by Eq. (3.37), it is seen both functions are affected by the observer gain matrix $\boldsymbol{L}$ throw the transfer function $\boldsymbol{O}(q^{-1},\boldsymbol{\theta}) = \big(\boldsymbol{I} - \boldsymbol{H}(q^{-1},\boldsymbol{\theta})\big)$ whose expression is given by Eq. (3.18). As a consequence of that, when forcing the isotonicity condition (4.3), the actuator fault residual sensitivity is affected such as it is the sensitivity to an output sensor fault. Thus, the residual sensitivity to a fault at time instant *k=0*, i.e., when it appears is

$$\boldsymbol{s}_{fa}(0) = \lim_{q\to\infty} \boldsymbol{S}_{fa}(q^{-1},\boldsymbol{\theta}) = \boldsymbol{\theta} \tag{4.20}$$

, independently of the observer gains such as it was shown in Eq. (3.56) and consequently, it is unaffected by condition (4.3) . Conversely, the steady-state value is given by Eq. (3.57) (*Section 3.3.4*) and it can be expressed in terms of matrices $\boldsymbol{L}_+$ and $\boldsymbol{L}_-$,such as in Eq. (4.15) for the output sensor fault case, as it follows:

$$\boldsymbol{s}_{fa}(\infty)=\lim_{q\to 1}\boldsymbol{S}_{fa}(q^{-1},\boldsymbol{\theta})=\left(\boldsymbol{I}+\boldsymbol{C}(\boldsymbol{\theta})\left(\boldsymbol{I}-\boldsymbol{A}(\boldsymbol{\theta})\right)^{-1}\left(\boldsymbol{L}_{+}+\boldsymbol{L}_{-}\right)\right)^{-1}\boldsymbol{C}(\tilde{\boldsymbol{\theta}})\left(\boldsymbol{I}-\boldsymbol{A}(\tilde{\boldsymbol{\theta}})\right)^{-1}\boldsymbol{F}_{a}(\tilde{\boldsymbol{\theta}}) \tag{4.21}$$

Thus, comparing Eq. (4.21) with Eq. (4.15) and taking into account what was mentioned in the beginning of this section, it is concluded that the steady-state value of the elements of $\boldsymbol{S}_{fa}(q^{-1},\boldsymbol{\theta})$ for every value of $\boldsymbol{\theta}\in\boldsymbol{\Theta}$ (Eq. (4.21)) may also increase its value regarding the case where that condition is not forced:

$$\left|\boldsymbol{s}_{fa_{i,j}}(\infty)_{\boldsymbol{L}_-\boldsymbol{C}=\boldsymbol{0}}\right|\leq\left|\boldsymbol{s}_{fa_{i,j}}(\infty)_{\boldsymbol{L}_-\boldsymbol{C}=\boldsymbol{A}_-}\right|\quad i=1,\cdots,ny\quad j=1,\cdots,nu \tag{4.22}$$

assuming all non-zero-valued elements of $\boldsymbol{C(\theta)}$ are positive. In a general case, the conclusions obtained for the output sensor case are also valid (*Section 4.3.1.1*). Thus, the relation given by Eq. (4.22) might be satisfied when the elements of the observation gain matrix $\boldsymbol{L}$ are required to be negative.

4.3.2 Influence of the isotonicity condition on the residual

In *Section 3.2.3* of *Chapter 3*, the effect of the observer gain matrix $\boldsymbol{L}$ on the residual time evolution was analyzed. Mainly, this effect is described by Eq. (3.30) and its derived relation, (3.31), obtained assuming that all the elements of matrices $\boldsymbol{A}$ and $\boldsymbol{L}$ are positive. Thereby, when these hypotheses are satisfied, the residual time evolution fulfils the relation given by Eq. (3.31), as demonstrated in *Appendix A*. Nonetheless, the use of the isotonicity condition (4.3) implies that $\boldsymbol{A}$ has some negative elements and therefore, as seen in *Section 4.2.2*, some elements of $\boldsymbol{L}$ may also be required to be negative ($\boldsymbol{L}_-$). As a result, relation (3.31) may not be satisfied. Recalling the expression of Eq. (3.30) in order to analyze it under the worst assumption that the isotonicity condition forces the non-zero-valued elements of $\boldsymbol{L}_-$ to be negative (non-zero-valued elements of $\boldsymbol{C(\theta)}$ are positive), this expression is re-written as:

$$\boldsymbol{r}(k)=\left(\boldsymbol{I}+\boldsymbol{H}_{r}(q^{-1},\boldsymbol{\theta})\right)^{-1}\boldsymbol{r}(k)_{\boldsymbol{L}=\boldsymbol{0}}=\left(\boldsymbol{I}+\boldsymbol{C}(\boldsymbol{\theta})\left(q\boldsymbol{I}-\boldsymbol{A}(\boldsymbol{\theta})\right)^{-1}\left(\boldsymbol{L}_{+}+\boldsymbol{L}_{-}\right)\right)^{-1}\boldsymbol{r}(k)_{\boldsymbol{L}=\boldsymbol{0}} \tag{4.23}$$

As it can be seen in Eq. (4.23), the influence of the observer gain on the time evolution of the residual is determine by the term $\left(\boldsymbol{I}+\boldsymbol{H}_{r}(q^{-1},\boldsymbol{\theta})\right)^{-1}$. If the expression of this term is compared with the expression of the function $\boldsymbol{S}_{fy}(q^{-1},\boldsymbol{\theta})$ (Eq. (3.38)), the following relation could be set

$$\left(\boldsymbol{I}+\boldsymbol{H}_{r}(q^{-1},\boldsymbol{\theta})\right)^{-1}=\boldsymbol{S}_{fy}(q^{-1},\boldsymbol{\theta})_{\boldsymbol{F}_{y}(\tilde{\boldsymbol{\theta}})=\boldsymbol{I}} \tag{4.24}$$

for every value of $\boldsymbol{\theta}\in\boldsymbol{\Theta}$. Considering just the steady state, it was aready explained in *Section 4.3.1.1* that when all the elements of matrices $\boldsymbol{A}$ and $\boldsymbol{L}$ are not positive, the relation given by Eq. (3.32) (*Section 3.2.3*) may not be satisfied and consequently, according to the contractivity property of a linear system (*Appendix B*) the relation (3.31), considered in steady state, may not be true when the condition (4.3) is forced. In this case, the residual may fulfil

$$\left|r_i(\infty)_{\boldsymbol{L}_-\boldsymbol{C}=\boldsymbol{0}}\right|\leq\left|r_i(\infty)_{\boldsymbol{L}_-\boldsymbol{C}=\boldsymbol{A}_-}\right|\quad i=1,\cdots,ny \tag{4.25}$$

for every value of $\boldsymbol{\theta}\in\boldsymbol{\Theta}$ and as a result,

$$\left[r_i(\infty)_{\boldsymbol{L}_-\boldsymbol{C}=\boldsymbol{0}}\right]\subseteq\left[r_i(\infty)_{\boldsymbol{L}_-\boldsymbol{C}=\boldsymbol{A}_-}\right]\quad i=1,\cdots,ny \tag{4.26}$$

what is an unexpected conclusion regarding the result mentioned in *Section 3.2.3* (Eq. (3.31)). Moreover, concerning the similarity between the expression of the residual $\boldsymbol{r(k)}$ and its associated adaptive threshold $\boldsymbol{r_0(k)}$ (*Section 3.2.2*), it must be taken into account that forcing the isotonicity condition may have a influence on the time evolution of the adaptive threshold very similar to the described one for the residual case (Eq. (4.25), Eq. (4.26)):

$$\left|r_{0_i}(\infty)_{\boldsymbol{L\_C=\theta}}\right| \leq \left|r_{0_i}(\infty)_{\boldsymbol{L\_C=A\_}}\right| \quad i=1,\cdots,ny \tag{4.27}$$

for every value of $\boldsymbol{\theta} \in \boldsymbol{\Theta}$ and

$$\left[r_{0_i}(\infty)_{\boldsymbol{L\_C=\theta}}\right] \subseteq \left[r_{0_i}(\infty)_{\boldsymbol{L\_C=A\_}}\right] \quad i=1,\cdots,ny \tag{4.28}$$

Regarding the time evolution of the system output estimation interval, it may be also affected by the isotonicity condition according to the definition of the interval residual given by Eq. (3.34) (*Section 3.2.2*). In consequence, the interval associated with every component of the computed vector $\hat{\boldsymbol{y}}(k)$ may satisfy the next relation:

$$\left[\hat{y}_i(\infty)_{\boldsymbol{L\_C=\theta}}\right] \subseteq \left[\hat{y}_i(\infty)_{\boldsymbol{L\_C=A\_}}\right] \quad i=1,\cdots,ny \tag{4.29}$$

In *Section 3.2*.3, it was signalled out that the interval $\left[\hat{\boldsymbol{y}}(k)\right]$ generated using the simulation approach encloses the one generated by the observer and predictor approaches while the observer system output estimation interval encloses the one generated by the predictor approach (Eq. (3.35)). Thus, according to Eq. (4.29), this result may not be true since the output interval generated when the isotonicity condition is forced may enclose the one generated if that condition would not be forced. Thereby, the system output estimation interval generated by an observer approach might enclose the one generated by a simulator.

In conclusion, when the isotonicity condition (4.3) is forced to avoid the wrapping effect, $\left[\hat{\boldsymbol{y}}(k)\right]$ may enclose the one generated if that condition would not be forced. Then, according to the fault detection condition given by Eq. (3.24) (*Section 3.2.2*), the interval observer will need a bigger fault in order to start indicating the fault. Then, it can be said that avoiding the wrapping effect using the observer gain matrix $\boldsymbol{L}$ worsens the fault detection performance of the interval observer model.

4.3.3 Influence of the isotonicity condition on the minimum detectable fault function

In *Section 3.4*, the minimum detectable concept was introduced (Eq. (3.67)) and particularized for the cases of output sensor fault (Eq. (3.72)), input sensor fault (Eq. (3.78)) and actuator fault (Eq. (3.81)). Moreover, the effect of the observer gain matrix $\boldsymbol{L}$ on the time evolution of these functions was also analyzed. Then, in this section, the effect of forcing the isotonicity condition (4.3) on the minimum detectable function is examined for each of the cases mentioned previously.

4.3.3.1 Minimum detectable output sensor fault

The minimum detectable output sensor fault function is given by Eq. (3.72) which can be expressed in terms of the matrices $\boldsymbol{L}_+$ and $\boldsymbol{L}_-$ as it follows:

$$\begin{aligned} &\boldsymbol{f}_{fy}^{min}(k-t_0) = -\boldsymbol{S}_{fy}(q^{-1},\boldsymbol{\theta})^{-1}\boldsymbol{r}_0(k) = -\boldsymbol{F}_y(\tilde{\boldsymbol{\theta}})^{-1}\left(\boldsymbol{I}+\boldsymbol{C}(\boldsymbol{\theta})\left(q\boldsymbol{I}-\boldsymbol{A}(\boldsymbol{\theta})\right)^{-1}(\boldsymbol{L}_+ + \boldsymbol{L}_-)\right)\boldsymbol{r}_0(k) \\ &k \geq t_0 \end{aligned} \tag{4.30}$$

where it must be taken into account that the observer adaptive threshold $\boldsymbol{r_0(k)}$ given by the Eq. (3.21) (*Section 3.2.2*) is affected by the isotonicity condition such as it was described in *Section 4.3.2* (Eq. (4.28)). At time instant $k=t_0$ when the fault appears, the value of Eq. (4.30) (*Section 3.4.4.1*) is given by

$$\boldsymbol{f}_{fy}^{\min}(0) = -\boldsymbol{F}_y(\tilde{\boldsymbol{\theta}})^{-1}\boldsymbol{r}_0(t_0) \tag{4.31}$$

Thus, given that forcing the isotonicity condition may widen the interval adaptive threshold regarding the case this condition is not used (Eq. (4.28)), the initial value of every component of the vector $\boldsymbol{f}_{fy}^{\min}$ may increase its absolute value.

$$\left|\left(\boldsymbol{f}_{fy}^{\min}(0)_{\boldsymbol{L\_C=0}}\right)_i\right| \leq \left|\left(\boldsymbol{f}_{fy}^{\min}(0)_{\boldsymbol{L\_C=A\_}}\right)_i\right| \quad i=1,\cdots,ny \tag{4.32}$$

Regarding the steady-state value of this minimum fault function (Eq. (4.30)), it was demonstrated in *Section 3.4.4.1* (Eq. (3.77)) that this value does not depend on the observer gain matrix $\boldsymbol{L}$ (Meseguer et al, 2007b).

In conclusion, when forcing the isotonicity condition, the minimum detectable output sensor fault vector is only affected during its transient-state and not once it reaches its steady-state value. The transient-state values of this function are bigger than the ones obtained when this condition is not used and consequently, this fact means that the interval observer requires a bigger output sensor fault during the residual transient state caused by the fault to start indicating the faulty situation.

4.3.3.2 Minimum detectable input sensor fault

The minimum detectable input sensor fault function is given by Eq. (3.78) which can be expressed in terms of the matrices $\boldsymbol{L}_+\boldsymbol{C}$ and $\boldsymbol{L}_-\boldsymbol{C}$ as it follows:

$$\boldsymbol{f}_{fu}^{min}(k-t_0) = -\boldsymbol{S}_{fu}(q^{-1},\boldsymbol{\theta})^{-1}\boldsymbol{r}_0(k) = \boldsymbol{F}_u(\boldsymbol{\theta})^{-1}\left(\boldsymbol{C}(\boldsymbol{\theta})(q\boldsymbol{I}-\boldsymbol{A}(\boldsymbol{\theta})-\boldsymbol{L}_+\boldsymbol{C}(\boldsymbol{\theta})-\boldsymbol{L}_-\boldsymbol{C}(\boldsymbol{\theta}))^{-1}\boldsymbol{B}(\boldsymbol{\theta})\right)^{-1}\boldsymbol{r}_0(k) \quad k \geq t_0 \tag{4.33}$$

where matrix $\boldsymbol{D}$ is considered to be null.

At time instant $k=t_0$ when the fault appears, the value of Eq. (4.33) (*Section 3.4.4.2*) is given by

$$\boldsymbol{f}_{fu}^{\min}(0) = \boldsymbol{\infty} \tag{4.34}$$

Regarding the steady-state value of this minimum fault function (Eq.(4.33)), it was demonstrated in *Section 3.4.4.2* (Eq. (3.80)) that this value does not depend on the observer gain matrix $\boldsymbol{L}$.

Although neither the initial value of this function (Eq. (4.34)) nor its steady-state value are affected by the isotonicity condition (4.3), its transient-state values may be influenced. Initially, they are basically affected by the threshold $\boldsymbol{r_0(k)}$ which may already be influenced (Eq. (4.28)) by this condition since time instant $k=0$ (*Section 4.3.2*). Conversely, since time instant $k=t_0$, the effect of that condition on the residual sensitivity function (Eq. (4.19)) starts counteracting the effect on the adaptive threshold $\boldsymbol{r_0(k)}$ until the function reaches its steady-state where its values does not depend on the observer gain matrix $\boldsymbol{L}$. Then, according to Eq. (4.28), the transient-state values of every component of the vector $\boldsymbol{f}_{fu}^{\min}$ may increase its absolute value satisfying the next relation:

$$\left|\left(\boldsymbol{f}_{fu}^{\min}(k-t_0)_{\boldsymbol{L\_C=0}}\right)_i\right| \leq \left|\left(\boldsymbol{f}_{fu}^{\min}(k-t_0)_{\boldsymbol{L\_C=A\_}}\right)_i\right| \quad i=1,\cdots,ny \quad t_0 < k < \infty \tag{4.35}$$

Thus, such as it was mentioned in the minimum detectable output sensor case, when forcing the isotonicity condition, the minimum detectable input sensor fault is also affected during its transient-state and not once it reaches its steady-state value. The transient-state absolute values are also bigger than the ones obtained when this condition is not used and consequently, the fault detection performance associated to the interval observer is also worsened when forcing the isotonicity condition.

4.3.3.3 Influence on the minimum detectable actuator fault

The minimum detectable actuator fault function is given by Eq. (3.78) which can be expressed in terms of the matrices $\boldsymbol{L}_+$ and $\boldsymbol{L}_-$ as it follows:

$$\boldsymbol{f}_{fa}^{min}(k-t_0)=-\boldsymbol{S}_{fa}(q^{-1},\boldsymbol{\theta})^{-1}\boldsymbol{r}_0(k)=-\boldsymbol{G}_{fa}(q^{-1},\tilde{\boldsymbol{\theta}})^{-1}\left(\boldsymbol{I}+\boldsymbol{C}(\boldsymbol{\theta})\left(q\boldsymbol{I}-\boldsymbol{A}(\boldsymbol{\theta})\right)^{-1}(\boldsymbol{L}_{+}+\boldsymbol{L}_{-})\right)\boldsymbol{r}_0(k) \qquad k\geq t_0 \tag{4.36}$$

where $\boldsymbol{G_{fa}}$ is the system transfer function regarding the actuator fault $\boldsymbol{f_a}$ which does not depend on the observer gain matrix $\boldsymbol{L}$ according to Eq. (3.5) (*Section 3.2.1*). On the other hand, comparing Eq. (4.36) with the obtained one for the output sensor case (Eq. (4.30)), it is seen that both are affected by the observer gain matrix $\boldsymbol{L}$ in the same way and consequently, the isotonicity condition (4.3) will also have the same effect on them. At time instant $k=t_0$ when the fault appears, the value of Eq. (4.36) (*Section 3.4.4.3*) is given by

$$\boldsymbol{f}_{fa}^{\min}(0)=\boldsymbol{\infty} \tag{4.37}$$

Regarding the steady-state value of this minimum fault function (Eq.(4.36)), it was demonstrated in *Section 3.4.4.3* (Eq. (3.83)) that this value does not depend on the observer gain matrix $\boldsymbol{L}$.

Then, such as it was explained for the input sensor case (*Section 4.3.3.2*), the effect of isotonicity condition on the transient-state values are basically established by the influence of that condition on the adaptive threshold $\boldsymbol{r_0(k)}$. In consequence, the next relation may be satisfied

$$\left|\left(\boldsymbol{f}_{fa}^{\min}(k-t_0)_{\boldsymbol{L\_C=0}}\right)_i\right|\leq\left|\left(\boldsymbol{f}_{fa}^{\min}(k-t_0)_{\boldsymbol{L\_C=A\_}}\right)_i\right| \quad i=1,\cdots,ny \qquad t_0<k<\infty \tag{4.38}$$

As a result, such as it was mentioned for output sensor and input sensor cases, when forcing the isotonicity condition, the transient-state absolute values of the minimum actuator fault function are also bigger than the ones obtained when this condition is not used and consequently, the fault detection performance associated to the interval observer is also worsened when forcing that condition.

4.3.4 Influence of the isotonicity condition on the fault detection persistency

In *Section 3.4.3*, it was explained that a fault is detected while its effect on the residual (residual disturbance $\boldsymbol{d_f(k)}$ given by Eq. (3.64)) surpasses the interval observer threshold $\boldsymbol{r_0(k)}$ which is originated by the effect of the model structured uncertainty on the residual. This fault indication condition is given by Eq. (3.71). On the other hand, when the isotonicity condition (4.3) is forced, both the interval observer threshold $\boldsymbol{r_0(k)}$ (*Section 4.3.2*) and the residual disturbance $\boldsymbol{d_f(k)}$ (*Section 4.3.1*) may be affected increasing their absolute values regarding the case where that condition is not used. However, it must be taken into account that $\boldsymbol{r_0(k)}$ is affected since $k=0$ while $\boldsymbol{d_f(k)}$ is since the fault occurrence time instant $k=t_0$ and is not fully affected until it does not reach its steady-state. In consequence, the fault indication might be affected negatively during the transient-state caused by the fault requiring more time instants to start indicating the fault or/and indicating the fault during less time instants.

4.4 Application example

4.4.1 Description

The application example proposed to illustrate the obtained results deals with an industrial smart actuator which has been proposed as an FDI benchmark in the context of the European research training network DAMADICS (*Fig. 4.1*). This smart actuator is used in the evaporation station of a sugar factory in Poland and it consists in a control valve, a pneumatic servomotor and a smart positioner (Bartys, 2002) (*Fig. 4.2*).

Fig. 4.1 DAMADICS smart actuator.

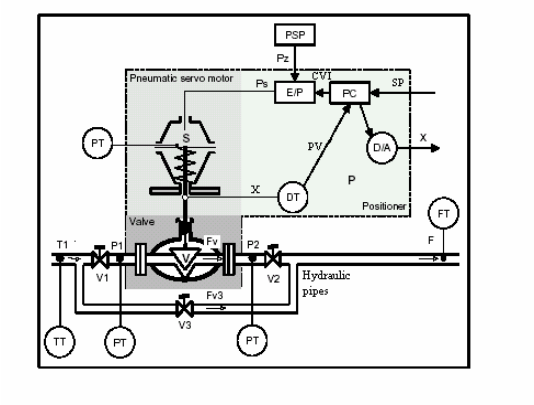

Fig. 4.2 DAMADICS smart actuator block diagram

Using physical modeling (Bartys, 2002) linearising around the operating point and a mixed optimization-identification algorithm as in (Ploix et al, 1999), the following linear interval model of the actuator valve position has been derived:

$$\begin{aligned} \hat{\boldsymbol{x}}(k+1) &= \boldsymbol{A}(\boldsymbol{\theta})\hat{\boldsymbol{x}}(k) + \boldsymbol{B}(\boldsymbol{\theta})\boldsymbol{u}(k) \\ \hat{\boldsymbol{y}}(k) &= \boldsymbol{C}(\boldsymbol{\theta})\hat{\boldsymbol{x}}(k) \end{aligned} \tag{4.39}$$

with: $\hat{\boldsymbol{x}}(k) = \left[\hat{x}_1(k) \quad \hat{x}_2(k) \quad \hat{x}_3(k)\right]^t$

$$\boldsymbol{A}(\boldsymbol{\theta}) = \begin{bmatrix} 0 & 0 & \theta_3 \\ 1 & 0 & \theta_2 \\ 0 & 1 & \theta_1 \end{bmatrix}, \quad \boldsymbol{B}(\boldsymbol{\theta}) = \begin{bmatrix} 0 \\ 0 \\ \theta_4 \end{bmatrix}, \quad \boldsymbol{C}(\boldsymbol{\theta}) = \begin{bmatrix} 0 & 0 & 1 \end{bmatrix} \text{ and } \boldsymbol{u}(k) = CVP(k-2)$$

where: $\hat{x}_3(k)$ is the valve position estimation, $\hat{\boldsymbol{y}}(k)$ is the estimation of this position measured by the displacement transducer (in Volt), ***CVP(k)*** is the command pressure (in Pascal) measured by a given input sensor and the uncertain parameters are bounded by their confidence intervals according to: $\theta_1 \in$ [1.1417 1.1471], $\theta_2 \in$ [0.3995 0.4103], $\theta_3 \in$ [-0.5537 -0.5484], and $\theta_4 \in$ [2.180e-4 2.183e-4] while their nominal values are given by θ^o_1=1.1444, θ^o_2=0.4049, θ^o_3= -0.5510, and θ^o_4=2.182e-4. In this application example, a constant command pressure whose value is ***u(k)= 1 Pa*** has been considered. According to (Cugueró et al, 2002), because some elements of $\boldsymbol{A}(\boldsymbol{\theta})$ are negative, this model suffers from the wrapping effect when the output interval $\left[\underline{\hat{\boldsymbol{y}}}(k), \overline{\hat{\boldsymbol{y}}}(k)\right]$ is calculated using a region-based algorithm. Besides, this wrapping effect is not stable because the system matrix $\boldsymbol{A}(\boldsymbol{\theta})$ is non-contractive ($\left\|\boldsymbol{A}(\boldsymbol{\theta})\right\|_\infty > 1$).

The aim of using this application example is to show the influence of the wrapping effect on the observer output interval generation when region-based algorithms are used. Then, when the isotonicity condition (4.3) is forced, the wrapping effect is avoided and consequently, both region and trajectory-based approaches estimate the same output interval at every time instant.

In order to obtain the system output estimation interval, $\left[\underline{\hat{\boldsymbol{y}}}(k), \overline{\hat{\boldsymbol{y}}}(k)\right]$, the interval observer defined by Eq. (4.1) is used. Thereby, its input-output form can be obtained from Eq. (4.39) considering $\boldsymbol{L}$=[k_3, k_2, k_1]$^{\mathrm{T}}$:

$$\begin{aligned} &\hat{\boldsymbol{y}}(k) = \boldsymbol{G}(q^{-1},\boldsymbol{\theta})\boldsymbol{u}(k) + \boldsymbol{H}(q^{-1},\boldsymbol{\theta})\boldsymbol{y}(k) = \\ &\frac{\theta_4 q^{-1}}{1+(k_1-\theta_1)q^{-1}+(k_2-\theta_2)q^{-2}+(k_3-\theta_3)q^{-3}}\boldsymbol{u}(k) + \frac{k_1 q^{-1}+k_2 q^{-2}+k_3 q^{-3}}{1+(k_1-\theta_1)q^{-1}+(k_2-\theta_2)q^{-2}+(k_3-\theta_3)q^{-3}}\boldsymbol{y}(k) \end{aligned} \tag{4.40}$$

where k_1, k_2 and k_3 are the observer gains used to avoid the wrapping effect and to enhance the interval fault detection performance regarding the needed requirements. Conversely, in line with the actuator model (4.39), the isotonicity condition (4.3) is satisfied whether

$$k_3 = \theta_3 \tag{4.41}$$

Considering the parameterisation $k_i = l_i \theta_i$, Eq. (4.41) implies $l_3 = 1$. Concerning l_1 and l_2, these observer gains must guarantee the observer stability apart from enhancing fault detection performance. Thus, analyzing the observer stability, the next values are considered

$$l_1 = l_2 = 0.5 \tag{4.42}$$

It must be taken into account that when the observer matrix $\boldsymbol{A}_o(\boldsymbol{\theta})$ fulfils the isotonicity property, the region and trajectory-based approaches compute the same system output estimation interval. Moreover, in this case, the trajectory-based approach obtain this interval using two well-known values of the model parameter set: according to (Cugueró et al., 2002), these values are $\overline{\boldsymbol{\theta}} \in \Re^{n\theta}$ for the upper envelope $\overline{\hat{\boldsymbol{y}}}(k)$ and $\underline{\boldsymbol{\theta}} \in \Re^{n\theta}$ for lower envelope $\underline{\hat{\boldsymbol{y}}}(k)$.

On the other hand, in this application example, in line with the done observer simulations and for the considered observation gains, it can also be accepted that those parameter values let obtain the output envelopes in spite the isotonicity condition is not fulfilled.

Regarding the observer residual, its expression is given by

$$\begin{aligned} \boldsymbol{r}(k,\boldsymbol{\theta}) &= -\boldsymbol{G}(q^{-1},\boldsymbol{\theta})\boldsymbol{u}(k) + \left(\boldsymbol{I} - \boldsymbol{H}(q^{-1},\boldsymbol{\theta})\right)\boldsymbol{y}(k) = \\ &- \frac{\theta_4 q^{-1}}{1+(k_1-\theta_1)q^{-1}+(k_2-\theta_2)q^{-2}+(k_3-\theta_3)q^{-3}}\boldsymbol{u}(k) + \frac{1-\theta_1 q^{-1}-\theta_2 q^{-2}-\theta_3 q^{-3}}{1+(k_1-\theta_1)q^{-1}+(k_2-\theta_2)q^{-2}+(k_3-\theta_3)q^{-3}}\boldsymbol{y}(k) \end{aligned} \tag{4.43}$$

In the following, the resulting system output estimation interval (4.40) is calculated using the region and trajectory-based approaches in order to show the influence of the isotonicity condition (4.41). Assuming a small constant additive fault affecting the system output sensor occurring at time instant $t_0=200$ and whose value is given by $f= 0.01$ *Volt* (roughly, *10%* of the system output nominal steady-state value), the time evolution of the system output estimation interval, its nominal value and the system output (*green line*) are plotted between the time instants $t_1=190$ and $t_2=220$ using $l_1=l_2=l_3=0.5$. In this case, while the trajectory-based approach produces an accurate output interval what let detect the fault (*Fig. 4.3)*; the corresponding interval generated by the region-based algorithm is useless because it suffers from unstable wrapping effect (*Fig. 4.4*) because the observer gains do not fulfil the isotonicity condition (4.41).

In *Fig. 4.5*, the isotonicity condition is applied (l_3=1) without changing the value of the others observer gains what let avoid the wrapping effect when the region-based approach is used and besides, both approaches estimate the same output interval and consequently and as a result, both of them can detect the fault.

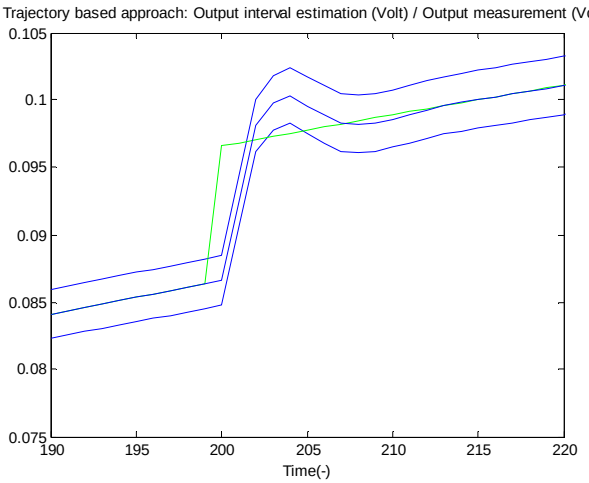

Fig. 4.3 Time evolution of the system output estimation interval, its nominal value and the output sensor measurement (green line) using a trajectory-based algorithm where l_1=l_2= l_3=0.5.

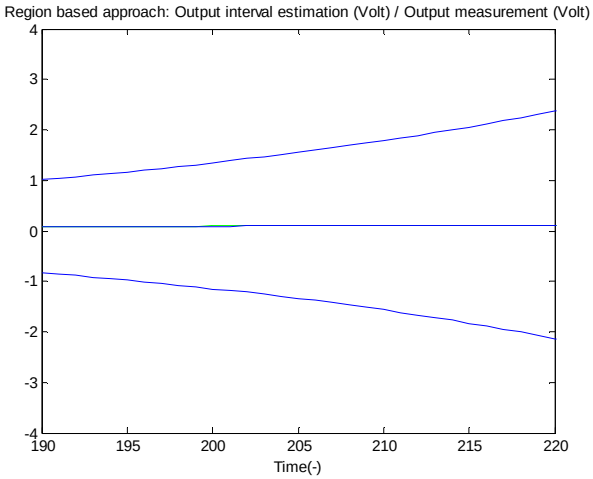

Fig. 4.4 Time evolution of the estimated interval output, its nominal value and the output sensor measurement (green line) using a region-based algorithm where l_1=l_2= l_3=0.5.

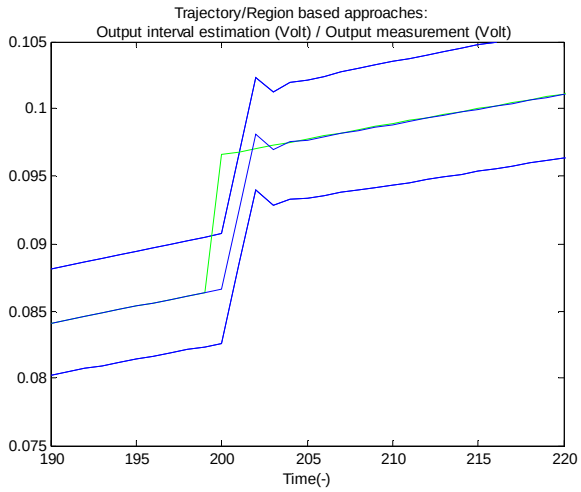

Fig. 4.5 Time evolution of the estimated interval output, its nominal value and the output sensor measurement (green line) using region and trajectory-based algorithms and being l_1=l_2=0.5 and l_3=1.

On the other hand, in *Fig. 4.6* (l_1=l_2=0.5 and l_3=0.97) it is shown the case the isotonicity condition is not satisfied but the region-based approach suffers from a stable wrapping effect because $\|\boldsymbol{A}_o(\boldsymbol{\theta})\|_\infty < 1$ as a consequence of the value

of l_3. In this case, the output interval generated by the region-based approach (*red lines*) is wider than the corresponding to the trajectory-based approach (*blue lines*) because of the output interval propagation error when a region algorithm is used.

In the next sections, the goal of the application example is to show the influence of the isotonicity condition (4.41) on the interval observer fault detection performance considering sensor and actuator faults. First, the effect on the residual sensitivity to a fault, on the residual and on the interval observer threshold is analyzed. Then, the effect on the minimum detectable fault function and on the residual disturbance caused by a fault is studied. Finally, some sensor and actuator faults are applied in order to illustrate the influence of condition (4.41) on their detection. This study is done considering two sets of observer gains: one of them fulfils condition (4.41) (l_1=l_2=0.5 and l_3=1) while the other does not (l_1=l_2=0.5 and l_3=0). Besides, in this example, all the variables (residual sensitivity, threshold, minimum detectable fault, residual disturbance caused by a fault) will be evaluated using the parameter lower bounds $\underline{\boldsymbol{\theta}} \in \Re^{n\theta}$ instead of the corresponding interval parameters $\boldsymbol{\theta}$ on behalf of the clearness of the plots shown in the following sections.

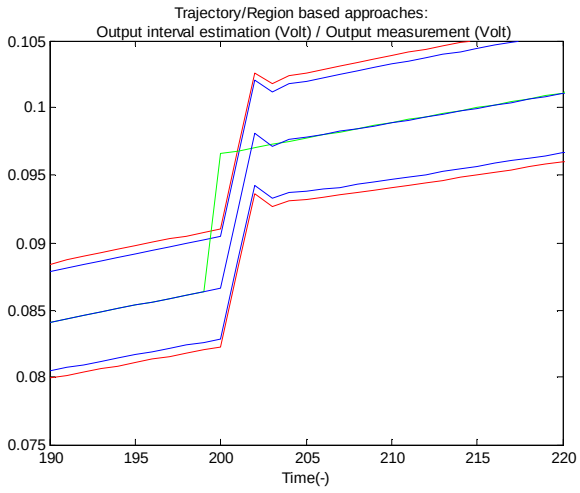

Fig. 4.6 Time evolution of the estimated interval output, its nominal value and the output sensor measurement (green line) using region and trajectory-based algorithms and being l_1=l_2=0.5 and l_3=0.97.

4.4.2 Influence of the isotonicity condition on the residual sensitivity to a fault function

The effect of forcing the isotonicity condition (4.3) on the time evolution of the residual sensitivity to a fault was described in *Section 4.3.1* for output sensors faults ($\boldsymbol{f_y}$), input sensors faults ($\boldsymbol{f_u}$) and actuators faults ($\boldsymbol{f_a}$). Thus, in this section, the results obtained in *Section 4.3.1* are particularized for the application example presented in *Section 4.4.*1.

4.4.2.1 Residual sensitivity to an output sensor fault

In the following, the application example is used to illustrate the effect of the isotonicity condition (4.3) on the residual sensitivity to an output sensor described in Section 4.3.1.1. Thereby, considering the general expression of this function given by Eq. (3.37) (*Section 3.3.1*) and particularizing for the example application (Eq. (4.39)) using its residual expression (Eq. (4.43)), the output sensor fault residual sensitivity associated to the application example is given by

$$\boldsymbol{S}_{fy}(q^{-1},\boldsymbol{\theta}) = \left(\boldsymbol{I} - \boldsymbol{H}(q^{-1},\boldsymbol{\theta})\right)\boldsymbol{G}_{fy}(q^{-1},\tilde{\boldsymbol{\theta}}) = \frac{1-\theta_1 q^{-1}-\theta_2 q^{-2}-\theta_3 q^{-3}}{1+(k_1-\theta_1)q^{-1}+(k_2-\theta_2)q^{-2}+(k_3-\theta_3)q^{-3}} \tag{4.44}$$

where $\boldsymbol{F_y}$ is assumed to be the identity matrix $\boldsymbol{I}$.

Then, the time evolution of the residual sensitivity to an output sensor fault (Eq. (4.44)) is plotted in *Fig. 4.7* assuming an abrupt fault modelled as a unit-step function and considering the observer gain sets mentioned previously: one that satisfies the isotonicity condition (l_1=l_2=0.5 and l_3=1) and another that does not (l_1=l_2=0.5 and l_3=0). Besides, as it was already mentioned, instead of using the interval parameters θ_i, their associated lower bounds $\underline{\theta_i}$ are used assuming the clearness of the plot,

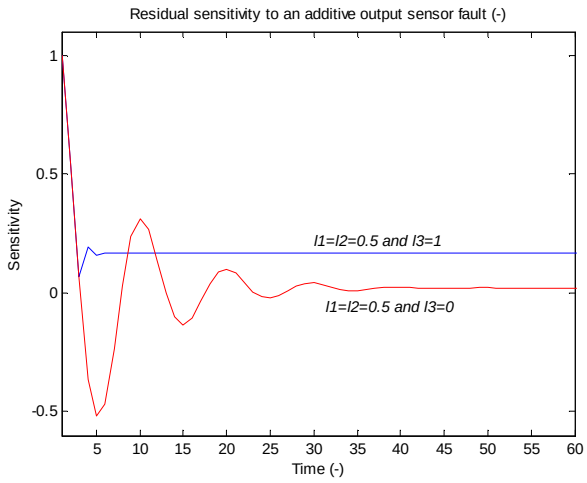

Fig. 4.7 Time evolution of the residual sensitivity associated to an additive abrupt output sensor fault considering two sets of observer gains and using the parameter lower bounds.

Thereby, *Fig. 4.7* shows that when the isotonicity condition (l_3=1) is forced, the absolute value of the residual sensitivity steady-state value increases (Eq.(4.16)). Regarding its dynamics, this is deeply affected but it is difficult to say anything in general since it also depends on the system model.

4.4.2.2 Residual sensitivity to an input sensor fault

Regarding the effect of the isotonicity condition (4.3) on the time evolution of the residual sensitivity to an input fault, it was described in *Section 4.3.1.2*. Thereby, when considering the application example, the residual sensitivity to an input sensor fault is obtained particularizing its general expression given by Eq. (3.47) using the residual expression associated to the application example (Eq. (4.43)):

$$\boldsymbol{S}_{fu}(q^{-1},\boldsymbol{\theta}) = -\boldsymbol{G}(q^{-1},\boldsymbol{\theta})\boldsymbol{F}_u(\boldsymbol{\theta}) = -\frac{\theta_4 q^{-1}}{1+(k_1-\theta_1)q^{-1}+(k_2-\theta_2)q^{-2}+(k_3-\theta_3)q^{-3}} \tag{4.45}$$

where $\boldsymbol{F_u}$ is equal to the identity matrix $\boldsymbol{I}$.

Considering the two observer gain sets mentioned above, (l_1=l_2=0.5 and l_3=1) and (l_1=l_2=0.5 and l_3=0), and assuming an abrupt fault modelled as a unit-step function, the time evolution of the residual sensitivity (Eq. (4.45))is plotted in *Fig. 4.8* using the parameter values given by $\underline{\theta_i}$ such as it was explained in the output sensor fault residual sensitivity case.

Fig. 4.8 shows the effect of forcing the isotonicity condition (4.3) on the residual sensitivity dynamics and steady-state value. According to Eq. (4.19), when that condition (l_3=1) is fulfilled, the absolute value of the input sensor fault residual sensitivity steady-state value increases. Regarding its dynamics, this is deeply affected but it is difficult to say anything in general since it also depends on the system model.

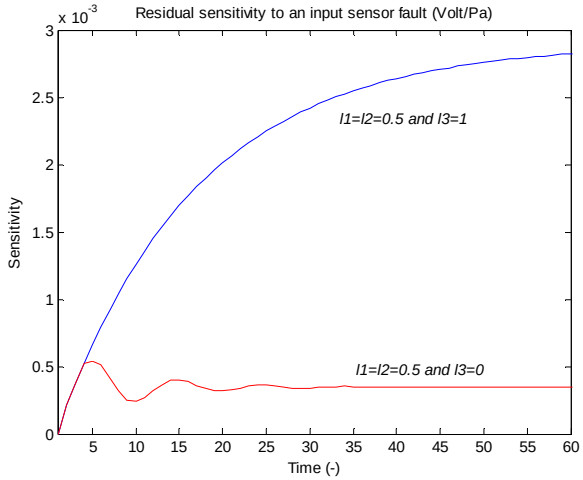

Fig. 4.8 Time evolution of the residual sensitivity associated to an additive abrupt input sensor fault considering two sets of observer gains and using the parameter lower bounds.

4.4.2.3 Residual sensitivity to an actuator fault

Regarding the effect of the isotonicity condition (4.3) on the time evolution of the residual sensitivity to an actuator fault, it was described in Section *Section 4.3.1.3*. Thus, when considering the application example, the residual sensitivity to an actuator fault (Eq. (3.54)) can be particularized using the residual expression given by Eq. (4.43):

$$\boldsymbol{S}_{fa}(q^{-1},\boldsymbol{\theta}) = \left(\boldsymbol{I} - \boldsymbol{H}(q^{-1},\boldsymbol{\theta})\right)\boldsymbol{G}_{fa}(q^{-1},\tilde{\boldsymbol{\theta}}) = \frac{1-\theta_1 q^{-1}-\theta_2 q^{-2}-\theta_3 q^{-3}}{1+(k_1-\theta_1)q^{-1}+(k_2-\theta_2)q^{-2}+(k_3-\theta_3)q^{-3}}\boldsymbol{G}_{fa}(q^{-1},\tilde{\boldsymbol{\theta}}) \tag{4.46}$$

where $\boldsymbol{G_{fa}}$ is given by Eq. (3.5). Then, for this application example, it is assumed that this transfer function satisfies the following expression:

$$\boldsymbol{G}_{fa}(q^{-1},\tilde{\boldsymbol{\theta}}) = \boldsymbol{G}(q^{-1},\tilde{\boldsymbol{\theta}})_{\boldsymbol{L=0}} \tag{4.47}$$

Considering the two observer gain sets mentioned previously, (l_1=l_2=0.5 and l_3=1) and (l_1=l_2=0.5 and l_3=0), and assuming an abrupt fault modelled as a unit-step function, the time evolution of the residual sensitivity (Eq. (4.46)) is drawn in *Fig. 4.9* using the parameter values given by $\underline{\theta}_i$.

Fig. 4.9 shows the effect of forcing the isotonicity condition (4.3) on the residual sensitivity dynamics and steady-state value. According to Eq.(4.22), when that condition (l_3=1) is fulfilled, the absolute value of the actuator fault residual sensitivity steady-state value increases. Regarding its dynamics, this is deeply affected but it is difficult to say anything in general since it also depends on the system model.

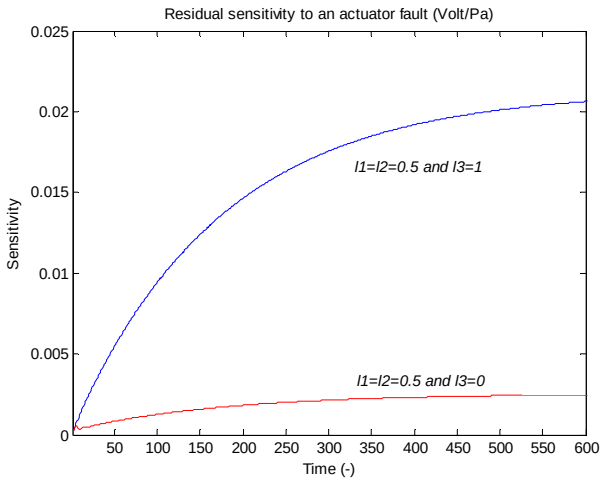

Fig. 4.9 Time evolution of the residual sensitivity associated to an additive abrupt actuator fault considering two sets of observer gains and using the parameter lower bounds.

4.4.3 Influence of the isotonicity condition on the adaptive threshold

In *Section 4.3.2*, the effect of the isotonicity condition (4.3) on time evolution of the residual and the adaptive threshold was analyzed. In this section, the obtained results are particularized for the application example case described in *Section 4.4.1*. Then, assuming a scenario free of faults and nuisance inputs, the observer adaptive threshold is given by Eq. (4.43) according to Eq. (3.62) (*Section 3.3.5*). Then, using the two observer gain sets mentioned above, (l_1=l_2=0.5 and l_3=1) and (l_1=l_2=0.5 and l_3=0), the time evolution of the observer threshold is plotted in *Fig. 4.10* using the parameter values given by $\underline{\theta}_i$.

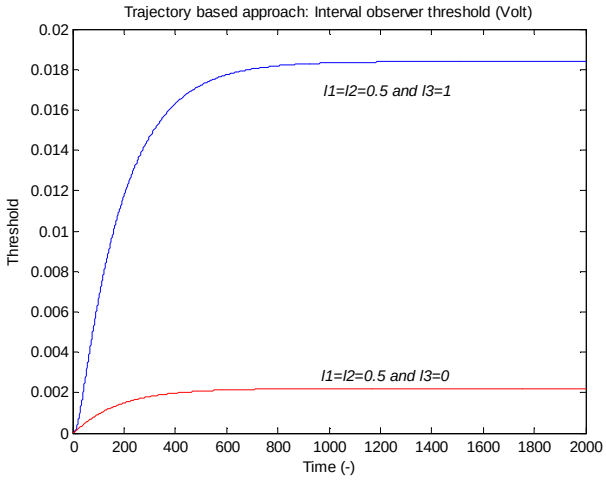

Fig. 4.10 Time evolution of the observer adaptive threshold considering two sets of observer gains and using the parameter lower bounds..

Fig. 4.10 confirms the conclusions mentioned previously (Eq. (4.28)) when the isotonicity condition (4.3) (l_3=1) is forced. In this case, the adaptive threshold generated by the interval observer increases its values worsening the fault detection as bigger faults will be required in order to detect them.

4.4.4 Influence of the isotonicity condition on the minimum detectable fault function

In *Section 4.3.3*, the effect of the isotonicity condition (4.3) on the minimum detectable fault function was analyzed particularizing this function for output sensor faults (*Section 4.3.3.1*), input sensor faults (*Section 4.3.3.2*) and actuator faults (*Section 4.3.3.3*). Then, in this section, the main obtained conclusions are illustrated when the monitored system is given by the application example described in *Section 4.4.1*.

4.4.4.1 Minimum detectable output sensor fault

In the following, using the application example, the effect of forcing the isotonicity condition on the minimum detectable output sensor fault function can be illustrated. In this case, this function is given by Eq. (3.67) using the fault residual sensitivity to an output sensor fault given by Eq. (4.44) and the interval observer threshold given by *Fig. 4.10*. Thus, the considered function can be expressed as it follows:

$$\boldsymbol{f}_{fy}^{min}(k-t_0) = -\frac{1+(k_1-\theta_1)q^{-1}+(k_2-\theta_2)q^{-2}+(k_3-\theta_3)q^{-3}}{1-\theta_1 q^{-1}-\theta_2 q^{-2}-\theta_3 q^{-3}}\boldsymbol{r}_0(k) \qquad (4.48)$$

$$k \geq t_0$$

Considering the two observer gain sets, (l_1=l_2=0.5 and l_3=1) and (l_1=l_2=0.5 and l_3=0), and assuming the fault occurrence time instant (t_0) is *400*, the time evolution of the minimum detectable fault function is plotted in *Fig. 4.11* using the parameter values given by $\underline{\theta}_i$.

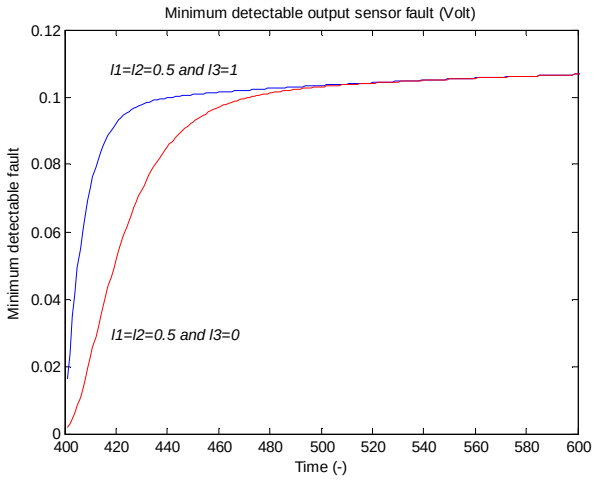

Fig. 4.11 Time evolution of the minimum detectable output sensor fault function considering two sets of observer gains and using the parameter lower bounds.

In *Fig. 4.11*, it is shown forcing the isotonicity condition (4.3) has no effect on the steady-state value of the minimum detectable output sensor fault function according to Eq. (3.77), since its effect on the residual sensitivity and on the interval observer threshold counteract each other. On the other hand, that function is affected during its transitory state because the influence of that condition on the interval observer threshold. It must be taken into account that the function value at fault occurrence time instant is basically determined by the threshold value at this time instant (Eq.(4.31)).

4.4.4.2 Minimum detectable input sensor fault

For the case of the minimum detectable input sensor fault (*Section 4.3.3.2*), this function is determined by Eq. (3.67) using the residual sensitivity to an input sensor fault given by Eq. (4.45) and the interval observer threshold given by *Fig. 4.10* when the application example system. Then, its expression is given by

$$\boldsymbol{f}_{fu}^{min}(k-t_0)=\frac{1+(k_1-\theta_1)q^{-1}+(k_2-\theta_2)q^{-2}+(k_3-\theta_3)q^{-3}}{\theta_4 q^{-1}}\boldsymbol{r}_0(k) \qquad (4.49)$$

$$k \geq t_0$$

In this case, it must be taken into account that this function is not causal (*Section 3.4.1*): it is not defined at its initial time instant ($k=t_0$). At this time instant, the function values do not depend on the observer gain: it is later when the observation gain influence appears. Thereby, such as it was mentioned en *Section 3.4.1*, the procedure given by (Peng et al., 1997) must be applied in order to turn Eq. (4.49) into a causal function. In this case, this procedure consists in delaying this function one time instant:

$$\boldsymbol{f}_{fu*}^{min}(k-t_0)=\boldsymbol{f}_{fu}^{min}(k-t_0)q^{-1} \qquad (4.50)$$

Considering the two observer gain sets, ($l_1=l_2=0.5$ and $l_3=1$) and ($l_1=l_2=0.5$ and $l_3=0$), and assuming the fault occurrence time instant (t_0) is *400*, the time evolution of the minimum detectable fault function is plotted in *Fig. 4.12* using the parameter values given by $\underline{\theta}_i$.

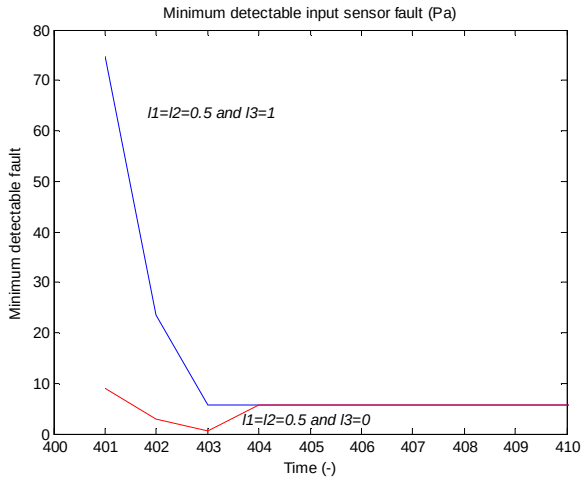

Fig. 4.12 Time evolution of the minimum detectable input sensor fault function considering two sets of observer gains and using the parameter lower bounds.

In this figure, it is seen that forcing the isotonicity condition has no effect on the steady-state value of this function, such as it was mentioned previously. In opposition, it is affected during its transitory-state as consequence of the influence of this condition on the interval observer threshold. In short, *Fig. 4.12* shows the influence of the isotonicity condition on the time evolution of that function is the same than the output sensor case seen in *Fig. 4.11*.

4.4.4.3 Influence on the minimum detectable actuator fault

In this case, considering the application example, the minimum detectable actuator fault function is given by Eq. (3.67) using the residual sensitivity to an actuator fault given by Eq. (4.46) and the interval observer threshold given by *Fig. 4.10*. Thus, this function can be expressed as it follows:

$$\boldsymbol{f}_{fa}^{min}(k-t_0) = -\left(\boldsymbol{G}(q^{-1},\tilde{\boldsymbol{\theta}})_{\boldsymbol{L=0}}\right)^{-1} \frac{1+(k_1-\theta_1)q^{-1}+(k_2-\theta_2)q^{-2}+(k_3-\theta_3)q^{-3}}{1-\theta_1 q^{-1}-\theta_2 q^{-2}-\theta_3 q^{-3}} \boldsymbol{r}_0(k) \qquad (4.51)$$

$k \geq t_0$

In this case, it must be taken into account that this function is not causal either (*Section 3.4.1*) as the function associated to the minimum input sensor fault (Eq. (4.49)) analyzed in the previous section. Consequently, the procedure given by (Peng et al., 1997) must be considered to turn Eq. (4.51) into a causal function. Then, Eq. (4.51) is delayed one time instant resulting the following equation:

$$\boldsymbol{f}_{fa*}^{min}(k-t_0) = \boldsymbol{f}_{fa}^{min}(k-t_0)q^{-1} \qquad (4.52)$$

Considering the two observer gain sets, (l_1=l_2=0.5 and l_3=1) and (l_1=l_2=0.5 and l_3=0), and assuming the fault occurrence time instant (t_0) is *400*, the time evolution of the minimum detectable fault function is plotted in *Fig. 4.13* using the parameter values given by $\underline{\theta}_i$.

Such as it was shown in the output and input sensor fault cases, *Fig. 4.13* shows that the minimum detectable actuator fault function is also only affected by the isotonicity condition during its transitory-state. Once this function reaches its steady-state value, this condition has no longer influence on the values of this function.

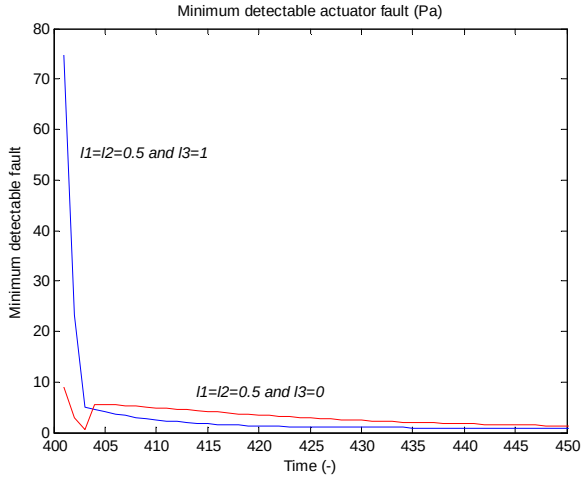

Fig. 4.13 Time evolution of the minimum detectable actuator fault function considering two sets of observer gains and using the parameter lower bounds.

4.4.5 Influence of the isotonicity condition on the fault detection persistency

In *Section 4.3.4*, the effect of the isotonicity condition (4.3) on the fault indication test (Eq. (3.71)) was described. Then, this effect is illustrated in the following subsections when considering the example application system considering output sensor faults, input sensor faults and actuator faults.

4.4.5.1 Influence on the residual disturbance caused by an output sensor fault and on the fault indication

In this example, a fault occurring at t_0=*400* whose value is *f=-0.02 Volt* (roughly, *20%* of the system output nominal steady-state value) is considered. Then, considering the two observer gain sets, (l_1=l_2=0.5 and l_3=1) and (l_1=l_2=0.5

and l_3=0), the time evolution of the interval adaptive threshold, [$\boldsymbol{r_0(k)}$] (*dashed line*), and the interval residual disturbance originated by the fault, [$\boldsymbol{-d_f(k)}$] (*solid line*), are plotted in *Fig. 4.14*. According to Eq. (3.71) (*Section 3.4.3*), the fault can not be indicated while [$\boldsymbol{r_0(k)}$] contains [$\boldsymbol{-d_f(k)}$] since the effect of the fault on the residual does not counteract the one caused by the model uncertainty.

Fig. 4.14 shows that when the isotonicity condition is forced (l_3=1) (*upper plot*), the interval adaptive threshold [$\boldsymbol{r_0(k)}$] widens regarding the case where that condition is not forced (*lower plot*) and consequently, the fault indication persistency worsens . As soon as the fault residual disturbance values decrease, as a consequence of the output sensor fault residual sensitivity time evolution (Eq. (4.44); *Fig. 4.7*), it is contained into the interval related to the adaptive threshold and as a result, the fault can no longer be indicated (Eq. (3.71)).

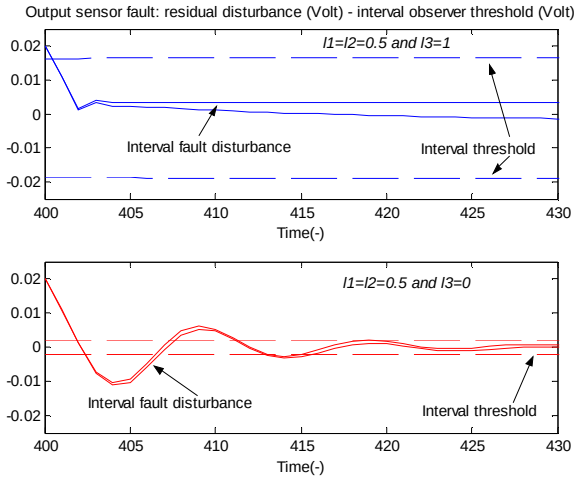

Fig. 4.14 Time evolution of the interval fault residual disturbance (solid line) and the interval observer threshold (dashed line) considering two sets of observer gains where the occurrence of a constant output sensor fault whose value is -0.02 *Volt* at time instant t_0=*400* is considered.

4.4.5.2 Influence on the residual disturbance caused by an input sensor fault and on the fault indication

In this case, an input sensor fault occurring at t_0=*400* whose value is *f=-9 Pa* (roughly, *9* times bigger than the input used in *Section 4.3*) is considered. Then, considering the two observer gain sets, (l_1=l_2=0.5 and l_3=1) and (l_1=l_2=0.5 and l_3=0), the time evolution of the interval adaptive threshold [$\boldsymbol{r_0(k)}$] and the interval residual disturbance originated by the fault [$\boldsymbol{-d_f(k)}$] are plotted in *Fig. 4.15*.

Such as it was mentioned in the output sensor fault case, when forcing the isotonicity condition (*upper plot*), the fault indication worsens regarding the case in which this condition was not forced (*lower plot*). In this case, as a consequence of the interval adaptive threshold widening, the input sensor fault residual disturbance requires more time to exceed the adaptive threshold than the case where the isotonicity condition is not forced.

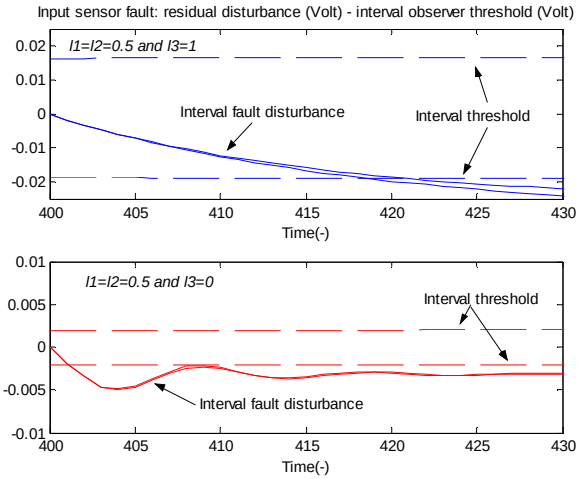

Fig. 4.15 Time evolution of the interval fault residual disturbance (solid line) and the interval observer threshold (dashed line) considering two sets of observer gains where the occurrence of a constant input sensor fault whose value is -9 *Pa* at time instant t_0=*400* is considered.

4.4.5.3 Influence on the residual disturbance caused by an actuator fault and on the fault indication

In this case, an actuator fault occurring at t_0=*400* whose value is *f*=*-9 Pa* (roughly, *9* times bigger than the input used in *Section 4.3*) is considered. Then, considering the two observer gain sets, (l_1=l_2=0.5 and l_3=1) and (l_1=l_2=0.5 and l_3=0), the time evolution of the interval adaptive threshold [$\boldsymbol{r_0(k)}$] and the interval residual disturbance originated by the fault [$\boldsymbol{-d_f(k)}$] are plotted in *Fig. 4.16*.

Such as it was mentioned in the input sensor fault case, when forcing the isotonicity condition (*upper plot*), the fault indication worsens regarding the case in which this condition is not forced (*lower plot*). In this case, when the isotonicity condition is forced, the actuator fault residual disturbance also requires more time to exceed the adaptive threshold as a consequence of the adaptive threshold interval widening.

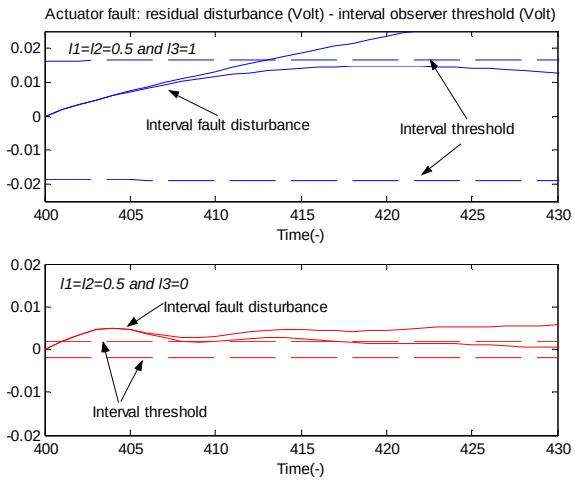

Fig. 4.16 Time evolution of the interval fault residual disturbance (solid line) and the interval observer threshold (dashed line) considering the two sets of observer gains where the occurrence of a constant actuator fault whose value is -9 *Pa* at time instant t_0=*400* is considered.

4.4.5.4 Output sensor fault detection

In this case, an output sensor fault occurring at time instant t_0=400 and whose value is given by *f*= *-0.06 Volt* (roughly, *60%* of the system output nominal steady-state value) is considered. In *Fig. 4.17*, the time evolution of the

system output estimation interval, its nominal value and the system output measurement (*green line*) is plotted using a trajectory-based approach and an observer gain set which does not satisfy the isotonicity condition: (l_1=l_2=0.5 and l_3=0). Besides, at the bottom of the figure, a fault indicator activated when the fault is detected (*red line*) is also plotted. On the other hand, in *Fig. 4.18,* the same functions are plotted but this time using an observer gain set which fulfils that isotonicity condition (l_1=l_2=0.5 and l_3=1).

Comparing *Fig. 4.18* where the isotonicity condition is forced regarding *Fig. 4.17* where it is not, it is seen clearly that this condition that allow avoiding the wrapping effect widens the system output estimation interval computed by the observer such as it was already mentioned in the relation (4.29) (*Section 4.4.2*). As a result, this comparison points out that the fault indication is worsened when the isotonicity condition is forced such as it was mentioned in *Section 4.4.2* and in *Section 4.4.4*.

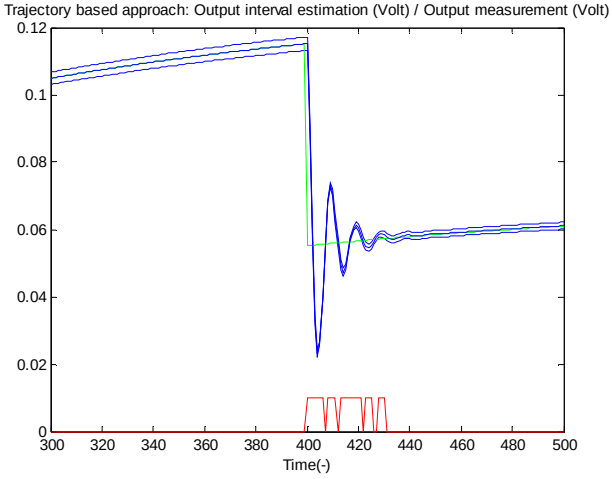

Fig. 4.17 Time evolution of the estimated interval output, its nominal value and the output sensor measurement (*green line*) using an observer gain set which does not fulfil the isotonicity condition (l_1=l_2=0.5 and l_3=0) and considering an output sensor fault whose value is *-0.06 Volt* at time instant t_0=400.

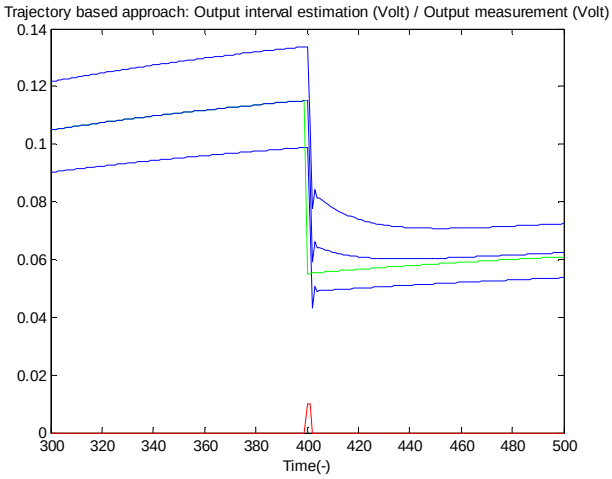

Fig. 4.18 Time evolution of the estimated interval output, its nominal value and the output sensor measurement (*green line*) using an observer gain set which fulfils the isotonicity condition (l_1=l_2=0.5 and l_3=1) and considering an output sensor fault whose value is *-0.06 Volt* at time instant t_0=400.

4.4.5.5 Input sensor fault detection

In this case, an input sensor fault occurring at time instant t_0=400 whose value is given by *f= -6 Pa* (roughly, *6* times bigger than the input used in *Section 4.3*) is considered. In *Fig. 4.19*, the time evolution of the system output

estimation interval, its nominal value and the system output measurement (*green line*) is plotted using a trajectory-based approach and an observer gain set which does not satisfy the isotonicity condition: (l_1=l_2=0.5 and l_3=0) while in *Fig. 4.20*, the same scenario is plotted but using an observer gain set which fulfils the isotonicity condition (l_1=l_2=0.5 and l_3=1).

Comparing *Fig. 4.20* (l_1=l_2=0.5 and l_3=1) and *Fig. 4.19* (l_1=l_2=0.5 and l_3=0), it is also seen clearly that the isotonicity condition widens the system output estimation interval (*Section 4.4.2*) and consequently, the observer fault detection performance is worsened such as it was shown in the previous section for the output sensor case.

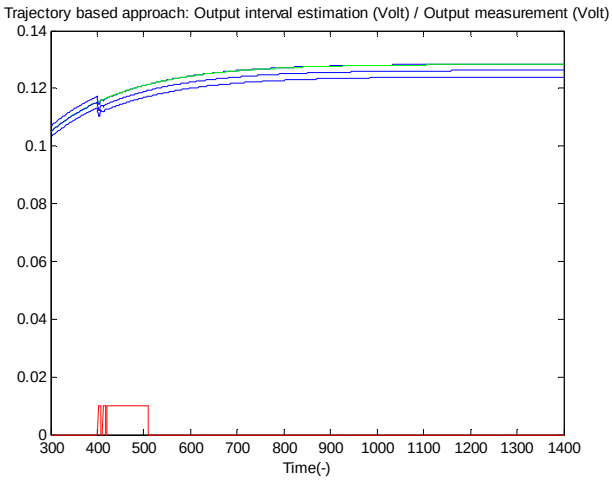

Fig. 4.19 Time evolution of the estimated interval output, its nominal value and the output sensor measurement (*green line*) using an observer gain set which does not fulfil the isotonicity condition (l_1=l_2=0.5 and l_3=0) and considering an input sensor fault whose value is *-6 Pa* at time instant t_0=400.

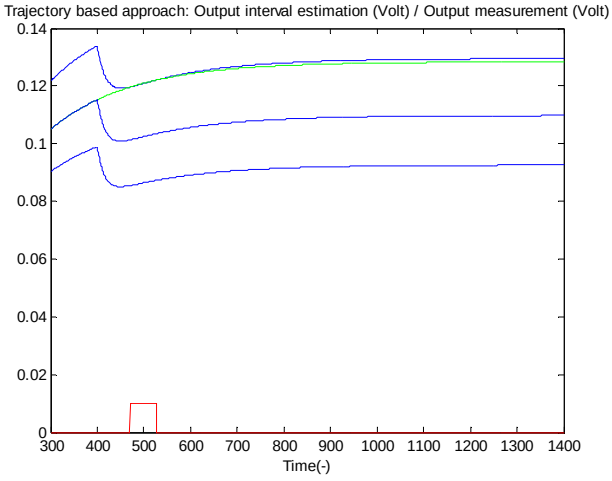

Fig. 4.20 Time evolution of the estimated interval output, its nominal value and the output sensor measurement (*green line*) using an observer gain set which fulfils the isotonicity condition (l_1=l_2=0.5 and l_3=1) and considering an input sensor fault whose value is *-6 Pa* at time instant t_0=400.

4.4.5.6 Actuator fault detection

In this case, an actuator fault occurring at time instant t_0=400 whose value is given by *f= -1 Pa* (roughly, *10* times bigger than the input used in *Section 4.3*) is considered. In *Fig. 4.21*, the time evolution of the system output estimation interval, its nominal value and the system output measurement (*green line*) is plotted using a trajectory-based approach and an observer gain set which does not satisfy the isotonicity condition: (l_1=l_2=0.5 and l_3=0) while

in *Fig. 4.22*, the same scenario is plotted but using an observer gain set which fulfils the isotonicity condition (l_1=l_2=0.5 and l_3=1).

Comparing *Fig. 4.22* (l_1=l_2=0.5 and l_3=1) and *Fig. 4.21* (l_1=l_2=0.5 and l_3=0), it is also seen clearly that the isotonicity condition widens the system output estimation interval (*Section 4.4.2*) such as mentioned for the output and input sensor fault cases shown in the previous sections. Thus, in the actuator fault case, the observer fault detection performance is also influenced negatively.

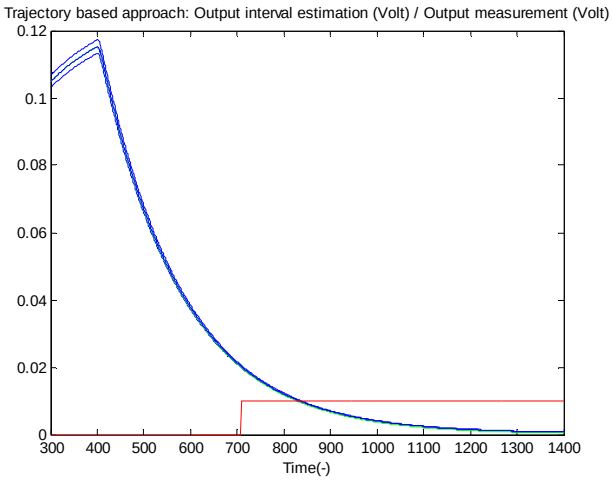

Fig. 4.21 Time evolution of the estimated interval output, its nominal value and the output sensor measurement (*green line*) using an observer gain set which does not fulfil the isotonicity condition (l_1=l_2=0.5 and l_3=0) and considering an actuator fault whose value is *-1 Pa* at time instant t_0=400.

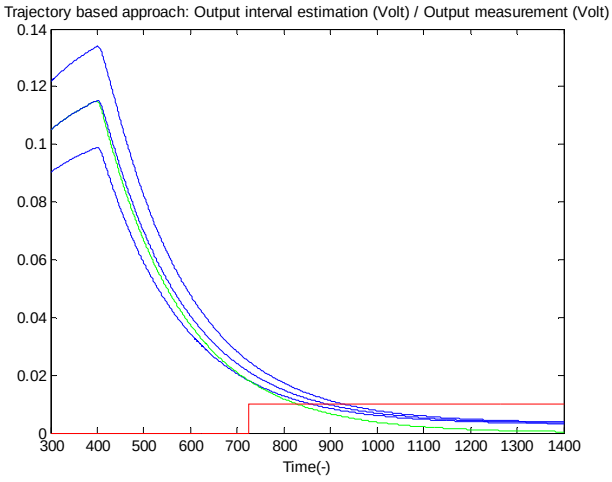

Fig. 4.22 Time evolution of the estimated interval output, its nominal value and the output sensor measurement (*green line*) using an observer gain set which fulfils the isotonicity condition (l_1=l_2=0.5 and l_3=1) and considering an actuator fault whose value is *-1 Pa* at time instant t_0=400.

4.5 Conclusions

According to the point (b) of fault detection objectives (*Section 2.5.1*), this chapter shows a method to avoid the wrapping effect which is affecting an interval model when it is computed using a low computational algorithm ("region-based approach"). It is demonstrated that it is not necessary to use a high computational algorithm ("trajectory-based approach") to avoid this effect but it is enough to consider an interval observer model whose observer gain matrix ***L*** has been properly designed. In fact, this method is only based on turning the non-isotonic

model matrix into an isotonic one using the mentioned matrix $\boldsymbol{L}_-$ ($\boldsymbol{L}=\boldsymbol{L}_+ + \boldsymbol{L}_-$). This chapter also shows that designing $\boldsymbol{L}$ to avoid the wrapping effect may apparently worsen the observer fault detection performance. However, analyzing the main observer fault detection properties, it can be seen that a proper design of $\boldsymbol{L}_+$ might counteract the negative effect of $\boldsymbol{L}_-$ regarding fault detection performance, although this task is out of the scope of this thesis.

CHAPTER 5

Approximating fault detection linear interval observers using λ-order interval predictors

5.1 Introduction

Model based fault detection can use different types of model representation in order to generate the residual. In case of model parameter uncertainty, a model whose parameter values are bounded by intervals, known as an interval model, is usually considered such as it was described in *Chapter 3* and *Chapter 4*. This chapter is focused on finding the equivalence between interval observers and λ-order interval predictors regarding fault detection since predictor models avoid those problems associated with the state estimation such as the wrapping effect (*Section 2.3.2.5* of *Chapter 2*). In (Chow et al, 1984), a minimum order predictor (*"dead-beat observer"* (Patton et al, 1991)) was obtained from a state-space model but regarding fault detection, this model does not show appealing properties as its fault indication persistence is minimum and given by the system order (Meseguer et al, 2006a). This chapter mainly deals with a generalization of the *"dead-beat observer"* method since given an interval observer whose fault detection properties have been carefully designed using the observation gain (Meseguer et al, 2006b), an equivalent λ-order predictor is obtained which has the same fault detection behaviour but avoids those drawbacks related to the state estimation when *region-based* (*set-based*) algorithms (*Section 2.3.2.5*) are used. According to (Gertler, 1998), an observer can be described by an ARMA model, i.e, by an IIR filter. On the other hand, a λ-order predictor can be described by a MA model of order λ, i.e, by an FIR filter. It is known from the literature that an IIR filter (i.e. ARMA model) can be approximated by a FIR filter (i.e, MA model) of infinite order. This fact will be used in this chapter to approximate fault detection linear interval observers by λ-order interval predictors. This will allow that given a particular linear interval observer, a predictor of order λ with an equivalent a fault detection performance can be found.

In the literature, the importance of the fault residual sensitivity regarding the quality of the fault indication is noticed by (Gertler, 1998). According to (Chen et al, 1999), when an interval observer is considered, the observer gain plays an important role because it determines the time evolution of the fault residual sensitivity and the associated adaptive threshold derived from the model structured uncertainty. As a result, and such as it was shown in *Chapter 3* based on (Meseguer et al., 2007b), the observer gain determines the observer fault detection properties.

However, as seen in *Chapter 4*, when the model matrix does not fulfil the isotonicity property (Cugueró et al, 2002), interval observers can suffer from wrapping effect if low computational algorithms, as the region-based approaches coming from the interval community, are used (Puig et al, 2005a). In this chapter based on (Meseguer et al., 2008a),

it was demonstrated that designing properly the observer gain matrix, the wrapping effect can be avoided. This design is based on forcing that the observer state-space matrix fulfils the isotonicity property. Nonetheless, if the equivalent λ-order predictor were used in this case, the wrapping effect would be also avoided as these models do not suffer from that effect since their estimations are only based on measurements. Besides, if the observer were isotonic using or not the conditions given by (Meseguer et al., 2008a), the equivalent predictor could be computed using two known point-wise trajectories given by the lower and upper bounds of the uncertain parameters (Cugueró et al, 2002) what has an appealing low computational cost. If the observer were not isotonic, the equivalent predictor would have to be computed using the general trajectory-based approach which has a high computational cost.

The structure of the *Chapter 5* remainder is the following: the way to obtain an λ-order predictor equivalent to an interval observer is presented in *Section 5.2*. In the following (*Section 5.3*), the behaviour of observers and their equivalent predictors is analyzed when applied to fault detection in order to show their equivalence. Finally (*Section 5.4*), an example based on an industrial servo actuator will be used to illustrate the derived results.

5.2 Equivalence between interval predictors and interval observers

As illustrated in *Chatper 3* (*Section 3.2.1*), the monitored system can be described by a MIMO linear uncertain dynamic model in discrete-time whose state-space form considering faults is

$$\begin{aligned} \boldsymbol{x}(k+1) &= \boldsymbol{A}(\tilde{\boldsymbol{\theta}})\boldsymbol{x}(k) + \boldsymbol{B}(\tilde{\boldsymbol{\theta}})\boldsymbol{u}_0(k) + \boldsymbol{F}_a(\tilde{\boldsymbol{\theta}})\boldsymbol{f}_a(k) \\ \boldsymbol{y}(k) &= \boldsymbol{C}(\tilde{\boldsymbol{\theta}})\boldsymbol{x}(k) + \boldsymbol{F}_y(\tilde{\boldsymbol{\theta}})\boldsymbol{f}_y(k) \end{aligned} \tag{5.1}$$

where $\boldsymbol{y}(k)\in\Re^{ny}$, $\boldsymbol{u_0}(k)\in\Re^{nu}$, $\boldsymbol{x}(k)\in\Re^{nx}$ are the system output, input and the state-space vectors respectively; $\boldsymbol{A}(\tilde{\boldsymbol{\theta}})\in\Re^{nx\times nx}$, $\boldsymbol{B}(\tilde{\boldsymbol{\theta}})\in\Re^{nx\times nu}$ and $\boldsymbol{C}(\tilde{\boldsymbol{\theta}})\in\Re^{ny\times nx}$ are the state, the input and the output matrices respectively; $\tilde{\boldsymbol{\theta}}\in\Re^{n\theta}$ is the system parameter vector; $\boldsymbol{f_y}(k)\in\Re^{ny}$ and $\boldsymbol{f_a}(k)\in\Re^{nu}$ are faults in the system output sensors and actuators respectively being $\boldsymbol{F_y}(\tilde{\boldsymbol{\theta}})$ and $\boldsymbol{F_a}(\tilde{\boldsymbol{\theta}})$ their associated matrices. Regarding the system model representation used in *Section 3.2.1* (Eq. (3.1)), the system model considered in this section (Eq. (5.1)) neglects the effect of direct transmission matrix $\boldsymbol{D}(\tilde{\boldsymbol{\theta}})$ since it has no influence in the derived results and genrally, it is considered zero-valued.

5.2.1 Observer

As it was mentioned in *Section 3.2.1*, assuming the observability for all $\tilde{\boldsymbol{\theta}}\in\boldsymbol{\Theta}$ the system described by Eq. (5.1) can be monitored using a linear observer with *Luenberger* structure based on an ***interval model*** whose model parameters $\boldsymbol{\theta}$ are bounded by an interval set $\boldsymbol{\Theta}=\left\{\boldsymbol{\theta}\in\Re^{n\theta}\middle|\underline{\boldsymbol{\theta}}\le\boldsymbol{\theta}\le\overline{\boldsymbol{\theta}}\right\}$ which represents the uncertainty about the exact knowledge of real system parameters $\tilde{\boldsymbol{\theta}}$. Thus, this ***interval observer*** can be written as:

$$\begin{aligned} \hat{\boldsymbol{x}}(k+1) &= (\boldsymbol{A}(\boldsymbol{\theta})-\boldsymbol{L}\boldsymbol{C}(\boldsymbol{\theta}))\hat{\boldsymbol{x}}(k) + \boldsymbol{B}(\boldsymbol{\theta})\boldsymbol{u}(k) + \boldsymbol{L}\boldsymbol{y}(k) = \boldsymbol{A}_o(\boldsymbol{\theta})\hat{\boldsymbol{x}}(k) + \boldsymbol{B}(\boldsymbol{\theta})\boldsymbol{u}(k) + \boldsymbol{L}\boldsymbol{y}(k) \\ \hat{\boldsymbol{y}}(k) &= \boldsymbol{C}(\boldsymbol{\theta})\hat{\boldsymbol{x}}(k) \end{aligned} \tag{5.2}$$

In *Chapter 3* (*Section 3.2.1*), it was noticed that two particular cases could be distinguished in the observer model structure: the ***simulator*** (***L=0*** assuming system stability (Chow et al, 1984)) and the ***predictor*** (***L= L_p*** (Chow et al, 1984)). According to (Patton et al, 1991), the predictor obtained forcing ***L= L_p*** is the predictor of minimum order

(*"dead-beat observer"*) which can only indicate a fault for a minimum time instants given by the system order. In line with the main conclusions of *Chapter 3* based on the results of (Meseguer et al, 2007b), when an observer is considered ($\boldsymbol{L}=\boldsymbol{L_o}$[14]), the fault indication is more persistent for a certain value of $\boldsymbol{L_o}$ than the corresponding one to the *dead-beat observer* and consequently, the observer model structure seems to be more suitable in order to enhance the fault detection performance of a certain model.

As it was shown in *Section 3.2.1*, the observer given by Eq. (5.2) can be expressed in transfer function form using the *q*-transform and considering zero initial conditions as it follows:

$$\hat{\boldsymbol{y}}(k)=\boldsymbol{G}_o(q^{-1},\boldsymbol{\theta})\boldsymbol{u}(k)+\boldsymbol{H}_o(q^{-1},\boldsymbol{\theta})\boldsymbol{y}(k) \tag{5.3}$$

where:

$$\boldsymbol{G}_o(q^{-1},\boldsymbol{\theta})=\boldsymbol{C}(\boldsymbol{\theta})(\boldsymbol{I}-q^{-1}\boldsymbol{A}_o(\boldsymbol{\theta}))^{-1}\boldsymbol{B}(\boldsymbol{\theta})q^{-1} \tag{5.4}$$

$$\boldsymbol{H}_o(q^{-1},\boldsymbol{\theta})=\boldsymbol{C}(\boldsymbol{\theta})(\boldsymbol{I}-q^{-1}\boldsymbol{A}_o(\boldsymbol{\theta}))^{-1}\boldsymbol{L}q^{-1} \tag{5.5}$$

The sub index '*o*' indicates these transfer functions are associated to the observer model. Besides, comparing these functions with those obtained in *Section 3.2.1* (Eq. (3.12) and Eq. (3.13)), it can be seen there is no difference neglecting the direct transmission matrix $\boldsymbol{D}(\tilde{\boldsymbol{\theta}})$. Regarding the system output measurement, ***y(k)***, and the system input measurement, ***u(k)***, it must be taken into account that their expressions are given by Eq. (3.2) and Eq. (3.8) respectively shown in *Section 3.2.1*

5.2.2 Predictor

On the other hand, the system described by Eq. (5.1) could be also monitored using a linear interval *predictor*. This model can be written as it follows

$$\hat{\boldsymbol{y}}(k+1)=\boldsymbol{A}_p(\boldsymbol{\theta})\boldsymbol{y}(k)+\boldsymbol{B}_p(\boldsymbol{\theta})\boldsymbol{u}(k) \tag{5.6}$$

where matrices $\boldsymbol{A_p(\theta)}\in\Re^{ny\times ny}$ and $\boldsymbol{B_p(\theta)}\in\Re^{ny\times nu}$ are obtained from the system model (5.1) and the predictor parameter vector is defined such it was in *Section 3.2.1*. Using the method given by (Patton et al, 1991) or (Ploix et al, 2006), the predictor of minimum order is obtained which behaves like an observer when the condition $\boldsymbol{L}=\boldsymbol{L_p}$ is satisfied. According to (Patton et al, 1991), the fault indication given by this predictor (*"dead-beat observer"*) has a minimum persistence when the fault is not persistently indicated (*weak fault detection*) (*Section 3.4.2*) what may origin a poor performance of the fault detection module causing a wrong fault diagnosis result. Considering this drawback, this chapter is focused on obtaining a λ-order predictor which behaves like an observer for a given value of $\boldsymbol{L}$. This method can be viewed as a generalization of the approaches given by (Patton et al, 1991) and (Ploix et al, 2006).

Equivalently, the predictor given by Eq. (5.6) can also be expressed in transfer function form using the shift operator q^{-1} and assuming zero initial conditions as it follows:

$$\hat{\boldsymbol{y}}(k)=\boldsymbol{G}_p(q^{-1},\boldsymbol{\theta})\boldsymbol{u}(k)+\boldsymbol{H}_p(q^{-1},\boldsymbol{\theta})\boldsymbol{y}(k) \tag{5.7}$$

where:

$$\boldsymbol{G}_p(q^{-1},\boldsymbol{\theta})=\boldsymbol{B}_p(\boldsymbol{\theta})q^{-1} \tag{5.8}$$

$$\boldsymbol{H}_p(q^{-1},\boldsymbol{\theta})=\boldsymbol{A}_p(\boldsymbol{\theta})q^{-1} \tag{5.9}$$

and the sub index '*p*' indicates these transfer functions are associated with the predictor model.

[14] $\boldsymbol{L_o}$ is a set of observer gains that places all the observer eigenvalues between the ones related to the monitored system (***simulation approach***) and the origin (***prediction approach***)

5.2.3 Equivalence between λ-order interval predictors and interval observers

Propagating the observer equation (5.2) k times forward, starting from $k=0$, the predicted output at time k can be determined as

$$\hat{\boldsymbol{y}}(k) = \boldsymbol{C}(\boldsymbol{\theta})\boldsymbol{A}_o(\boldsymbol{\theta})^k \hat{\boldsymbol{x}}(0) + \sum_{v=1}^{k} \boldsymbol{C}(\boldsymbol{\theta})\boldsymbol{A}_o(\boldsymbol{\theta})^{v-1}\boldsymbol{B}(\boldsymbol{\theta})\boldsymbol{u}(k-v) + \sum_{v=1}^{k} \boldsymbol{C}(\boldsymbol{\theta})\boldsymbol{A}_o(\boldsymbol{\theta})^{v-1}\boldsymbol{L}\boldsymbol{y}(k-v) \tag{5.10}$$

for every value of $\boldsymbol{\theta} \in \boldsymbol{\Theta}$.

The current estimated output not only depends on the initial state, but also on the last k measurements of the system inputs and outputs. The contribution of the states depends on the dynamics of the observer and as a result, if k is large enough, the contribution of the initial state $\hat{\boldsymbol{x}}(0)$ to the output estimation $\hat{\boldsymbol{y}}(k)$ can be dismissed. Thereby, this simplification can be assumed if the next relation is satisfied:

$$\boldsymbol{A}_o(\boldsymbol{\theta})^k = (\boldsymbol{A}(\boldsymbol{\theta}) - \boldsymbol{L}\boldsymbol{C}(\boldsymbol{\theta}))^k \approx 0 \quad \forall \boldsymbol{\theta} \in \boldsymbol{\Theta}, k > \lambda \tag{5.11}$$

where λ is the time window which assures the fulfilment of the relation (5.11). Equivalently, it can be said that the dynamics of the observer has vanished some steps ago. Then, the predicted output can be approximated through

$$\hat{\boldsymbol{y}}(k) \approx \left[\sum_{v=1}^{\lambda} \boldsymbol{C}(\boldsymbol{\theta})\boldsymbol{A}_o(\boldsymbol{\theta})^{v-1}\boldsymbol{B}(\boldsymbol{\theta})q^{-(v-1)}\right]\boldsymbol{u}(k-1) + \left[\sum_{v=1}^{\lambda} \boldsymbol{C}(\boldsymbol{\theta})\boldsymbol{A}_o(\boldsymbol{\theta})^{v-1}\boldsymbol{L}q^{-(v-1)}\right]\boldsymbol{y}(k-1) \tag{5.12}$$

which is exactly equal to the predictor expression given by Eq. (5.6) and therefore, this especial interval observer ,where the contribution of the initial $\hat{\boldsymbol{x}}(0)$ can be obviated if the relation (5.11) is satisfied, can be seen as a interval predictor of order λ which compute at every time instant, roughly, the same system output estimation interval. Comparing Eq. (5.6) with Eq. (5.12), the matrices of the predictor model related to those of the interval observer are obtained resulting

$$\boldsymbol{A}_p(q^{-1},\boldsymbol{\theta}) = \sum_{v=1}^{\lambda} \boldsymbol{C}(\boldsymbol{\theta})\boldsymbol{A}_o(\boldsymbol{\theta})^{v-1}\boldsymbol{L}q^{-(v-1)} \tag{5.13}$$

$$\boldsymbol{B}_p(q^{-1},\boldsymbol{\theta}) = \sum_{v=1}^{\lambda} \boldsymbol{C}(\boldsymbol{\theta})\boldsymbol{A}_o(\boldsymbol{\theta})^{v-1}\boldsymbol{B}(\boldsymbol{\theta})q^{-(v-1)} \tag{5.14}$$

The inspection of these equations shows that the relationship between the interval observer and the interval predictor scheme is given in terms of the observer matrix $\boldsymbol{A_o}$, which depends on the observer gain matrix $\boldsymbol{L}$. This gain not only determines the observer behaviour but also the order λ of the equivalent predictor. The interval predictor given by Eq (5.12) is a ***closed-loop predictor*** since it uses measurements of past system inputs and outputs to predict the present system output.

From Eq. (5.12), it follows that if the particular case of $\boldsymbol{L}=\boldsymbol{0}$ corresponding to a simulator were considered, predictor (5.12) would have been an ***open-loop predictor*** that only uses measurements of past system inputs to predict the present system output.

In order to derive analytically the order λ of the equivalent interval predictor to a given interval observer, the following proposition can be used:

Proposition 1 (Puig et al, 2003b). Let us consider that the interval observer given by Eq. (5.2) is asymptotic stable. Then, for a $k>l_\varepsilon$ where

$$l_\varepsilon = \max_{\theta \in \Theta} \left[\frac{\log \varepsilon - \log \kappa(\theta)}{\log \rho(\theta)} \right] \tag{5.15}$$

,the condition given by Eq. (5.16) is fulfilled with a desired degree of approximation ε:

$$\left\| A_o(\theta)^k \right\|_\infty = \left\| \left[A(\theta) - LC(\theta) \right]^k \right\|_\infty = \varepsilon \approx 0 \quad \forall \theta \in \Theta \tag{5.16}$$

, where ρ is the spectral radius of the interval observer matrix A_o determined by the maximum absolute value of all the eigenvalues of this matrix and κ is the condition number of A_o whose value is determined by the result of the following matrix product: $\|A_o\|.\|A_o^{-1}\|$. A matrix with a high κ is said to be ill-conditioned, otherwise it is considered well-conditioned.

Thus, Eq. (5.15) describes the equivalent predictor order dependence regarding the observer gain matrix L. The bigger is the norm of L, the observer poles tend to zero and consequently, so does the spectral radius. Then, according to Eq. (5.15), the lower is the order λ of the obtained equivalent predictor. When $L = L_p$, the observer is a *"dead-beat observer"* (Patton et al, 1991), and thus, ρ tends to zero what provokes l_ε to tend to its minimum value given by the system order. Otherwise, when $L = 0$, the observer is a simulator (Chow et al, 1984), and ρ tends to its maximum value given by one, and thus, l_ε tends to an infinite value.

5.2.4 Computational complexity

(Puig et al, 2005a) shows the problem of interval observation can be translated to an interval simulation. As it is noticed by (Ploix et al, 2006), interval simulation requires lots of computations at each sample time, being generally incompatible with real-time constraint needed by the fault detection module when applied to complex dynamic system (*trajectory-based algorithm*). The reason is that, except for some particular cases, the recurrence leads to replace state-space value sets by simpler outer value sets, such as boxes or ellipsoids what yields some over-estimations. The propagation of these approximations (using a region-based algorithm) induces an accumulation of errors leading to an explosion of the computed sets (*wrapping effect*) (Puig et al, 2005a) such as it was also analyzed along the *Chapter 4*. On the other hand, checking on a finite horizon, such as parity space approach does, avoids this drawback because the integration over a long time window is not required. However, as noticed in previous section, parity space approach produces a minimum order predictor that has a response equivalent to a *"dead-beat observer"*. Thus, as it is known (Puig et al, 2002a), when applied to fault detection, the minimum order predictor (or *"dead-beat observer"*) is highly sensitive to noise and, depending on the fault, only indicates the fault at its occurrence time instant. Conversely, observer models through the observer gain can filter noise and indicate the fault presence for longer time as illustrated in *Chapter 3* derived from the results obtained in (Meseguer et al, 2007b). This motivates the use of higher order predictors with a fault detection performance equivalent to the behaviour of an observer but without the drawback of being affected by the wrapping effect, such as demonstrated in *Chapter 4*. However, although the wrapping effect problem is avoided, computational complexity still remains since optimization problems related to compute a higher-order predictor equivalent to a given observer are non-linear regarding the parameters (*trajectory-based algorithms*). Then, in order to guarantee the tightest interval bounding output prediction, a global optimization algorithm should be used since the optimization problem is non-convex. The only case in which such computational complexity can be reduced is when higher order predictor comes from an observer whose matrix $A_o(\theta)$ has all elements positive (isotonic matrix). In this case, the estimation interval for each system output prediction can be obtained evaluating the model uncertain parameters using two point-wise sets determined by their lower and upper interval bound ($\overline{\hat{y}}_i(k) = \hat{y}_i(k, \overline{\theta})$ and $\underline{\hat{y}}_i(k) = \hat{y}_i(k, \underline{\theta})$) (Cugueró et al, 2002). Then, the equivalent

λ-order predictor interval output can be also computed using these two known point-wise trajectories as Eq. (5.15) forces each observer trajectory to be equivalent to the associated predictor trajectory. In this case, the output estimation generated by the equivalent interval observer would also be computationally cheap since a set propagation based approach (*region-based algorithm*) can be applied. This is because in this case the interval observer is unaffected by the wrapping effect (Puig et al, 2005a). Besides, it should be taken into account that the elements of $\boldsymbol{A}_o(\boldsymbol{\theta})$ can be forced to be positive through the observer gain matrix $\boldsymbol{L}$ (Meseguer et al, 2008a) such as it was shown in *Chapter 4* (*Section 4.2.2*).

5.3 Application to fault detection

5.3.1 Residual generation and evaluation

As mentioned in *Chapter 3* (*Section 3.2.2*), fault detection is based on calculating at every time instant a residual comparing the measurements of physical variables $\boldsymbol{y}(k)$ associated with the monitored system with their estimation $\hat{\boldsymbol{y}}(k)$ provided by the associated system model:

$$\boldsymbol{r}(k) = \boldsymbol{y}(k) - \hat{\boldsymbol{y}}(k) \tag{5.17}$$

According to (Gertler, 1998) and such as it was shown in *Section 3.2.2*, a general expression for the residual, known as its *computational form*, is given by

$$\boldsymbol{r}(k,\boldsymbol{\theta}) = \boldsymbol{V}(q^{-1},\boldsymbol{\theta})\boldsymbol{u}(k) + \boldsymbol{O}(q^{-1},\boldsymbol{\theta})\boldsymbol{y}(k) \tag{5.18}$$

where: $\boldsymbol{r}(k) \in \Re^{ny}$ is the residual set, $\boldsymbol{V}(q^{-1},\boldsymbol{\theta})$ and $\boldsymbol{O}(q^{-1},\boldsymbol{\theta})$ are transfer functions.

When the interval observer model is considered, the transfer functions $\boldsymbol{V}(q^{-1},\boldsymbol{\theta})$ and $\boldsymbol{O}(q^{-1},\boldsymbol{\theta})$ can be obtained using Eq. (5.3) and Eq. (5.17) what results in:

$$\boldsymbol{V}_o(q^{-1},\boldsymbol{\theta}) = -\boldsymbol{G}_o(q^{-1},\boldsymbol{\theta}) = -\boldsymbol{C}(\boldsymbol{\theta})(\boldsymbol{I} - q^{-1}\boldsymbol{A}_o(\boldsymbol{\theta}))^{-1}\boldsymbol{B}(\boldsymbol{\theta})q^{-1} \tag{5.19}$$

$$\boldsymbol{O}_o(q^{-1},\boldsymbol{\theta}) = \boldsymbol{I} - \boldsymbol{H}_o(q^{-1},\boldsymbol{\theta}) = \boldsymbol{I} - \boldsymbol{C}(\boldsymbol{\theta})(\boldsymbol{I} - q^{-1}\boldsymbol{A}_o(\boldsymbol{\theta}))^{-1}\boldsymbol{L}q^{-1} \tag{5.20}$$

Comparing these expressions with the calculated ones in *Section 3.2.2* (Eq. (3.17) and Eq. (3.18)), it can be seen they are equal if $\boldsymbol{D}(\tilde{\boldsymbol{\theta}})$ is neglected.

In the interval predictor case, those transfer functions can be obtained using Eq. (5.7) and Eq. (3.18) what results in:

$$\boldsymbol{V}_p(q^{-1},\boldsymbol{\theta}) = -\boldsymbol{G}_p(q^{-1},\boldsymbol{\theta}) = -\boldsymbol{B}_p(\boldsymbol{\theta})q^{-1} \tag{5.21}$$

$$\boldsymbol{O}_p(q^{-1},\boldsymbol{\theta}) = \boldsymbol{I} - \boldsymbol{H}_p(q^{-1},\boldsymbol{\theta}) = (\boldsymbol{I} - \boldsymbol{A}_p(\boldsymbol{\theta})q^{-1}) \tag{5.22}$$

In the fault detection and fault isolation interface used in (Puig et al. 2005b), the residual (5.17) is computed regarding the nominal observer model $\hat{\boldsymbol{y}}^{\boldsymbol{o}}(k)$ obtained using the observer parameter set $\boldsymbol{\theta} = \boldsymbol{\theta}^o \in \boldsymbol{\Theta}$,

$$\boldsymbol{r}^{\boldsymbol{o}}(k) = \boldsymbol{y}(k) - \hat{\boldsymbol{y}}^{\boldsymbol{o}}(k) \tag{5.23}$$

Such as it was mentioned in *Chapter 3* (*Section 3.2.2*), when considering model uncertainty located in parameters, the residual generated by (5.23) will not be zero even in a non-faulty scenario. In this case, the possible values of each component of this residual vector, $\boldsymbol{r}^{\boldsymbol{o}}(k)$, can be bounded using the following interval (neglecting couplings among outputs), such as illustrated by (Puig et al, 2002a):

$$[\underline{r}_i^o(k), \overline{r}_i^o(k)] \tag{5.24}$$

where:

$$\underline{r}_i^o(k) = \underline{\hat{y}}_i(k) - \hat{y}_i^o(k) \text{ and } \overline{r}_i^o(k) = \overline{\hat{y}}_i(k) - \hat{y}_i^o(k) \tag{5.25}$$

being $\underline{\hat{y}}_i(k)$ and $\overline{\hat{y}}_i(k)$ the bounds of the i^{th}-system output estimation computed using the interval observer (5.2) or its equivalent interval predictor (5.12) and obtained according to Eq. (3.10).

In this case, this residual interval constitutes the ***adaptive threshold*** since the comparison of every component of the nominal residual vector, $r^o{}_i(k)$, with its corresponding bounding interval (Eq. (5.24)) allows the indication of the fault if the following relation is satisfied.

$$r_i^o(k) \notin [\underline{r}_i^o(k), \overline{r}_i^o(k)] \tag{5.26}$$

It should be noticed that this fault detection test is fully equivalent to the one given by Eq. (3.24) in *Chapter 3* (Section *3.2.2*).

5.3.2 Equivalence between the interval observer and its associated interval predictor regarding fault indication

As it was mentioned in the previous section, the indication of a fault by the fault detection stage is just determined by the test given by the Eq. (5.26). Thus, two models (interval observer and its equivalent λ-order predictor) which generate at every time instant the same residual $r_i^o(k)$ having the same adaptive threshold $[\underline{r}_i^o(k), \overline{r}_i^o(k)]$ will indicate the fault equivalently.

According to Eq. (5.15) which sets the order of the equivalent predictor to the given interval observer, the system output estimations given by both models fulfil the following condition:

$$\left\| \hat{\boldsymbol{y}}_o(k,\boldsymbol{\theta}) - \hat{\boldsymbol{y}}_p(k,\boldsymbol{\theta}) \right\| \approx 0 \quad \forall \boldsymbol{\theta} \in \boldsymbol{\Theta} \tag{5.27}$$

where the sub index '*o*' is set for the observer model while sub index *p* for the equivalent predictor model.

Therefore, according to the residual expression given by Eq. (5.17), the residuals generated by both models also fulfil an equivalent condition:

$$\left\| \boldsymbol{r}_o(k,\boldsymbol{\theta}) - \boldsymbol{r}_p(k,\boldsymbol{\theta}) \right\| \approx 0 \quad \forall \boldsymbol{\theta} \in \boldsymbol{\Theta} \tag{5.28}$$

Then, considering the conditions given by Eq. (5.27) and Eq. (5.28), the observer and its equivalent predictor are generating at every time instant the same residual $r_i^o(k)$ and the same adaptive threshold $[\underline{r}_i^o(k), \overline{r}_i^o(k)]$ and consequently, both models have an equivalent performance regarding the fault indication.

5.3.3 Sensitivity of the residual to a fault

In *Chapter 3* (*Section 3.3*), the concept of ***fault sensitivity of the residual*** (Gertler, 1998) was recalled extending this concept to interval models focusing on the dynamical aspects of this model property. In this section, a complete analysis regarding the influence of the observer gain $\boldsymbol{L}$ on the time evolution of this property was carried out. According to (Gertler, 1998) regarding non-interval models and (Meseguer et al, 2007b) regarding interval observer models and such as it was shown along *Chapter 3*, the fault residual sensitivity is a key property of the considered model concerning its fault detection behaviour as it determines the adaptive threshold, the minimum detectable fault and the time a fault is indicated.

In this section, it will be demonstrated that interval observers and their equivalent λ-order predictors must have the same residual sensitivity to whatever kind of fault affecting to the monitored system.

The residual internal form given by Eq. (3.62) (*Section 3.3.5*) determines that the value of the residual at every time instant is given by the disturbance caused by different faults which can affect the monitored system (actuator fault, $\boldsymbol{f_a}$, output sensor fault, $\boldsymbol{f_y}$ and input sensor fault, $\boldsymbol{f_u}$) and the disturbance caused by the model parameter uncertainty. This residual form shows that the residual disturbance caused by a fault vector is determined by the residual sensitivity to this kind of fault (residual sensitivity to an actuator fault, $\boldsymbol{S_{fa}}$, given by Eq. (3.54), residual sensitivity to an output sensor fault, $\boldsymbol{S_{fy}}$, given by Eq. (3.37), residual sensitivity to an input sensor fault, $\boldsymbol{S_{fu}}$ given by Eq. (3.47)) while the residual disturbance caused by the model parameter uncertainty is given by the adaptive threshold, $\boldsymbol{r_\theta}$ (Eq. (3.21)). Then, considering the monitored system is affected by a fault vector $\boldsymbol{f}$ whose occurrence time instant is t_0, the expression of the residual according to Eq. (3.62) will be given by

$$\boldsymbol{r}(k,\boldsymbol{\theta}) = \begin{cases} \boldsymbol{r}_0(k,\boldsymbol{\theta}) + \boldsymbol{S}_f(q^{-1},\boldsymbol{\theta})\boldsymbol{f}(k)q^{-t_0} & k \geq t_0 \\ \boldsymbol{r}_0(k,\boldsymbol{\theta}) & k < t_0 \end{cases} \tag{5.29}$$

where $\boldsymbol{S_f}$ is the residual sensitivity to the fault vector $\boldsymbol{f}$. Then, according to Eq. (5.28), at whatever time instant k, the interval observer and its equivalent predictor generate the same residual (Eq. (5.28)). As a result of this statement, it is concluded both models must have the same residual sensitivity to the fault vector $\boldsymbol{f}$ if condition (5.15) is fulfilled. This equivalence can be written as it follows:

$$\boldsymbol{S}_{of}(q^{-1},\boldsymbol{\theta}) \approx \boldsymbol{S}_{pf}(q^{-1},\boldsymbol{\theta}) \quad \forall \boldsymbol{\theta} \in \boldsymbol{\Theta} \tag{5.30}$$

where the sub index '*o*' is set for the observer model while sub index *p* for the equivalent predictor model.

This result shows that such as in *Section 3*.3 (*Chapter 3*) the fault residual sensitivity dynamics was described regarding the observation gain $\boldsymbol{L}$, the same sensitivity dynamics can also be achieved with the equivalent predictor calculating its order using Eq. (5.15). In the following, *Table 5.1* describes the sensitivity dynamics in terms of $\boldsymbol{L}$ and λ such as it was done in terms of $\boldsymbol{L}$ in *Table 3.1* (*Section 3.6*).

	Simulation $\boldsymbol{L=0}$ *or* $\lambda \to \infty$	***Observation*** $\boldsymbol{L=L_o}$ *or* $n < \lambda < \infty$	***Prediction*** $\boldsymbol{L=L_p}$ *or* $\lambda = n$
$\boldsymbol{S}_{fy}$	Constant	Pulse	Deadbeat
$\boldsymbol{S}_{fu}$	Dynamic response	Dynamic response	Constant
$\boldsymbol{S}_{fa}$	Dynamic response	Dynamic response	Constant

Table 5.1 Fault residual sensitivity dinamics[15]

5.4 Application example

5.4.1 Description

The application example proposed to illustrate the obtained results is the industrial smart actuator FDI Benchmark used in *Chapter 4* (*Section 4.4*) to demonstrate how an interval observer can avoid the wrapping effect forcing the observer gain to satisfy a especial condition (*Section 4.2.2*) and to illustrate the effect of this condition on its fault detection performance. Although the properties of the considered model of this smart actuator are equal to the ones presented in *Chapter 4* (*Section 4.4*), in this section are recalled for the clarity of the given results. Thereby, such as it was shown in *Section 4.4,* the following linear interval model of this smart actuator is considered:

$$\begin{aligned} \hat{\boldsymbol{x}}(k+1) &= \boldsymbol{A}(\boldsymbol{\theta})\hat{\boldsymbol{x}}(k) + \boldsymbol{B}(\boldsymbol{\theta})\boldsymbol{u}(k) \\ \hat{\boldsymbol{y}}(k) &= \boldsymbol{C}(\boldsymbol{\theta})\hat{\boldsymbol{x}}(k) \end{aligned} \tag{5.31}$$

with: $\hat{\boldsymbol{x}}(k) = \begin{bmatrix} \hat{x}_1(k) & \hat{x}_2(k) & \hat{x}_3(k) \end{bmatrix}^t$,

$\boldsymbol{A}(\boldsymbol{\theta}) = \begin{bmatrix} 0 & 0 & \theta_3 \\ 1 & 0 & \theta_2 \\ 0 & 1 & \theta_1 \end{bmatrix}$, $\boldsymbol{B}(\boldsymbol{\theta}) = \begin{bmatrix} 0 \\ 0 \\ \theta_4 \end{bmatrix}$, $\boldsymbol{C}(\boldsymbol{\theta}) = \begin{bmatrix} 0 & 0 & 1 \end{bmatrix}$ and $\boldsymbol{u}(k) = CVP(k-2)$

where: $\hat{x}_3(k)$ is the valve position estimation, $\hat{\boldsymbol{y}}(k)$ is the estimation of this position measured by the displacement transducer (in Volt), ***CVP(k)*** is the command pressure (in Pascal) measured by a given input sensor. Then, as used in *Chapter 4* (*Section 4.4*), the model uncertain parameters are bounded by their confidence intervals: $\theta_1 \in$ [1.1417 1.1471], $\theta_2 \in$ [0.3995 0.4103], $\theta_3 \in$ [-0.5537 -0.5484], and $\theta_4 \in$ [2.180e-4 2.183e-4] while their nominal values are given by $\theta^o{}_1$=1.1444, $\theta^o{}_2$=0.4049, $\theta^o{}_3$= -0.5510, and $\theta^o{}_4$=2.182e-4. Regarding the command pressure, a constant value given by $u(k) = 1Pa$ has been considered.

5.4.2 Output estimation and residual analysis

As shown in *Section 4.4.1* and according to Eq. (5.3), the interval observer estimation of the system output can be obtained from Eq. (5.31) considering the following observer gain matrix $\boldsymbol{L}$=[k_3, k_2, k_1]$^{\mathrm{T}}$:

$$\begin{aligned} &\hat{\boldsymbol{y}}(k) = \boldsymbol{G}_o(q^{-1},\boldsymbol{\theta})\boldsymbol{u}(k) + \boldsymbol{H}_o(q^{-1},\boldsymbol{\theta})\boldsymbol{y}(k) = \\ &= \frac{\theta_4 q^{-1}}{1+(k_1-\theta_1)q^{-1}+(k_2-\theta_2)q^{-2}+(k_3-\theta_3)q^{-3}}\boldsymbol{u}(k) + \frac{k_1 q^{-1}+k_2 q^{-2}+k_3 q^{-3}}{1+(k_1-\theta_1)q^{-1}+(k_2-\theta_2)q^{-2}+(k_3-\theta_3)q^{-3}}\boldsymbol{y}(k) \end{aligned} \tag{5.32}$$

where k_1, k_2 and k_3 are the observer gains. Regarding the residual expression, its form can be inferred from Eq. (5.18), Eq. (5.19) and Eq. (5.20) using Eq. (5.32):

$$\begin{aligned} &\boldsymbol{r}(k,\boldsymbol{\theta}) = \boldsymbol{V}_o(q^{-1},\boldsymbol{\theta})\boldsymbol{u}(k) + \boldsymbol{O}_o(q^{-1},\boldsymbol{\theta})\boldsymbol{y}(k) = \left(-\boldsymbol{G}_o(q^{-1},\boldsymbol{\theta})\right)\boldsymbol{u}(k) + \left(\boldsymbol{I} - \boldsymbol{H}_o(q^{-1},\boldsymbol{\theta})\right)\boldsymbol{y}(k) = \\ &= -\frac{\theta_4 q^{-1}}{1+(k_1-\theta_1)q^{-1}+(k_2-\theta_2)q^{-2}+(k_3-\theta_3)q^{-3}}\boldsymbol{u}(k) + \frac{1-\theta_1 q^{-1}-\theta_2 q^{-2}-\theta_3 q^{-3}}{1+(k_1-\theta_1)q^{-1}+(k_2-\theta_2)q^{-2}+(k_3-\theta_3)q^{-3}}\boldsymbol{y}(k) \end{aligned} \tag{5.33}$$

As it was said in *Chapter 4* (*Section 4.4.1*), the state-space matrix $\boldsymbol{A}(\boldsymbol{\theta})$ of the application example model (Eq. (5.31)) does not fulfil the isotonicity property and consequently, the system output estimation using the interval observer given by Eq. (5.32) is affected by the wrapping effect when a *region-based algorithm* is used and the isotonicity condition given by Eq. (4.3) is not forced. As it was seen, this condition is satisfied when

$$k_3 = \theta_3 \tag{5.34}$$

which using the known observer gain parameterization $k_i = l_i\theta_i$ implies l_3=*1*. In case, condition given by Eq. (5.34) is not forced, the output estimation done by the interval observer should be obtained using a *trajectory-based approach* or, according to *Section 5.2.2*, using its equivalent λ-order interval predictor as both approaches estimate the same system output interval according to Eq. (5.27).

---

[15] *n* stands for the predictor minimum order.

Thereby, let us assume a constant additive fault affecting the system output sensor occurring at time instant t_0=200 and whose value is given by *f= 0.01 Volt* (roughly, *10%* of the steady-state system output nominal value) and let us also consider an observation gain set determined by $l_1= l_2=l_3=0.5$. Then, in *Fig. 5.1*, the time evolution of the system output estimation interval and its nominal estimation and the output sensor measurement (*green line*) are plotted between the time instants $t_1=190$ and $t_2=220$ using the interval observer input-output form given by Eq. (5.32) and considering a *trajectory-based algorithm* (*upper plot*) and a *region-based algorithm* (*lower plot*). Thereby, according to the mentioned above, while the trajectory based approach produces an accurate interval what allows to detect the fault; the corresponding interval produced using a region based approach is useless because of the wrapping effect which causes an unstable growing system output estimation interval.

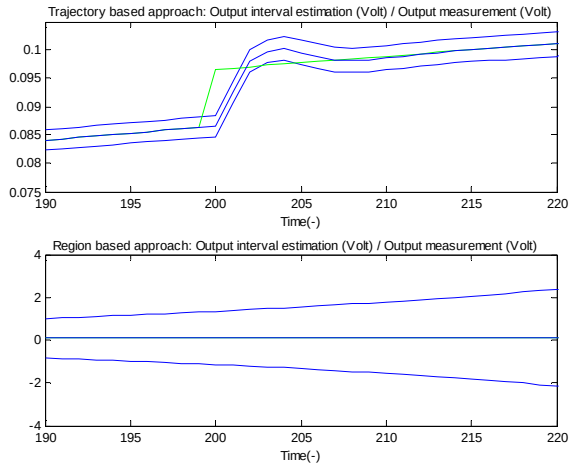

Fig. 5.1 Time evolution of the system output estimation interval, its nominal value, and the system output sensor measurement (*green line*) using a trajectory and region-based algorithm and where the observers gains are given by $l_1=l_2= l_3$=0.5

5.4.3 Equivalence between observers and predictors

Using the application example, in this section, the evolution of the equivalent predictor order, λ, regarding the observation gain of its associated interval observer is described. Thus, for a given observer gain, using Eq. (5.15), the order λ of the equivalent predictor is obtained for a certain degree of approximation ε. Then, in *Fig. 5.2*, the evolution of the predictor order versus the observer gain is plotted considering the parameterization $k_i = l\theta_i$ varying the l from simulation ($l=0$) to prediction ($l=1$) and using an approximation degree given by $\varepsilon=1e\text{-}5$. It must be taken into account that for a certain value of l, Eq. (5.15) is evaluated considering all the possible trajectories related to the interval observer determined for the uncertainty related to the parameters. It can be noticed that when the observer works as a simulator ($l \to 0$), the order of its equivalent predictor is affected by a fast growing, *i.e.*, the memory of the predictor increases fastly. On the other hand, when the observer works as a predictor ($l \to 1$) (*predictor* of order $n=3$, being n the system order), the equivalent predictor tends to the order of the system (*"dead-beat observer"* (Patton et al, 1991)), *i.e.*, the memory of the predictor decreases until the system order.

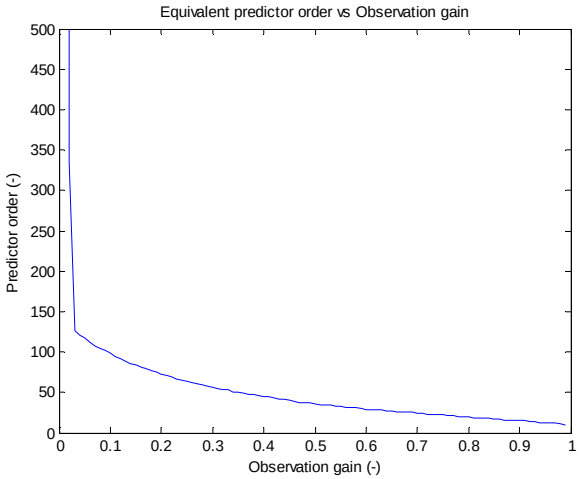

Fig. 5.2 Evolution of the equivalent predictor order regarding the observation gain of its associated interval observer

5.4.4 Time evolution of the residual sensitivity to a fault

In *Section 5.3.3*, it was shown that the fault residual sensitivity functions of the interval observer and its equivalent λ-order predictor are equal when the degree of approximation ε can be underestimated since it is roughly zero-valued. Thus, the goal of this section is to exemplify this statement using the application example and considering the residual sensitivity to an output sensor fault, $\boldsymbol{S_{fy}}$, and the residual sensitivity to an input sensor fault, $\boldsymbol{S_{fu}}$.

Such as it was seen in *Chapter 3* (*Section 3.3*), the functions $\boldsymbol{S_{fy}}$ and $\boldsymbol{S_{fu}}$ are given by Eq. (3.37) and Eq. (3.47), respectively. Concerning these expressions, it must be noticed that they are valid for the interval observer and also for its equivalent predictor. The fault residual sensitivity functions associated with the interval observer are obtained when the transfer function matrices $\boldsymbol{O}(q^{-1},\boldsymbol{\theta})$ and $\boldsymbol{V}(q^{-1},\boldsymbol{\theta})$ are calculated using Eq. (5.20) and Eq. (5.19), respectively. On the other hand, if Eq. (5.22) and Eq. (5.21) were used to calculate those transfer functions, the fault residual sensitivity functions associated with the equivalent predictor would be obtained.

Focusing on the application example, when an interval observer is considered, according to Eq. (3.37) and Eq. (5.33), its residual sensitivity to an output sensor fault is given by

$$\boldsymbol{S}_{ofy}(q^{-1},\boldsymbol{\theta}) = \boldsymbol{O}_o(q^{-1},\boldsymbol{\theta})\boldsymbol{G}_{fy}(q^{-1},\tilde{\boldsymbol{\theta}}) = \frac{1-\theta_1 q^{-1}-\theta_2 q^{-2}-\theta_3 q^{-3}}{1+(k_1-\theta_1)q^{-1}+(k_2-\theta_2)q^{-2}+(k_3-\theta_3)q^{-3}} \tag{5.35}$$

assuming matrix $\boldsymbol{F_y}$ is equal to the identity matrix $\boldsymbol{I}$. Conversely, according to Eq. (3.47) and Eq. (5.33), the interval observer residual sensitivity to an input sensor fault can be written as it follows:

$$\boldsymbol{S}_{ofu}(q^{-1},\boldsymbol{\theta}) = \boldsymbol{V}_o(q^{-1},\boldsymbol{\theta})\boldsymbol{F}_u(\boldsymbol{\theta}) = -\frac{\theta_4 q^{-1}}{1+(k_1-\theta_1)q^{-1}+(k_2-\theta_2)q^{-2}+(k_3-\theta_3)q^{-3}} \tag{5.36}$$

assuming matrix $\boldsymbol{F_u} = \boldsymbol{I}$.

Concerning the equivalent predictor associated with the interval observer given by Eq. (5.32), its residual sensitivity to an output sensor fault can be obtained using Eq. (3.37), Eq. (5.22), Eq. (5.13) and considering the matrices $\boldsymbol{A}$ and $\boldsymbol{C}$ associated with the monitored system (Eq. (5.31)).

$$\begin{aligned}\boldsymbol{S}_{pfy}(q^{-1},\boldsymbol{\theta}) &= \boldsymbol{O}_p(q^{-1},\boldsymbol{\theta})\boldsymbol{G}_{fy}(q^{-1},\tilde{\boldsymbol{\theta}}) = \boldsymbol{I}-\boldsymbol{H}_p(q^{-1},\boldsymbol{\theta}) = \ (\boldsymbol{I}-\boldsymbol{A}_p(\boldsymbol{\theta})q^{-1}) = \\ &= \boldsymbol{I}-\left(\sum_{v=1}^{\lambda}\boldsymbol{C}(\boldsymbol{\theta})\left(\boldsymbol{A}(\boldsymbol{\theta})-\boldsymbol{LC}\right)^{v-1}\boldsymbol{L}q^{-(v-1)}\right)q^{-1}\end{aligned} \tag{5.37}$$

where $\boldsymbol{F_y} = \boldsymbol{I}$, λ is obtained using Eq. (5.15) and $\boldsymbol{L}$=[k_3, k_2, k_1]$^{\mathrm{T}}$.

Then, using Eq, (3.47), Eq. (5.21), Eq. (5.14) and the matrices ***A, B, C*** and ***L*** associated to the monitored system (Eq. (5.31)), the equivalent predictor residual sensitivity to an input sensor fault can be calculated computing the following equation

$$\begin{aligned} \boldsymbol{S}_{pfu}(q^{-1},\boldsymbol{\theta}) &= \boldsymbol{V}_p(q^{-1},\boldsymbol{\theta})\boldsymbol{F}_u(\boldsymbol{\theta}) = -\boldsymbol{G}_p(q^{-1},\boldsymbol{\theta}) = -\boldsymbol{B}_p(\boldsymbol{\theta})q^{-1} = \\ &= -\sum_{v=1}^{\lambda} \boldsymbol{C}(\boldsymbol{\theta})\left(\boldsymbol{A}(\boldsymbol{\theta}) - \boldsymbol{LC}\right)^{v-1} \boldsymbol{B}(\boldsymbol{\theta})q^{-(v-1)}q^{-1} \end{aligned} \tag{5.38}$$

assuming $\boldsymbol{F_u} = \boldsymbol{I}$.

In the following, considering an abrupt fault modelled as a unit-step function, the time evolution of those residual sensitivity functions are plotted using the observer gain set given by $k_1=k_2=k_3=0.5$ and considering just the nominal value of the uncertain parameters ($\boldsymbol{\theta} = \boldsymbol{\theta}^o \in \boldsymbol{\Theta}$). In this case, the equivalent predictor order is given by $l=36$ *(Fig. 5.2)* considering a predictor approximation degree $\varepsilon=1e\text{-}5$ (Eq. (5.15)).

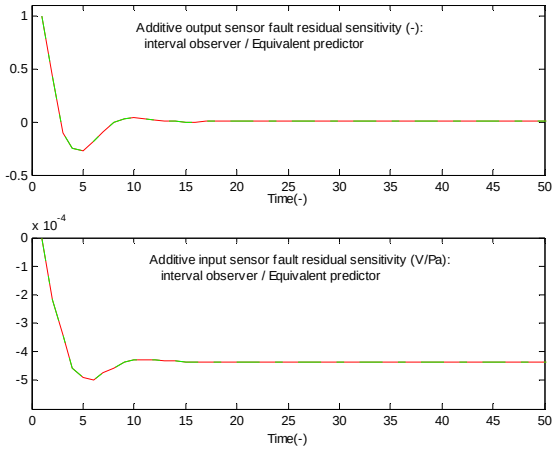

Fig. 5.3 Time evolution of the residual sensitivity function to an output sensor fault (*upper plot*) and the residual sensitivity function to an input sensor fault (*lower plot*) using the nominal observer (*green line*) and its equivalent predictor (*red line*)

In *Fig.* 5.3, the residual sensitivity functions to an output sensor fault (*upper plot*) and to an input sensor fault (*lower plot*) are drawn using both the nominal observer (*green line*) and its associated equivalent predictor (*red line*). As it can be seen in this figure, comparing the time evolution of the residual sensitivity to an input/output fault related to the nominal observer with the one related to the equivalent predictor, they are almost undistinguishable when both schemes are really equivalent.

On the other hand, in *Fig. 5.4*, the case in which both models are not equivalent is plotted. This is achieved considering $l<36$, for example $l=3$. In this case, such as it can be seen in *Fig. 5.4*, the time evolution of the residual sensitivity to an output/input sensor related to both models is different since they are not equivalent.

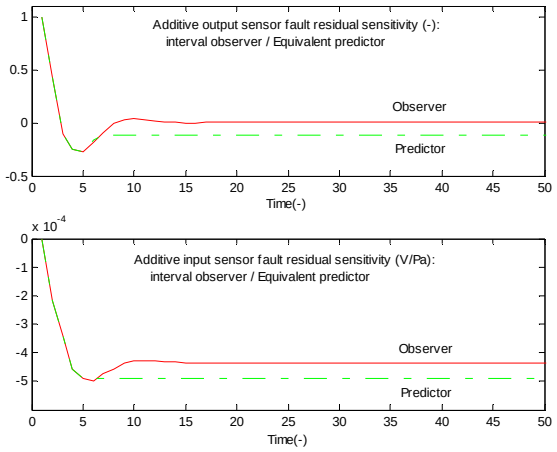

Fig. 5.4 Time evolution of the residual sensitivity function to an output sensor fault (*upper plot*) and the residual sensitivity function to an input sensor fault (*lower plot*) using the nominal observer (*green line*) and its equivalent predictor (*red line*) which does not satisfy condition (5.15)

5.4.5 Predictor and observer behaviour in fault scenario

The goal of this section is to compare the fault detection performance of an interval observer whose system output estimations are obtained using the *trajectory based approach* (*Section 2.3.2.5.4*) (Puig et al, 2003b) with the fault detection performance of its corresponding equivalent predictor considering the fault scenario used in *Section 5.4.2* and assuming a predictor approximation degree ε*=1e-5* (Eq. (5.15)). In addition, this behaviour comparison is also used to confirm the equivalent predictor also avoids the wrapping effect such as the interval observer when it is computed using the *trajectory based approach* as it was mentioned along *Chapter 4*.

Firstly, a case where both type of models are fully equivalent regarding fault detection is shown in *Fig.* 5.5. This is achieved when the order of the equivalent predictor *'λ'* is equal to *36* according to Eq. (5.15) and the observer gains mentioned in *Section 5.4.2* are used (l_1*= *l_2*=*l_3*=0.5*). Then, in *Fig.* 5.5, the time evolutions of the nominal residual (*green line*) (Eq. (5.33), $\boldsymbol{\theta} = \boldsymbol{\theta}^o \in \boldsymbol{\Theta}$) and its associated adaptive threshold (*blue line*) (Eq. (5.24)) are plotted between the time instants *190* and *220* using both models (*interval observer: upper plot*; *equivalent predictor: lower plot*) showing the full equivalence between them. As a result, the interval observer and its correspondent predictor are also equivalent regarding their fault detection properties according to the fault detection test given by Eq. (5.26).

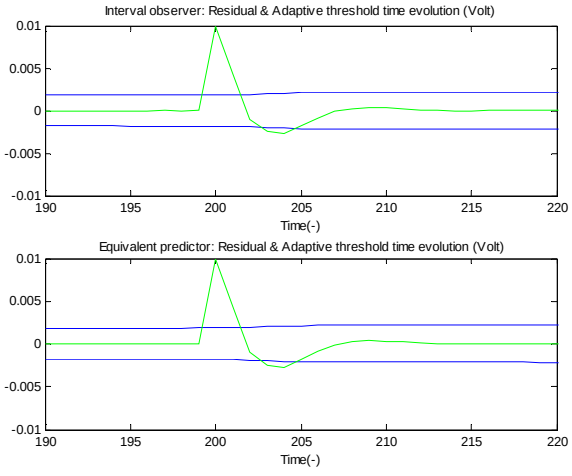

Fig. 5.5 Time evolution of the nominal residual (*green line*) and its adaptive threshold (*blue line*) using the interval observer (*upper plot*) and its equivalent predictor (*lower plot*)

In the following, a case where the predictor is not equivalent to its associated interval observer is considered. This is achieved when the equivalent predictor order is smaller than the obtained by Eq. (5.15). In this case, an order given by $\lambda=7$ is used. Then, the nominal residual (*green line*) and its adaptive threshold (*blue line*) corresponding to both models (*interval observer: upper plot*; *equivalent predictor: lower plot*) are plotted in *Fig.* 5.6 between the time instants *190* and *220*. Analyzing this figure, it can be noticed that while the interval observer nominal residual is null when the fault does not exist (k<200), the associated with the equivalent predictor is not due to its non-accurate system output approximation and according to the fault detection condition given by Eq. (5.26), this model would be indicating the fault existence although the fault does not appear till time instant t_0=200.

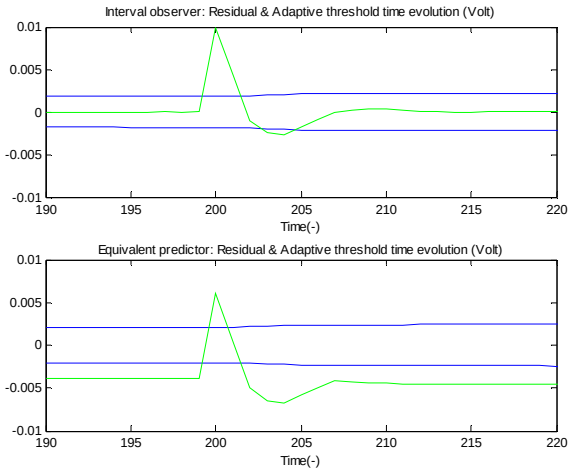

Fig. 5.6 Time evolution of the nominal residual (*green line*) and its adaptive threshold (*blue line*) using the interval observer (*upper plot*) and its equivalent predictor (*lower plot*)

5.4.6 Computing the equivalent predictor interval output using two known point-wise trajectories

When the observation gain condition given by Eq. (5.34) ($l_3=1$) is forced, the observer output interval can be computed using the *region-based approach* avoiding the wrapping effect (Meseguer et al, 2008a). That is because the interval observer matrix ($\boldsymbol{A_o = A - LC}$) fulfils the isotonicity property (all its elements are positive) and thus, according to (Cugueró et al, 2002), the trajectory of the output interval upper bound is obtained when the uncertain parameters are equal to their interval upper bound ($\overline{\hat{y}}(k) = \hat{y}(k, \overline{\theta}_1, \overline{\theta}_2, \overline{\theta}_3, \overline{\theta}_4)$) while the trajectory of the output interval lower bound is obtained when the parameters are equal to their interval lower bound ($\underline{\hat{y}}(k) = \hat{y}(k, \underline{\theta}_1, \underline{\theta}_2, \underline{\theta}_3, \underline{\theta}_4)$). Conversely, these two output interval trajectories could also be generated by the equivalent predictor using the uncertain parameter lower and upper bounds what means that the output interval can be also generated by the equivalent predictor using only two known point-wise trajectories and consequently, its computational cost is lower than the corresponding to the general *trajectory-based approach*.

In the following, the next observations gains are considered: $l_1=l_2=0.5$ and $l_3=1$. Then, assuming an equivalent predictor approximation degree $\varepsilon=1e\text{-}5$, the equivalent predictor order is given by $l=112$. Considering those observer and predictor parameters, the system output estimation interval and its nominal value are generated (*blue lines*) in *Fig.* 5.7 using the interval observer computed by the *region-based approach* (*upper plot*) and its equivalent predictor computed using only the two known point-wise trajectories (*lower plot*) such as it was mentioned above. Besides, the time evolution of the system output measurement is also plotted (*green line*) . *Fig.* 5.7 shows how both methods

generate exactly the same interval output and consequently, they are equivalent regarding their fault detection performance.

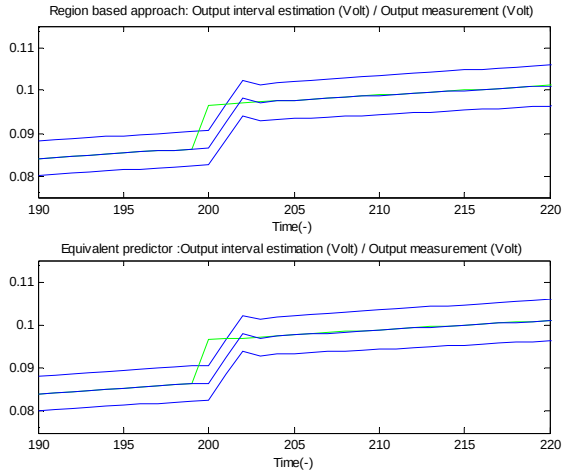

Fig. 5.7. Time evolution of the system output estimation interval and its nominal value (*blue lines*), and the output sensor measurement (*green line*) using the interval observer (*upper plot*) and its equivalent predictor (*lower plot*)

5.4.7 Influence of the equivalent predictor order λ on the fault indication persistence

(Meseguer et al., 2007b) shows that when interval observers are used, the observer gain has an important influence on the fault indication persistence. In general, the fault indication persistence depends on the observer gain, on the dynamics of the fault residual sensitivity and on the parameter uncertainty. Moreover, as indicated in (Meseguer et al, 2007b), when the simulation approach can not detect the fault and the 'dead-beat observer' (Patton et al, 1991) can only detect during a number of time instants equal to its order, optimum observer gain values between *Simulation* and *Prediction ('dead-beat observer')* can be applied to such that the fault indication persistence can be enhanced. When instead of using the interval observer, its equivalent λ-order predictor is used; the order λ of this model plays the same role regarding the fault indication persistence than the observer gain, derived from the shown equivalence between both models.

Next, assuming a constant additive fault affecting the system output sensor occurring at time instant t_0=200 and whose value is given by *f= 0.1 Volt* (roughly, *1 time* of the steady-state system output nominal value), the time evolutions of the system output estimation interval and its nominal value (*blue lines*) generated by the equivalent predictor are plotted. In addition, the time evolution of the system output measurement (*green line*) and the fault detection indicator (*red line*) are also plotted. In *Fig. 5.8*, a predictor whose order is $l=117$ is considered. This is equivalent to the observer given by Eq. (5.32) when $l_1=l_2=l_3=0.05$ and $\varepsilon=1e\text{-}5$. On the other hand, in *Fig. 5.9*, the predictor of minimum order is used ($\lambda=3$) which is equivalent to the interval observer when $l_1=l_2=l_3=1$ and $\varepsilon=1e\text{-}5$.

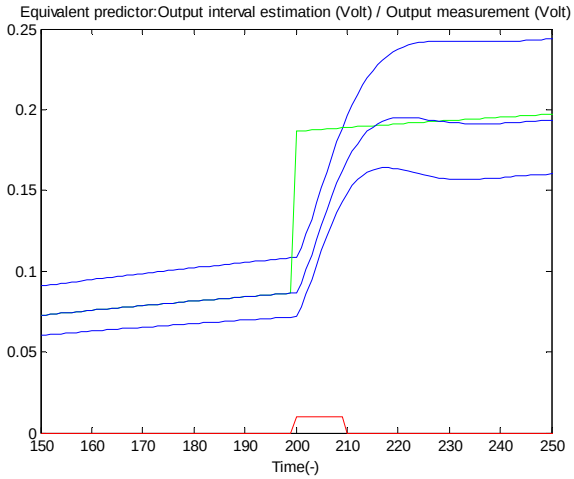

Fig. 5.8. Time evolution of the system output estimation interval and its nominal value (*blue lines*), and the output sensor measurement (*green line*) using a λ-order predictor (λ=*117*). The fault indicator is plotted in *red line*

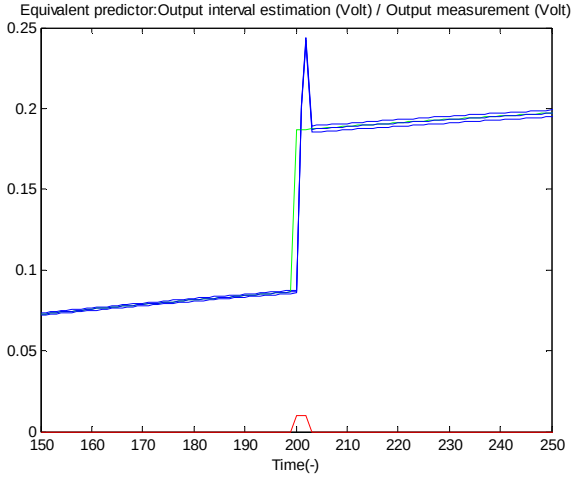

Fig. 5.9 Time evolution of the system output estimation interval and its nominal value (*blue lines*), and the output sensor measurement (*green line*) using a λ-order predictor (λ=*3*). The fault indicator is plotted in *red line*

5.5 Conclusions

This chapter demonstrates that it is possible to determine an interval λ-order predictor which is fully equivalent to an interval observer with a certain observer gain $\boldsymbol{L}$ when applied to fault detection applications. The presented method is an extension of the approach presented by (Ploix et al, 1999) where the predictor of minimum order ("*dead-beat observer*" (Patton et al, 1991)) was obtained. In the presented approach, the order of the equivalent predictor is determined by the observer gain matrix $\boldsymbol{L}$ and offers to the predictor model the same fault indication persistence than the corresponding to the interval observer. Such equivalence is based on the fact that an interval observer can be represented by an ARMA model, while a predictor by a MA model and it is known from the literature that an ARMA model can be approximated by a MA model of infinite order. On the other hand, this chapter shows that the use of the λ-order equivalent predictor is very interesting in fault detection applications because it avoids those problems associated with the state estimation as the initial state value problem or the wrapping effect. In addition, the equivalent predictor can be computed efficiently if the associated interval observer fulfils the isotonicity property

which can always be forced using the observer gains (Meseguer et al, 2008a). In this case, the interval output generated by the equivalent predictor is determined by two known point-wise trajectories obtained when the uncertain parameters are equal to their interval upper and lower bounds (Cugueró et al, 2002).

Part II

Fault diagnosis using interval observers

CHAPTER 6

On the integration of fault detection and isolation in model based fault diagnosis

6.1 Introduction

As mentioned in *Section 2.4*, model-based diagnosis has been approached from two different scientific communities (Venkatasubrarnanian et al., 2003a): Artificial Intelligence, also known as the ***DX approach*** (Hamscher et al, 1992) (Reiter, 1987), and Automatic Control, also known as ***FDI approach*** (Blanke et al, 2003)(Gertler, 1998)(Patton et al, 2000). Nonetheless, both approaches are considering separately the fault detection and the fault isolation tasks. Thereby, elements of comparison between both approaches have been included in (Cordier et al, 2000), which provides a common framework for research from both communities. In such trend, some recent works have tried to merge the best of each approach (Ploix et al, 2003) (*BRIDGE project*). In this merging process, the fault diagnosis task has been again separated in the task of fault detection and isolation.

However, most of the research in both communities has been focused either in the detection task or in the isolation task but very few papers deal with the interface between these two modules. Only few researchers have pointed out the importance of this interface but only from one of the two approaches (Combastel et al, 2003). The aim of this chapter is to recall that the interface between fault detection and fault isolation modules should be carefully designed in order to avoid the loss of information which derives in decreasing the quality of final fault diagnosis result, specially when dynamic systems are diagnosed (Puig et al, 2004c).

This remainder of *Chapter 6* is organized as follows: *Section 6.2* analyses the limitations of the binary interface between fault detection and fault isolation; *Section 6.3* proposes a motivational example which illustrates the fault isolation problems when every fault signal has its own dynamics and consequently, every fault signal may appear at different time instants; *Section 6.4* proposes some improvements on the existing *FDI* and *DX* fault isolation schemes in order to deal with the problems presented in *Section 6.3*. Finally, *Section 6.5* presents the obtained main conclusions.

6.2 Limitations of FDI fault isolation and DX fault isolation

As mentioned in *Chapter 2*, model-based fault detection tests are based on the evaluation of a certain set of *n* numerical fault indicators, residuals ***r(k)***, (also known as ***analytical redundancy relations*** (*ARRs*) in the FDI community or ***potential conflicts*** in the DX community) derived from the elementary models of system components and the available measurements coming from sensors (Ploix et al, 2003):

$$\boldsymbol{r}(k) = \boldsymbol{\Psi}(\boldsymbol{y}(k), \boldsymbol{u}(k)) \tag{6.1}$$

where $\boldsymbol{\Psi}$ is the residual generator function that allows computing the residual set at every time instant using the measurements of the system inputs and outputs (*i.e.* set by Eq. (3.16) in *FDI approach*).

Using either an approach coming from FDI (as for example, Staroswiecki's structural analysis (Staroswiecki et al, 1989)) or an approach coming from DX (as for example, Pulido's GDE based algorithm (Pulido et al, 2001)), the whole set of residuals *r(k)* (ARRs) for a certain system and a certain set of sensors can be generated. Each detection test ($r_i(k)$) should be evaluated on-line in order to decide if it is or not violated at a given time instant (typically a binary codification is used: *0* indicated not violation and *1* violation):

$$\phi_i(k) = \begin{cases} 0 & \text{if } |r_i(k)| < \tau_i \quad \text{(no fault)} \\ 1 & \text{if } |r_i(k)| \geq \tau_i \quad \text{(fault)} \end{cases} \tag{6.2}$$

where τ_i is the threshold associated to the detection test $r_i(k)$. This residual test constitutes the detection phase of the fault diagnosis process. Finally, the evaluation of each detection test will let obtain the ***observed fault signature*** of the system: $\boldsymbol{\phi}(k) = \left[\phi_1(k), \phi_2(k), \cdots, \phi_{n_\phi}(k)\right]$ such as indicated in *Chapter 2*. This vector can be considered as a set of fault signals which will be used by the fault isolation module in order to isolate the fault.

6.2.1 FDI fault isolation

The *observed fault signature* is, then, supplied to the fault isolation module that will try to isolate the fault so that a *fault diagnosis* result can be given. This module is able to produce such a fault diagnosis since it has the knowledge about the binary relation between the considered fault hypothesis set $\boldsymbol{f}(k) = \left\{f_1(k), f_2(k), \cdots, f_{n_f}(k)\right\}$ and the fault signal set $\phi(k)$. This relation is stored in the called *theoretical binary fault signature matrix* (***FSM***). Thereby, an element FSM_{ij} of this matrix is equal to *1* if the fault hypothesis $f_j(k)$ is expected to affect the residual $r_i(k)$ such that the related fault signal $\phi_i(k)$ is equal to *1* when this fault is affecting to the monitored system. Otherwise, the element FSM_{ij} is zero-valued. Then, fault isolation lies in looking for the ***theoretical fault signature*** of the ***fault signature matrix FSM*** which matches with the observed signature $\phi(k)$. For example, in case of having the following fault signature matrix

	f_1	f_2	f_3
ϕ_1	1	1	1
ϕ_2	1	0	1
ϕ_3	1	1	0

Table 6.1 Fault signature matrix

then, the following logical tests allow isolating the different faults without considering that noise or perturbations may cause detection errors:

$$\begin{aligned} f_1 &= \phi_1 \wedge \phi_2 \wedge \phi_3 \\ f_2 &= \phi_1 \wedge \overline{\phi_2} \wedge \phi_3 \\ f_3 &= \phi_1 \wedge \phi_2 \wedge \overline{\phi_3} \end{aligned} \tag{6.3}$$

Thereby, fault isolation FDI approach can be viewed as a ***parallel diagnostic inference*** (***column view***) approach (Gerter, 1998) (*Section 2.4.2.1.1*).

6.2.2 DX fault isolation

According to (Cordier et al, 2000), FDI fault detection approach using *ARRs* and DX fault detection approach using *potential conflicts* can be considered equivalent. However, fault isolation can be tackled in two different ways within the DX community: *consistency-based*, *CBD*, or *abduction-based* (Hamscher et al, 1992). Thereby, while consistency-based diagnosis tries to reject those behavioural modes which are not consistent with current observations, abduction-based diagnosis tries to explain current observation with a consistent behavioural mode assignment. In this line, the abduction-based diagnosis is closer to the FDI approach than the consistency-based approach. Nevertheless, for real complex dynamic systems there is no direct translation from the static consistency test to the dynamic one (Chantler et al, 1996).

Based on the framework proposed by Cordier (Cordier et al, 2000), the fault signature matrix presented in *Table 6.1* is interpreted in fault isolation CBD approach considering separately each line associated with a violated *ARR*, isolating *R-conflicts* (*i.e*., a set of components which must be considered abnormal in order to be consistent with the *observed fault signature*) before a common explanation can be given (*i.e*, it follows a ***series diagnostic inference*** **(*row view*)** of the table (Gerter, 1998) (*Section 2.4.2.1.1*).

6.2.3 Common limitations

Given that every fault signal $\phi_i(k)$ may exhibit different dynamics, some information is lost between fault detection and fault isolation modules when fault diagnosis of dynamic systems is carried out applying the above mentioned DX and FDI approaches. This is a consequence of considering just a binary interface between both modules which is obtained using a binary codification of every fault detection test (Eq. (6.2)) related to a given set of residuals ***r(k)*** (*ARR's* or *potential conflicts*). This loss of information might result in a wrong fault diagnosis or even though, faults might not be isolated since they are undistinguishable regarding the binary property of the fault signals. Among the

fault signal lost information when considering the mentioned binary interface, the following properties are highlighted:

- The sensitivity of the fault signal regarding to each considered fault.
- The sign of the fault signal.
- The fault signal occurrence order of a given *ARR* regarding the others is not recorded.
- Once the fault occurs, every fault signal $\phi_i(k)$ has its own persistency.
- The time window required so that all fault signals caused by a fault can be observed is not considered although every fault signal has its own dynamics and consequently, they may have different apparition time instants.
- The instability of the fault detection test indicator (chattering) as a consequence of the presence of noise and the used binary test is not considered.

Thus, if this information were considered in the interface between fault detection and fault isolation modules, the fault diagnosis result could be improved remarkably. Following the analysis done in (Puig et al, 2004c), in the next section some clues of the importance of considering fault signal dynamical properties are given using the approaches coming from both communities.

6.3 Motivational example

In order to show the importance of considering the fault signal dynamics when diagnosing dynamical systems, an example is used. In this example, in spite of the system dynamical properties, once the effect of faults on the considered fault signals has been determined, the following *binary theoretical fault signature matrix*, ***FSM***, is used:

	f_{y1}	f_{y2}	f_{c1}	f_{c2}
ϕ_1	1	1	1	0
ϕ_2	1	1	0	1

Table 6.2 Fault signature matrix

Such as it can be seen in this matrix, faults f_{c1} and f_{c2} are isolable since their binary fault signature is different from the signature of faults f_{y1} and f_{y2}. However, faults f_{y1} and f_{y2} are not isolable when a binary fault isolation approach is applied since they have the same binary fault signature.

The isolation approaches presented in *Section 6.2* uses a set of binary fault detection tests (Eq. (6.2)) to compose the *observed fault signature*. Given the isolation decision at time instant *k* only depends on the results of these tests at this time instant, this scheme is purely static, independently of the followed approach and consequently, it may cause false fault isolation decisions, especially when some fault detection tests have a transient behaviour (especially in dynamic slow/delayed systems) in response to the faults.

When using the previous static FDI or DX fault isolation approaches in dynamical systems where each fault signal $\phi_i(k)$ has its own dynamics, their behavior is very different during the transient time and as result, an erratic diagnosis may be provided.

Fig. 6.1 describes the time evolution of fault signals when a fault f_{y1} occurs. As it can be seen, the fault signals ϕ_1 and ϕ_2 do not appears at the same time because of the dynamics of the system. Thereby, *Table 6.3* illustrates the

corresponding FDI and DX CBD diagnostics at the time instants t_1 and t_2 in which each fault signal appears. Then, using the fault signature presented in *Table 6.2*, FDI approach, which follows the *column view approach*, provides the following diagnosis: between $t_1<k<t_2$, the observed fault signature correspond to the associated one with fault f_{c1}, while at $k>t_2$, the observed fault signature corresponds to f_{y1} or f_{y2}. As a conclusion, while all fault signals associated with a given fault do not have been observed because of the different appearance times, an FDI isolation approach will provide erratic diagnosis during the transient-state (see *Table 6.3*).

On the other hand, if a DX CBD isolation approach is used since it follows the *row view approach*, those components associated with activated fault signals will be considered as possible faulty candidates. Using the example used in the FDI case which deals with the occurrence of a fault f_{y1}, the activation of fault signal ϕ_1 will provide as possible faults f_{y1}, f_{y2} and f_{c1}, considering only single faults. Then, the activation of symptom ϕ_2 will allow reducing the set of possible faults to f_{y1} and f_{y2}. Thereby, DX approach allows refining incrementally the first diagnosis which already includes the fault which is affecting the considered system without providing erratic diagnosis in the transient-state (see *Table 6.3*).

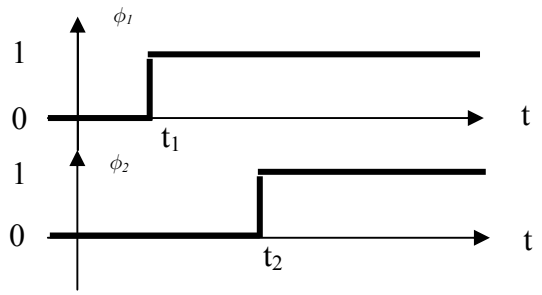

Fig. 6.1 Sequence of fault symptoms

Time	t_1	t_2
Fault Signals	$\phi_1=1$ $\phi_2=0$	$\phi_1=1$ $\phi_2=1$
FDI	$\boldsymbol{f_{c1}}$	$\boldsymbol{f_{y1} \vee f_{y2}}$
DX CBD	$\boldsymbol{f_{c1} \vee f_{y1} \vee f_{y2}}$	$\boldsymbol{f_{y1} \vee f_{y2}}$

Table 6.3 Diagnosis with FDI and DX CBD approaches (in black the provided diagnostic)

6.4 Approaches to deal with fault isolation considering fault signals with different apparition time instants

After a review of the existent approaches, a set of improvements was proposed in (Puig et al, 2004c) to deal with fault isolation applied to dynamical systems. As mentioned, the fault signals related to this kind of systems have their own dynamics and consequently, their apparition time instants may be different. Thereby, as illustrated in *Section 6.3*, if the dynamics of every fault signal is not taken into account, wrong fault diagnosis results can be obtained. Such as demonstrated in (Puig et al, 2004c), these enhancements can be used in the existent fault isolation approaches (either FDI or DX) without increasing the complexity related to the fault isolation algorithm.

6.4.1 Introduction

Delayed/slow systems are an important class of dynamic systems, which generally are composed by many subsystems with important delay times in their behaviour or with large transient responses. Some examples of delayed/slow systems are energy and water distribution networks, chemical processes, etc. In this class of systems, when a fault occurs, their associated fault signals never appear simultaneously. If the fault isolation decision procedure is static, as illustrated in *Section 6.3*, the fault propagation may produce a fault diagnosis result changing during the system transient-state caused by the fault. This problem has already been noticed by Kościelny (Kościelny, 1995) (Kościelny, 2000), Console (Console et al, 2001) and by Quevedo (Quevedo et al, 2001) among others. In both DX and FDI communities, there are recent works where the inclusion of information associated with the model dynamics and the fault signal occurrence time instants allow improving the fault diagnosis results when applied to dynamical systems.

Most DX methods take advantage of implicit temporal knowledge in the structure of the model, which can be represented as a set of QSIM/QDEs (Dvorak et al, 1992) (Ng, 1990), temporal causal graphs (Mostermann et al, 1997) or causal influences (Travé-Massuyes et al, 1997). These pieces of knowledge allow enhancing the isolation process in the transient period caused by the fault. This model temporal information can also be used to predict later deviations or to estimate delayed consequences. Moreover, this information can be used to favouring fault diagnosis candidates according to the dynamics of their observed fault signals (Mostermann et al, 1999) (Travé-Massuyes et al, 1997) or to reject them if their effects are not present at a given time instant (Alonso et al, 2000). In general these techniques use rules which, given a fault signal at time k, compute the diagnosis result taking into account the observations in time instants earlier than time instant k. Thus, these approaches let obtain a final fault isolation result after a sequence of transient diagnostics. Console (Console et al, 2001) proposes temporal decision trees which take into account temporal information on the fault signals and temporal constraints on the recovery actions to be performed, increasing the fault discrimination.

On the other hand, in the FDI community, the works of Kościelny (Kościelny, 1995)(Kościelny, 2000) propose a new fault signature matrix replacing binary *1's* by an interval of time $[t_{min},t_{max}]$,where t_{min} and t_{max} are the minimum and maximum time period between fault occurrence and the fault signal appearance. The conclusion of this approach is that the fault isolation performance can be improved taking into account the time of fault signal appearance. Moreover, this approach suggests that once the fault occurs, the final fault isolation result can be obtained in a certain number of time instants determined by the number of affected fault signals and their appearance time instants.

6.4.2 Fault isolation considering fault signals with different appearance time instants

According to (Puig et al., 2004), one possible approach to deal with fault signals with different appearance time instants, independently of the fault isolation approach, consists in not allowing an isolation decision until a prefixed waiting time (T_w) has elapsed from the first fault signal appearance. This reference proposes that T_w must be calculated from the largest transient time response (T_{lt}) from non-faulty situation to any faulty situation. Moreover, depending on the nature of the faults (abrupt or incipient), there is usually a detection time that should be added.

In the example described in *Section 6.3*, T_w must be calculated from the largest transient time response from non-faulty situation to any faulty situation, being, in this case, the transient time response from $\phi_1=\phi_2=0$ to $\phi_1=\phi_2=1$ resulting in $T_{lt}=max(t_1,t_2)$. Moreover, taking into account the uncertainty about the knowledge of the delays t_1 and t_2

and the detection time, a security time period should be added to T_w in order to enhance the fault diagnostic decision reliability. In this example, then $T_w > T_{lt} = max(t_1,t_2)$ (see *Table 6.4*).

In the case of some DX approaches, it is also possible to exonerate those components not involved in the violated detection tests once the waiting time T_w has elapsed. This will allow obtaining the same isolation results than FDI approach.

Time	t_1	t_2	T_w
Fault Signals	$\phi_1=1\ \phi_2=0$	$\phi_1=1\ \phi_2=1$	$\phi_1=1\ \phi_2=1$
FDI	f_{c1}	$f_{y1} \vee f_{y2}$	$\boldsymbol{f_{y1} \vee f_{y2}}$
DX CBD	$f_{c1} \vee f_{y1} \vee f_{y2}$	$f_{y1} \vee f_{y2}$	$\boldsymbol{f_{y1} \vee f_{y2}}$

Table 6.4 Diagnosis with FDI and DX CBD approaches (in black the provided diagnostic)

6.4.3 Fault isolation considering the appearance order of fault signals

A second improvement described in (Puig et al, 2004c) is based on taking into account the appearance order of fault signals.

The *binary theoretical fault signature matrix*, ***FSM***, (*Section 2.4.2.1.1*) gives a static relation between faults ***f*** and fault signals ϕ. Thereby, when taking into account the order of fault signal appearance, the fault isolation algorithm increases its capacity to discriminate one fault from the rest since this fault signal property allow to distinguish those faults which have the same static theoretical fault signature but a different dynamic fault signature, *i.e,* different appearance order of their associated fault signals.

As a result, the approach presented in (Puig et al, 2004c) proposes the use of a new fault signature matrix named dynamic fault signature matrix (***DFSM***) ($\boldsymbol{\Sigma_d}$) (Quevedo et al, 2001). This matrix is composed using an analysis of the propagation of each fault. Each element of this matrix has two digits: the first digit (index) codifies the result of the detection test (*0* means non-fired test while *1* means fired test) and the second digit (sub index) codifies the logical sequential order of appearance of the fault signal for every fault hypothesis. This sub index describes in a simple way the propagation of the fault effect on the system and can be inferred from the analytical redundancy relations or by analysis of the fault effects on the model.

Considering again the fault signature matrix presented in *Table 6.2*, the faults f_{y1} and f_{y2} have identical static fault signature and consequently, they are not isolable. However, considering the fault signal appearance order, these faults can be isolated if their associated fault signals have different appearance order, as assumed in the following. In this case, the dynamic fault signature matrix can be written as shown in Table 6.5

	f_{y1}	f_{y2}	f_{c1}	f_{c2}
ϕ_1	1_1	1_2	1_1	0
ϕ_2	1_2	1_1	0	1_1

Table 6.5 Dynamic fault signature matrix

Such as it can be seen in this dynamic (*Table 6.5*), when the fault signal appearance order is considered, all the theoretical fault signatures are different and as a result, this approach can isolate faults f_{y1} and f_{y2}. (Puig et al., 2004) defines these two faults as sequentially isolable but not static isolable. In *Table 6.6*, considering the faulty scenario used in *Section 6.3*, the fault diagnosis result is given when the dynamic fault signature matrix is used.

Time	t_1	t_2	T_w
Fault Signals	ϕ_1=1 ϕ_2=0	ϕ_1=1 ϕ_2=1	ϕ_1=1 ϕ_2=1
FDI	f_{c1}	f_{y1}	**f_{y1}**
DX CBD	$f_{c1} \vee f_{y1}$	f_{y1}	**f_{y1}**

Table 6.6 Diagnosis with FDI and DX CBD approaches (in black the provided diagnostic)

6.4.4 Fault isolation considering the fault signal appearance time instant

A third improvement shown in (Puig et al, 2004c) consists in considering not only the fault signal appearance order but also their appearance time instant which is bounded by the time interval $\left[\varphi_j\right]=\left[\underline{\varphi}_j,\overline{\varphi}_j\right]$ where $\underline{\varphi}_j$ and $\overline{\varphi}_j$ are the minimum and maximum appearance time instant of all fault signals related to the fault f_j from the first fault signal appearance.

Regarding *Table 6.5*, if the monitored system were affected by a new fault f_5 with the same dynamic fault signature than f_{y1}, it would not be possible to isolate both faults even considering their appearance order. Conversely, according to (Puig et al., 2004) when the interval $\left[\varphi_j\right]$ for each fault is known, these two faults could be isolated if their associated appearance time intervals do not have an intersection.

Then, taking into account the interval $\left[\varphi_j\right]$ and considering the new fault f_5, the matrix ***DFSM*** given by Table 6.5 can be re-written as follows:

	f_{y1}	f_{y2}	f_{c1}	f_{c2}	f_5
ϕ_1	1_1	1_2	1_1	0	1_1
ϕ_2	1_2	1_1	0	1_1	1_2
$[\varphi]$	$[\varphi_{y1}]$	$[\varphi_{y2}]$	$[\varphi_{c1}]$	$[\varphi_{c2}]$	$[\varphi_5]$

Table 6.7 Modified dynamic fault signature matrix (assuming the case $\overline{\varphi}_{y1} < \underline{\varphi}_5$)

In order to check this modified dynamic fault signature matrix, three different single-fault scenarios corresponding to faults f_{y1}, f_5 and f_{c1} are considered and analysed in *Table 6.8*, *Table 6.9* and *Table 6.10*, respectively. These tables present how this matrix allows isolating two faults that are not isolable using the fault signal occurrence order. In this case, the fault isolation is possible due to the knowledge of the time interval in which fault signals should appear.

Time	t_1	$\underline{\varphi}_{y1} < t_2 < \overline{\varphi}_{y1}$
Fault Signals	$\phi_1=1\ \phi_2=0$	$\phi_1=1\ \phi_2=1$
FDI	f_{c1}	$\boldsymbol{f_{y1}}$
DX CBD	$f_{c1} \vee f_{y1} \vee f_5$	$\boldsymbol{f_{y1}}$

Table 6.8 Diagnosis with FDI and DX CBD approaches (in black the provided diagnostic)

Time	t_1	$\underline{\varphi}_5 < t_2 < \overline{\varphi}_5$
Fault Signals	$\phi_1=1\ \phi_2=0$	$\phi_1=1\ \phi_2=1$
FDI	f_{c1}	$\boldsymbol{f_5}$
DX CBD	$f_{c1} \vee f_{y1} \vee f_5$	$\boldsymbol{f_5}$

Table 6.9 Diagnosis with FDI and DX CBD approaches (in black the provided diagnostic)

Time	t_1	$\max([\varphi_{y1}],[\varphi_{c1}],[\varphi_5])$
Fault Signals	$\phi_1=1\ \phi_2=0$	$\phi_1=1\ \phi_2=1$
FDI	f_{c1}	$\boldsymbol{f_5}$
DX CBD	$f_{c1} \vee f_{y1} \vee f_5$	$\boldsymbol{f_5}$

Table 6.10 Diagnosis with FDI and DX CBD approaches (in black the provided diagnostic)

6.5 Conclusions

Chapter 6 is based on the results obtained in (Puig et al., 2004) and presents a set of problems that appear when fault detection and isolation are handled by separated modules such as it is usual in the FDI methods. Regarding the DX community, there is also a current trend where these two tasks are considered separately: mostly, when integrating methods of both communities using for example detection tests based on FDI techniques and isolation methods based on DX techniques. Consequently, the fault diagnosis problems presented in this section should be interesting for both the FDI community and the DX community.

This chapter identifies the fault diagnosis problems of dynamical systems which result of considering a binary codification of the fault detection tests when a static reasoning scheme is applied. The effect of these problems is remarkable when the monitored system has a large transient state once the fault occurs. The solutions proposed in (Puig et al., 2004) are based on some improvements of the basic FDI and DX CBD schemes considering temporal aspects related to the fault signal dynamics.

CHAPTER 7

Towards a better integration of passive robust interval-based FDI algorithms

7.1 Introduction

As mentioned in *Chapter 6*, fault detection and fault isolation tasks are usually considered separately in model-based fault diagnosis. The typical interface between these two modules is based on a binary codification of the evaluation of each residual (fault signal) what allow obtaining a binary observed fault signature (*Section 2.4.2.1.1*). Then, the fault isolation process consists in matching the observed fault signature with some of the theoretical fault signatures which are obtained using a binary codification of the effect of every fault on every residual (fault signal) generating a theoretical signature for every fault hypothesis (*Section 2.4.1.1*). As a result, if the observed signature matches with one theoretical signature related to a certain fault hypothesis, this process let isolate the fault. Such as it was introduced in *Chapter 6* and in *Section 2.4.2.2* of *Chapter 2*, this binary approach has some important drawbacks which are due to the loss of information between the fault detection module and the fault isolation module. This weakness has been also noticed by (Combastel et al., 2003) which suggests that the whole fault diagnosis performance can be highly increased by improving this interface between fault detection and isolation modules. In particular, the interface can be improved taking into account the following information:

- The effect of model uncertainty on the fault detection threshold what let generate an adaptive threshold as shown in *Chapter 3* (*Section 3.2.2*).
- The residual signs since faults can cause positive or negative residual values.
- The size of the residual value (fault signal). Thus, the fault can cause a big violation of the threshold or only a small fault signal-activation.
- The sensitivity of a residual with respect to a certain fault (*Section 3.3*).
- The dynamics related to a fault signal which determines both its appearance time instant and its time evolution.
- The appearance order of the fault signals which can be estimated when considering the dynamics of every fault signal.

In addition, it should not be forgotten that when using a binary evaluation of the residual (Eq. (6.2)), the presence of noise affecting the sensor measurements may cause chattering effect on the result of this evaluation.

In this chapter, a new interval-based FDI algorithm that improves the integration between the fault detection and fault isolation modules is presented which uses the information mentioned previously. The core of this fault-isolation method for the non-uncertainty systems was proposed in (Puig et al, 2005b). Thus, the approach presented in this chapter is an extension of the one proposed in (Puig et al, 2005b) for the uncertain system case and it is the first step of a set of improvements which will be introduced in the following chapters. Thereby, the following strengtheners of the method proposed in this chapter regarding the presented one in (Puig et al, 2005b) can be highlighted:

- Uncertain systems are considered which let obtain an adaptive threshold used in the residual evaluation stage in order to decide if the monitored system is affected or not by a fault.
- The method is tested using real data of the Barcelona's urban sewer system such as it will be explained below.

Conversely, both this method and the one presented in (Puig et al., 2006) are affected by the following weaknesses:

- The time evolution of the dynamical properties of the fault signals is not considered.
- The theoretical occurrence time instant of every fault signal is not used. In (Puig et al, 2005b) a first definition of this pattern was given without showing how it can be estimated using the considered model.
- These methods do not say anything about how to obtain the waiting time T_w required for the appearance of all fault signals once the fault occurs. Thus, although the drawback of a static fault diagnosis reasoning (*Chatper 6*) is known, this method still uses it.
- The estimation of the system output is obtained using a predictor of minimum order in spite of the drawbacks mentioned in *Chapter 3* and *Chapter 5*.

In the following chapters of this *II Part* of the thesis, these weaknesses will be tackled in order to enhance the whole fault diagnosis process.

The fault isolation method proposed in this section is applied to the limnimeters of Barcelona's urban sewer system: a telemetry network containing more than 100 limnimeters and some quality sensors connected to a Supervisory Control and Data Acquisition system (SCADA) which has been in operation since 1994. This SCADA is carrying out a real-time global control in the whole Barcelona network with the objective of reducing flooding and the combined sewers overflow (CSO) (Cembrano et al., 2002). The achievement of these goals avoid realising untreated water to the environment and let take full advantage of the storage capacity of the urban drainage network and the treatment plants. On the other hand, it must be taken into account that the control of the urban sewer system depends on the reliability of the measurements given by the instruments, specially by the limnimeters used to measure the water level in the storage tanks. Thus, if a set of limnimeters were affected by a certain fault, the data obtained from the faulty instruments could confuse the control module and as a result, the control objective might not be achieved resulting in some disastrous consequences. These negative consequences justify the use of a fault diagnosis system in order to detect and isolate faulty instruments and to reconstruct faulty measurements using the measurements of the non-faulty instruments. In this chapter, the fault diagnosis method has been applied to a real faulty scenarios collected from limnimeters of Barcelona's network in order to test the goodness of its performance.

Regarding the structure of the remainder of *Chapter 7*, passive robust fault detection using interval models is recalled in *Section 7.2*. In *Section 7.3*, the integration of robust interval based methods with a new fault isolation method is discussed. In *Section 7.4*, the introduced fault isolation approach is applied to diagnose faults affecting to the limnimeters of the Barcelona sewer network considering different real fault scenarios. Finally, in *Section 7.5*, the main conclusions are presented.

7.2 Fault detection using interval models based on a passive robustness approach

7.2.1 Fault detection test based on a passive robustness approach

In this section, the fault detection test which was already introduced in *Chapter 5* (*Section 5.3.1*) is recalled since it will allow introducing the manner in which fault signals are computed at every time instant. Thus, such as it was already mentioned in *Section 3.2.2*, model-based fault detection tests let determine the existence of a fault affecting the monitored system comparing the measurements of physical variables $\boldsymbol{y}(k)$ of the process with their estimation $\hat{\boldsymbol{y}}(k)$ provided by the associated system model. However, since model uncertainty located in the parameters is considered ($\boldsymbol{\theta} \in \Re^{n\theta}$ is the vector of uncertain parameters with their values bounded by a compact set $\boldsymbol{\theta} \in \boldsymbol{\Theta}$ of box type, *i.e.,* $\boldsymbol{\Theta} = \left\{ \boldsymbol{\theta} \in \Re^{n\theta} \middle| \underline{\boldsymbol{\theta}} \le \boldsymbol{\theta} \le \overline{\boldsymbol{\theta}} \right\}$), the residual may be computed using the nominal model $\hat{\boldsymbol{y}}^o(k, \boldsymbol{\theta}^o)$ related to the interval model which is obtained when using $\boldsymbol{\theta} = \boldsymbol{\theta}^o \in \boldsymbol{\Theta}$.

$$\boldsymbol{r}^o(k) = \boldsymbol{y}(k) - \hat{\boldsymbol{y}}^o(k) \tag{7.1}$$

In a non-faulty scenario, $\boldsymbol{r}^o(k)$ should be zero-valued at every time instant k considering an ideal situation. Nevertheless, it will never be satisfied since the system can be affected by unknown inputs (*i.e.* noise, nuisance disturbances, etc) and the model might be affected by some error assumptions (model errors) apart from its considered parameter uncertainty. Thus, the residual generated by Eq. (7.1) can not be expected to be zero-valued in a non-faulty scenario. However, propagating the interval observer parameter uncertainty to the residual, the values of the nominal residual (Eq. (7.1)) will be bounded by the interval (neglecting couplings among outputs) (Puig et al., 2002):

$$[\underline{r}_i^o(k), \overline{r}_i^o(k)] \tag{7.2}$$

where as indicated in *Section 5.3.1*:

$$\underline{r}_i^o(k) = \underline{\hat{y}}_i(k) - \hat{y}_i^o(k) \text{ and } \overline{r}_i^o(k) = \overline{\hat{y}}_i(k) - \hat{y}_i^o(k) \tag{7.3}$$

As a result, while the nominal residual $r_i^o(k)$ satisfies the following relation, a fault can not be indicated since the measurements related to the system outputs satisfy the relation given by Eq. (3.9) (*Section 3.2.1*)

$$r_i^o(k) \in [\underline{r}_i^o(k), \overline{r}_i^o(k)] \tag{7.4}$$

Thereby, according to the fault detection strategy given by relation (7.4), the interval given by Eq. (7.2) can be seen as an ***adaptive threshold***. Such as presented by (Puig et al, 2002a), the main goal of the fault detection module consists in checking for every residual $r_i^o(k)$ if the relation (7.4) holds or not what can be seen as a passive robust strategy based on generating an ***adaptive threshold***. Conversely, it must be taken into account that this strategy is totally equivalent to the one presented in *Section 3.2.2* of *Chapter 3* (Eq. (3.24)).

7.2.2 Fault signal generation

The fault detection test (7.4) relies on the comparison of the numerical value of the nominal residual $r_i^o(k)$, which may be affected by noise, with its associated adaptive threshold. This binary procedure may lead to undesirable decision instability (chattering) because of the effect of noise on the sensor measurements and consequently, a persistency criterion should be introduced (Theillol et al., 1997). Such as indicated by the *DMP-approach* (Petti et al., 1990), a gradual reasoning involved by the use of fuzzy logic is an appealing alternative to bypass this chattering phenomenon. Then, as it was proposed in (Puig et al. 2005), the fault diagnostic signal (or fault signal) for each residual is calculated in the approach presented in this paper using the Kramer function (Petti et al., 1990):

$$\phi_i(k) = \begin{cases} \dfrac{(r_i^o(k)/\overline{r}_i^o(k))^4}{1+(r_i^o(k)/\overline{r}_i^o(k))^4} & if \quad r_i^o(k) \geq 0 \\ \\ -\dfrac{(r_i^o(k)/\underline{r}_i^o(k))^4}{1+(r_i^o(k)/\underline{r}_i^o(k))^4} & if \quad r_i^o(k) < 0 \end{cases} \tag{7.5}$$

The appealing performance of this function is due to its introduced grading when evaluating the residual in order to conclude the existence or not of a fault. When using the Kramer function given by Eq. (7.5), the residuals are normalized to a metric between -1 and 1, $\phi_i(k) \in [-1,1]$, which indicates the degree of satisfaction of Eq. (7.4) for every nominal residual $r_i^o(k)$: *0* for perfectly satisfied, *1* for severely violated high and *-1* for severely violated low. In the following, a fault signal will be notated as $\phi_i(k)$ and it is considered that it exists while $|\phi_i(k)| \geq 0.5$. Otherwise, $|\phi_i(k)| < 0.5$, the fault signal does not exist from fault detection and isolation point of view. Conversely, the set of all fault signals will be notated as $\phi = \{\phi_i : i = 1,2,....n_y\}$.

7.3 Architecture of the fault isolation approach

7.3.1 Architecture components

The passive robustness-based fault detection approach presented in previous section is integrated with a fault isolation algorithm in order to diagnose those faults affecting the monitored system. In *Fig. 7.1*, the fault isolation module architecture proposed in (Puig et al, 2005b) is presented which consists in three main components. The first one is called the memory component and determines the interface between the fault detection and fault isolation modules. It is based on a memory which stores information related to the time evolution of every fault signal and is updated cyclically by the fault detection module. The second element of this fault isolation architecture is the pattern comparison component which compares the fault signal information stored in the memory component with the theoretical one stored in different fault signature matrices: one for each considered fault signal pattern. The last element is the decision logic component which diagnoses the most probable fault according to the monitored properties of the observed fault signals.

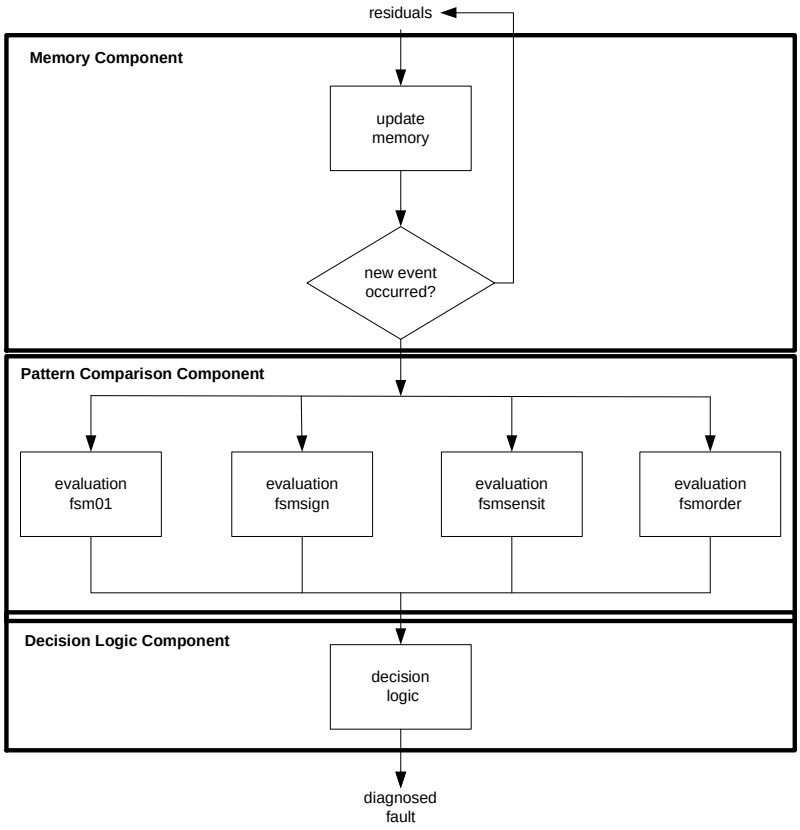

Fig 7.1 Architecture of the fault isolation approach

7.3.2 Memory component

The memory component is built on the grounds of a table which stores some information related to the time evolution of every fault signal $\phi_i(k)$. Thereby, once the first fault signal is observed, for each fault signal $\phi_i(k)$ ($|\phi_i(k)| \geq 0.5$) computed according to Eq. (7.5), the memory component stores the occurrence time instant ($k_{\phi i}$), defined as the first time instant where $|\phi_i(k_{\phi i})| = 0.5$, and the fault signal value (ϕ_{imax})[16] whose absolute value is maximum. Every time the fault detection module detects a new fault signal or an observed fault signal reaches a new value ϕ_{imax}, this memory is updated with the new information situation.

Such as it was discussed in *Chapter 6* (*Section 6.4*), fault signals associated with dynamical systems do not appear at the same time instant since each of them has its own dynamics. This fact, such as it was already discussed, can confuse the fault isolation module obtaining a wrong fault diagnosis result if a suitable strategy is not used. According to (Puig et al., 2004) and such as it was presented in *Section 6.4*, this problem can be solved if a fault diagnosis result is not given until all fault signals have appeared once the first one is observed. This waiting time T_w (*Section 6.4.2*) is calculated from the larger transient time response T_{lt} from the non-faulty situation to any faulty situation. After this time has been elapsed, a fault diagnosis result is proposed and the memory component is reset being ready to start the diagnosis of a new fault. This reset consists in deleting the information related to all vanished

[16] $\phi_{i\max} = \phi_i(k_{i\max})$ where $|\phi_{i\max}| = \max_{k \geq k_{\phi i}} \left(|\phi_i(k)| \right)$

fault signals ($|\phi_i(k)|<0.5$) and the value ϕ_{imax} of those fault signals which can still be observed at this time instant ($|\phi_i(k)|\geq 0.5$). Following the method given by (Combastel et al., 2003), inside the diagnosis time window T_w, the value ϕ_{imax} registered for every observed fault signal changes at time instant k if $|\phi_i(k)| > |\phi_{imax}|$. Then, $\phi_{imax} = \phi_i(k)$. According to this strategy, the value $|\phi_{imax}|$ can only rise and not fall inside the time window T_w, in spite the associated fault signal has already vanished. This behaviour provides two advantages to the fault isolation algorithm performance:

- The effect of noise is partially filtered out. That leads to smoother diagnosis results without flickering.
- The problem of non-persistence fault signals inside the diagnosis time window T_w is filtered since just the peaks of activation are stored. However, this strategy does not solve the general problem of the non-persistence of the fault signals. In general, some observed fault signals $\phi_i(k)$ might vanish ($|\phi_i(k)|<0.5$) once T_w has elapsed and this fact do not let conclude that the fault has also disappeared since the model estimations could be affected by the fault following effect analysed in *Chapter 3* and introduced in *Section 2.3.2.6* of *Chapter 2*. Consequently, the model might have lost its capacity to detect faults and therefore, wrong fault diagnosis results may be concluded. Conversely, if the value ϕ_{imax} were never deleted, the fault would always be diagnosed in spite it could already have vanished being the system affected by no fault. The influence of this problem on the fault diagnosis result will be analysed in *Chapter 8*.

This memory component makes the information related to the fault signal time evolution accessible for later computation by explicitly storing that data. In this way, time aspects of fault isolation can be tackled in a very easy and straightforward way.

7.3.3 Pattern comparison component

Once the time window T_w has elapsed and while at least one fault signal is observed ($|\phi_i(k)|\geq 0.5$), the pattern comparison component compares the fault signal information registered in the memory component with the theoretical one which describes the theoretical influence of a fault f_j on the time evolution of the fault signal set ϕ regarding to some of their properties or patterns. The manner of storing the theoretical influence of faults on the fault signals is based on the concept of the ***theoretical fault signature matrix*** (***FSM***). As mentioned in *Section 2.4.1.1* (*Chapter 2*), an element $\boldsymbol{FSM}_{ij}$ of this matrix is *'1'* when the sensitivity function of the residual $r_i(k)$ to fault f_j is not null (*Section 3.3*), otherwise, this element is *'0'*. This interpretation assumes that the occurrence of f_j is observable in $r_i(k)$ and therefore, the fault signal $\phi_i(k)$ ($|\phi_i(k)|\geq 0.5$) will appear during at least few time instants. This hypothesis is known as fault exoneration or no compensation. In this proposed approach, the fault signature matrix concept is generalized since the binary interface is extended taking into account more fault signal properties. Thus, there will be as many ***FSM*** matrices as different properties are taken into account: binary property (***FSM****01*), sign property (***FSM****sign*), fault residual sensitivity property (***FSM****sensit*) and occurrence order property (***FSM****order*).

Finally, this process which is carried out by the comparison component allows computing one factor at the end of the time window T_w for every considered fault signal property and for each fault hypothesis f_j. Every factor estimates the occurrence probability of a certain fault hypothesis f_j comparing the fault signal observations related to a certain property (*binary, sign, residual sensitivity* and *order*) with the theoretical values for this fault hypothesis f_j and for

this property stored in the corresponding ***FSM*** matrix. In the following sections of this chapter, more detailed information about these factors will be given.

It should be taken into account that in this first approach presented in *Chapter 7*, the time evolution of the fault signal properties is not considered yet but their steady-state values. It will be in the following chapters where this approach will be extended considering the dynamical aspects of the fault signals.

7.3.3.1 FSM01: Evaluation of fault signal occurrence

The ***FSM***01-table contains the theoretical binary patterns that faults produce in the residual equations which can be codified using the values *'0'* for no influence, *'1'* otherwise. Thereby, this matrix can be obtained such as the theoretical fault signature matrix ***FSM*** introduced by (Gertler, 1998)(*Section 2.4.1.1*). Then, an element $\boldsymbol{FSM01}_{ij}$ of this matrix is *'1'* when the sensitivity function of the residual $r_i^0(k)$ to fault f_j is not null, otherwise, this element is *'0'*. This statement can be expressed by the following equation:

$$\boldsymbol{FSM}01_{\mathrm{ij}} = \begin{cases} 1, & \text{if} \quad S_{f_{i,j}}(q^{-1}) \neq 0 \\ 0, & \text{if} \quad S_{f_{i,j}}(q^{-1}) = 0 \end{cases} \tag{7.6}$$

where $S_{f_{i,j}}$ is the sensitivity function of the nominal residual $r_i^o(k)$ regarding the fault hypothesis f_j (*Section 3.3*).

Such as it was mentioned previously, the occurrence probability of the fault hypothesis f_j regarding the binary property of the observed fault signals can be obtained calculating $\boldsymbol{factor01}_j$ according to the following equation:

$$\boldsymbol{factor}01_j(k) = \frac{\sum_{i=1}^{ny}\left(boolean\left(\phi_i(k)\right)\boldsymbol{FSM}01_{ij}\right)}{\sum_{i=1}^{ny}\boldsymbol{FSM}01_{ij}}\,\boldsymbol{zvf}_j \tag{7.7}$$

with

$$boolean(\phi_i(k)) = \begin{cases} 0, & \text{if} \quad \phi_{i\max} = 0 \\ 1, & \text{if} \quad \phi_{i\max} \neq 0 \end{cases} \tag{7.8}$$

and where $\boldsymbol{zvf}_j$ is the zero-violation-factor whose expression is

$$\boldsymbol{zvf}_j = \begin{cases} 0, & \text{if}\ \exists\ i \in \{1,\ldots,ny\} \ \text{ with } \ \boldsymbol{FSM}01_{ij} = 0 \\ & \qquad\qquad \text{and } \ \phi_{i\max} \neq 0 \\ 1, & \text{otherwise} \end{cases} \tag{7.9}$$

Thus, computing $\boldsymbol{factor01}_j$ such as it is indicated by Eq. (7.7), the following behaviour is obtained: those expected and observed fault signals $\phi_i(k)$ support the fault hypothesis f_j while the observation of an unexpected fault signal let reject that fault hypothesis of the final diagnosis result. Moreover, those missing fault signals also affect indirectly the supportability of the fault hypothesis via the denominator of Eq. (7.7).

7.3.3.2 FSMsign: Evaluation of fault signal signs

The ***FSMsign***-table contains the theoretical sign patterns that faults produce in the residual equations. Those patterns can be codified using the values *'0'* for no influence, *'+1'* or *'-1'* for positive/negative deviation for every $\boldsymbol{FSMsign}_{ij}$. In this approach, the element $\boldsymbol{FSMsign}_{ij}$ related to the fault signal $\phi_i(k)$ (nominal residual $r_i^o(k)$) and the fault hypothesis f_j is obtained evaluating the sign of the steady-state value of the associated residual sensitivity function $S_{f_{i,j}}$ to a fault f_j (Section 3.3) considering an unit step as an input. Thus, $\boldsymbol{FSMsign}_{ij}$ is calculated evaluating the following equation:

$$\boldsymbol{FSM}\text{sign}_{ij} = \begin{cases} 0 & \text{if} \quad S_{f_{i,j}}(q^{-1}) = 0 \\ 1 & \text{if} \quad s_{f_{i,j}}(\infty) > 0 \\ -1 & \text{if} \quad s_{f_{i,j}}(\infty) < 0 \end{cases} \tag{7.10}$$

where $s_{f_{i,j}}(\infty)$ is the steady-state value of $S_{f_{i,j}}$ when an unit step input is considered (*Section 3.3*). The reason of using the fault residual sensitivity function $S_{f_{i,j}}$ is because according to the residual internal form expression (Eq. (3.62)) (*Section 3.3.5*) and to the fault residual sensitivity concept (Eq. (3.36)) (*Section 3.3.1*), the influence of a fault on the residual is just determined by this function once the fault signal is observed ($|\phi_i(k)| \geq 0.5$).

On the other hand, in this approach the observed signs associated with every observed fault signal $\phi_i(k)$ are determined by the sign of its corresponding value ϕ_{imax} stored in the memory component such as it is illustrated in the following expression:

$$sign(\phi_i(k)) = \begin{cases} 0 & \text{if} \quad \phi_{i\max} = 0 \\ 1 & \text{if} \quad \phi_{i\max} > 0 \\ -1 & \text{if} \quad \phi_{i\max} < 0 \end{cases} \tag{7.11}$$

Thereby, with regard to the fault signal sign property, the probability of the occurrence of the fault hypothesis f_j will be set by the $\boldsymbol{factor}sign_j$. This factor is computed comparing the theoretical fault signal signs for the hypothesis f_j stored in the j^{th}-column of matrix $\boldsymbol{FSM}sign$ with the fault signal observed signs stored in the memory component. This comparison requires counting the number of signs of the fault signal vector $\phi(k)$ which coincide with the ones related to every fault hypothesis f_j, considering both the case in which all residuals have been violated positively and the case in which they are violated negatively. Thus, this number of signs can be counted using the following expression:

$$numsign_j(k) = \max\left(\sum_{i=1}^{ny} ckecksign(\phi_i(k), \boldsymbol{FSM}sign_{ij}), \sum_{i=1}^{ny} ckecksign(\phi_i(k), -\boldsymbol{FSM}sign_{ij})\right) \tag{7.12}$$

where

$$ckecksign(\phi_i(k), \boldsymbol{FSM}sign_{ij}) = \begin{cases} 0 & \text{if } \phi_{i\max} = 0 \\ 0 & \text{if } sign(\phi_i(k)) \neq \boldsymbol{FSM}sign_{ij} \text{ and } \phi_{i\max} \neq 0 \\ 1 & \text{if } sign(\phi_i(k)) = \boldsymbol{FSM}sign_{ij} \text{ and } \phi_{i\max} \neq 0 \end{cases} \tag{7.13}$$

Then, the $\boldsymbol{factor}sign_j$ is obtained as follows:

$$\boldsymbol{factor}sign_j(k) = \frac{numsign_j(k)}{\sum_{i=1}^{ny} \left|\boldsymbol{FSM}sign_{ij}\right|} \boldsymbol{zvf}_j \tag{7.14}$$

It should be taken into account that the approach presented in this section to calculate this factor is just an approximation since, such as it was shown in *Section 3.3*, the fault residual sensitivity $S_{f_{i,j}}$ is a function of time and consequently, the sign property of a fault signal can fluctuate along the time. In *Chapter 9*, the fault signal dynamics will be considered allowing to introduce more accurate approaches. On the other hand, an appealing approximation to calculate this factor is based on evaluating both the observed and the theoretical property of the fault signal at its occurrence time instant, $k_{\phi i}$. This approach can be viewed as an evaluation of the theoretical and observed residual derivative regarding time at time instant $k_{\phi i}$.

7.3.3.3 FSMsensit: Evaluation of fault sensitivities

The value of an element of the table ***FSM**sensit, **FSM**sensit*$_{ij}$, describes how easily a fault f_j will cause the i^{th}-residual $r_i^o(k)$ to violate its associated adaptive threshold given by the interval $[\underline{r}_i^o(k), \overline{r}_i^o(k)]$ (Eq. (7.2)), such as it is described by Eq. (7.4), originating the occurrence of the fault signal $\phi_i(k)$ ($|\phi_i(k)| \geq 0.5$). Thereby, according to the residual internal form (Eq. (3.62)) (*Section 3.3.5*) and the main results of *Section 3.3*, every element ***FSM**sensit*$_{ij}$ must be directly proportional to the fault residual sensitivity function $S_{f_{i,j}}$ and inversely proportional to the associated threshold $\overline{r}_i^o(k)$ or $\underline{r}_i^o(k)$ (Eq. (7.2)). In consequence, the expression of ***FSM**sensit*$_{ij}$ can be written as it follows:

$$\boldsymbol{FSM}sensit_{ij} = \begin{cases} 0 & \text{if} \quad S_{f_{i,j}}(q^{-1}) = 0 \\ \dfrac{s_{f_{i,j}}(\infty)}{\left|\overline{r}_i^o(k)\right|} & \text{if} \quad r_i^o(k) \geq 0 \\ \dfrac{s_{f_{i,j}}(\infty)}{\left|\underline{r}_i^o(k)\right|} & \text{if} \quad r_i^o(k) < 0 \end{cases} \tag{7.15}$$

where $s_{f_{i,j}}(\infty)$ is the steady-state value of $S_{f_{i,j}}$ when an unit step input is considered (*Section 3.3*).

Although the fault residual sensitivity $S_{f_{i,j}}$ is a function of time such as it was demonstrated in *Section 3.3*, its steady-state value is just considered in the approach presented in this chapter such as it was also suggested by (Gertler, 1998). This is just an initial approximation which will be discussed and improved in *Chapter 9* where the time evolution of the function $S_{f_{i,j}}$ will be considered.

Conversely, regarding the fault residual sensitivity property related to every fault signal, the comparison component computes at the end of the time window T_w for every fault signal $\phi_i(k)$ and for every fault hypothesis f_j the factor $factorsensit_{ij}$. Thus, this factor uses the values ϕ_{imax} of every fault signal $\phi_i(k)$ weighted by the corresponding elements $FSMsensit_{ij}$ related to the fault hypothesis f_j in order to determine the occurrence probability of this fault hypothesis. Nevertheless, it should be noticed that those values ϕ_{imax} related to non-observed fault signals are considered zero-valued in the memory component. As a reference, the approach used to obtain $factorsensit_{ij}$ can be also found in the DMP-method (Petti et al., 1990). Then, the expression of this factor can be written as it follows:

$$\boldsymbol{factor}sensit_j(k) = \frac{\left|\sum_{i=1}^{ny}\left(\phi_{i\max}\boldsymbol{FSM}sensit_{ij}\right)\right|}{\sum_{i=1}^{ny}\left|\boldsymbol{FSM}sensit_{ij}\right|}\boldsymbol{zvf}_j \tag{7.16}$$

7.3.3.4 FSMorder: Fault signal occurrence order evaluation

Such as it was shown in *Chapter 6*, when a fault f_j affects a dynamical system, the fault signals do not appear at the same time but each of them has its own dynamics and time evolution. As a result, the occurrence of a fault will originate the appearance of a set of fault signals ϕ in a characteristic order which will help to isolate the fault from the set $\boldsymbol{f}$ of possible faults. Thereby, for the fault hypothesis f_j, the j^{th}-column of the table ***FSM**order* contains the theoretical occurrence order of those affected fault signals which is codified using ordinal numbers, starting with *'1'*. Moreover, if two fault signals appear at the same time or if they explicitly may commute their order, then they should

share the same ordinal number. Regarding those fault signals which are theoretically not affected by that fault hypothesis, they get the code *'0'* in the corresponding cells of matrix ***FSM**order*.

$$\boldsymbol{FSM}order_{ij} = \begin{cases} \eta_{ij} & \text{if} \quad S_{f_{i,j}}(q^{-1}) \neq 0 \\ 0 & \text{if} \quad S_{f_{i,j}}(q^{-1}) = 0 \end{cases} \tag{7.17}$$

where η_{ij} is the ordinal number that determines the theoretical occurrence order of the fault signal $\phi_i(k)$ regarding the fault hypothesis f_j. According to the residual internal form (Eq. (3.62)) (*Section 3.3.5*), it can be seen that the fault signal occurrence order for a given fault hypothesis is determined basically by the fault residual sensitivity function and by the adaptive threshold. In *Chapter 9*, an approximated method to determine the theoretical values of this fault signal property will be presented.

Conversely, the occurrence order of all observed fault signals is indirectly stored in the memory component since for every observed fault signal $\phi_i(k)$, this element stores its appearance time instant ($k_{\phi i}$). Thereby, for those non-observed fault signals, the corresponding parameter $k_{\phi i}$ stored in the memory component will be zero-valued.

Then, comparing the fault signal observed information with the theoretical one stored in the matrix ***FSM**order*, the comparison component can compute ***factor**order*$_j$ for every fault hypothesis f_j at the end of the time window T_w in order to estimate the occurrence probability of every fault hypothesis. Thus, the expression of ***factor**order*$_j$ is given by the following equation:

$$\boldsymbol{factor}order_j(k) = \frac{\sum_{i=1}^{ny}\left(ckeckorder\left(\phi_i(k), \boldsymbol{FSM}order_{ij}\right)\right)}{\sum_{i=1}^{ny} boolean(\boldsymbol{FSM}order_{ij})} \boldsymbol{zvf}_j \tag{7.18}$$

where

$$ckeckorder(\phi_i(k), \boldsymbol{FSM}order_{ij}) = \begin{cases} 0 & \text{if} \quad k_{\phi i} = 0 \\ 0 & \text{if} \quad order(\phi_i(k)) \neq \boldsymbol{FSM}order_{ij}) \text{ and } k_{\phi i} \neq 0 \\ 1 & \text{if} \quad order(\phi_i(k)) = \boldsymbol{FSM}order_{ij}) \text{ and } k_{\phi i} \neq 0 \end{cases} \tag{7.19}$$

and $order(\phi_i(k))$ is the occurrence order of the fault signal $\phi_i(k)$ which can be inferred from the information stored in the memory component such as it was already mentioned above.

7.3.4 Decision logic component

The last task of the considered diagnosis algorithm is the decision logic component. At the end of the time window T_w, this element determines the occurrence probability d_j of every fault hypothesis f_j using the associated factors: ***factor**01*$_j$, ***factor**sign*$_j$, ***factor**sensit*$_j$ and ***factor**order*$_j$. Thereby, d_j may be calculated using two possible alternatives:

- the highest factor

$$d_j = \max(\boldsymbol{factor}01_j, \boldsymbol{factor}sign_j, \boldsymbol{factor}sensit_j, \boldsymbol{factor}order_j) \tag{7.20}$$

- or weighting these factors according to its significance in the fault diagnosis process

$$d_j = (\alpha_1 \boldsymbol{factor}01j + \alpha_2 \boldsymbol{factor}sign_j + \alpha_3 \boldsymbol{factor}sensit_j + \alpha_4 \boldsymbol{factor}order_j) \tag{7.21}$$

where α_1 , …., $\alpha_4 \in [0,1]$ are the weighing parameters proposed by fault diagnosis designer.

As an initial approximation, ***factor**sensit*$_j$ and ***factor**order*$_j$ are considered more important than the rest of the factors. However, this issue will be discussed in *Chapter 9* and in *Chapter 10*. Finally, the diagnosed fault given by the

decision logic component will be the one whose occurrence probability d_j is the highest of all possible fault hypotheses f_j.

7.4 Case of study

7.4.1 Description

To illustrate the fault diagnosis approach proposed in this paper, a real case of study based on the Barcelona urban drainage system is used. The city of Barcelona, with a population of 3,000,000 inhabitants in an area of 98 square Km^2, has a combined sewer system (waste and rainwater go into the same sewers) of approximately 1,500 Km. Additionally, the yearly rainfall is not very high (600 mm/year), but it includes heavy storms typical of the Mediterranean climate that cause a lot of flooding problems and combined sewer overflows to the sea that cause pollution (*CSO*). Such a complex system is conducted through the control centre in CLABSA (Barcelona Sewer Company) using a remote control system (in operation since 1994) that includes sensors, regulators, remote stations and communications (*Fig. 7.2*). The real-time control of the sewer network is based on model predictive control (*MPC*), as the global control law which sets the references for local controllers located on different actuator (gates and pumps) elements of the sewer network using measurements taken from sensors distributed along the network and rain sensors. These references are computed in real-time using an operational model to predict time ahead the network dynamics, the current state of the system, provided by sensors, the current rain intensity measures and appropriate rainfall predictions. The control objective is to minimize flooding and combined sewer overflow to the environment, and to maximize the utilization of wastewater treatment plants. However, the global optimal control of the sewer network is vulnerable to faults. Faults in sensors (rain-gauges and limnimeters) and actuators (gates and pumps), especially in heavy rain scenarios are usual. If these faults are not detected and isolated, and if it is possible, also corrected introducing some mechanism that assures fault tolerance, the global optimal control should be stopped, moving the control to the local mode. Since in every rain scenario, several faults, especially in sensors, occur, it is highly probable that it will be stopped. This will make very difficult the success of the global control system.

The application example of this chapter is based on a part of this network that covers 12 of the twenty catchments of the city and it contains 3 diversion gates and only one real detention tank, whose capacity is 35000 m^3. It includes the main sewer which carries water to the treatment plant and the four main seafront sea pollution points. Moreover, there are five passive flow-diversion (overflow) devices and the network is metered by means of 4 rain-gauges and 14 limnimeters (water level meters). The aim of the fault diagnosis algorithm proposed in this paper will be to detect and isolate faults in those limnimeters.

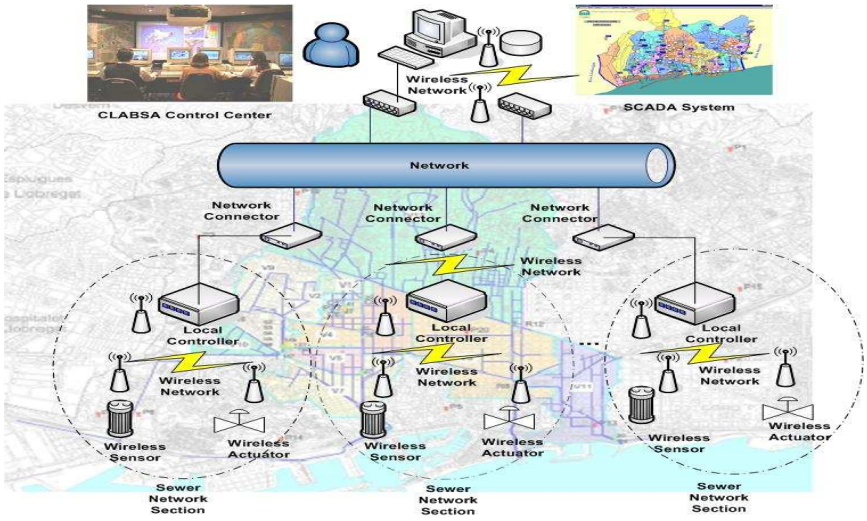

Fig. 7.2 Barcelona sewer network control system

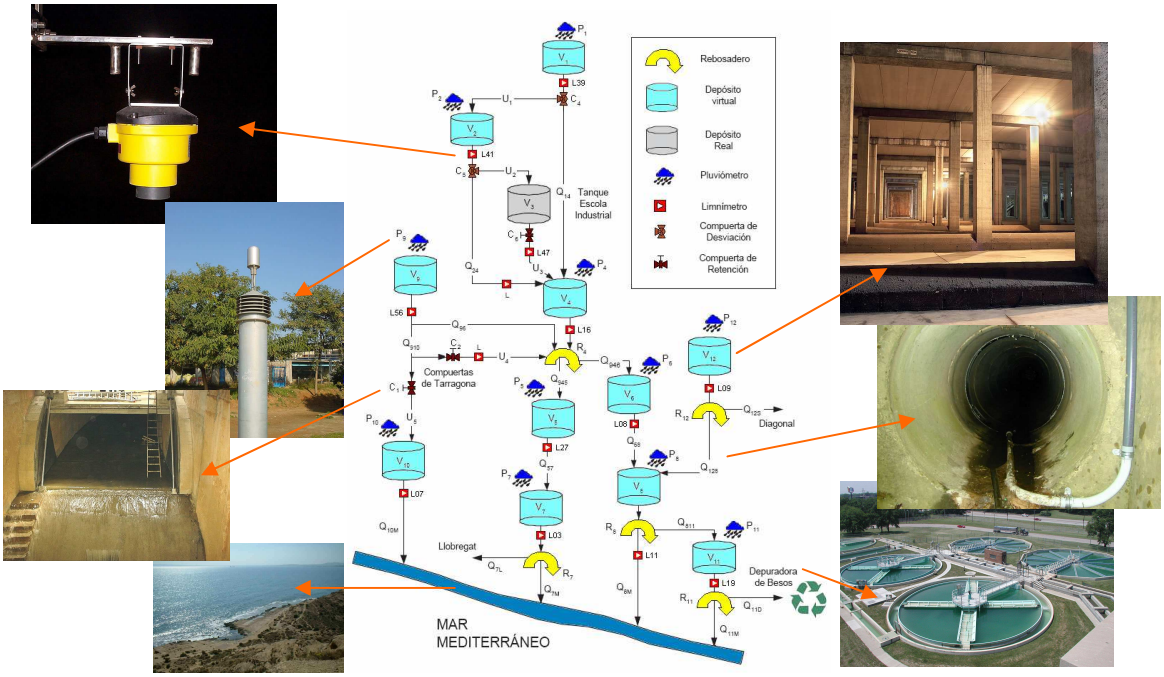

Fig. 7.3 Virtual reservoir model of Barcelona network prototype

7.4.2 Modelling limnimeters

Limnimeters can be monitored using a rainfall-runoff on-line model of the sewerage network. Complex non-linear rainfall-runoff models are very useful for off-line operations (calibration and simulation) of the sewerage network, but for on-line purposes, as the global optimal control and fault diagnosis, a much simpler structure of the model must be selected. One possible model methodology to derive a rainfall-runoff real-time model of a sewerage network is through a simplified graph relating the main sewers and a set of virtual and real reservoirs (Cembrano, 2002). A ***virtual reservoir*** is an aggregation of the sewer network catchment which approximates the hydraulics of the retention of rain, runoff and sewage water. The hydraulics of a virtual reservoir can be described by the following equation:

$$\frac{dV(t)}{dt} = Q_{up}(t) - Q_{down}(t) + P(t)S \tag{7.22}$$

where: V is the water volume accumulated in the catchment, Q_{up} and Q_{down} are flows entering and exiting the catchment, P is the rain intensity falling in the catchment and S its surface. Input and output sewer levels are measured using limnimeters and they can be related with flows using a linearised Manning relation: $Q_{up}(t) = M_{up}L_{up}(t)$ and $Q_{down}(t) = M_{down}L_{down}(t)$. Moreover, it is assumed that: $Q_{down}(t) = K_v V(t)$. Then, substituting these relations in Eq. (7.22) and considering that the measurement sample time is T_s=*300 s*, the following discrete-time model for every limnimeter can be derived:

$$L_{down}(k+1) = aL_{down}(k) + bL_{up}(k) + cI(k)) \tag{7.23}$$

where: $a = (1 - K_v T_s)$, $b = M_{up}K_v T_s / M_{down}$ and $c = SK_v / M_{down}$. Using this modelling methodology, a model of the selected part of the Barcelona's sewer network is presented in *Fig. 5.3*.

7.4.3 Interval models for limnimeter fault detection

Thereby, this methodology applied to the selected sewer network allow diagnosing faults of a set $\boldsymbol{f_{Lm}}$ related to 14 limnimeters (L_{03}, L_{07}, L_{08}, L_{09}, L_{16}, L_{27}, L_{39}, L_{41}, L_{45}, L_{47}, L_{53}, L_{56}, L_{80} and L_{54}) modelling a set $\boldsymbol{L_m}$ of 12 limnimeters (L_{03}, L_{07}, L_{08}, L_{09}, L_{16}, L_{27}, L_{39}, L_{41}, L_{45}, L_{56}, L_{80} and L_{54}) according to the procedure indicated in *Section 7.4.2* (Eq. (7.23)). In this chapter, the fault detection model for every limnimeter of the set $\boldsymbol{L_m}$ is given by an interval predictor whose general structure is given by Eq. (7.23) and whose parameters must be estimated using real data from the sensors installed in the network. In this case, the measurements provided by the limnimeters related to the set $\boldsymbol{f_{Lm}}$ and by a set $\boldsymbol{G}$ of 4 rain-gauges (G_{13}, G_{14}, G_{16} and G_{20}). These rain-gauges measure the rain intensity which is falling to every virtual reservoir. Thus, according to the real topology of the sewer network, the rain-gauge G_{13} measures the rain intensity P_{11} falling into the virtual reservoir V_{11}, G_{14} measures P_7, G_{16} measures P_1, P_2, P_9 and P_{10} and G_{20} measures P_4, P_5, P_6, P_8 and P_{12}. Moreover, in spite it can not be seen in *Fig. 7.3*, it must be taken into account that limnimeter L_{45} is installed into the real tank V_3 what allows measuring its water level, L_{53} let measure the entering flow of the virtual reservoir V_{10} and L_{54} is installed close to the gate C_2 measuring its related water flow.

The interval predictor related to every limnimeter must be calibrated in order to guarantee that its estimated interval output includes all the limnimeter non-modelled effects. Thus, an algorithm inspired by the one proposed in (Ploix et al., 1999) is used. It is based on the use of classical identification methods, such as the least-squares method, to provide the nominal values of the model parameters. Then, using optimization tools, the output intervals are adjusted until all the limnimeter measurements are covered by the estimated output interval.

According to Eq. (7.1), the estimations given by the limnimeter models of the set $\boldsymbol{L_m}$ allow obtaining a set $\boldsymbol{r}$ of 12 residuals (or ARR). Thus, according to Eq. (7.5), each residual of the set $\boldsymbol{r}$ determines a fault signal being ϕ the set of all possible fault signals caused by the faults of the set $\boldsymbol{f_{Lm}}$. Such as mentioned along this chapter, the properties of the observed fault signals let the fault isolation algorithm introduced in *Section 7.3* predict a diagnosis result.

Concerning the influence of the limnimeter faults of the set $\boldsymbol{f_{Lm}}$ on the fault signal set ϕ, it is described by the four theoretical fault signature matrices (***FSM**01*, ***FSM**sign*, ***FSM**sensit* and ***FSM**order*)(*Section 7.3.3*) showed below which are derived from the sewer network topology (*Figure 7.3*) and from the presented limnimeter modelling approach (Eq. (7.23)).

***FSM** 01* Matrix

	f_{L03}	f_{L07}	f_{L08}	f_{L09}	f_{L16}	f_{L27}	f_{L39}	f_{L41}	f_{L45}	f_{L47}	f_{L53}	f_{L56}	f_{L80}	f_{L54}
ϕ_{L03}	1	0	0	0	0	1	0	0	0	0	0	0	0	0
ϕ_{L07}	0	1	0	0	0	0	0	0	0	0	1	0	0	0
ϕ_{L08}	0	0	1	0	1	0	0	0	0	0	0	0	1	0
ϕ_{L09}	0	0	0	1	0	0	0	0	0	0	0	0	0	0
ϕ_{L16}	0	0	0	0	1	0	0	0	0	0	0	0	1	0
ϕ_{L27}	0	0	0	0	0	1	0	0	0	0	0	0	0	0
ϕ_{L39}	0	0	0	0	0	0	1	0	0	0	0	0	0	0
ϕ_{L41}	0	0	0	0	0	0	1	1	0	0	0	0	0	0
ϕ_{L45}	0	0	0	0	0	0	0	1	1	1	0	0	0	0
ϕ_{L54}	0	0	0	0	0	0	0	0	0	0	1	1	0	1
ϕ_{L56}	0	0	0	0	0	0	0	0	0	0	0	1	0	0
ϕ_{L80}	0	0	0	0	0	0	0	0	0	1	0	0	1	0

Table 7.1 Theoretical fault signature matrix related to the binary property

***FSM** sign* Matrix

	f_{L03}	f_{L07}	f_{L08}	f_{L09}	f_{L16}	f_{L27}	f_{L39}	f_{L41}	f_{L45}	f_{L47}	f_{L53}	f_{L56}	f_{L80}	f_{L54}
ϕ_{L03}	+1	0	0	0	0	-1	0	0	0	0	0	0	0	0
ϕ_{L07}	0	+1	0	0	0	0	0	0	0	0	-1	0	0	0
ϕ_{L08}	0	0	+1	0	-1	0	0	0	0	0	0	0	-1	0
ϕ_{L09}	0	0	0	+1	0	0	0	0	0	0	0	0	0	0
ϕ_{L16}	0	0	0	0	+1	0	0	0	0	0	0	0	-1	0
ϕ_{L27}	0	0	0	0	0	+1	0	0	0	0	0	0	0	0
ϕ_{L39}	0	0	0	0	0	0	+1	0	0	0	0	0	0	0
ϕ_{L41}	0	0	0	0	0	0	-1	+1	0	0	0	0	0	0
ϕ_{L45}	0	0	0	0	0	0	0	-1	+1	-1	0	0	0	0
ϕ_{L54}	0	0	0	0	0	0	0	0	0	0	-1	-1	0	+1
ϕ_{L56}	0	0	0	0	0	0	0	0	0	0	0	+1	0	0
ϕ_{L80}	0	0	0	0	0	0	0	0	0	-1	0	0	+1	0

Table 7.2 Theoretical fault signature matrix related to the sign property

***FSM** sensit* Matrix

	f_{L03}	f_{L07}	f_{L08}	f_{L09}	f_{L16}	f_{L27}	f_{L39}	f_{L41}	f_{L45}	f_{L47}	f_{L53}	f_{L56}	f_{L80}	f_{L54}
ϕ_{L03}	0.241	0	0	0	0	-0.156	0	0	0	0	0	0	0	0
ϕ_{L07}	0	0.115	0	0	0	0	0	0	0	0	-0.033	0	0	0
ϕ_{L08}	0	0	0.360	0	-0.193	0	0	0	0	0	0	0	-0.294	0
ϕ_{L09}	0	0	0	0.128	0	0	0	0	0	0	0	0	0	0
ϕ_{L16}	0	0	0	0	0.383	0	0	0	0	0	0	0	-0.246	0
ϕ_{L27}	0	0	0	0	0	0.082	0	0	0	0	0	0	0	0
ϕ_{L39}	0	0	0	0	0	0	0.379	0	0	0	0	0	0	0
ϕ_{L41}	0	0	0	0	0	0	-0.958	0.042	0	0	0	0	0	0
ϕ_{L45}	0	0	0	0	0	0	0	-0.254	0.014	0.187	0	0	0	0
ϕ_{L54}	0	0	0	0	0	0	0	0	0	0	-0.810	-0.393	0	1
ϕ_{L56}	0	0	0	0	0	0	0	0	0	0	0	0.080	0	0
ϕ_{L80}	0	0	0	0	0	0	0	0	0	-0.580	0	0	0.256	0

Table 7.3 Theoretical fault signature matrix related to the fault residual sensitivity property

***FSM**order* Matrix

	f_{L03}	f_{L07}	f_{L08}	f_{L09}	f_{L16}	f_{L27}	f_{L39}	f_{L41}	f_{L45}	f_{L47}	f_{L53}	f_{L56}	f_{L80}	f_{L54}
ϕ_{L03}	1	0	0	0	0	2	0	0	0	0	0	0	0	0
ϕ_{L07}	0	1	0	0	0	0	0	0	0	0	2	0	0	0
ϕ_{L08}	0	0	1	0	2	0	0	0	0	0	0	2	0	0
ϕ_{L09}	0	0	0	1	0	0	0	0	0	0	0	0	0	0
ϕ_{L16}	0	0	0	0	1	0	0	0	0	0	0	0	2	0
ϕ_{L27}	0	0	0	0	0	1	0	0	0	0	0	0	0	0
ϕ_{L39}	0	0	0	0	0	0	1	0	0	0	0	0	0	0
ϕ_{L41}	0	0	0	0	0	0	2	1	0	0	0	0	0	0
ϕ_{L45}	0	0	0	0	0	0	0	2	1	2	0	0	0	0
ϕ_{L54}	0	0	0	0	0	0	0	0	0	0	1	1	0	1
ϕ_{L56}	0	0	0	0	0	0	0	0	0	0	0	1	0	0
ϕ_{L80}	0	0	0	0	0	0	0	0	0	1	0	0	1	0

Table 7.4 Theoretical fault signature matrix related to the occurrence order property

It must be taken into account that the elements of ***FSM**sensit* matrix showed in *Table 7.13* are just the fault residual sensitivity steady-state values, $s_{f_{i,j}}(\infty)$, instead of the ones derived from the use of Eq. (7.15). However, the presented fault isolation algorithm does use Eq. (7.15) to obtain the elements of ***FSM**sensit*.

7.4.4 Fault scenario

The fault diagnosis algorithm presented in *Section 7.3* has been tested using several real fault scenarios in spite of its weaknesses mentioned in *Section 7.1* in order to illustrate the goodness of this approach. In this section, a real scenario occurred the 28/09/2001 is presented in which the Barcelona sewer network operators registered a faulty behaviour of the limnimeter L_{47}. The aim of this initial test is to show the general performance of the presented fault isolation algorithm without carrying out a deep analysis since it will be done from *Chapter 8*.

Thereby, such as shown by the *binary fault signature matrix* ***FSM***01 (*Table* 7.1), this faulty scenario has just an influence on the residuals (fault signals) associated with the models of limnimeters L_{45} and L_{80}. Consequently, both must be activated in order to diagnose that fault.

The nominal predictor model related to L_{45} is given by

$$\hat{L}_{45}(k+1) = a_{45}L_{45}(k) + b_{45}L_{41}(k) + c_{45}L_{47}(k) \tag{7.24}$$

where a_{45}=0.985, b_{45}=0.254 and c_{45}=-0.186.

Regarding the nominal predictor that models the behaviour of L_{80}, it is given by

$$\hat{L}_{80}(k+1) = a_{80}L_{80}(k) + b_{80}L_{47}(k) \tag{7.25}$$

where a_{80}=0.744 and b_{45}=0.58.

In the approach used in this section, the output intervals associated with the nominal predictor models are adjusted statistically until all the limnimeter measurements are covered by the estimated output intervals when there is none of the faults of the set $\boldsymbol{f_{Lm}}$. Conversely, from *Chapter 8* the output intervals will be computed using models with uncertain parameters since according to (Puig et al., 2002), this kind of models may show a better performance in applications where an on-line computation is required.

As seen in *Fig. 7.4*, the occurrence of the fault in L_{47}, f_{L47}, provoked the nominal residuals associated with L_{45} and L_{80}, r^o_{L45} and r^o_{L80}, to violate their associated adaptive thresholds (Eq. (7.2)) and as a result, the associated fault signals, ϕ_{L45} and ϕ_{L80}, could be observed for a period of time since their associated absolute values were greater or equal than 0.5 (*Section 7.2.2*), such as it can be viewed in *Fig. 7.5*; in other words, r^o_{L45} and r^o_{L80} did not satisfy the

fault detection condition (7.4) for a certain period of time. Thus, according to these observations and to the information stored in the four theoretical fault signature matrices, the fault isolation algorithm could isolate the fault affecting to L_{47}.

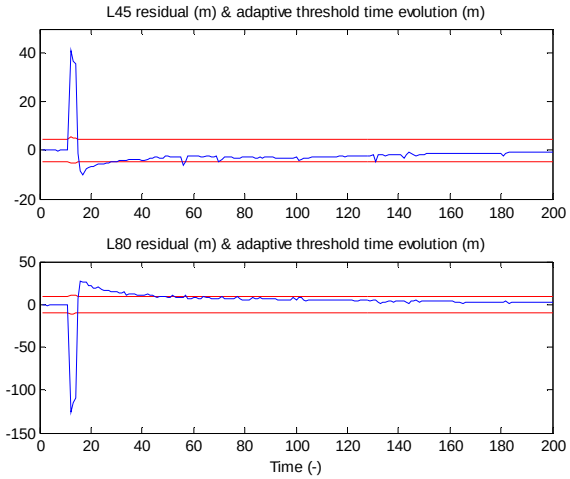

Fig. 7.4 Time evolution of the residuals and their corresponding adaptive thresholds

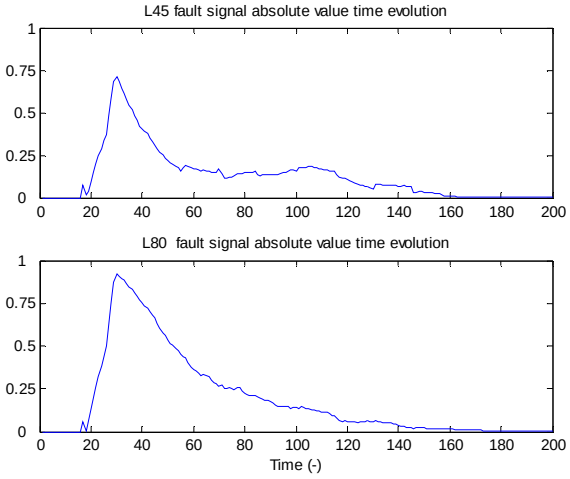

Fig. 7.5 Time evolution of the fault signals considering their absolute value

Fig. 7.4 and *Fig. 7.5* show clearly that the fault is not persistently indicated (*weak-fault detection*; *Section 3.4.2*) by the residuals (Eq. (7.4)) and therefore, the observation of the fault signals is only possible for a certain period of time. As it can be seen, this fact could affect the isolation of the fault if a suitable strategy were not use. This issue will be analyzed in *Chapter 8* as an extension of the main conclusions derived from *Chapter 3* where this model performance was already analyzed focusing only in fault detection.

In *Fig. 7.6*, the time evolution of the fault isolation factors (***factor***01_j, ***factor***$sign_j$, ***factor***$sensit_j$ and ***factor***$order_j$) (*Section 7.3*) related to every fault hypothesis of the set $\boldsymbol{f_{Lm}}$ is plotted. Regarding the value of the waiting time window T_w, it is equal to the sampling time period T_s in spite of knowing that it is not its optimum value. Thus, the fault isolation factors are computed at every time instant and consequently, the influence of the fault indication persistence on the fault isolation result can be noticed. It will be in *Chapter 9* where the optimum value of T_w will be discussed.

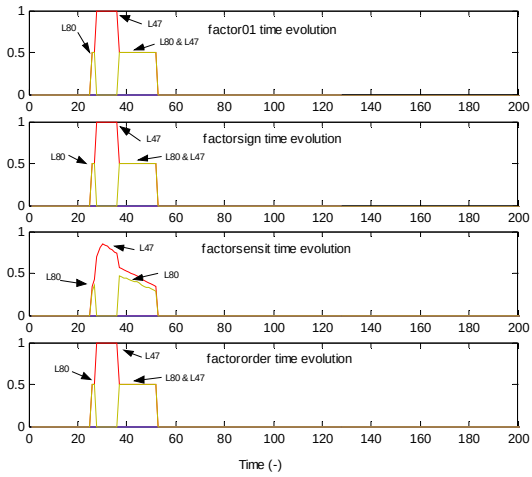

Fig 7.6 Time evolution of the fault isolation factors

Such as it can be deduced from the theoretical fault signatures matrices (***FSM**01*, ***FSM**sign*, ***FSM**sensit* and ***FSM**order*) shown in *Section 7.4.3* and according to the time evolution of the fault signals showed in *Figure 7.5*, the only two fault hypotheses whose factors have non-null values, at least for a certain period of time, are f_{L47} and f_{L80} indicating L_{47} and L_{80} as the faulty limnimeters. Conversely, observing *Fig. 7.6* and assuming that the fault does not disappears once it occurs (at least, it is quite unlikely), it would not be hardly to think that the *decision logic component* (*Section 7.3.4*) of the proposed fault isolation architecture would give f_{L47} as the best candidate since all its associated factors reaches bigger values than the ones corresponding to f_{L80}. Moreover, it would not be hardly to think either, that using an incremental fault diagnosis approach, instead of an static one, and considering a suitable value of T_w, this fault isolation algorithm could avoid the confusion when just one fault signal is observed at the beginning, ϕ_{L45}, and the confusion once ϕ_{L45} vanishes, since f_{L47} hypothesis is the only one that fulfils that all its associated fault signals were observed and besides, they appeared in the expected occurrence order. Nevertheless, once all fault signals vanish, it is even assumed that the fault still persists and consequently, the diagnosed result is still valid. If the fault would have vanished, something else should be done in order to detect this event. In the following chapters, the effect of the non-persistence of the fault signals on the fault isolation result and suitable strategies to avoid this drawback are deeper analyzed.

7.5 Conclusions

In this chapter, an interval model-based fault diagnosis method that improves the integration between the fault detection and isolation modules has been proposed. This method is based on a new interface between both stages which takes into account the information about the degree of fault signal activation and the dynamics associated with each fault signal. The fault isolation process uses a combination of four theoretical fault signature matrices which store the knowledge about the faulty system behaviour determined by the properties of the observed fault signals (binary property, sign property, fault residual sensitivity property and occurrence order property). In this chapter, some weaknesses of this fault diagnosis method are remarked in order to introduce the analysis which will be presented in the following chapters.

CHAPTER 8

Fault isolation using linear interval observers: influence of the observer gain

8.1 Introduction

These last years, the integration between fault detection and fault isolation tasks in model-based fault diagnosis has been a very active research area (see among others (Combastel et al., 2003), (Pulido et al., 2005) or (Puig et al, 2005b)) since it plays an important role in the final result given by the fault diagnoser, as illustrated in *Chapter 6* and *Chapter 7*. Consequently, the typical binary interface between these two modules has been improved using additional information what let improve the fault diagnoser performance as it was shown in *Chapter 6*. One example is the fault isolation architecture (*Fig. 7.1*) presented in *Chapter 7* where different aspects associated with the time evolution of the fault signals are considered in order to give an accurate result: binary property, sign property, fault residual sensitivity property and occurrence order property.

However, model-based fault detection methods still have some weaknesses as lack of fault indication persistence (*Chapter 3*), noise sensitivity and model errors. Therefore, as a result of these inherent problems, their fault detection performance can be worse than the one it might be required in order to give a reliable fault diagnosis result. Moreover, this fact might also confuse the fault isolation module when a subset of fault signals must be observed during the same period of time so that the right fault diagnosis result can be derived. This happens when the ***FSM*** matrices (*theoretical fault signature matrices*) are not diagonal with respect to the fault hypotheses what the most likely situation is.

When using fault detection methods based on observers, the observer gain plays an important role in their fault detection performance as it determines the time evolution of the residuals, their fault sensitivity functions and as a consequence, the minimum detectable fault function at any time instant (Chen et al., 1999). Therefore, such as it was demonstrated in *Chapter 3*, the ***fault indication persistence*** also depends on the observer gain (Meseguer et al., 2006). On the other hand, as it was presented in that chapter, faults can be classified in three types depending on their detectability. Thus, there will be faults ***permanently detected*** (*strong detection*), ***non-permanently detected*** (*weak detection*) and ***non-detected***. Regarding this issue, the reference (Meseguer et al, 2006) shows that the observer gain does also have an influence on how a fault will be detected: permanently, non-permanently or non-detected.

The above mentioned fault detection problems and their influence on the fault isolation module have been already noticed by (Combastel et al., 2003) who suggests registering the maximum absolute value of the residual value once reached. However, this strategy introduces an additional problem, since then, it is not possible to know when the fault disappears. Another approach would be using structured residuals in a diagonal form (Gertler, 1998) but it might be too complicated in this case because of the parameter uncertainty. When using an interval observer method, the effect of those fault detection problems might be partially avoided designing properly the observer gain matrix and therefore, the fault isolation result might be also improved.

The goal of this chapter is to illustrate how different fault isolation results are obtained depending on the observer gain for a given fault scenario in spite of using an accurate fault isolation algorithm: *right persistent fault isolation*, *right non-persistent fault isolation*, *wrong fault isolation* and *lack of fault isolation*. The applied fault isolation architecture is the one introduced in *Chapter 7* (*Fig. 7.1*). Thereby, concerning the weaknesses of this approach mentioned in *Section 7.1*, just one is improved. This is the considered models will no be given by uncertain predictors but by interval observers with uncertain parameters such as the ones showed in *Chapter 3*. Thus, the effect of the fault detection stage and the observer gain on the fault isolation module can be analyzed. Nevertheless, this analysis is carried out considering a qualitative approach since it will be in *Chapter 9* where a more quantitative approach will be considered.

The interval observer-based fault diagnosis algorithm will be applied to real faulty scenarios affecting to limnimeters of Barcelona's urban sewer system application described in Section 7.4.

Regarding the structure of the remainder of *Chapter 8*, passive robust fault detection using interval observers is recalled in *Section 8.2*. In *Section 8.3*, the integration of robust fault detection interval observer methods with the considered fault isolation algorithm is discussed. In *Section 8.4*, for a given limnimeter fault scenario, several observer gain sets are applied in order to illustrate their influence on the resulting fault isolation. Finally, in *Section 8.5*, the main conclusions are presented.

8.2 Passive robust based fault detection using interval observers

As assumed in *Chapter 3*, *Chapter 4* and *Chapter 5*, from this chapter it is considered that the monitored system can be described analytically by a *MIMO* linear uncertain dynamic model in discrete-time and state-space form, including faults, as follows

$$\begin{aligned} \boldsymbol{x}(k+1) &= \boldsymbol{A}(\tilde{\boldsymbol{\theta}})\boldsymbol{x}(k) + \boldsymbol{B}(\tilde{\boldsymbol{\theta}})\boldsymbol{u}_0(k) + \boldsymbol{F}_a(\tilde{\boldsymbol{\theta}})\boldsymbol{f}_a(k) \\ \boldsymbol{y}(k) &= \boldsymbol{C}(\tilde{\boldsymbol{\theta}})\boldsymbol{x}(k) + \boldsymbol{F}_y(\tilde{\boldsymbol{\theta}})\boldsymbol{f}_y(k) \end{aligned} \tag{8.1}$$

noticing that this equation is equal to Eq. (3.1) assuming that the direct transmission matrix $\boldsymbol{D}$ is zero-valued. As mentioned in *Section 3.2.1,* $\boldsymbol{y}(k)\in\Re^{ny}$, $\boldsymbol{u_0}(k)\in\Re^{nu}$, $\boldsymbol{x}(k)\in\Re^{nx}$ are the system output, input and the state-space vectors respectively; $\boldsymbol{A}(\tilde{\boldsymbol{\theta}})$, $\boldsymbol{B}(\tilde{\boldsymbol{\theta}})$ and $\boldsymbol{C}(\tilde{\boldsymbol{\theta}})$ are the state, the input and the output matrices respectively; $\tilde{\boldsymbol{\theta}}$ is the system parameter vector; $\boldsymbol{f_y}(k)\in\Re^{ny}$ and $\boldsymbol{f_a}(k)\in\Re^{nu}$ represent faults in the system output sensors and actuators respectively being $\boldsymbol{F_y}(\tilde{\boldsymbol{\theta}})$ and $\boldsymbol{F_a}(\tilde{\boldsymbol{\theta}})$ their associated matrices.

8.2.1 Interval observer expression

As done in *Chapter 3* and *Chapter 5*, from this chapter it is assumed that the system described by Eq. (8.1) can be monitored using a linear observer with *Luenberger* structure based on an ***interval model*** whose model parameters $\boldsymbol{\theta}$ are time-invariant but bounded by an interval set $\boldsymbol{\Theta}=\left\{\boldsymbol{\theta}\in\Re^{n\theta}\,\middle|\,\underline{\boldsymbol{\theta}}\le\boldsymbol{\theta}\le\overline{\boldsymbol{\theta}}\right\}$ which represents the uncertainty about the exact knowledge of real system parameters $\tilde{\boldsymbol{\theta}}$. Thus, the resulting ***interval observer*** assuming the observability of the system (Eq. (8.1)) for all $\tilde{\boldsymbol{\theta}}\in\boldsymbol{\Theta}$ can be expressed using Eq. (3.7) (*Section 3.2.1*) but this time matrix $\boldsymbol{D}$ is considered to be zero-valued:

$$\begin{aligned}\hat{\boldsymbol{x}}(k+1) &= (\boldsymbol{A}(\boldsymbol{\theta}) - \boldsymbol{L}\boldsymbol{C}(\boldsymbol{\theta}))\hat{\boldsymbol{x}}(k) + \boldsymbol{B}(\boldsymbol{\theta})\boldsymbol{u}(k) + \boldsymbol{L}\boldsymbol{y}(k) = \boldsymbol{A}_o(\boldsymbol{\theta})\hat{\boldsymbol{x}}(k) + \boldsymbol{B}(\boldsymbol{\theta})\boldsymbol{u}(k) + \boldsymbol{L}\boldsymbol{y}(k) \\ \hat{\boldsymbol{y}}(k) &= \boldsymbol{C}(\boldsymbol{\theta})\hat{\boldsymbol{x}}(k)\end{aligned} \tag{8.2}$$

where $\boldsymbol{u}$ is the measured system input vector, $\hat{\boldsymbol{x}}$ is the estimated system space-state vector and $\hat{\boldsymbol{y}}$ is the estimated system output vector. Besides, it must taken into account that as indicated in *Section 3.2.1*, the observer gain matrix $\boldsymbol{L}$ is designed to stabilise the matrix $\boldsymbol{A}_o(\boldsymbol{\theta}) = \boldsymbol{A}(\boldsymbol{\theta}) - \boldsymbol{L}\boldsymbol{C}(\boldsymbol{\theta})$ and to guarantee a desired performance regarding fault detection for all $\boldsymbol{\theta} \in \boldsymbol{\Theta}$. Conversely, the effect of the uncertain parameters $\boldsymbol{\theta}$ on the observer temporal response will allow obtaining a system output estimation interval: $[\ \underline{\hat{y}}(k)\ ,\ \overline{\hat{y}}(k)\ ]$,where for each output (neglecting couplings among outputs):

$$\underline{\hat{y}}_i(k) = \min_{\boldsymbol{\theta}\in\boldsymbol{\Theta}}(\hat{y}_i(k,\boldsymbol{\theta})) \ \text{ and } \ \overline{\hat{y}}_i(k) = \max_{\boldsymbol{\theta}\in\boldsymbol{\Theta}}(\hat{y}_i(k,\boldsymbol{\theta})) \tag{8.3}$$

Thereby, in case that there is no fault, each system output fulfils:

$$y_i(k) \in [\ \underline{\hat{y}}_i(k), \overline{\hat{y}}_i(k)\ ] = [\hat{y}_i(k)] \tag{8.4}$$

Finally, the interval observer given by Eq. (8.2) can be expressed in transfer function form using the *q*-transform and considering zero initial conditions as it follows:

$$\hat{\boldsymbol{y}}(k) = \boldsymbol{G}(q^{-1},\boldsymbol{\theta})\boldsymbol{u}(k) + \boldsymbol{H}(q^{-1},\boldsymbol{\theta})\boldsymbol{y}(k) \tag{8.5}$$

where:

$$\boldsymbol{G}(q^{-1},\boldsymbol{\theta}) = \boldsymbol{C}(\boldsymbol{\theta})(\boldsymbol{I} - q^{-1}\boldsymbol{A}_o(\boldsymbol{\theta}))^{-1}\boldsymbol{B}(\boldsymbol{\theta})q^{-1} \tag{8.6}$$

$$\boldsymbol{H}(q^{-1},\boldsymbol{\theta}) = \boldsymbol{C}(\boldsymbol{\theta})(\boldsymbol{I} - q^{-1}\boldsymbol{A}_o(\boldsymbol{\theta}))^{-1}\boldsymbol{L}q^{-1} \tag{8.7}$$

Noticing that Eq. (8.5) is fully equivalent to Eq. (3.11) presented in *Section 3.2.1*.

8.2.2 Fault detection using interval observers

This section is an extension of *Section 7.2* (*Chapter 7*) when using interval observers to model the monitored system and it is based on some conclusions of *Section 3.2.2* (*Chapter 3*). Thus, as already exposed, fault detection is based on calculating at every time instant a residual comparing the measurements of physical variables $\boldsymbol{y}(k)$ with their estimation $\hat{\boldsymbol{y}}(k)$ provided by the interval observer:

$$\boldsymbol{r}(k) = \boldsymbol{y}(k) - \hat{\boldsymbol{y}}(k) \tag{8.8}$$

According to (Gertler, 1998), the *computational form* of the residual (*Section 3.2.2*) is given by

$$\boldsymbol{r}(k,\boldsymbol{\theta}) = \boldsymbol{V}(q^{-1},\boldsymbol{\theta})\boldsymbol{u}(k) + \boldsymbol{O}(q^{-1},\boldsymbol{\theta})\boldsymbol{y}(k) \tag{8.9}$$

where considering the observer input-output form (Eq. (8.5)), the transfer functions $\boldsymbol{V(q^{-1},\theta)}$ and $\boldsymbol{O(q^{-1},\theta)}$ can be written as it follows:

$$\boldsymbol{V}(q^{-1},\boldsymbol{\theta}) = -\boldsymbol{G}(q^{-1},\boldsymbol{\theta}) = -\boldsymbol{C}(\boldsymbol{\theta})(\boldsymbol{I} - q^{-1}\boldsymbol{A}_o(\boldsymbol{\theta}))^{-1}\boldsymbol{B}(\boldsymbol{\theta})q^{-1} \tag{8.10}$$

$$\boldsymbol{O}(q^{-1},\boldsymbol{\theta}) = \boldsymbol{I} - \boldsymbol{H}(q^{-1},\boldsymbol{\theta}) = \boldsymbol{I} - \boldsymbol{C}(\boldsymbol{\theta})(\boldsymbol{I} - q^{-1}\boldsymbol{A}_o(\boldsymbol{\theta}))^{-1}\boldsymbol{L}q^{-1} \tag{8.11}$$

As illustrated in *Section 7.2.1*, residual (8.9) can be computed regarding the nominal observer model $\hat{\boldsymbol{y}}^o(k)$ obtained using $\boldsymbol{\theta} = \boldsymbol{\theta}^o \in \boldsymbol{\Theta}$,

$$\boldsymbol{r}^o(k) = \boldsymbol{y}(k) - \hat{\boldsymbol{y}}^o(k) \tag{8.12}$$

where propagating the interval observer parameter uncertainty to the residual (8.8), the values of every component of the nominal residual (Eq. (8.12)) will be bounded by the interval (Puig et al., 2002):

$$[\underline{r}_i^o(k), \overline{r}_i^o(k)] \tag{8.13}$$

where:

$$\underline{r}_i^o(k) = \underline{\hat{y}}_i(k) - \hat{y}_i^o(k) \text{ and } \overline{r}_i^o(k) = \overline{\hat{y}}_i(k) - \hat{y}_i^o(k) \tag{8.14}$$

Then, taking into account the definition of the nominal (Eq. (8.12)) and its associated *adaptive threshold* (Eq. (8.13)), no fault will be indicated while the following fault detection condition is satisfied

$$r_i^o(k) \in [\underline{r}_i^o(k), \overline{r}_i^o(k)] \tag{8.15}$$

noticing the equivalence of this condition and the one expressed in terms of system output measurements and their associated estimation (Eq. (8.4))

On the other hand, instead of using the fault detection test (8.15), the fault diagnostic signal (fault signal) $\phi_i(k)$ for every residual $r_i(k)$ (Eq. (7.5)) is calculated as indicated in *Section 7.2.2*. Then, when there is no fault, the values of every fault signal satisfies the expression $|\phi_i(k)|<0.5$ and consequently, they are not observable. Otherwise ($|\phi_i(k)|\geq 0.5$), the fault signals are observable which indicates that a given fault is affecting the monitored system.

8.2.3 Fault signal dynamics

In general, the occurrence of a fault signal can be caused by different faults and therefore, what let distinguish one fault from another are the fault signal dynamic properties: they should be different for each different fault. According to (Gertler, 1998), these theoretical dynamic properties of a fault signal $\phi_i(k)$ caused by a given fault f_j are set by the sensitivity of the associated residual $r_i(k)$ to this fault f_j introduced in *Section 3.3* of *Chapter 3*. As exposed in that section, the concept of the ***residual sensitivity to a fault*** (Eq. (3.36)) can be expressed analytically as

$$\boldsymbol{S}_f = \frac{\partial \boldsymbol{r}}{\partial \boldsymbol{f}} \tag{8.16}$$

Thus, the residual sensitivity to a fault is a dynamic time function which describes how a fault is affecting the residual and consequently, the dynamic properties of the fault signals caused by this fault.

Concerning fault detection stage whose main task is the generation of fault signals, *Chapter 3* based on the reference (Meseguer et al, 2007b) shows the importance of this concept both in the residual time evolution and in the quality of the fault detection.

Particularizing Eq. (8.16) for a certain type of fault ($\boldsymbol{f_y}$, $\boldsymbol{f_u}$ and $\boldsymbol{f_a}$), *Section 3.3.2* shows that the residual sensitivity for the case of an output sensor fault $\boldsymbol{f_y}=\{f_{yj} : j = 1,2,....n_y\}$ is given by a matrix $\boldsymbol{S}_{fy} \in \Re^{ny} \text{x} \Re^{ny}$ whose expression is

$$\begin{aligned} &\boldsymbol{S}_{fy}(q^{-1},\boldsymbol{\theta}) = \left(\boldsymbol{I} - \boldsymbol{H}(q^{-1},\boldsymbol{\theta})\right)\boldsymbol{G}_{fy}(q^{-1},\tilde{\boldsymbol{\theta}}) = \left(\boldsymbol{I} - \boldsymbol{C}(\boldsymbol{\theta})\left(q\boldsymbol{I} - \left(\boldsymbol{A}(\boldsymbol{\theta}) - \boldsymbol{L}\boldsymbol{C}(\boldsymbol{\theta})\right)\right)^{-1}\boldsymbol{L}\right)\boldsymbol{F}_y(\tilde{\boldsymbol{\theta}}) = \\ &= \begin{pmatrix} S_{fy_{1,1}}(q^{-1},\boldsymbol{\theta}) & \cdots & S_{fy_{1,ny}}(q^{-1},\boldsymbol{\theta}) \\ \vdots & \ddots & \vdots \\ S_{fy_{ny,1}}(q^{-1},\boldsymbol{\theta}) & \cdots & S_{fy_{ny,ny}}(q^{-1},\boldsymbol{\theta}) \end{pmatrix} \end{aligned} \tag{8.17}$$

In the same way, the residual sensitivity to an input sensor fault $\boldsymbol{f_u}=\{f_{uj} : j = 1,2,....n_u\}$ (*Section 3.3.3*) is given by a matrix $\boldsymbol{S}_{fu} \in \Re^{ny} \text{x} \Re^{nu}$ whose expression is:

$$\boldsymbol{S}_{fu}(q^{-1},\boldsymbol{\theta}) = -\boldsymbol{G}(q^{-1},\boldsymbol{\theta})\boldsymbol{F}_u(\boldsymbol{\theta}) = -\Big(\boldsymbol{C}(\boldsymbol{\theta})\big(q\boldsymbol{I}-\big(\boldsymbol{A}(\boldsymbol{\theta})-\boldsymbol{LC}(\boldsymbol{\theta})\big)\big)^{-1}\big(\boldsymbol{B}(\boldsymbol{\theta})-\boldsymbol{LD}(\boldsymbol{\theta})\big)+\boldsymbol{D}(\boldsymbol{\theta})\Big)\boldsymbol{F}_u(\boldsymbol{\theta}) =$$
$$= \begin{pmatrix} S_{fu_{1,1}}(q^{-1},\boldsymbol{\theta}) & \cdots & S_{fu_{1,nu}}(q^{-1},\boldsymbol{\theta}) \\ \vdots & \ddots & \vdots \\ S_{fu_{ny,1}}(q^{-1},\boldsymbol{\theta}) & \cdots & S_{fu_{ny,nu}}(q^{-1},\boldsymbol{\theta}) \end{pmatrix} \tag{8.18}$$

Thereby, the residual sensitivity to an actuator fault $\boldsymbol{f_a} = \{f_{aj} : j = 1,2,....n_u\}$ (*Section 3.3.4*) is given by a matrix $\boldsymbol{S}_{fa} \in \Re^{ny}\text{x}\Re^{nu}$ whose expression is:

$$\boldsymbol{S}_{fa}(q^{-1},\boldsymbol{\theta}) = \big(\boldsymbol{I}-\boldsymbol{H}(q^{-1},\boldsymbol{\theta})\big)\boldsymbol{G}_{fa}(q^{-1},\tilde{\boldsymbol{\theta}}) =$$
$$= \Big(\boldsymbol{I}-\boldsymbol{C}(\boldsymbol{\theta})\big(q\boldsymbol{I}-\big(\boldsymbol{A}(\boldsymbol{\theta})-\boldsymbol{LC}(\boldsymbol{\theta})\big)\big)^{-1}\boldsymbol{L}\Big)\boldsymbol{C}(\tilde{\boldsymbol{\theta}})\big(q\boldsymbol{I}-\boldsymbol{A}(\tilde{\boldsymbol{\theta}})\big)^{-1}\boldsymbol{F}_a(\tilde{\boldsymbol{\theta}}) = \tag{8.19}$$
$$= \begin{pmatrix} S_{fa_{1,1}}(q^{-1},\boldsymbol{\theta}) & \cdots & S_{fa_{1,nu}}(q^{-1},\boldsymbol{\theta}) \\ \vdots & \ddots & \vdots \\ S_{fa_{ny,1}}(q^{-1},\boldsymbol{\theta}) & \cdots & S_{fa_{ny,nu}}(q^{-1},\boldsymbol{\theta}) \end{pmatrix}$$

Then, as demonstrated in *Section 3.3.5* of *Chapter 3*, the residual computational form (Eq. (8.9)) can be expressed in terms of the fault residual sensitivity matrices ($\boldsymbol{S_{fy}}$, $\boldsymbol{S_{fu}}$ and $\boldsymbol{S_{fa}}$) and the adaptive threshold $\boldsymbol{r_0}(k)$(Eq. (3.21)) as it follows:

$$\boldsymbol{r}(k,\boldsymbol{\theta}) = \boldsymbol{r}_0(k,\boldsymbol{\theta}) + \boldsymbol{S}_{fa}(q^{-1},\boldsymbol{\theta})\boldsymbol{f}_a(k) + \boldsymbol{S}_{fy}(q^{-1},\boldsymbol{\theta})\boldsymbol{f}_{fy}(k) + \boldsymbol{S}_{fu}(q^{-1},\boldsymbol{\theta})\boldsymbol{f}_{fu}(k) \tag{8.20}$$

Thereby, taking into account that the fault signals $\phi_i(k)$ are generated evaluating residual given by Eq, (8.20) such as indicated by Eq. (8.12) and Eq. (8.13) and then, applying Eq. (7.5), the next conclusions can be obtained regarding the influence of the fault residual sensitivity functions on the fault signal set ϕ according to Eq. (8.20):

- the fault residual sensitivity functions establish which residual $r_i(k)$ (fault signal $\phi_i(k)$) is affected by which fault (f_{yj}, f_{uj}, f_{aj}),
- the fault residual sensitivity functions establish the dynamics of a given fault signal regarding a given fault,
- the knowledge of the dynamic properties of the fault residual sensitivity functions allow inferring the theoretical dynamic properties of the fault signals generated by the occurrence of a given fault and as a result, the set of the *theoretical fault signature matrices* ***FSM*** presented *Section 7.3.3* can be inferred in order to be to be used by the fault isolation algorithm, as presented in *Section 7.3* when using the fault isolation architecture given by *Fig. 7.1*.

In *Chapter 3*, the importance of the fault residual sensitivity matrices ($\boldsymbol{S_{fy}}$, $\boldsymbol{S_{fu}}$ and $\boldsymbol{S_{fa}}$) (*Section 3.3*) in the whole fault detection process is demonstrated. This residual property determines both the persistence of the fault indication and the minimum detectable fault function, $\boldsymbol{f}_f^{\min}(k)$, at every time instant. Moreover, *Section 3.3* demonstrates that when using interval observers, the dynamics and the structure of matrices $\boldsymbol{S_{fy}}$ (Eq. (8.17)), $\boldsymbol{S_{fu}}$ (Eq. (8.18)) and $\boldsymbol{S_{fa}}$ (Eq. (8.19)) are set by the observer gain matrix $\boldsymbol{L}$. The influence of $\boldsymbol{L}$ on the fault residual sensitivity matrices is analyzed in detail along *Section 3.3* but briefly, as shown in *Section 3.6*, the influence of $\boldsymbol{L}$ on the dynamics of $\boldsymbol{S_{fy}}$, $\boldsymbol{S_{fu}}$ and $\boldsymbol{S_{fa}}$ can be characterized by the following table:

	Simulation ***L=0***	***Observation*** ***L= L_o***	***Prediction*** ***L= L_p***
$\boldsymbol{S}_{fy}$	Constant	Pulse	Deadbeat
$\boldsymbol{S}_{fu}$	Dynamic response	Dynamic response	Constant
$\boldsymbol{S}_{fa}$	Dynamic response	Dynamic response	Constant

Table 8.1 Observer gain influence on the fault residual sensitivity dynamics

One of the main conclusions of *Chapter 3* is that the performance of the fault detection module may be varied using the observer gain matrix $\boldsymbol{L}$ what may allow enhancing the fault indication result if this matrix is designed properly. The goal of designing $\boldsymbol{L}$ properly is to achieve more reliable fault diagnosis results.

Concerning the fault isolation process, the influence of the fault residual sensitivity matrices on this process was mentioned above derived from Eq. (8.20) but nothing was said regarding the influence of matrix $\boldsymbol{L}$. Thus, taking into account the influence of $\boldsymbol{L}$ on $\boldsymbol{S_{fy}}$, $\boldsymbol{S_{fu}}$ and $\boldsymbol{S_{fa}}$, summarized in *Table 8.1* but analyzed in detail in *Section 3.3*, the following conclusions can be derived from the influence of $\boldsymbol{L}$ on the fault signal set ϕ and therefore, on the fault isolation process:

- Given that the structure of the matrices $\boldsymbol{S_{fy}}$ (Eq. (8.17)), $\boldsymbol{S_{fu}}$ (Eq. (8.18)) and $\boldsymbol{S_{fa}}$ (Eq. (8.19)) sets which residual $r_i(k)$ (fault signal $\phi_i(k)$) is affected by which fault (f_{yj}, f_{uj}, f_{aj}) (Eq. (8.20)) and given that their structure depends on the observer gain matrix $\boldsymbol{L}$, it can be concluded that $\boldsymbol{L}$ may determine the fault signals which are affected by a certain fault and consequently, the structure of the *theoretical fault signature matrices* ***FSM***. As a result, a proper design of matrix $\boldsymbol{L}$ may obtain matrices ***FSM*** whose structure might enhance the fault diagnosis result adding more fault distinguishability.
- Given that the dynamics of matrices $\boldsymbol{S_{fy}}$ (Eq. (8.17)), $\boldsymbol{S_{fu}}$ (Eq. (8.18)) and $\boldsymbol{S_{fa}}$ (Eq. (8.19)) depends on $\boldsymbol{L}$ and given that the dynamics of the fault signals $\phi_i(k)$ depends on these matrices, it can be concluded that the fault signals dynamics may be influenced by matrix $\boldsymbol{L}$ and consequently, a proper design of this matrix may also add more fault distinguishability what can improve the accurateness of the fault isolation algorithm.

All the dynamical aspects related to the fault signals will be analyzed more in detail in the following chapters illustrating how the matrices ***FSM*** can be obtained.

8.3 Fault isolation algorithm

In this section, the fault isolation algorithm presented in *Section 7.3* (*Fig. 7.1*) is used taking into account two main changes:

- This algorithm is integrated with the interval observer-based fault detection approach presented in *Section 8.2.1* and consequently, the four different *theoretical fault signature matrices* (***FSM***01, ***FSM****sign*, ***FSM****sensit* and ***FSM****order*) are obtained using this fault detection approach. Although the theoretical fault signal properties regarding a certain fault hypothesis are still considered in steady-state. It will be in the following chapter where the procedure to obtain the set of matrices ***FSM*** will be illustrated considering all the fault signal dynamical aspects described in *Section 8.2.1*.

- The waiting time T_w is equal to the sample period T_s in order to show clearly the observer gain effect on the fault isolation result.
-

Recalling the general performance of this fault isolation algorithm (*Section 7.3*), the first component between the fault detection and fault isolation modules (*memory component*) is an interface based on a memory that stores along a time window given by T_w and for every residual (fault signal), the time instant ($k_{\phi i}$) in which the fault signal appears ($|\phi_i(k_{\phi i})|\geq 0.5$) and the fault signal value (ϕ_{imax})[1] whose absolute value is maximum. Then, at the end of this time window, an isolation result is given based on the memory stored information and on a *pattern comparison component*. This component compares the observed properties of the observed fault signals $\phi_i(k)$ with the theoretical ones regarding to every fault hypothesis f_j (binary property, sign property, fault residual sensitivity property and occurrence order property) which are stored in the four ***FSM*** matrices (***FSM***01, ***FSM***$sign$, ***FSM***$sensit$ and ***FSM***$order$). Thus, for every fault hypothesis f_j and for every fault property, a factor (***factor***01_j, ***factor***$sign_j$, ***factor***$sensit_j$ and ***factor***$order_j$) is computed determining the occurrence probability of this fault hypothesis regarding the observations of this fault property. At the end, using these factors, the *logic decision component* chooses the best candidate.

This fault isolation algorithm needs the time window T_w in order to avoid fault detection problems as the lack of fault indication persistence (*Section 3.4.2*) and the fact that all fault signals do not appear at the same time since they have different dynamics. This opens a new problem: which is the length of this time window and how can it be calculated? This fault isolation approach is known as *relative fault isolation*. However, in the algorithm version considered in this chapter, there is no memory component and consequently, a fault isolation result is given at every time instant (T_w=T_s): *absolute fault isolation*. As it was already mentioned above, this assumption is done in order to show the effect of the observer gain on the fault isolation result and how these gains might avoid the fault detection problems.
The efficiency of the *absolute* approach relies basically on a proper design of the observer gain matrix in order to avoid the mentioned fault detection problems. On the other hand, the efficiency of the *relative* approach based on *predictors* relies on determining an optimal time window T_w since in this case, residual activation lasts only few time instants as it was already illustrated in *Chapter 3*. Once observed the first fault signal, the length of this time window T_w must be enough so that all the affected fault signals can be observed during at least one time instant, otherwise a wrong isolation result could be set. Conversely, taking into account that fault signal dynamics are ruled by the corresponding residual sensitivity function matrix (*Section 8.2.3*), the T_w dependency regarding to this function can be stated. Besides, when using observers, the observer gain $\boldsymbol{L}$ will also have an influence on this time window since it determines the time evolution of the fault residual sensitivity function (*Section 3.3*).
In fault isolation where normally a subset of fault signals $\phi_i(k)$ must be active at the same time in order to isolate the fault, the lack of fault indication persistence presented by a residual $r_i(k)$ (*Section 3.4.2*) or its associated fault signal $\phi_i(k)$ and the fact that fault signals have different dynamics (*Section 8.2.3*) may confuse the isolation module and consequently, different fault isolation results may appear:

- ***Right persistent fault isolation***: the fault isolation module can isolate the fault and its result lasts while the fault is affecting the system. This is because the associated fault signals can always be observed once the fault appears.
- ***Right non-persistent fault isolation:*** the fault isolation algorithm can precisely isolate the fault during just a certain period of time since either fault signals are not persistently observable or they require different periods of time in order to be observable.
- ***Wrong fault isolation:*** the fault isolation algorithm can not give a right fault isolation result since there are some fault signals which are not observable.
- ***Lack of fault isolation***: this is the case when fault signals are not observable according to the adaptive threshold of the fault detection module.

On the other hand, given that observer gain matrix $\boldsymbol{L}$ affects the dynamics of the fault signals $\phi_i(k)$ (Section 8.2.3), different types of fault isolation result could be obtained varying the observer gain. That means that the observer gain could be designed in order to enhance the fault isolation (*Section 8.2.3*). On the other hand, when using a predictor or simulator model, the observer gain is already fixed and consequently, the fault isolation result can not be enhanced.

8.4 Application example

8.4.1 Application description

This section uses the application example based on 12 limnimeters of the Barcelona urban drainage system which was already explained in *Section 7.4*. However, in this case the limnimeters related to the set $\boldsymbol{L_m}$ (*Section 7.4.3*) are modelled using *interval reduced observers* with uncertain parameters instead of interval predictors. The structure of this interval observer model is derived from Eq. (7.23).

As explained when using interval predictor models (*Section 7.4.3*), the interval observer related to every limnimeter must be calibrated in order to guarantee that its estimated interval output includes all the limnimeter non-modelled effects. Thus, an algorithm inspired by the one proposed in (Ploix et al., 1999) can be used. It is based on the use of classical identification methods, such as the least-squares method, to provide the nominal values of the model parameters. Then, using optimization tools, the uncertain parameter intervals of the considered reduced observer are adjusted using a *worst-case approach* (Puig et al, 2003b) until all the measured data is covered by the interval of prediction for the considered observer gain.

In this setion, a real limnimeter fault scenario is analyzed in order to illustrate that when varying the observer gain, different fault isolation results could be obtained. In particular, for the analyzed case, the fault isolation result will be:

- right persistent fault isolation,
- right non-persistent fault isolation,
- wrong fault isolation,
- and lack of fault isolation.

8.4.2 Fault scenario

The proposed interval observer-based fault diagnosis approach has been tested using a faulty scenario affecting the limnimeter L_{39}. In this fault scenario, the limnimeter output was zero-valued from time instant $k=150$. According to the binary fault signature matrix *FSM*01 shown in *Table 7.1*, this faulty scenario has just an influence on the

residuals associated to limnimeters L_{39} and L_{41} and thus, both must be activated in order to isolate that fault or in other words, the fault signals ϕ_{L39} and ϕ_{L41} must be observed.

The *reduced observer* associated with L_{39} is given by

$$\hat{L}_{39}(k+1) = a_{39}(1-l_{39})\hat{L}_{39}(k) + c_{39}P_1(k) + a_{39}l_{39}L_{39}(k) \tag{8.21}$$

where l_{39} (l_{39}=0, *simulation*; l_{39}=1, *prediction*) is the associated observer gain using the parameterization $k_{39}=l_{39}a_{39}$, P_1 is the rain intensity measured by the rain gauge G_{16} and $a_{39}\in$ [0.496, 0.744], $c_{39}\in$ [0.601, 0.901]. These interval parameter values are valid for the observer gains tested in this section.

Regarding L_{41}, its associated *reduced interval observer* is

$$\hat{L}_{41}(k+1) = a_{41}(1-l_{41})\hat{L}_{41}(k) + b_{41}L_{39}(k) + c_{41}P_2(k) + a_{41}l_{41}L_{41}(k) \tag{8.22}$$

where l_{41} ($k_{41}=l_{41}a_{41}$) is the associated observer gain, P_2 is the rain intensity which is also measured by the rain gauge G_{16} and $a_{41}\in$ [0.869, 1.063], $b_{41}\in$ [-0.296, -0.245], $c_{39}\in$ [0.734, 0.897]. These interval parameter values are valid for the observer gains tested in this section.

First, the observer gains are set so that a *right persistent fault isolation* result can be diagnosed. Then, new observer gain values are given so that the fault almost becomes *non-detectable* (*Section 3.4.2*). Finally, new values are assigned so that the fault isolation result becomes *non-permanent* and *partially wrong*.

8.4.3 Persistent fault isolation case

In this case, the used observer gains are: $\boldsymbol{l_{39}=0.35}$ and $\boldsymbol{l_{41}=0.4}$, the fault isolation algorithm indicates L_{39} as the faulty sensor from the fault occurrence time instant. The observer gains have been chosen so that none of the fault signals $\boldsymbol{\phi_L}$ can be observed in a non-faulty scenario and their values are as low as possible so that the fault does not fully contaminate the observer model estimation. Thus, once the fault has occurred, the fault signals ϕ_{L39} and ϕ_{L41} associated with L_{39} and L_{41} are observed ($|\phi_{L41}|\geq 0.5$ and $|\phi_{L39}|\geq 0.5$) while the fault lasts.

In *Fig. 8.1*, the time evolution of the nominal residuals (r^o_{L39} and r^o_{L41}) and their associated adaptive thresholds are plotted. This figure shows that both r^o_{L39} and r^o_{L41} are out of their associated adaptive thresholds from fault time occurrence ($k=150$) and thus, both of them are indicating persistently that fault (*Section 3.4.2*).

In *Fig. 8.2*, the time evolution of the absolute value of the fault signals ϕ_{L39} and ϕ_{L41} is plotted. Indeed, in order to avoid the noise effect, the diagnosis algorithm does not use the instant values of ϕ_{L39} and ϕ_{L41} but an average of the last values associated with a given time window and this is what is plotted in *Fig. 8.2*. These fault signals indicate the fault while their absolute value is bigger than 0.5 ($|\phi_{L41}|\geq 0.5$ and $|\phi_{L39}|\geq 0.5$) what happens from few time instants once the fault has appeared ($k=150$) till the end of the scenario. Consequently, derived from this figure, the fault is persistently detected by the interval observers related to both limnimeters.

In *Fig. 8.3*, the fault isolation result time evolution is plotted: ***factor**01* (Eq. (7.7)), ***factor**sign* (Eq. (7.14)), ***factor**sensit* (Eq. (7.16)) and ***factor**order* (Eq. (7.18)) related to every fault hypothesis of the set $\boldsymbol{f_{Lm}}$ (*Section 7.4*). In this fault scenario and for the used observer gains, only the fault indicators related to a fault affecting L_{39} are activated and they do persistently from fault occurrence time instant till the end of the scenario. Consequently, the fault is clearly isolated by the interval observers for the applied observer gains.

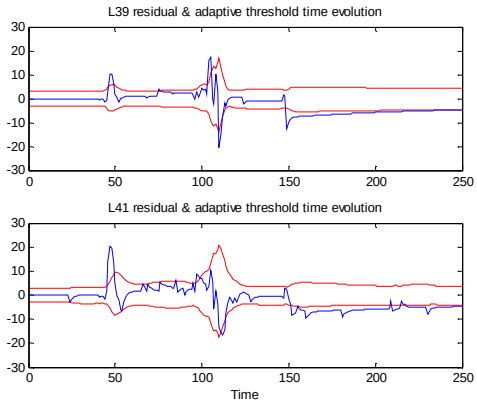

Fig. 8.1.Time evolution of the residuals (m) and their adaptive thresholds (m)

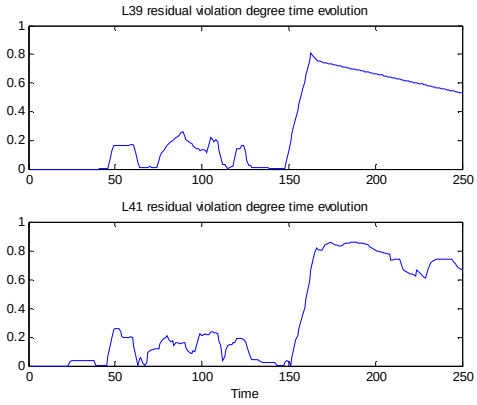

Fig. 8.2 Time evolution of the fault signal absolute values

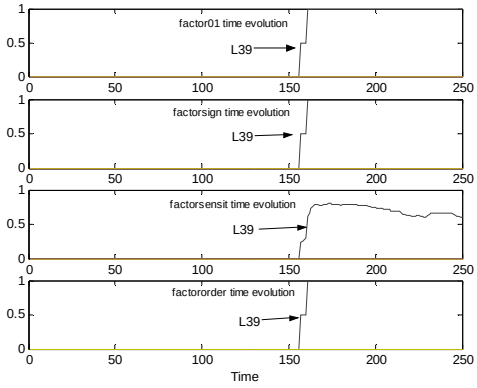

Fig. 8.3 Time evolution of the fault isolation factors

8.4.4 Almost non-fault isolation case

In this case, using the same fault scenario, the isolation algorithm can just isolate the fault for very few time instants because the fault detection does not last longer. This is because the interval observers associated with both limnimeters are using high observer gain (l_{39}***=0.85*** and l_{41}***=0.85***) values and consequently, their performance is quite close to the one related to a *predictor*: the model predicted values are almost fully contaminated by the fault since few time instants once the fault has occurred (*Section 3.3*).

In *Fig. 8.4*, the time evolution of the nominal residuals (r^o_{L39} and r^o_{L41}) and their associated adaptive thresholds are plotted. This figure illustrates that, once the fault has occurred, both r^o_{L39} and r^o_{L41} are into their associated adaptive thresholds for the most of the time instants. Consequently, the fault signals ϕ_{L39} and ϕ_{L41} (*Fig. 8.5*) are hardly observed for very few time instants. As a result, the fault isolation indicators (***factor***01 (Eq. (7.7)), ***factor***sign (Eq. (7.14)), ***factor***sensit (Eq. (7.16)) and ***factor***order (Eq. (7.18))) of L_{39} fault hypothesis, f_{L39}, are hardly activated ($|\phi_{L41}| \geq 0.5$ and $|\phi_{L39}| \geq 0.5$) and therefore, the fault can not be isolated. The time evolution of these indicators is plotted in *Fig. 8.6*.

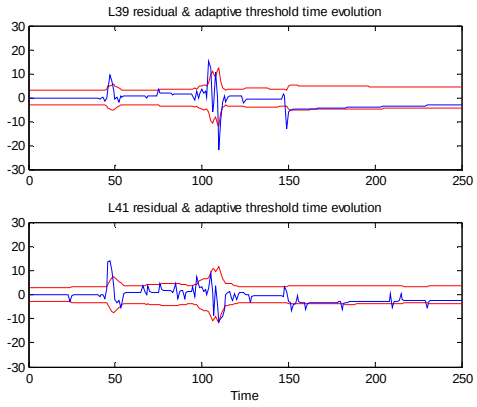

Fig. 8.4 Time evolution of the residuals (m) and their adaptive thresholds (m)

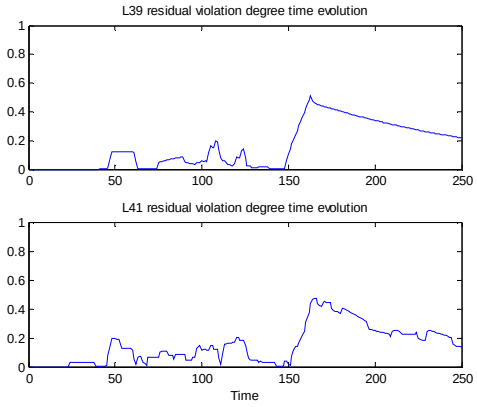

Fig. 8.5 Time evolution of the fault signal absolute values

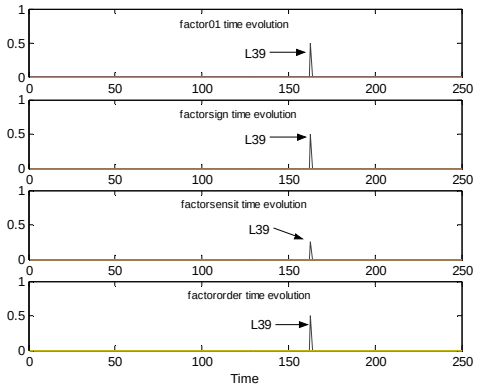

Fig. 8.6 Time evolution of the fault isolation factors

8.4.5 Non-persistent fault indication and partially wrong fault isolation

In this case, using the same fault scenario, the fault is clearly isolated from its occurrence but it is just for a certain time window since ϕ_{L39} is not persistently observed. Then, the isolation algorithm decreases the values of the factor indicators (***factor***01_{fL39}, ***factor***$sign_{fL39}$, ***factor***$sensit_{fL39}$ and ***factor***$order_{fL39}$) associated with the fault hypothesis f_{L39} and on the other hand, it activates the indicators associated with f_{L41}. This fact could lead to a wrong fault isolation result from that time instant. The fault isolation behavior described previously is obtained when L_{39} model uses an observer gain quite similar to the one used in *Section 8.4.4* while the corresponding one to L_{41} is quite similar to the one used in *Section 8.4.4* (***l***$_{39}$***=0.7*** and ***l***$_{41}$***=0.5***).

In *Fig. 8.7*, the time evolution of the nominal residuals (r^o_{L39} and r^o_{L41}) and their associated adaptive thresholds are plotted, while *Fig. 8.8* shows the time evolution of the fault signals ϕ_{L39} and ϕ_{L41} (absolute values). Both figures are in line with the behavior described previously.

Conversely, the time evolution of the fault isolation indicators (***factor***01 (Eq. (7.7)), ***factor***$sign$ (Eq. (7.14)), ***factor***$sensit$ (Eq. (7.16)) and ***factor***$order$ (Eq. (7.18))) associated with fault hypotheses f_{L39} and f_{L41} is plotted. This figure describes how the fault isolation algorithm might be confused between the hypotheses f_{L39} and f_{L41} once fault signal ϕ_{L39} becomes non-observable ($|\phi_{L39}|<0.5$). In spite of this fact, the factor ***factor***$sensit_{fL39}$ continues having a bigger value than ***factor***$sensit_{fL41}$ and consequently, this fault hypothesis might still be the best candidate.

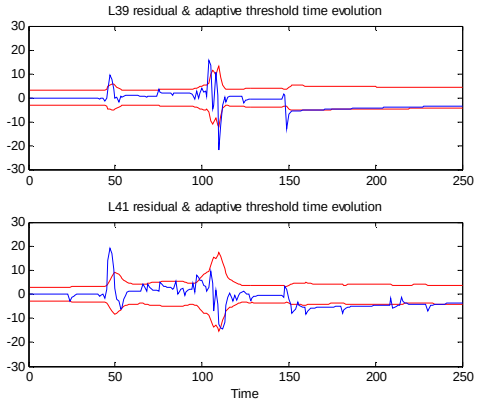

Fig. 8.7 Time evolution of the residuals (m) and their adaptive thresholds (m)

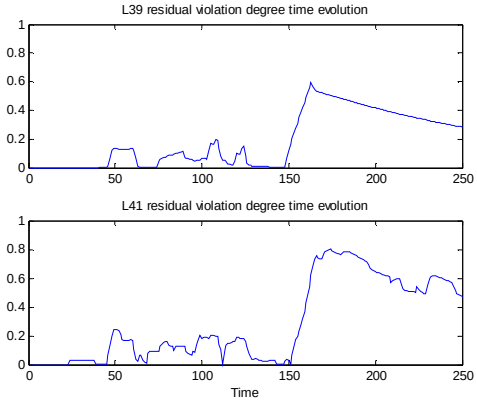

Fig. 8.8 Time evolution of the fault signal absolute values

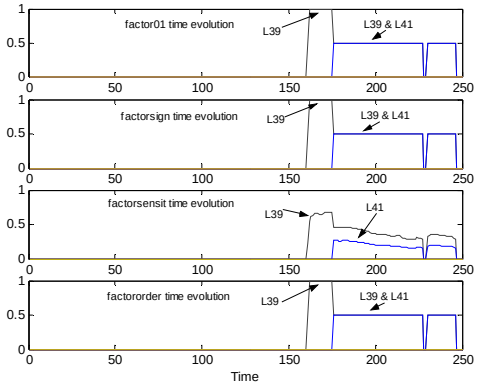

Fig. 8.9 Time evolution of the fault isolation factors

8.5 Conclusions

In general, model-based fault detection methods have inherent problems as the lack of fault indication persistence, noise sensitivity or model errors and as a result, fault detection performance is not as good as it might be needed in order to give a reliable fault diagnosis result. This fact may confuse the fault isolation module and consequently, wrong faults may be diagnosed. According to the points *(d)* and *(e)* of the fault isolation objectives of this thesis (*Section 2.5.2*), *Chapter 8* shows fault isolation results may be very sensitive to the fault indication persistence provided by the fault detection module. It also shows that this lack of persistence can deteriorate the integration between the fault model-based detection module and the fault isolation module and as a consequence, both modules should not be considered separately. Moreover, when using interval observers, the fault indication persistence might be improved designing properly the observer gain matrix. Therefore, the fault isolation results might be also enhanced. Thereby, this chapter describes qualitatively the influence of the observer gain on the fault isolation module.

CHAPTER 9

Fault diagnosis using linear interval observers: obtaining *FSM* matrices

9.1 Introduction

This chapter is based on the interval model-based fault diagnosis method described in *Chapter 8* which improves the integration of fault detection and isolation tasks considering the degree of fault signal activation and using a combination of several *theoretical fault signature matrices* which store the theoretical properties of fault signals when a fault occurs. As mentioned in *Chapter 8*, model-based fault detection methods still have some problems as lack of fault indication persistence, noise sensitivity and model errors (Meseguer et al. 2006a). As a result, fault detection performance can be worse than the required one in order to give a reliable fault diagnosis result. As a consequence, the fault isolation module might be confused when a subset of fault signals must be observed during the same period of time so that the right fault diagnosis result can be derived. However, there is another type of influence of fault detection on the fault isolation module. This influence is derived from the matter that the performance of the fault detection and fault isolation modules depends on the structure of the residual generator, as illustrated along the *Chapter 3* for the fault detection case and in *Section 8.2.3* for the fault isolation case. Consequently, when designing the residual generator to enhance the fault detection result, the fault isolation module is also affected. As a consequence of this integration between both modules, the design of the residual generator structure must be planned to enhance the whole fault diagnosis process and not just one of the both modules. Thereby, in fault diagnosis, fault detection and fault isolation can not be considered separately. Otherwise, the enhancement of the performance of one of the modules might worsen the performance of the other.

On the other hand, as mentioned in *Section 8.2.3*, the structure of the residual generator sets the knowledge the fault isolation module has about faults regarding their influence on the fault signal set what allows obtaining the set of *theoretical fault signature matrices* (***FSM***). In this chapter, the obtaining process of these matrices is illustrated when using a passive robust fault detection approach based on interval observers.

Finally, applying the obtained ***FSM*** matrices, the interval observer-based fault diagnosis algorithm used in *Chapter 8* will be applied to the limnimeters of Barcelona's urban sewer system to assess the validity of the derived results.

Thereby, regarding to the weaknesses of the fault isolation approach used in *Chapter 8,* all of them are improved:

- The time evolution of the dynamical properties of the fault signals is considered.
- The theoretical occurrence time instant of every fault signal is used.
- The waiting time T_w required for the appearance of all fault signals once the fault occurs is obtained.
- The estimation of the system output is obtained using an interval observer with uncertain parameters.

Regarding the structure of the chapter remainder, in *Section 9.2* the influence of fault detection on the fault isolation module is explained more in detail. Then, (*Section 9.3*) a method to obtain the *theoretical fault signature matrices* is

presented describing the influence of the observer gain $\boldsymbol{L}$. *Section 9.4* is focused on how the fault isolation result is obtained and the effect of the observer gain on this stage. Finally, (*Section 9.5*) the application example is used to illustrate the main points described along this chapter.

9.2 Integration between fault detection and fault isolation when using interval observers

One of the main conclusions obtained *Chapter 3* is that the fault detection performance is established by the structure of the residual generator whose *computational form* (Eq. (3.19)) is described in *Section 3.2.2*. Thereby, assessing at every time instant the computed residual interval (Eq. (3.22)) against the fault detection condition (3.24), the fault is indicated or not. On the other hand, the fault residual sensitivity concept introduced in *Section 3.3* and the *internal form* of the residual generator (Eq. (3.20)) presented in *Section 3.2.2* let conclude that the residual generator can be written in terms of the residual sensitivity to an output sensor fault, $\boldsymbol{S_{fy}}$ (Eq. (3.37)), to an input sensor fault, $\boldsymbol{S_{fu}}$ (Eq. (3.47)), and to an actuator, $\boldsymbol{S_{fa}}$ (Eq. (3.54)), such as shown in *Section 3.3.5* and *Section 8.2.3*:

$$\boldsymbol{r}(k,\boldsymbol{\theta}) = \boldsymbol{r}_0(k,\boldsymbol{\theta}) + \boldsymbol{S}_{fa}(q^{-1},\boldsymbol{\theta})\boldsymbol{f}_a(k) + \boldsymbol{S}_{fy}(q^{-1},\boldsymbol{\theta})\boldsymbol{f}_{fy}(k) + \boldsymbol{S}_{fu}(q^{-1},\boldsymbol{\theta})\boldsymbol{f}_{fu}(k) \tag{9.1}$$

This expression shows that the structure of the residual generator is basically determined by the structure of the fault residual sensitivity matrices and consequently, as mentioned along the *Chapter 3*, the performance of the fault detection module depends basically on their structure and dynamics. On the other hand, as derived from the equations of matrices $\boldsymbol{S_{fy}}$, $\boldsymbol{S_{fu}}$ and $\boldsymbol{S_{fa}}$, both their structure and dynamics depends on the observation gain matrix $\boldsymbol{L}$ and this is the reason which let conclude that the whole performance of the fault detection module can be tuned using $\boldsymbol{L}$ (*Chapter 3*).

Concerning fault isolation, *Section 8.2.3* sets the importance of matrices $\boldsymbol{S_{fy}}$, $\boldsymbol{S_{fu}}$ and $\boldsymbol{S_{fa}}$ on the fault isolation module derived also from the residual generator structure expressed in its *internal form* (Eq. (9.1)). Mainly, as described in that section, this importance is because the structure and dynamics of matrices $\boldsymbol{S_{fy}}$, $\boldsymbol{S_{fu}}$ and $\boldsymbol{S_{fa}}$ determine the residuals $r_i(k)$ (fault signals $\phi_i(k)$) affected by a certain fault (f_{yj}, f_{uj}, f_{aj}) and the dynamics of the observed fault signals when the fault occurs. As a consequence, according to the definition of the *theoretical fault signature matrix* $\boldsymbol{FSM}$ (*Section 7.3.3*), the knowledge of matrices $\boldsymbol{S_{fy}}$, $\boldsymbol{S_{fu}}$ and $\boldsymbol{S_{fa}}$ will allow building up the set of matrices $\boldsymbol{FSM}$ used by the fault isolation algorithm. Moreover, as demonstrated in detail in *Section 3.3* and summarized by *Table 8.1*, each fault residual sensitivity matrix ($\boldsymbol{S_{fy}}$, $\boldsymbol{S_{fu}}$ and $\boldsymbol{S_{fa}}$) related to a certain type of fault (f_{yj}, f_{uj}, f_{aj}) has its own dynamical properties what implies that the fault signal subset caused by this type of fault has also different dynamical properties regarding the fault signal subset caused by another fault type. Then, if matrices $\boldsymbol{S_{fy}}$, $\boldsymbol{S_{fu}}$ and $\boldsymbol{S_{fa}}$ are known, more fault distinguishability is added to the fault isolation algorithm allowing to enhance its performance, as it will be seen in the following section. In conclusion, the fault residual sensitivity matrices ($\boldsymbol{S_{fy}}$, $\boldsymbol{S_{fu}}$ and $\boldsymbol{S_{fa}}$) play also a crucial role in the performance of the fault isolation module. In addition, because the dependence of this matrices regarding the observer gain $\boldsymbol{L}$ (*Section 3.3*), it can be concluded that the performance of the fault isolation module may also be tuned using the observer gain.

Therefore, the fault residual sensitivity matrices ($\boldsymbol{S_{fy}}$, $\boldsymbol{S_{fu}}$ and $\boldsymbol{S_{fa}}$) play significant role both in fault detection and in fault isolation setting the performance of the whole fault diagnosis process. Conversely, when using interval observers, the observer gain $\boldsymbol{L}$ may allow tuning the behaviour of this process enhancing the final result. Derived from these statements, it can be affirmed that fault detection and fault isolation are closely integrated throw the matrices $\boldsymbol{S_{fy}}$, $\boldsymbol{S_{fu}}$ and $\boldsymbol{S_{fa}}$ and consequently, these matrices should be designed taking into account the whole fault

diagnosis process and not just one of its modules (fault detection or fault isolation). Otherwise, when enhancing just one module, the other could be affected negatively.

9.3 Fault detection and isolation interface: *FSM* matrices

In *Section 7.3* (*Chapter 7*) and in *Section 8.3* (*Chapter 8*), the interface between fault detection and fault isolation was illustrated. On the one hand, this interface consist in a *memory component* (*Section 7.3.2*) which registers for every observed fault signal ($|\phi_i(k)| \geq 0.5$) its occurrence time instant ($k_{\phi i}$) and its value ϕ_{imax}[1] whose absolute value is maximum. Then, on the other hand, this interface considers also the theoretical influence on the fault signal set $\boldsymbol{\phi}$ of every fault f_j belonging to the set $\boldsymbol{f}$ of faults which wanted to be isolated. As mentioned in *Section 7.3* and in *Section 8.3*, this theoretical influence is stored in four different *theoretical fault signature matrices*, ***FSM***, applying a method that is an extension of the proposed by (Gertler, 1998) in which just the fault signal binary property was considered. Thus, as described in these sections, the four matrices are: the *binary fault signal activation matrix* (***FSM***01), the *fault signal sign matrix* (***FSM****sign*), the *fault residual sensitivity matrix* (***FSM****sensit*), and the *fault signal occurrence order matrix* (***FSM****order*). As described, the structure of those matrices is set by the following: the element $\boldsymbol{FSM}_{ij}$ of one of these matrices contains the expected influence of fault f_j on the nominal residual $r_i^0(k)$ (Eq. (7.1)) related to the fault signal $\phi_i(k)$ (Eq.(7.5)). Then, the *comparison component* (*Section 7.3.3*) of the fault isolation algorithm determines for every fault signal property a occurrence probability ($\boldsymbol{factor}01_j$, $\boldsymbol{factor}sign_j$, $\boldsymbol{factor}sensit_j$ and $\boldsymbol{factor}order_j$) for every fault hypothesis f_j applying the fault signal observed and theoretical properties registered by the fault detection and isolation interface.

In this section, a new important fault signal property will be introduced. This is the *fault signal occurrence time instant* is introduced. Its theoretical value related to a fault signal $\phi_i(k)$ and to a fault hypothesis f_j will be stored in the element of the i^{th}-file and j^{th}-column of the matrix ***FSM****time*. The following subsections illustrate how to obtain matrices ***FSM****sensit* and ***FSM****time* and how they are affected by the observer gain matrix $\boldsymbol{L}$ taking into account that, as mentioned in *Section 9.2*, these matrices can be derived from the fault residual sensitivity matrices ($\boldsymbol{S_{fy}}$, $\boldsymbol{S_{fu}}$ and $\boldsymbol{S_{fa}}$). Moreover, it will be illustrated how the other matrices can be derived from them.

Regarding the fault isolation algorithm used in *Chapter 8*, this approach is also used in this chapter but improving its weaknesses. Thereby, the time evolution of the dynamical properties of the fault signals is considered, the theoretical occurrence time instant of every fault signal is used and the waiting time T_w required for the appearance of all fault signals once the fault occurs will be obtained using ***FSM****time*.

Finally, it must be taken into account that the influence of a fault affecting the output sensor y_i on its associated residual r_i is registered in the diagonal element $\boldsymbol{FSM_{ii}}$ of the corresponding *theoretical fault signature matrix*.

9.3.1 ***FSM****sensit*: fault sensitivity matrix

The fault residual sensitivity matrix $\boldsymbol{S_f}$ sets the residual capacity to detect faults (Gertler, 1998) and as described in *Section 9.2*, its importance in the whole fault diagnosis process is crucial. In *Section 7.3.3.3*, matrix ***FSM****sensit,* was defined as a matrix whose element $\boldsymbol{FSM}sensit_{ij}$ establish how easily a fault f_j will cause the i^{th}-residual $r_i^o(k)$ to violate its associated adaptive threshold. However, although *Section 3.3* determines this property has a time evolution

and is influenced by the observer gain matrix $\boldsymbol{L}$, the values of every element $\boldsymbol{FSM}sensit_{ij}$ were obtained considering the steady-state value of the residual sensitivity to a fault. Thus, in this section $\boldsymbol{FSM}sensit$ is obtained considering the time evolution of the property. Thereby, the following equation describes how to compute the entries $\boldsymbol{FSM}sensit_{ij}$

$$\boldsymbol{FSM}sensit_{ij} = \begin{cases} \dfrac{S_{f_{i,j}}(q^{-1})\eta(k-t_0)}{\left|\overline{r}_i^{\,o}(k)\right|} & if \quad r_i^o(k) \geq 0 \text{ and } k \geq t_0 \\ \dfrac{S_{f_{i,j}}(q^{-1})\eta(k-t_0)}{\left|\underline{r}_i^{\,o}(k)\right|} & if \quad r_i^o(k) < 0 \text{ and } k \geq t_0 \\ 0 \quad if \quad k < t_0 \text{ or } S_{f_{i,j}}(q^{-1}) = 0 \end{cases} \tag{9.2}$$

where $\eta(k)$ is an unitary abrupt step input, $S_{f_{i,j}}(q^{-1})$ is the sensitivity associated with the nominal residual $r_i^o(k)$ regarding the fault hypothesis f_j (f_{yj}, f_{uj}, f_{aj}) and t_0 is the fault occurrence time instant. When t_0 is unknown, it must be estimated using the occurrence time instant $k_{\phi i}$ of the first observed fault signal $\phi_i(k)$. As consequence of the fault residual sensitivity time dependency, $\boldsymbol{FSM}sensit_{ij}$ evolves dynamically since the fault occurrence time instant t_0. This function is corrected using the detection threshold as the bigger it is, the more difficult fault signals will be observed, according to Eq. (8.15).

9.3.1.1 Influence of fault residual sensitivity matrix S_f on *FSMsensit*

Focusing on the properties of fault residual sensitivity matrices ($\boldsymbol{S_{fy}}$, $\boldsymbol{S_{fu}}$ and $\boldsymbol{S_{fa}}$) described in detail *Section 3.3* and on the structure of the matrix $\boldsymbol{FSM}sensit$ (Eq. (9.2)), in general, the next information may be derived concerning the fault isolation stage:

- if an abrupt output sensor fault f_{yj} is detected, it must be from time instant t_0 since the residual sensitivity to this output sensor fault regarding its associated residual $r_j(k)$ ($r_j(k) = y_j(k) - \hat{y}_j(k)$), ($S_{f_{j,j}}(q^{-1})$) (Eq. (3.43)), is maximum at fault occurrence time instant (*Section 3.3.2*) causing the observation of the fault signal $\phi_j(k)$. Therefore, when an abrupt output sensor fault occurs, the fault occurrence time instant t_0 is always known since it is equal to the occurrence time instant $k_{\phi i}$ of the first observed fault signal. Conversely, regarding the sensitivity of the other residuals $r_i(k)$ ($S_{f_{i,j}}(q^{-1})$) to this fault f_{yj}, it is zero-valued (Eq. (3.40)) at fault occurrence time instant, t_0, and consequently, the corresponding fault signals $\phi_i(k)$ ($i \neq j$) are not observed yet
- the residual sensitivity to an input sensor fault f_{uj} (Eq. (3.48)) (assuming $\boldsymbol{D} \approx \boldsymbol{0}$) and to an actuator fault f_{aj} (Eq. (3.56)) are null at t_0 (*Section 3.3.3* and *Section 3.3.4*) and consequently, these faults can not be detected at this time instant and they associated fault signals will not be observed either.

9.3.1.2 Deriving FSM01 and FSMsign from FSMsensit

According to *Section 7.3.3.1*, the $\boldsymbol{FSM}$01-table contains the theoretical binary influence that faults f_j produce in the residual equations $r_i(k)$ which can be codified using the values 0 for no influence, 1 otherwise. This matrix can be obtained such as the theoretical fault signature matrix $\boldsymbol{FSM}$ introduced by (Gertler, 1998) (*Section 7.3.3.1*) but besides, it can be derived from the matrix $\boldsymbol{FSM}sensit$ (Eq. (9.2)) described in the previous section. Thereby, its expression is

$$\boldsymbol{FSM}01_{ij} = \begin{cases} 1, & \boldsymbol{FSM}\text{sensit}_{ij} \neq 0 \\ 0, & \boldsymbol{FSM}\text{sensit}_{ij} = 0 \end{cases} \tag{9.3}$$

Concerning ***FSMsign***-table, this matrix contains the theoretical sign patterns (*Section 7.3.3.2*) faults f_j produce in the residual equations $r^0{}_i(k)$. As described by *Section 7.3.3.2*, those patterns can be codified using the values 0 for no influence, +1/-1 for positive/negative deviation for every $\boldsymbol{FSMsign}_{ij}$. Concerning the value of $\boldsymbol{FSMsign}_{ij}$, according to the residual internal form (Eq. (8.20)) and the definition given in *Section 7.3.3.2*, the fault residual sensitivity sets the sign pattern a given fault f_j produces in a given residual $r^0{}_i(k)$. Thereby, the element $\boldsymbol{FSMsign}_{ij}$ related to the fault signal $\phi_i(k)$ (nominal residual $r_i^o(k)$) and the fault hypothesis f_j (f_{yj}, f_{uj}, f_{aj}) can be derived from matrix ***FSMsensit*** (Eq.(9.2)) as it follows:

$$\boldsymbol{FSM}\text{sign}_{ij} = \begin{cases} 0 & \text{if} \quad k < t_0 \text{ or } \boldsymbol{FSMsensit}_{ij} = 0 \\ sign(\boldsymbol{FSMsensit}_{ij}) & \text{if } k \geq t_0 \text{ and } \boldsymbol{FSMsensit}_{ij} \neq 0 \end{cases} \tag{9.4}$$

On the other hand, the observed signs associated with every observed fault signal $\phi_i(k)$ will be obtained as it follows:

$$sign(\phi_i(k)) = \begin{cases} 0 & \text{if} \quad |\phi_i(k)| < 0.5 \\ 1 & \text{if} \quad \phi_i(k) \geq 0.5 \\ -1 & \text{if} \quad \phi_i(k) \leq -0.5 \end{cases} \tag{9.5}$$

9.3.2 ***FSMtime***: fault signal occurrence time matrix

When a fault f_j (f_{yj}, f_{uj}, f_{aj}) occurs, the affected residuals $r^0{}_i(k)$ need different periods of time to start indicating that fault or equivalently, the fault signals $\phi_i(k)$ require different periods of time to appear. Each element of the j^{th} -column of the matrix ***FSMtime*** contains the time interval $[\underline{\varphi}_{ij}, \overline{\varphi}_{ij}]$ in which the fault signal $\phi_i(k)$ is expected to appear. The value $\overline{\varphi}_{ij}$ is associated to the minimum f_j-type fault which is considered to be isolated, while $\underline{\varphi}_{ij}$ is associated with the maximum f_j-type fault the monitored system might suffer. Thus, the values $\underline{\varphi}_{ij}$ for a given fault f_j could be estimated carrying out a test for every residual which compares the residual disturbance (Eq. (3.64)) (*Section 3.4.1*) caused by a fault in the nominal residual $r_i^o(k)$ with the adaptive threshold given by Eq. (8.13). Derived from fault detection test given by Eq. (8.15) and from the residual internal form (Eq. (8.20)), this test can be written as:

$$S_{f_{i,j}}(q^{-1}) f_j^*(k) q^{-t_0} \notin [\underline{r}_i^o(k), \overline{r}_i^o(k)] \quad k \geq t_0 \tag{9.6}$$

where $f_j^*(k)$ is the worst case of a f_j-type fault the monitored system might suffer. Then, the time the residual requires to start indicating the fault ($\underline{\delta}_{ij}$) is obtained using the minimum time instant k_{min} that satisfies Eq. (9.6).

$$\underline{\delta}_{ij} = k_{\min} - t_0 \tag{9.7}$$

When monitoring a system, the fault occurrence time instant t_0 is unknown in general. Hence, the values $\underline{\delta}_{ij}$ associated with the fault hypothesis f_j must be referred to the first observed fault signal. Then,

$$\underline{\varphi}_{ij} = \underline{\delta}_{ij} - \min_{\forall i}(\underline{\delta}_{ij}) \tag{9.8}$$

The value $\overline{\varphi}_{ij}$ might also be calculated using test (9.6) but in this case, $f_j^*(k)$ must be the minimum f_j-type fault

which is considered to be isolated. Thus, the values $\overline{\delta}_{ij}$ are obtained and then,

$$\overline{\varphi}_{ij} = \overline{\delta}_{ij} - \min_{\forall i}(\underline{\delta}_{ij}) \tag{9.9}$$

Regarding the elements of matrix ***FSM**time*,

$$\boldsymbol{FSM}time_{ij} = \begin{cases} [\underline{\varphi}_{ij}, \overline{\varphi}_{ij}] & if \quad S_{f_{i,j}}(q^{-1}) \neq 0 \\ [-1,-1] & if \quad S_{f_{i,j}}(q^{-1}) = 0 \end{cases} \tag{9.10}$$

it is remarkable the influence of the observer gain $\boldsymbol{L}$ on the interval $[\underline{\varphi}_{ij}, \overline{\varphi}_{ij}]$ derived from its influence on the fault residual sensitivity matrices ($\boldsymbol{S_{fy}}$, $\boldsymbol{S_{fu}}$ and $\boldsymbol{S_{fa}}$) (*Section 3.3*) and consequently, a proper design of $\boldsymbol{L}$ might help so that all the fault signals were observed at the same time instant.

Derived from ***FSM**time*, one of the most important parameters of the fault isolation algorithm can be obtained. This is the time window T_w which determines the maximum period of time required once the first fault signal is observed so that all fault signals can appear. In other words, T_w is the period of time needed, once the first fault signal is detected, to give an accurate fault diagnosis result unless there were only one fault hypothesis left supporting the observed fault signal temporal sequence before T_w would have ended. Thereby, T_w can be obtained as it follows:

$$T_w = \max_{\forall i,j}(\overline{\varphi}_{ij}) \tag{9.11}$$

On the other hand, in order to compare the occurrence time instant of the observed fault signal sequence with the stored one in matrix ***FSM**time,* the factor ***factor**time*$_j$ is calculated for every fault hypothesis as it follows:

$$\boldsymbol{factor}time_j(k) = \frac{\sum_{i=1}^{ny}\left(ckecktime\left(k_{\phi i}, k_{ref}, \boldsymbol{FSM}time_{ij}\right)\right)}{\sum_{i=1}^{ny} boolean(\boldsymbol{FSM}time_{ij})} \boldsymbol{zvf}_j \tag{9.12}$$

where $k_{\phi i}$ is the apparition time instant of the fault signal $\phi_i(k)$, k_{ref} is the apparition time instant of the first observed fault signal,

$$ckecktime\left(k_{\phi i}, k_{ref}, \boldsymbol{FSM}time_{ij}\right) = \begin{cases} 0 \quad if \quad k_{\phi i} - k_{ref} \notin \boldsymbol{FSM}time_{ij} \text{ or } |\phi_i(k)| < 0.5 \\ 1 \quad if \quad k_{\phi i} - k_{ref} \in \boldsymbol{FSM}time_{ij} \text{ and } |\phi_i(k)| \geq 0.5 \end{cases} \tag{9.13}$$

$$boolean(\boldsymbol{FSM}time_{ij}) = \begin{cases} 0, & \text{if } \boldsymbol{FSM}time_{ij} = [-1,-1] \\ 1, & \text{if } \boldsymbol{FSM}time_{ij} \neq [-1,-1] \end{cases} \tag{9.14}$$

and where $\boldsymbol{zvf_j}$ is the zero-violation-factor (Eq. (7.9)) (*Section 7.3.3.1*) whose expression is

$$\boldsymbol{zvf}_j = \begin{cases} 0, & \text{if } \exists\ i \in \{1,...,n\} \text{ with } \boldsymbol{FSM}01_{ij} = 0 \\ & \qquad\qquad \text{and } |\phi_i(k)| \geq 0.5 \\ 1, & \text{otherwise} \end{cases} \tag{9.15}$$

9.3.2.1 Influence of fault residual sensitivity matrix S_f on *FSMtime*

When applying all the fault isolation particulars described in *Section 9.3.1.1* regarding the influence of the properties of matrices ($\boldsymbol{S_{fy}}$, $\boldsymbol{S_{fu}}$ and $\boldsymbol{S_{fa}}$) (*Section 3.3*) on matrix ***FSM**sensit*, a simplification can be done concerning the expression of ***FSM**time*. Mainly, these particulars are:

- Assumption of abrupt output sensor fault f_{yi}. Then, at fault occurrence time instant t_0, the residual related to sensor $y_i(k)$ ($r_i(k) = y_i(k) - \hat{y}_i(k)$) is the only residual which has the capacity to indicate the fault causing the observation of the fault signal $\phi_i(k)$.
- Input sensor faults f_{uj} (assuming $\boldsymbol{D \approx 0}$) and actuator faults f_{aj} are not indicated by none residual at fault occurrence time instant t_0.
- As already mentioned, regarding the structure of the *theoretical fault signature matrices*, ***FSM***, it is assumed that the influence of a fault affecting the output sensor y_i on its associated residual r_i is registered in the diagonal element $\boldsymbol{FSM_{ii}}$ of the corresponding *theoretical fault signature matrix*.

As a consequence of all these particulars, the elements of matrix ***FSMtime*** can be expressed as it follows:

$$\boldsymbol{FSMtime}_{ij} = \begin{cases} [0,0] & \text{if} \quad i = j \\ [\underline{\varphi}_{ij}, \overline{\varphi}_{ij}] & \text{if} \quad i \neq j \text{ and } S_{f_{i,j}}(q^{-1}) \neq 0 \\ [-1,-1] & \text{if} \quad S_{f_{i,j}}(q^{-1}) = 0 \end{cases} \tag{9.16}$$

9.3.2.2 Deriving FSMorder from *FSMtime*

According to Section 7.3.3.4 where matrix ***FSM****order* was introduced, this matrix contains the observation order of the fault signals caused for every fault hypothesis. Thereby, the elements of this matrix for a f_j-type fault can be obtained from ***FSM****time* as

$$\boldsymbol{FSMorder}_{ij} = \begin{cases} \sigma & \text{where} \quad \boldsymbol{\delta}_j(\sigma) = \underline{\varphi}_{ij} \\ & \text{and } \boldsymbol{FSMtime}_{ij} \neq [-1,-1] \\ 0 & \text{if} \quad \boldsymbol{FSMtime}_{ij} = [-1,-1] \end{cases} \tag{9.17}$$

where $\boldsymbol{\delta_j}$ is a vector that contains the non-repeated elements $\underline{\varphi}_{ij}$ of the j^{th} -column of ***FSM****time* ordered ascendant and whose values are not equal to *-1*.

When considering the fault isolation particulars described in *Section 9.3.2*.1, the elements of matrix ***FSM****order* satisfies the following relation according to the expression of the elements ***FSM****time* given by Eq. (9.16),:

$$\boldsymbol{FSMorder}_{ij} = \begin{cases} 1 & \text{if} \quad i = j \\ \sigma > 1 & \text{if} \quad i \neq j \text{ and } \boldsymbol{FSMtime}_{ij} \neq [-1,-1] \\ 0 & \text{if} \quad \boldsymbol{FSMtime}_{ij} = [-1,-1] \end{cases} \tag{9.18}$$

assuming the model associated to each system output is not static. Thus, when considering just abrupt output sensor faults, the first observed fault signal will allow isolating the faulty sensor according to Eq (9.18).

9.4 Diagnosis result: Logic decision

As shown in the proposed fault isolation architecture (*Fig. 7.1*), the last task of the considered diagnosis algorithm is the *decision logic component* (*Section 7.3.4*). At the end of the time window T_w, this component gives a fault diagnosis result based on the occurrence probability d_j related to every fault hypothesis f_j calculated using one of the proposals given in *Section 7.3.4* and all the factors related to f_j: $\boldsymbol{factor}01_j$, $\boldsymbol{factor}sign_j$, $\boldsymbol{factor}sensit_j$, $\boldsymbol{factor}order_j$, $\boldsymbol{factor}time_j$. This result indicates the most probable fault which is affecting to the considered system.

As illustrated in *Section 9.3*, matrices ***FSM****01*, ***FSM****sign* and ***FSM****order* may be derived from ***FSM****time* and ***FSM****sensit*. Consequently, another proposal to obtain the occurrence probability d_j related to every fault hypothesis f_j

would be using just $\boldsymbol{factor}sensit_j$ and $\boldsymbol{factor}time_j$. Concerning $\boldsymbol{factor}order_j$, it is not always accurate to consider that its significance can be obviated since the observation order property of a fault signal is related to a set of fault signals while the occurrence time instant property is just related to one fault signal, for a given f_j. Thereby, d_j may be calculated using these two new possible alternatives:

- the highest factor

$$d_{j,} = \max\left(\boldsymbol{factor}sensit_j, \boldsymbol{factor}order_j, \boldsymbol{factor}time_j\right) \tag{9.19}$$

- or weighting these factors according to its significance in the fault diagnosis process

$$d_{j,} = \left(\alpha_1 \boldsymbol{factor}sensit_j + \alpha_2 \boldsymbol{factor}order_j + \alpha_3 \boldsymbol{factor}time_j\right) \tag{9.20}$$

where α_1 , α_2, $\alpha_3 \in [0,1]$ are the weighing parameters proposed by fault diagnosis designer.

In these new proposals, $\boldsymbol{factor}order_j$ and $\boldsymbol{factor}time_j$ play a significant role on the final result as this factors are very robust regarding the non-persistence fault indication given by the fault detection module while $\boldsymbol{factor}sensit_j$ is not so robust. On the other hand, if the fault diagnosis result might be very influenced by the model errors, all three factors should be used since $\boldsymbol{factor}order_j$ and $\boldsymbol{factor}time_j$ might be inaccurate.

Finally, regarding the influence of the observation gain matrix $\boldsymbol{L}$, *Section 9.2* describes the key influence of the fault residual sensitivity matrices ($\boldsymbol{S_{fy}}$, $\boldsymbol{S_{fu}}$ and $\boldsymbol{S_{fa}}$) on the whole fault diagnosis process (*fault detection* and *fault isolation module*). As recalled in this section and demonstrated in detail in *Section 3.3*, the dynamics and structure of these matrices is set by $\boldsymbol{L}$ and consequently, so do the dynamics and structure of the *theoretical fault signature matrices* $\boldsymbol{FSM}time$ and $\boldsymbol{FSM}sensit$. As a consequence, the result given by the *decision logic component* may also be influenced by the applied design of matrix $\boldsymbol{L}$

9.5 Case of study: Barcelona urban drainage system

9.5.1 Fault isolation scenario description

This section uses the application example of 12 limnimeters of the Barcelona urban drainage system which was already described in *Section 7.4* and in *Section 8.4* where a set $\boldsymbol{L_m}$ of limnimeters are modelled using *interval reduced observers* with *uncertain parameters*. However, unlike *Section 7.4* and *Section 8.4*, the measurements of the limnimeters and the rain-gauges will not be obtained from real data but from a simulator of the Barcelona urban drainage system. Thereby, some unknown effects of the measurements can be avoided in order to focus this analysis on the effect of the observer gain $\boldsymbol{L}$ on the fault isolation result.

In this *Chapter 9*, only the fault signal set ϕ_{L03} and ϕ_{L27} associated with the limnimeters L_{03} and L_{27} will be considered to illustrate the results and conclusions described in previous sections of this chapter. According to the theoretical binary fault signature matrix $\boldsymbol{FSM}01$ given by *Table 7.1* (*Chapter 7*), this fault signal set allow diagnosing faults affecting to the limnimeters L_{03} and L_{27}, f_{L03} and f_{L27} and is composed by two residuals, one for each limnimeter. Thus, the expressions of the interval reduced observers used to monitor L_{03} and L_{27} are given by

$$\hat{L}_{03}(k+1) = a_{03}(1-l_{03})\hat{L}_{03}(k) + b_{03}L_{27}(k) + c_{03}P_{07}(k) + a_{03}l_{03}L_{03}(k) \tag{9.21}$$

$$\hat{L}_{27}(k+1) = a_{27}(1-l_{27})\hat{L}_{27}(k) + c_{27}P_{05}(k) + a_{27}l_{27}L_{27}(k) \tag{9.22}$$

where l_{03} and l_{27} are the associated observer gains using the parameterizations $k_{03}=l_{03}a_{03}$ and $k_{27}=l_{27}a_{27}$. P_{07} and P_{05} are the rain intensities measured by the rain gauges G_{14} and G_{20}, respectively. Conversely, the model parameters are obtained using parameter estimation from experimental data considering that the following intervals describes the possible values of each parameter: $a_{03}\in[0.8816,\ 0.9084]$, $b_{03}\in[0.0381,\ 0.0393]$, $c_{03}\in[1.4469e4,\ 1.4910e4]$,

$a_{27} \in [0.9544, 0.9737]$ and $c_{27} \in [6.2641e3, 6.3907e3]$. These interval parameter values are valid for the observer gains tested in this section.

The nominal residual associated to limnimeter L_{03} using the observer (9.21) is given by

$$r_{03}^{o}(k) = \frac{1 - a_{03}^{o} q^{-1}}{1 + a_{03}^{o}(l_{03}^{o} - 1) q^{-1}} L_{03}(k) - \frac{b_{03}^{o} q^{-1}}{1 + a_{03}^{o}(l_{03}^{o} - 1) q^{-1}} L_{27}(k) - \frac{c_{03}^{o} q^{-1}}{1 + a_{03}^{o}(l_{03}^{o} - 1) q^{-1}} P_{07}(k) \tag{9.23}$$

According to the fault residual sensitivity concept presented in *Section 3.3* and in *Section 8.2.3*, the sensitivity of this residual to an additive fault in L_{03} ($\boldsymbol{F}_{y}(\boldsymbol{\theta})=\boldsymbol{I}$) is

$$S_{03}^{o}(q^{-1}) = \frac{1 - a_{03}^{o} q^{-1}}{1 + a_{03}^{o}(l_{03}^{o} - 1) q^{-1}} \tag{9.24}$$

which satisfies that when an additive abrupt fault affecting L_{03} occurs, the fault signal ϕ_{L03} is observed from the fault occurrence time instant t_0 if the fault is detected (*Section 9.3.1.1*). On the other hand, in case of an additive fault affecting L_{27} ($\boldsymbol{F}_{u}(\boldsymbol{\theta})=\boldsymbol{I}$), the sensitivity of the residual associated to the limnimeter L_{03} is

$$S_{03-27}^{o}(q^{-1}) = - \frac{c_{03}^{o} q^{-1}}{1 + a_{03}^{o}(l_{03}^{o} - 1) q^{-1}} \tag{9.25}$$

According to *Section 9.3.1.1*, fault signal ϕ_{L27} is never observed at t_0 as its fault residual sensitivity is null at this time instant.

Analogously, in case of the limnimeter L_{27}, its nominal residual is

$$r_{27}^{o}(k) = \frac{1 - a_{27}^{o} q^{-1}}{1 + a_{27}^{o}(l_{27}^{o} - 1) q^{-1}} L_{27}(k) - \frac{c_{27}^{o} q^{-1}}{1 + a_{27}^{o}(l_{27}^{o} - 1) q^{-1}} P_{05}(k) \tag{9.26}$$

Thus, the sensitivity of this residual to an additive fault affecting L_{27} is

$$S_{27}^{o}(q^{-1}) = \frac{1 - a_{27}^{o} q^{-1}}{1 + a_{27}^{o}(l_{27}^{o} - 1) q^{-1}} \tag{9.27}$$

while its sensitivity to an additive fault affecting L_{03} is

$$S_{27-03}^{o}(q^{-1}) = 0 \tag{9.28}$$

Such as for the fault signal ϕ_{L03} case, the residual sensitivity given by Eq. (9.27) shows that the fault signal ϕ_{L27} is observed from the occurrence time instant t_0 if the fault is detected and assuming a abrupt fault scenario.

9.5.2 ***FSM*** matrices

In this section, considering the fault isolation scenario described in *Section 9.5.1*, the value of the *theoretical fault signature matrices* (***FSM***01, ***FSM****sign*, ***FSM****sensit*, ***FSM****order* and ***FSM****time*) is obtained and analyzed.

9.5.2.1 FSMsensit, FSM01 and FSMsign

Considering the residual generator associated with limnimeters L_{03} and L_{27} (Eq. (9.21) and Eq.(9.22)), the corresponding matrices ***FSM****sensit,* ***FSM****01* and ***FSM****sign* are analyzed in this section.

In the proposed fault isolation algorithm, the fault residual sensitivity pattern $\boldsymbol{FSM}sensit_{ij}$ is calculated dynamically at every time instant once a fault is detected (Eq. (9.2)). The fact of considering the residual sensitivity as a time function instead of a steady-state value really matters in the fault diagnosis result as, for instance, the residual sensitivity to an abrupt output sensor fault may be maximum at t_0 while it is null if the fault affects an input sensor

(*Section 9.3.1.1*). On the other hand, the observer gains have an influence on the elements of ***FSMsensit*** which might help to differentiate the effect a fault produces in the fault signal set (*Section 9.3.1*). Concerning the case of study and according to Eq. (9.2), the elements of this matrix are given by *Table 9.1* when $k \geq t_0$ and $r_{03}{}^0$, $r_{27}{}^0$ are positive.

	f_{L03}	f_{L27}
ϕ_{L03}	$\frac{S_{03}^0(q^{-1})\eta(k-t_0)}{\left\|\overline{r}_{03}^o(k)\right\|}$	$\frac{S_{03-27}^0(q^{-1})\eta(k-t_0)}{\left\|\overline{r}_{03}^o(k)\right\|}$
ϕ_{L27}	0	$\frac{S_{27}^0(q^{-1})\eta(k-t_0)}{\left\|\overline{r}_{27}^o(k)\right\|}$

Table 9.1 ***FSMsensit*** Matrix

Regarding matrices ***FSM01*** and ***FSMsign***, they are derived from ***FSMsensit*** according to Eq. (9.3) and Eq. (9.4), respectively. Then, in line with *Table 9.1*, their values in this study case are given by *Table 9.2* and *9.3*.

	f_{L03}	f_{L27}
ϕ_{L03}	1	1
ϕ_{L27}	0	1

Table 9.2 ***FSM01*** Matrix

	f_{L03}	f_{L27}
ϕ_{L03}	1	-1
ϕ_{L27}	0	1

Table 9.3 ***FSMsign*** Matrix

9.5.2.2 FSMtime and FSMorder

In this section, considering residual generator associated with limnimeters L_{03} and L_{27} (Eq. (9.21) and Eq.(9.22)), the matrices corresponding *FSMtime* and *FSMorder* are analyzed.

In this case, the expression (9.16) can be used to calculate the ***FSMtime*** matrix elements (*Section 9.3.2.1*). Thus, all elements of this matrix are determined except for the element $\boldsymbol{FSMtime}_{12}$ which is calculated dynamically when the first fault signal is observed. When test (9.6) is carried out, a simplification is done regarding the considered adaptive threshold ($[\underline{r}_i^o(k), \overline{r}_i^o(k)]$): a constant adaptive threshold is used whose value is given by the worst-case regarding the detection of the fault. This is

$$[-\tau_i, \tau_i] \tag{9.29}$$

where $\tau_i = \max\left\{\max_{\forall k \geq t_0}\left(abs\left(\underline{r}_i^o(k)\right)\right), \max_{\forall k \geq t_0}\left(abs\left(\overline{r}_i^o(k)\right)\right)\right\}$

where *abs* is the absolute value function.

The worst sensor fault of type f_j is assumed to be an abrupt step whose gain $f_j^{\max}$ is equal to the maximum estimated value of all sensors affected by this type of fault. The minimum fault of type f_j which is considered to be isolated is assumed to be an abrupt step whose gain $f_j^{\min}$ is derived from the minimum detectable fault functions (*Section 3.4*) of type f_j associated with each residual. This gain is calculated as it follows:

$$f_j^{\min} = \max_{\forall i} \left\{ abs(f_{i,j}^{\min}) \right\} \tag{9.30}$$

where $f_{i,j}^{\min}$ is the steady-state value of the minimum detectable fault of type f_j regarding the i^{th} -residual considering its associated threshold is given by the Eq. (9.29).

$$f_{i,j}^{\min} = \frac{\tau_i}{s_{f_{i,j}}(\infty)} \tag{9.31}$$

where $s_{f_{i,j}}(\infty)$ is the steady-state value of the fault residual sensitivity functions shown in *Section 9.5.1*.

In the following, the values in seconds of the ***FSM**time* matrix associated with residuals (9.23) (ϕ_{L03}) and (9.26) (ϕ_{L27}) are shown for two specific scenarios: *Scenario 1* (*Table 9.4*) where t_0***=4000 s*** (Sampling Time T_s*=300 s*), $l_{03}^o = 0.01$, $l_{27}^o = 0.01$ and ***Scenario 2*** *(Table 9.5)* where t_0***=4000 s*** , $l_{03}^o = 0.01$, $l_{27}^o = 0.5$

	f_{L03}	f_{L27}
ϕ_{L03}	[0,0]	[900, 6300]
ϕ_{L27}	[-1,-1]	[0,0]

Table 9.4 ***FSM**time* Matrix

	f_{L03}	f_{L27}
ϕ_{L03}	[0,0]	[900, 3900]
ϕ_{L27}	[-1,-1]	[0,0]

Table 9.5 ***FSM**time* Matrix

These tables confirm the influence of the observer gain on matrix ***FSM**time*.

Concerning ***FSM**order*, the expression (9.18) can be applied (*Section 9.3.2.1*) according to the considered fault scenario. Thus, the elements of the ***FSM**order* matrix are fully determined independently of the observer gain.

	f_{L03}	f_{L27}
ϕ_{L03}	1	2
ϕ_{L27}	0	1

Table 9.6 ***FSM**order* Matrix

9.5.3 Fault scenarios

In this section, considering the residual generator associated with the limnimeters L_{03} and L_{27} (Eq. (9.21) and Eq.(9.22)), the time evolution of the residuals and the fault isolation factors (***factor***$sensit_j$ and ***factor***$time_j$) are plotted considering the two scenarios introduced in the last section when a constant additive fault appears at time instant t_0=*4000 s* affecting L_{27}. The value of this fault is equal to the minimum isolable fault according to the *Scenario 1* f_{L27}=*0.5566 m*. The difference between these scenarios is only the values of the observer gains in order to show their influence and the importance of ***factor***$time_j$ when the result given by ***factor***$sensit_j$ is confusing. In those fault scenarios, the factors are calculated at every time instant k (T_w=*300 s* corresponding to one sample since T_s=*300 s*) since then, the effect of the observer gains on them can be seen more clearly. Besides, a third scenario is considered which is like *Scenario 2* but where the right value of T_w is used according to *Table 9.5* and Eq. (9.11).

Scenario 1: t_0=4000 s, T_w=300 s, $l_{03}^o = 0.01$ ***and*** $l_{27}^o = 0.01$

In this fault scenario, the fault is clearly detected and isolated as illustrated by the time evolution of the residuals (*Fig. 9.1*) and by the time evolution of the fault isolation factors (*Fig. 9.2*).

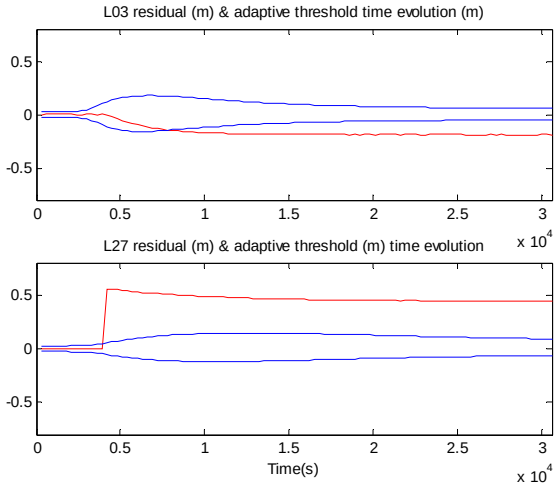

Fig. 9.1 Time evolution of the residuals and their adaptive thresholds in scenario 1.

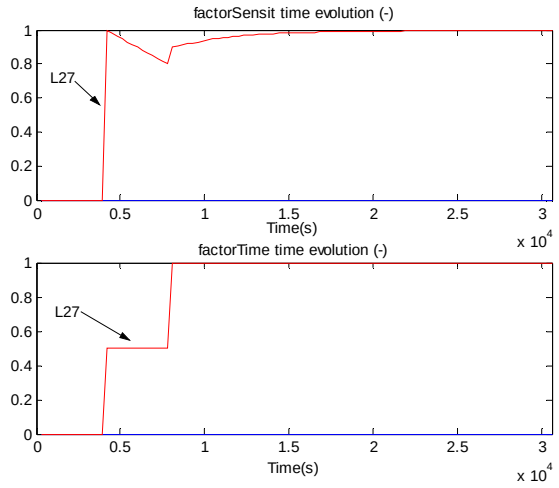

Fig. 9.2 Time evolution of the fault isolation factors in scenario 1.

It can be noticed from *Fig. 9.1* that the fault is detected at its occurrence time instant by the residual associated with L_{27}, as expected according to its fault sensitivity function (Eq. (9.27)) while the residual related to L_{03} does not detect it till later such as it was also expected according to its fault sensitivity (Eq. (9.25)) and the values of matrix ***FSM****time* (*Table 9.4*). Finally, it should be taken into account that while only one fault signal is observed (ϕ_{L27}), only ***factor****sensit*$_{L27}$ reaches its maximum value as the residual sensitivity of L_{03} is nearly zero-valued when fault appears. This is because the dynamics of the residual sensitivity functions has been taken into account when computing matrix ***FSM****sensit*.

Scenario 2: t_0=4000 s, T_w=300 s, $l_{03}^o = 0.01$ ***and*** $l_{27}^o = 0.5$

In this scenario once the fault occurs, it is only clearly indicated by the residual associated with L_{27} during few time instants (*Fig. 9.3*). Concerning the other residual, the fault is detected such as it was in the *Scenario 1*. This inaccurate behaviour of the fault detection module causes ***factor****sensit*$_j$ to be also inaccurate regarding the fault isolation result (*Fig. 9.4*). Conversely, because the observed fault signal occurrence time instants satisfy the theoretical values stored in matrix ***FSM****time*, the factor ***factor****time*$_j$ is not affected by this lack of fault indication and it let clearly isolate the fault.

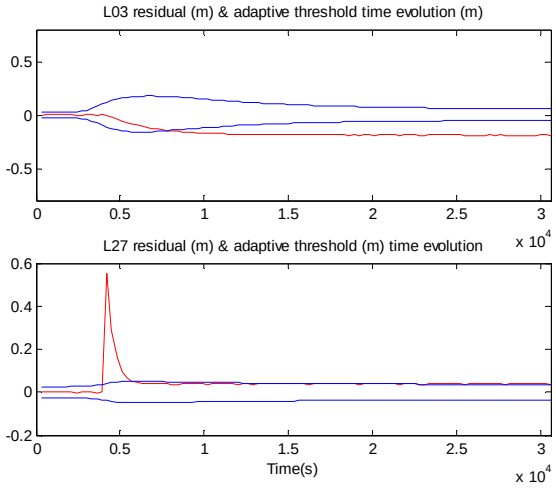

Fig. 9.3 Time evolution of the residuals and their adaptive thresholds, scenarios 2 and 3.

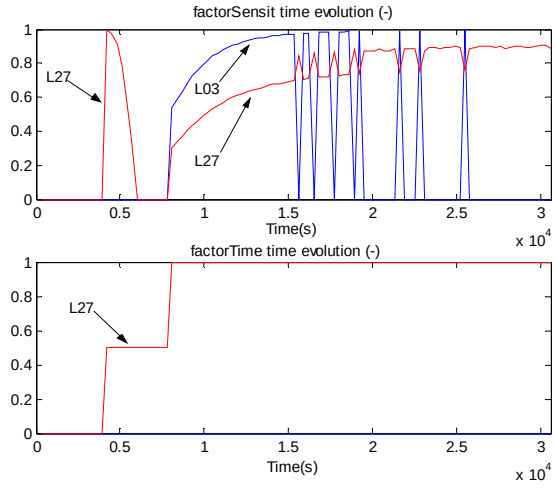

Fig. 9.4 Time evolution of the fault isolation factors in scenario 2.

Scenario 3: t_0=4000 s, T_w=3900 s, $l_{03}^o = 0.01$ ***and*** $l_{27}^o = 0.5$

Unlike *Scenario 2*, in this scenario the right value of the time window T_w, according to Eq. (9.11) is used: T_w=*3900 s*. This value assures that once the first fault signal is observed (ϕ_{L27} at t_0=*4000 s*: see *Fig. 9.3*), the rest of the fault signals (ϕ_{L03}) will have been observed, at least, during few time instants, at the end of this time window ($t=t_0+T_w$=*7900s*). Then, the first diagnosis result is given which already let isolate clearly the fault (*Fig. 9.5*). This result is kept constant till the end of the next time window.

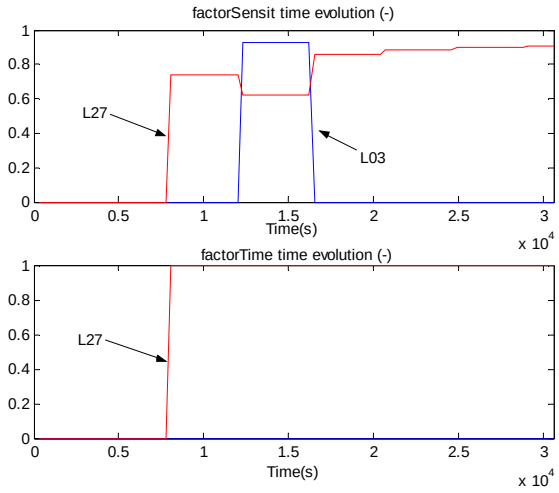

Fig. 5.19. Time evolution of the fault isolation factors in scenario 3.

9.6 Conclusions

Fault isolation is influenced by fault detection as both of them use the residual generator as a key element. This element allows the fault isolation algorithm to know the expected properties of the fault signal set when a fault hypothesis occurs. In consequence, the theoretical fault signature matrices can be obtained analyzing the effect of faults on the residual generator and taking into account that this effect is set by the dynamics and structure of the fault residual sensitivity matrices. Moreover, because the residual generator depends on the observer gain $\boldsymbol{L}$, the influence of this matrix on the fault isolation module is also concluded. This influence allow to add more fault distinguishability designing properly the theoretical fault signature matrices using the observation gain matrix. This fact is unrelated to the type of fault, in spite this chapter is focusing more in sensor faults due to the use application example.

This chapter follows the trend in FDI to analyze the influence of the detection stage in the isolation results (Combastel et. al 2003). The main contribution is the method provided for on-line computation of the ***FSM*** including temporal information about the evolution of the fault signals –*i.e.* fault signal values -, which can be used to support or reject fault modes in the isolation stage. Moreover, related to recent works in BRIDGE, the interval model-based observer ,which is used to estimate the system behaviour for detection purposes, provides a different way to cope with uncertainty in model parameters: modal intervals (Armengol et al. 2001), or different techniques for envelope generation (Loiez et al. 1998;Rinner et al., 2004). Finally, from a pure DX perspective, this work can be seen as an initial step towards on-line calculation of temporal fault signal evolution as needed in diagnosis chronicles (Cordier et al. 2000).

CHAPTER 10

Fault diagnosis using a timed discrete-event approach based on interval observers

10.1 Introduction

In model-based fault diagnosis applied to dynamic processes (systems), it is possible to distinguish between models applied to fault detection (*Section 2.3*) and models used for fault isolation (or system state recognition) (*Section 2.4*) (Kościelny et al. 2004a). Models used for fault detection (either, in the ***DX community*** or in the ***FDI community***) describe relationships existing between the system inputs and outputs (using *qualitative* or *quantitative* approaches), and allow detecting inconsistencies caused by faults generating fault diagnostic signals (fault signals). Typically, inconsistencies are detected by computing a residual signal as the difference between the real and the modelled system behaviour. More precisely, a fault signal appears when the residual evaluation stage associated with the fault detection task concludes that the residual time evolution is caused by the effect of a fault (Chow et al., 1984). Thus, although the fault signal is characterized by a given dynamics, it can be considered as a discrete event caused by the fault effect on the monitored system. The goal of the fault detection model is to generate fault signals so that the fault can be isolated. The type of the model used in fault detection (*qualitative* or *quantitative*), in general, depends on the system knowledge and the effort required to obtain an accurate model. If an accurate analytical model can be obtained using a reasonable effort, this type of models seems to be a better choice than the qualitative models. Otherwise, qualitative models seem to be better in fault detection.

On the other hand, models used for fault isolation (*qualitative* or *analytical*) define the relationship existing between observed fault signals and faults. The basic idea of a fault diagnosis system is that the occurrence of a fault will generate a unique sequence of observable fault signals (*events*) that will establish the presence of a given fault. In general, the model type (*qualitative* or *quantitative*) used in fault isolation depends on the type of the fault detection model. However, since a fault signal can be seen as a *discrete-time event* with a given occurrence time instant, dynamics and duration, the use of those qualitative models known as *timed discrete events models* (Lunze et al. 2005) follows naturally. In this sense, (Daigle et al, 2007) uses a ***temporal labelled transition system*** which is built on the grounds of a ***temporal causal graph*** that models the behaviour of the monitored systems. Conversely, ***temporal dynamic table of states*** (***T-DTS) method*** (Kościelny et al., 2004c) models the relationship between fault signals and faults using the called ***Fault Information System (FIS)***. The fault isolation algorithm used by this method is based on series inference where the occurrence of a new fault signal let narrow the possible fault hypotheses checking its observed properties and the information stored in the ***FIS***. However, this kind of models is not very common when fault detection stage is modeled using an analytical model (at least in the ***FDI community***).

In this chapter, the proposed fault diagnosis approach will combine a fault isolation *qualitative timed discrete event model* with the fault detection analytical model based on interval observers presented in *Section 3.2* (*Chapter 3*) and recalled in *Section 7.2* (*Chapter 7*). This chapter follows forward the work developed in *Chapter 7*, *Chapter 8* and

Chapter 9. Recalling this line of research, *Chapter 7* demonstrates that the typical binary interface proposed by (Gertler, 1998) between fault detection and fault isolation can lead to inaccurate fault isolation results and shows that fault isolation performance can be enhanced when other fault signal properties are considered: the fault signal sign, its static fault residual sensitivity, the fault signal occurrence order and the fault signal occurrence time instant. In *Chapter 8*, the interface presented in *Chapter 7* is used and the monitored system is modelled using an interval observer model. This last section characterizes the influence of the fault detection stage on the fault isolation result. As a result, this chapter illustrates that observation gain matrix may be designed to enhance the fault detection and isolation results. *Chapter 9* continues the work developed in both previous sections showing that the relationship between faults and the fault signal dynamical properties can be obtained analytically using the residual generator structure related to the monitored system interval observer. This chapter demonstrates the crucial importance of the fault residual sensitivity matrices in the whole fault diagnosis process and the importance of considering the fault signal dynamics.

The aim of this chapter is to propose a fault diagnosis method using a *timed discrete-event approach* based on interval observers which improves the integration of fault detection and isolation tasks. The proposed method can be considered as a ***BRIDGE approach*** that tries to benefit from the best of the *FDI* and *DX* diagnosis communities. Thereby, in this approach, fault signals are represented as a temporal sequence of discrete events using a qualitative approach while fault detection is based on the analytical model represented by an interval observer described in *Section 8.2*. In this way, it will be shown that all available and useful information of the fault detection and isolation tasks is considered. The interface between fault detection and fault isolation is based on the presented one in *Section 9.3*. Thereby, the diagnosis result will be enhanced since the occurrence of a fault generates a unique sequence of observable events (fault signals) that will be recognized by the isolation module implemented as a timed discrete event system. The states and transitions that characterize such a system can be inferred directly from the relation between fault signals and faults. The proposed fault diagnosis approach is applied to detect and isolate faults of the Barcelona's urban sewer system limnimeters (level meter sensors).

Regarding the proposed fault diagnosis process, this chapter focuses just on the fault isolation module since both the fault detection module and the interface between fault detection and fault isolation were already illustrated in *Chapter 8* and *Chapter 9*, respectively. In consequence, concerning the structure of the remainder, in the next section, an overview of the proposed approach is presented in order to point out its motivation. Then, in *Section 10.3,* the fault isolation algorithm based on a *timed discrete event system* is shown. Then, in *Section 10.4*, the interval observer-based fault diagnosis algorithm will be applied to the limnimeters of Barcelona's urban sewer system to assess the validity of the derived results.

10.2 Overview of the proposed approach

10.2.1 Motivation

As described in *Section 6.2*, model-based fault diagnosis is based on a certain set of n numerical fault indicators, known as *residuals* $\boldsymbol{r}(k)$ which connect the measured inputs $\boldsymbol{u}(k)$ and the measured outputs $\boldsymbol{y}(k)$ of the monitored system:

$$\boldsymbol{r}(k) = \boldsymbol{\Psi}(\boldsymbol{y}(k), \boldsymbol{u}(k)) \tag{10.1}$$

where $\boldsymbol{\Psi}$ is the residual generator function that allows computing the residual set at every time instant using the measurements of the system inputs and outputs. Ideally, according to (Gertler, 1998), this function is a residual generator if the computational form of the residual set, which can also be expressed as a set of analytical redundancy relations (*ARR*),is null when no fault is affecting the system (*Section 2.3.2.1*).

According to (Gertler, 1998), the fault detection task consists in deciding if there is a fault affecting the monitored system by checking each residual $r_i(k)$ of the residual set against a threshold τ_i that takes into account model uncertainty, noise and the unknown disturbances. The result of this test applied to every residual $r_i(k)$ produces an *observed fault signature* $\phi(k)$ (observed fault signal set): $\boldsymbol{\phi}(k) = \left[\phi_1(k), \phi_2(k), \cdots, \phi_{n_\phi}(k)\right]$. As mentioned in *Section 6.2* and *Section 2.4.2.1*, a basic way of obtaining these observed fault signals could be throw a binary evaluation of every residual $r_i(k)$ against a certain threshold τ_i (Gertler, 1998):

$$\phi_i(k) = \begin{cases} 0 & \text{if} \quad |r_i(k)| \le \tau_i \\ 1 & \text{if} \quad |r_i(k)| > \tau_i \end{cases} \tag{10.2}$$

The observed fault signature is, then, supplied to the fault isolation module that will try to isolate the fault so that a fault diagnosis result can be given. This module is able to produce such a fault diagnosis since it has the knowledge about the binary relation between the considered fault hypothesis set $\boldsymbol{f}(k) = \left\{f(k)_1, f_2(k), \cdots, f_{n_f}(k)\right\}$ and the fault signal set $\phi(k)$. This relation is stored in the called *theoretical binary fault signature matrix* (***FSM***) described in *Section 2.4.1.1* and *Section 6.2.1*. In short, an element FSM_{ij} of this matrix is equal to 1 if the fault hypothesis $f_j(k)$ is expected to affect the residual $r_i(k)$ such that the related fault signal $\phi_i(k)$ is equal to 1 when this fault is affecting to the monitored system. Otherwise, the element FSM_{ij} is zero-valued.

However, as mentioned along *Chapter 6* and *Chapter 7*, this basic fault detection an isolation scheme has the following drawbacks, among others:

(a) The threshold τ_i should be determined and adapted on-line according to the system inputs and outputs taking into account the model uncertainty.

(b) The presence of the noise produces chattering when using the binary evaluation of the residual.

(c) All fault signals $\phi_i(k)$ affected by a certain fault $f_j(k)$ according to the structure of the matrix ***FSM*** should be activated at the same time instant and they should be persistently observed during the whole fault isolation process. Otherwise, a wrong fault diagnosis result could be given. Nonetheless, because fault signals have their own dynamics, neither they necessarily have to be activated at the same time nor they are persistently observed.

(d) Restricting the relation between faults and fault signals to a binary one causes a loss of useful information that can add fault distinguishability and accurateness to the fault isolation algorithm preventing possible wrong fault diagnosis results. The occurrence of a fault causes the apparition of a certain subset of fault signals such that each of them have characteristic dynamical properties for this fault which can improve the performance of the fault isolation algorithm if they are taken into account.

Some of these problems should be considered by the fault detection module (for example, (a) and (b)), while the others by the fault isolation module (for example, (c) and (d)), or by the interface between both stages.

10.2.2 Proposed approach

As described briefly in *Section 2.5.4* of *Chapter 2*, *Chapter 10* proposes a new fault diagnosis approach which tries to take into account the problems indicated previously by using the architecture presented in *Fig. 10.1*.

This architecture consists in the following modules:

- ***Fault detection module*** which generates fault signals measuring the system inputs and outputs taking into account model uncertainty. This module is carried out using the *passive robust fault detection method* based on *intervals observers* as presented in *Chapter 3* and *Chapter 8*. This approach allows computing an adaptive threshold that evolves along time (*drawback (a)*) which is applied to evaluate robustly the consistency between the available measurements and the set of considered residuals. Concerning the chattering effect produced by the presence of noise when evaluating the residual using a binary approach (*drawback (b)*), this problem has been faced using the fault signal generation method based on the Kramer function described in *Section 7.2.2*.
- ***Fault detection/isolation interface module*** which evaluates fault signals generated by the fault detection module in order to register their dynamical properties. This will allow the fault isolation module to isolate the fault among the considered fault hypotheses. These properties are summarized using several indicators which take into account not only the activation value of the fault signal but also its fault sensitivity/sign and its occurrence time instant/order. This proposed interface module is described in *Chapter 9* and tries to handle the problems (*drawback (d)*) associated with the fault signal persistence, the residual sensitivity to a fault, the fault signal occurrence order and the fault signal occurrence time instant. As a result, the interface between fault detection and fault isolation modules is improved enhancing the performance of the used fault diagnosis system,
- ***Fault isolation module*** reasons with the information used to build all the indicators provided by the improved fault detection and isolation interface using a *discrete-event fault diagnosis model* that can be automatically built from the analytical redundancy relations obtained from the monitored system model equations and the system available measurements. This approach is based on the issue that the occurrence of a fault will generate a unique temporal sequence of fault signals whose dynamical properties allow isolating the fault. This method tries to tackle the *drawback (c)* and apart from new components which will be presented in this chapter, uses the *memory component* and some parts of the *comparison component* of the fault isolation architecture presented in *Fig. 7.1* and described in *Section 7.3*.

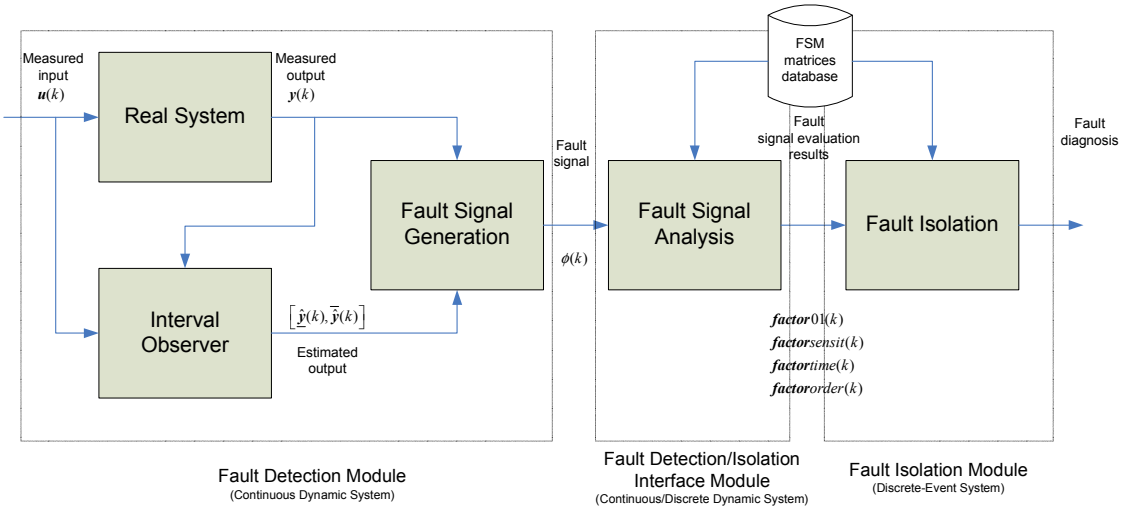

Fig. 10.1 Block diagram of the fault diagnosis system

10.3 Fault isolation module

10.3.1 Fault isolation algorithm as a ***DES***

The fault isolation module and the interface between fault detection and fault isolation can be formalized as a *discrete event system* (*DES*)[17] since a given fault affecting to the monitored system will cause a unique sequence of fault signals (*events*) whose dynamical properties should allow obtaining a fault diagnosis result. Taking into account temporal aspects in the sequence of fault signals (order and time instant of occurrence), a *timed discrete event model* (*TDES*) will allow modeling more accurately the fault isolation process from the occurrence of the first fault signal of the temporal sequence until a fault isolation result is given. A *timed discrete event model* of this type is known as a *timed labeled transition model* (*TLTS*) (Daigle et al., 2007). Using this modeling approach, the fault signals would be the events, the states would be given by all the fault hypotheses supporting the observed fault signal sequence and the transitions would be set by the comparison between the theoretical and the observed dynamical properties of the fault signals.

10.3.2 Fault isolation and interface module components

10.3.2.1 Description

Figure 10.2 presents the components of the fault isolation and interface modules which are an evolution of the fault isolation architecture proposed in *Fig. 7.1* (*Chapter 7*). As mentioned in *Section 10.3.1*, the main idea of this new fault isolation approach is based on the fact that a given fault affecting to the monitored system will cause a unique temporal sequence of fault signals what will allow obtaining a diagnosis result comparing the dynamical properties of the observed fault signals with the ones stored for each fault hypothesis in the *theoretical fault signature matrices*, ***FSM*** (*Section 9.3*).

[17] Fault isolation methods built using a *DES* consist in a set of states connected by transitions (Sampath *et al*, 1996). The transitions are related to events generated by the fault effect on the monitored system, while the states indicate a certain situation of the whole fault isolation process. Moreover, when these transitions are built taking into account some temporal aspects, the *discrete event model* (***DES***) is known as a *timed discrete event model* (***TDES***) (Chen et al, 1997).

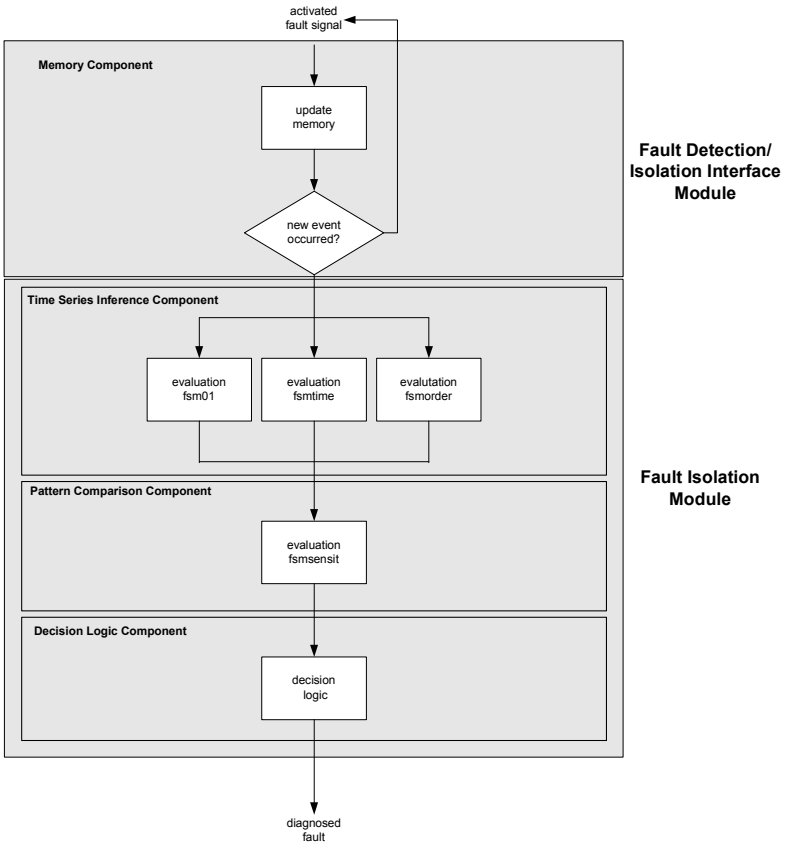

Fig. 10.2 Components related to the interface and fault isolation modules

The fault isolation algorithm starts with the occurrence of the first fault signal ($|\phi_i(k)|\geq 0.5$) and ends when there is only one fault hypothesis supporting the observed temporal sequence of fault signals or when the diagnosis time window T_w (Eq. (9.11)) (*Section 9.3.2*) has ended. Thereby, the first element of this algorithm is a ***memory component*** which registers some information of the observed fault signals, such as described in *Section 7.3.2*. The second element is a ***timed series inference component*** which compares the stored information of a new observed fault signal with the information stored in matrices ***FSM**01*, ***FSM**time*, and ***FSM**order* for those non-rejected fault hypotheses. The result of this series inference component is the rejection of those fault hypotheses that do not support the observations. When there is only one fault hypothesis left, the algorithm ends giving that hypothesis as the fault diagnostic result. Otherwise, when the time window T_w has ended, the third element, the ***pattern comparison component***, computes ***factor**sensit*$_j$ for those non-rejected fault hypotheses. Then, the last element, the ***logic decision component***, gives as a diagnostic result the fault with the biggest absolute value of the factor ***factor**sensit*$_j$.

Concerning the ***timed series inference component***, this is a new component regarding the architecture presented in *Fig. 7.1* and tries to take benefit from the event nature of fault signals and from the fact that a fault affecting the system will generate a unique temporal sequence of fault signals. In the following section, more detailed explanation of the performance of this component will be given. Finally, regarding the ***pattern comparison*** and ***logic decision components***, they work as described in *Section 7.3* using the architecture shown in *Fig. 7.1*. However, in the new architecture described by *Fig. 10.2*, these components are restricted to the fault residual sensitivity property since the binary, the fault occurrence time instant and the occurrence order properties are checked by the ***timed series***

inference component. This approach assumes that the fault signal sign property is already set by the fault residual sensitivity property, as mentioned in *Section 9.3.1.2*.

10.3.2.2 Timed series inference component

The ***timed series inference component*** is based on the fact that each new fault signal allows rejecting those hypotheses that do not support the observations and in consequence, a diagnosis result can be given before the time window T_w (Eq. (9.11)) (*Section 9.3.2*) ends. Thereby, the rejection of a certain fault hypothesis when a new fault signal is observed is based on the comparison between the information related to this fault signal which is stored in the *memory component* and the theoretical properties of this fault signal for this fault hypothesis, which are stored in the matrices ***FSM****01*, ***FSM****time*, and ***FSM****order*. In consequence, the observation of a new fault signal will allow narrowing the subset of fault hypotheses which are still supporting the observations and consequently, the ones which are still candidates to set the diagnosis result. When there is just one fault hypothesis left, the reasoning process ends giving this hypothesis as diagnosis result. Otherwise, the process ends once the period of time T_w has elapsed since the observation of the first fault signal.

This component can be built using a *timed labelled transition system* (Daigle et al., 2007) where the initial state is the non-faulty state, then, each fault hypotheses (set $\boldsymbol{f}$) have a *TLTS* representation which are connected to this initial state. The *TLTS* representation associated with a given fault hypothesis shows the fault signal temporal sequence caused by this fault. In each state transition, the properties of the new observed fault signal are compared with those stored in ***FSM****01*, ***FSM****order* and/or ***FSM****time* for this fault hypothesis. The present state of a fault hypothesis *TLTS* representation just indicates that this fault hypothesis is still supporting the observed fault signal temporal sequence. When a new fault signal occurs, for each non-rejected fault hypotheses, the state transition starting in the present state is evaluated. If this evaluation fails, the fault hypothesis is rejected. At the end of the diagnosis time window T_w, those non-rejected fault hypotheses will establish the final fault diagnosis result.

According to the definition given by (Daigle et al., 2007), a *TLTS* can be seen as the following tuple

$$\mathcal{T}_j=(Q_j,q_0,\boldsymbol{\Sigma}_j,\boldsymbol{\delta}_j) \tag{10.3}$$

where Q_j is the set of states, q_0 is the initial state, $\boldsymbol{\Sigma}_j$ is the set of labels and $\boldsymbol{\delta}_j$ is the set of transitions. Thus, when applying this *TLTS* definition to model the presented *timed series inference component,* there will be a tuple $\mathcal{T}_j$ related to every fault hypothesis f_j that belongs to the set $\boldsymbol{f}$ of all the considered fault hypotheses. All these set of elements $\mathcal{T}_j$ will just have one element in common: the state q_0 related to the non-faulty state. Regarding the states $Q_{pj} \in Q_j$, its number n_{Qj} is set by the number of fault signals $\phi_i(k)$ affected by the fault hypothesis f_j. This is

$$n_{Qj} = \sum_{i=1}^{ny} \boldsymbol{FSM}01_{ij} \tag{10.4}$$

The present state Q_{pj} of $\mathcal{T}_j$ just have the meaning that the fault hypothesis f_j is still supporting the observations.

Regarding the transitions $\boldsymbol{\delta}_{pj}$ of the set $\boldsymbol{\delta}_j$, they connect $Q_{(p-1)j}$ with Q_{pj} being q_0 , the first state. Thus, there will be for a certain $\mathcal{T}_j$, a transition for every fault signal related to the fault hypothesis f_j: this is $n_{Qj.}$ In this way, the transition $\boldsymbol{\delta}_{pj}$ will be related to the fault signal $\phi_i(k)$ whose theoretical occurrence order for this fault hypothesis is given by *'p'* (***FSM****order*$_{ij}$=*p*). Thereby, concerning the sequence of transitions and states in $\mathcal{T}_j$, they have an ascendant order set by $p = 1,\ldots, n_{Qj}$.

About the labels Σ_{pj} of the set Σ_j, there is one for each transition δ_{pj} and consequently, for each fault signal $\phi_i(k)$ related to the fault hypothesis f_j. Thereby, the evaluation of all the labels Σ_{pj} is carried out when the p^{th} -fault signal $\phi_i(k)$ is observed. If the evaluation of Σ_{pj} fails, the fault hypothesis f_j is rejected. Otherwise, the state Q_{pj} becomes the present state of $\mathcal{T}_j$. Thereby, Σ_{pj} is carried out evaluating the following relation

$$\sum_{pj} = \left(ckeckorder\left(\phi_i(k), \boldsymbol{FSM}order_{ij}\right)\right) \text{and} \left(ckecktime\left(k_{\phi i}, k_{ref}, \boldsymbol{FSM}time_{ij}\right)\right) \tag{10.5}$$

where the functions *checkorder* and *checktime* are given by Eq. (7.19) and Eq.(9.13), respectively.

According to the mentioned previously, a diagram of the set of elements $\mathcal{T}_j$ which models the performance of this *timed series inference component* is presented in *Fig.10 3*.

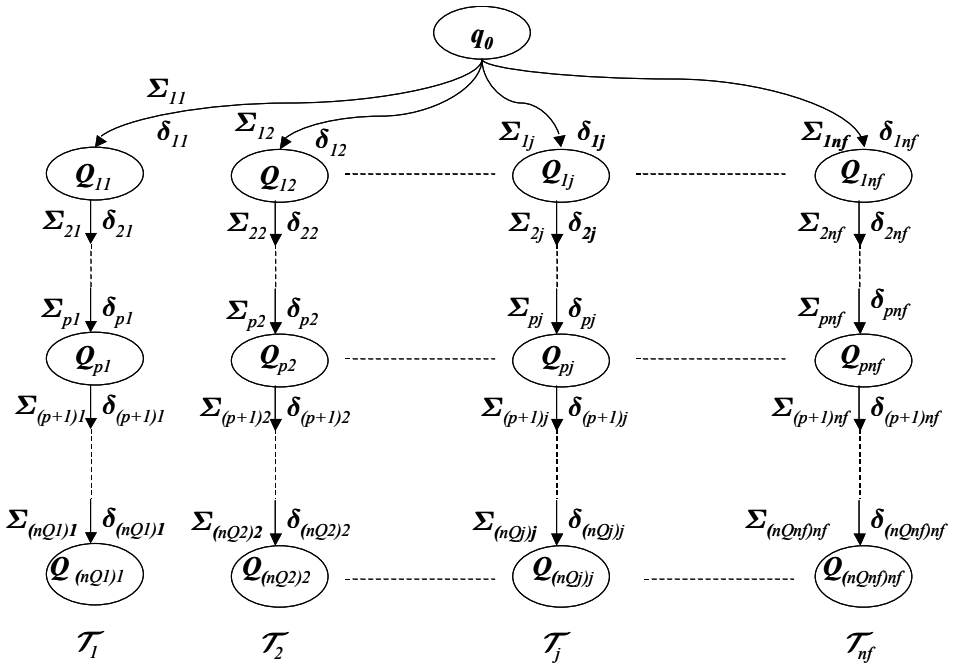

Fig. 10.3 Timed series inference component modelled using a timed labelled transition system

10.4 Case of study

10.4.1 Description

This section uses the application example of 12 limnimeters of the Barcelona urban drainage system which was already explained in previous sections (*Section 9.3*). As mentioned, the used methodology applied to the selected sewer network (*Fig. 7.3*) let diagnose faults of a set $\boldsymbol{f_{Lm}}$ composed by 14 limnimeters modelling a set $\boldsymbol{L_m}$ of 12 limnimeters using interval reduced observers with uncertain parameters. Thereby, the estimations given by the limnimeter models of the set $\boldsymbol{L_m}$ allow obtaining a set $\boldsymbol{r}$ of 12 residuals. Thus, according to Eq. (7.5), every residual of the set $\boldsymbol{r}$ determines a fault signal being ϕ the set of all possible fault signals caused by the faults of the set $\boldsymbol{f_{Lm}}$.

Then, a fault affecting a limnimeter of the set $\boldsymbol{f_{Lm}}$ will cause a temporal sequence of fault signals (a subset of ϕ**)** whose properties will let detect and isolate the fault using the new fault isolation algorithm presented in *Section 10.3.2* (*Fig. 10.2*).

10.4.2 Fault Signature Matrices

In this section, fault signature matrices ***FSM**sensit* and ***FSM**time* related to the considered case of study are given. These matrices are computed as shown in *Section 9.3* assuming the observer gains l_i ($k_i=l_i a_i$)(Eq. (9.21)) of all interval observers associated with the limnimeter set $\boldsymbol{L_m}$ are equal to *0.01* and the occurrence of the first fault signal is detected at time instant $t_0=4000\ s$. Thereby, they show the relationship between the limnimeter fault set $\boldsymbol{f_{lm}}$ and the properties of the fault signal temporal sequence ϕ originated by these faults and consequently, they let isolate limnimeter faults using either the fault isolation algorithm described in *Section 10.3*. As mentioned in *Section 9.3*, the other three matrices (***FSM**01, **FSM**sign* and ***FSM**order*) of the interface can be easily obtained from ***FSM**sensit* and ***FSM**time*.

Regarding ***FSM**sensit* (see *Section 9.3.1*), it must be taken into account that each element of this matrix is a time function, mainly, based on the sensitivity of residual related to a certain fault signal to a given fault hypothesis (Eq. (9.2)). Thus, in the following, the elements of ***FSM**sensit* matrix showed in *Table 10.1* are just the fault residual sensitivity steady-state values instead of the ones derived from the use of Eq. (9.2). However, the presented fault isolation algorithm does use this equation to obtain the elements of ***FSM**sensit.* In this table, f_{Lmj} is a fault affecting the limnimeter L_{mj} while ϕ_{Lmi} is the fault signal associated with the residual r_{Li} obtained using the interval observer model of L_{mi}.

***FSM**sensit Matrix*

	f_{L03}	f_{L07}	f_{L08}	f_{L09}	f_{L16}	f_{L27}	f_{L39}	f_{L41}	f_{L45}	f_{L47}	f_{L53}	f_{L56}	f_{L80}	f_{L54}
ϕ_{L03}	0.921	0	0	0	0	-0.340	0	0	0	0	0	0	0	0
ϕ_{L07}	0	0.933	0	0	0	0	0	0	0	0	-0.150	0	0	0
ϕ_{L08}	0	0	0.951	0	-0.752	0	0	0	0	0	0	-0.406	0	-5.162
ϕ_{L09}	0	0	0	0.946	0	0	0	0	0	0	0	0	0	0
ϕ_{L16}	0	0	0	0	0.977	0	0	0	0	0	0	0	-0.255	0
ϕ_{L27}	0	0	0	0	0	0.789	0	0	0	0	0	0	0	0
ϕ_{L39}	0	0	0	0	0	0	0.964	0	0	0	0	0	0	0
ϕ_{L41}	0	0	0	0	0	0	-0.908	0.955	0	0	0	0	0	0
ϕ_{L45}	0	0	0	0	0	0	0	-57.243	0	97.484	0	0	0	0
ϕ_{L54}	0	0	0	0	0	0	0	0	0	0	0.265	-0.183	0	1
ϕ_{L56}	0	0	0	0	0	0	0	0	0	0	0	0.802	0	0
ϕ_{L80}	0	0	0	0	0	0	0	0	0	-14.085	0	0	1	0

Table 10.1 Theoretical fault signature matrix related to the fault residual sensitivity property

Table 10.2 presents ***FSM**time* matrix (see *Section 9.3.2*), where the fault occurrence time intervals are expressed in seconds. According to the value of the presented ***FSM**time* and Eq. (9.11), the value of the diagnosis time window for this scenario is $T_w = 30600\ s$.

FSMtime Matrix

	f_{L03}	f_{L07}	f_{L08}	f_{L09}	f_{L16}	f_{L27}	f_{L39}	f_{L41}	f_{L45}	f_{L47}	f_{L53}	f_{L56}	f_{L80}	f_{L54}
ϕ_{L03}	[0,0]	[-1,-1]	[-1,-1]	[-1,-1]	[-1,-1]	[900,6300]	[-1,-1]	[-1,-1]	[-1,-1]	[-1,-1]	[-1,-1]	[-1,-1]	[-1,-1]	[-1,-1]
ϕ_{L07}	[-1,-1]	[0,0]	[-1,-1]	[-1,-1]	[-1,-1]	[-1,-1]	[-1,-1]	[-1,-1]	[-1,-1]	[-1,-1]	[2100,5400]	[-1,-1]	[-1,-1]	[-1,-1]
ϕ_{L08}	[-1,-1]	[-1,-1]	[0,0]	[-1,-1]	[600,4200]	[-1,-1]	[-1,-1]	[-1,-1]	[-1,-1]	[-1,-1]	[-1,-1]	[900,4200]	[-1,-1]	[300,4200]
ϕ_{L09}	[-1,-1]	[-1,-1]	[-1,-1]	[0,0]	[-1,-1]	[-1,-1]	[-1,-1]	[-1,-1]	[-1,-1]	[-1,-1]	[-1,-1]	[-1,-1]	[-1,-1]	[-1,-1]
ϕ_{L16}	[-1,-1]	[-1,-1]	[-1,-1]	[-1,-1]	[0,0]	[-1,-1]	[-1,-1]	[-1,-1]	[-1,-1]	[-1,-1]	[-1,-1]	[-1,-1]	[300,2400]	[-1,-1]
ϕ_{L27}	[-1,-1]	[-1,-1]	[-1,-1]	[-1,-1]	[-1,-1]	[0,0]	[-1,-1]	[-1,-1]	[-1,-1]	[-1,-1]	[-1,-1]	[-1,-1]	[-1,-1]	[-1,-1]
ϕ_{L39}	[-1,-1]	[-1,-1]	[-1,-1]	[-1,-1]	[-1,-1]	[-1,-1]	[0,0]	[-1,-1]	[-1,-1]	[-1,-1]	[-1,-1]	[-1,-1]	[-1,-1]	[-1,-1]
ϕ_{L41}	[-1,-1]	[-1,-1]	[-1,-1]	[-1,-1]	[-1,-1]	[-1,-1]	[300,3900]	[0,0]	[-1,-1]	[-1,-1]	[-1,-1]	[-1,-1]	[-1,-1]	[-1,-1]
ϕ_{L45}	[-1,-1]	[-1,-1]	[-1,-1]	[-1,-1]	[-1,-1]	[-1,-1]	[-1,-1]	[300,1800]	[0,0]	[300,30600]	[-1,-1]	[-1,-1]	[-1,-1]	[-1,-1]
ϕ_{L54}	[-1,-1]	[-1,-1]	[-1,-1]	[-1,-1]	[-1,-1]	[-1,-1]	[-1,-1]	[-1,-1]	[-1,-1]	[-1,-1]	[0,0]	[0,0]	[-1,-1]	[0,0]
ϕ_{L56}	[-1,-1]	[-1,-1]	[-1,-1]	[-1,-1]	[-1,-1]	[-1,-1]	[-1,-1]	[-1,-1]	[-1,-1]	[-1,-1]	[-1,-1]	[0,0]	[-1,-1]	[-1,-1]
ϕ_{L80}	[-1,-1]	[-1,-1]	[-1,-1]	[-1,-1]	[-1,-1]	[-1,-1]	[-1,-1]	[-1,-1]	[-1,-1]	[0,0]	[-1,-1]	[-1,-1]	[0,0]	[-1,-1]

Table 10.2 Theoretical fault signature matrix related to the fault signal occurrence time instant property

10.4.3 Fault isolation method using the timed discrete-event approach

In this section and for the considered case of study, a fault isolation process will be designed following the fault isolation architecture presented in *Section 10.3* focusing on the *timed labelled transition system* used to model the *timed series inference component* (see *Fig. 10.2*) (*Section 10.3.2.1*). In this case, this fault isolation model will be built just considering a subset of 6 fault hypotheses affecting to L_{16}, L_{27}, L_{39}, L_{41}, L_{03} and L_{54} of the fault set $\boldsymbol{f_{lm}}$ (*Fig. 10.4*). In this figure, the label of the transition related to the fault signal ϕ_{Lmi} for the fault hypothesis f_{Lmj} (fault affecting limnimeter L_{mj}) will be noted as $\Sigma_{Lmi-\,Lmj}$ (Eq. (10.5)) while all the states related to a certain fault hypothesis will be notated as f_{Lmj} .

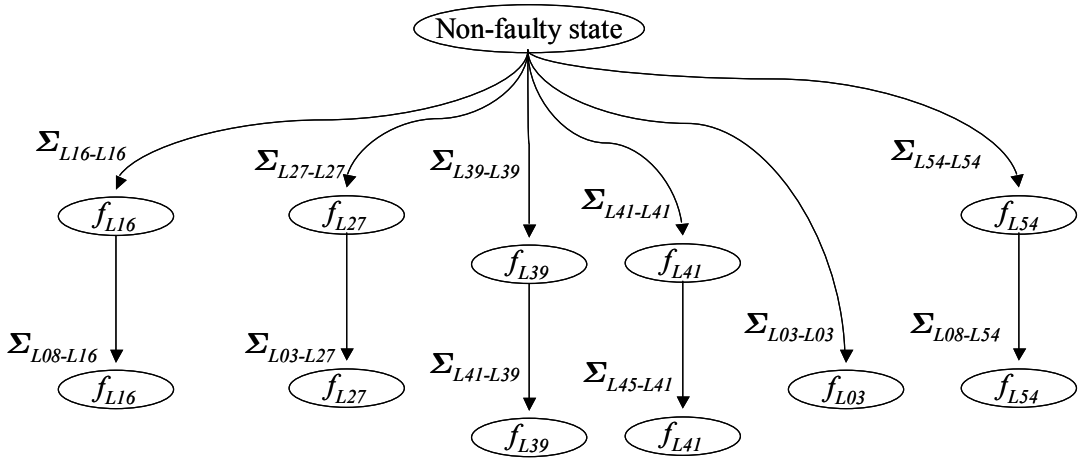

Fig. 10.4 Limnimeter fault isolation based on a timed LTS model

The associated representation of this *timed labelled transition system* can be seen as the integration of all the information stored in ***FSM***01, ***FSM***order and ***FSM***time in the same structure, as has been described in *Section 10.3.2*.

Focusing on a fault scenario where a fault affecting limnimeter L_{27} occurs at t_0= *4000s*, the time evolution of the affected residuals and their associated adaptive thresholds (Eq. (8.15)) are plotted in *Fig. 10.5*.

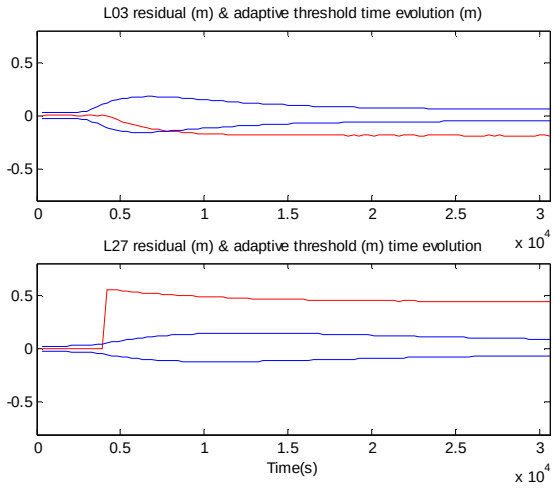

Fig. 10.5 Time evolution of the residuals and their adaptive thresholds.

Analyzing the time evolution of those residuals and according to Eq. (8.15) and Eq.(7.5), the first observed fault signal will be ϕ_{L27} (fault signal related to limnimeter L_{27} observer model) since time instant $t=t_0$. The value of $\boldsymbol{factor}sensit_j$ (Eq.(7.16)) and $\boldsymbol{factor}time_j$ (Eq. (9.12)) related to all fault hypotheses of the set $\boldsymbol{f_{Lm}}$ is presented in *Fig. 10.6*. It can be seen that only those factors related to the fault hypothesis f_{L27} are activated from the fault occurrence time instant. Then, according to the fault isolation discrete-event model presented *Fig. 10.4* and the information stored in ***FSM**01*, ***FSM**order* and ***FSM**time*, all fault hypotheses except f_{L27} (fault affecting L_{27}) will be rejected. Afterwards, the fault signal ϕ_{L03} is observed supporting the *LTS* representation associated with f_{L27}.

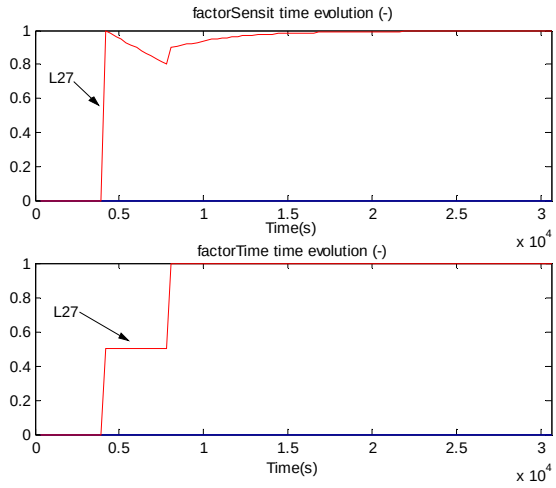

Fig. 10.6 Time evolution of $\boldsymbol{factor}sensit_j$ and $\boldsymbol{factor}time_j$ related to all fault hypotheses of the set $\boldsymbol{f_{Lm}}$.

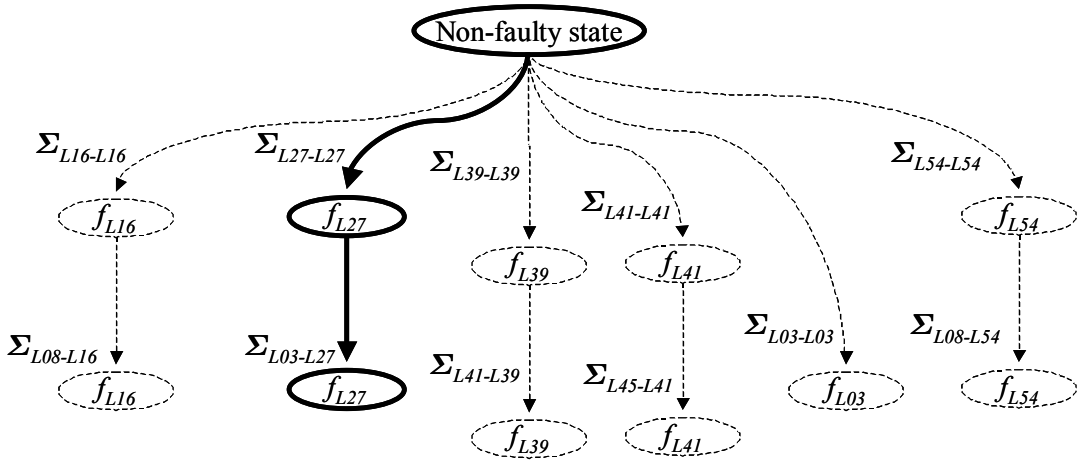

Fig. 10.7 Isolation of a fault affecting L_{27} using a Timed LTS model

10.5 Conclusions

This chapter proposes a model-based fault diagnosis method using a *timed discrete-event approach* based on *interval observers* which improves the integration of fault detection and isolation tasks. The interface between fault detection and fault isolation module considers the degree of fault signal activation and the occurrence time instant of the fault signals using a combination of several fault signature matrices which store the knowledge of the relationship between diagnostic signals and faults. Such fault signatures matrices can be derived from the system model using a fault residual sensitivity analysis. Moreover, exploiting the discrete-time event nature of the fault signals generated by the fault detection module, a fault diagnoser based on a timed discrete-event model can automatically be implemented. Using such approach, faults can be diagnosed since their occurrence generates a unique sequence of observable events (fault signals) that can be recognized by the isolation module. The states and transitions that characterize such a model can be inferred directly from the relationship between fault signals and faults. To exemplify the use and illustrate the effectiveness of the proposed approach, a real case study consisting in diagnosing faults of the limnimeters used for the global control of the Barcelona sewer network is used.

Concluding remarks

11.1 Introduction

According to the PhD thesis objectives determined in *Section 2.5* (*Chapter 2*) and the work carried out in the previous chapters, this chapter summarize the main contributions of this PhD thesis. It must be noticed that this contributions were already described in each corresponding chapter. Moreover, in this chapter it is also pointed out the further work derived from the main obtained results.

Without taking into account the introduction chapter (*Chapter 1*) and the chapter of the state of the art (*Chapter 2*), the obtained contributions and conclusions will be described showing their relations regarding the planned objectives (*Section 2.5*).

11.2 Contributions

In the following subsections of this section, the contributions derived from every general group of objectives (*Section 2.5*) will be illustrated, as mentioned above.

11.2.1 Fault detection objectives

The contributions related to this group of objectives were obtained in *Chapter 3*, *Chapter 4* and *Chapter 5* of this PhD thesis document. Thereby, regarding the fault detection objectives set in point *(a)* of *Section 2.5.1*, the main contributions are:

(a) Illustration of the influence of the observer gain on the time evolution of the fault residual sensitivity function.

(b) Determination of the minimum detectable fault function when considering an interval observer-based approach pointing out its dynamical aspects and the influence of the observer gain. This point can be considered as an extension of the *triggering limit* concept introduced by (Gertler 1998).

(c) Determination of a fault classification according to the time evolution of their detectability: permanently detected (*strong fault detection*), non-permanently detected (*weak fault detection*) or just non-detected.

(d) Determination of the adaptive threshold related to the interval observer and the effect of the observer gain on it.

(e) Determination of the influence of the observer gain on the envelopes associated with the system output estimation interval computed by the interval observer.

(f) Illustration of the influence of the observer gain on the fault detectability.

These contributions were mainly derived from *Chapter 3* which illustrates that the performance of the fault detection module is established by the adaptive threshold related to the interval observer. Thereby, this adaptive threshold depends on the uncertainty, and by the different fault residual sensitivity functions related to the residual generator built up using the interval observer model. This chapter signals out that both observer fault detection properties have

an associated dynamics which depends basically on the observer gain. As a result, the observer gain can be seen as the tuning parameter of the interval observer which may allow obtaining the required fault detection performance.

On the other hand, *Chapter 4* tackles the set of fault detection goals enumerated in point *(b)* of *Section 2.5.1* being its main contributions:

(g) Observer gain design procedure to avoid the wrapping effect when using low computational algorithms (set/region-based approaches) to compute the system output estimation interval at every time instant.

(h) Influence of this observer gain design procedure on the performance of the fault detection module.

The main conclusion of this chapter is that designing properly certain elements of the observer gain matrix, the wrapping effect can be avoided when using low computational algorithms. A drawback of this procedure is that the interval observer fault detection performance might be affected negatively. Nonetheless, this effect might be counteracted setting properly the values of the other elements of the observer gain matrix.

Concerning the last set of fault detection objectives (point *(c)* of *Section 2.5.1*), they are carried out in *Chapter 5* obtaining the following contributions:

(i) Design procedure to obtain a λ-order interval predictor equivalent to a certain interval observer from their fault detection performance point view.

(j) Illustration that when state-space matrix of the interval observer satisfies the isotonicity property (*Chapter 4*), the system output estimation interval can be obtained by the fault detection equivalent predictor using two known point-wise trajectories.

The main conclusion of *Chapter 4* is that a $\lambda!!$-order interval predictor equivalent to a certain interval observer regarding their fault detection performance can be obtained. It must be noticed that predictors do not suffer either from the wrapping effect or from the *initial condition sensitivity problem* (*Table 2.1*). Moreover, if the interval observer is isotonic, the system output estimation interval related to the equivalent interval predictor can be computed using two known point-wise trajectories.

11.2.2 Fault detection/isolation interface objectives

This group of objectives was tackled in *Chapter 6*, *Chapter 7* and part of *Chapter 9*. However, *Chapter 6* has only a motivational function regarding the non-accurateness associated with a binary interface between fault detection and fault isolation. Thereby, the main conclusion of this chapter is that the fault detection module and the fault isolation modules can not be considered separately such as it is proposed by those methods using a binary interface but the dynamical properties of the fault signals must be considered. This non-binary fault detection/isolation interface allows adding more fault distinguishability to the fault isolation algorithm and besides, takes into account the effect of the fault detection module on the fault isolation result.

Concerning *Chapter 7*, this chapter is based on the fault isolation method proposed by (Puig et al, 2005b) focusing on the interface between fault detection and fault isolation. In (Puig et al, 2005b), the properties of a non-binary interface are described without giving a procedure for its construction. In this chapter, the different steps which must be followed to build up this interface according to a passive robust fault diagnosis approach based on interval observers are given. The most of these steps will be tackled in *Chapter 8*, *Chapter 9* and *Chapter 10*. Thereby, the main contributions of this chapter are:

(a) Adaptation of the method proposed by (Puig et al, 2005b) to a passive robustness approach based on interval models.

(b) Procedure to model the Barcelona sewer network in order to detect and isolate faults affecting the limnimeter sensors.

The main conclusion of *Chapter 7* is that the accurateness of the whole fault diagnosis process is notably enhanced when a set of properties related to fault signals is considered to isolate the fault instead of just considering the binary property. It is in the following where this interface is further tested using an interval observer-based fault diagnosis approach.

As mentioned, the last contributions in this group of objectives related to the interface between fault detection and isolation were obtained in *Chapter 9*:

(c) Illustration of the importance of the fault residual sensitivity functions on the fault isolation process since they determine the dynamics of the fault signals and the structure of the theoretical fault signature matrices (***FSM***).

(d) Procedure to compute the theoretical fault signature matrices when using interval observers and when considering the time evolution of the fault signal properties.

The main conclusion of this chapter regarding this interface is that for those fault diagnosis approaches based on analytical models it is very important to know the expressions of the fault residual sensitivity functions since they rule not only the results of the fault detection stage but also the results of the fault isolation module. They determine the dynamics of the generated fault signals and the fault signals which will be affected by a given fault (structure of the ***FSM*** matrices).

11.2.3 Fault isolation objectives

As described in *Section 2.5*, the last group of objectives is related to the fault isolation module which was tackled in *Chapter 8*, part of *Chapter 9* and *Chapter 10* obtaining a set of new contributions. Thereby, *Chapter 8* focuses on the fault isolation objectives shown in point *(d)* of *Section 2.5.2* being its main contributions:

(a) Adaptation of the method proposed by (Puig et al, 2005b) applying interval observers.

(b) Illustration that the result obtained by the fault isolation module is influenced by the fault detections module and therefore, both modules can not be considered separately. This influence is due to problems affecting the fault detection module (*Table 2.1*) and to the fact that the isolation of a fault requires the activation of a subset the residuals in a certain period of time. This result justifies the use of the interface proposed by (Puig et al, 2005b).

(c) Illustration that the observer gain has a key influence on the result given by the observer gain. This influence derives from the effect of the fault detection module on the fault isolation process and from the fact that the detectability of a fault depends on the observer gain, such as depicted in *Chapter 3*.

(d) Adaptation of the procedure to model the Barcelona sewer network in order to detect and isolate faults affecting the limnimeter sensors applying interval observers.

The main conclusion of this chapter is that the fault detection and fault isolation modules can not be considered separately when designing a fault diagnosis process. This is due to the fact that the results given by the fault isolation module depend significantly on the time evolution of the fault signals generated by the fault detection stage. The importance of this aspect is remarkable since, as mentioned previously (*Table 2.1*), fault detection is affected by some inherent problems and fault isolation requires the activation of a subset of fault signals in order to isolate the fault without any error. Moreover, this influence of the fault detection module on the fault isolation process stands out even more the fact of considering a set of fault signal properties in the interface between both modules instead of considering just the binary property. As a last conclusion of this chapter, the influence of the observer gain on the

fault isolation result is derived from since, as concluded in *Chapter 3*, the generation of fault signal by the fault isolation stage is ruled by the observer gain.

Concerning the fault isolation goal described in point *(e)* of *Section 2.5.2*, *Chapter 9* allow obtaining the following contribution:

(e) Illustration of the importance of the observer gain matrix $\boldsymbol{L}$ on the fault isolation process since its influence on the dynamics of the fault residual sensitivity functions, such as demonstrated in *Chapter 3*.

The main conclusion of this chapter regarding this aspect is that the observer gain matrix $\boldsymbol{L}$ have also a key influence on the fault isolation module since, as demonstrated in *Chapter 3*, this matrix determines the dynamics of the fault residual sensitivity functions. In consequence, a proper design of this matrix might allow enhancing the fault isolation result according to a certain requirements.

The last contributions are achieved in *Chapter 10* which focuses on the fault isolation objectives shown in point *(f)* of *Section 2.5.2*:

(f) Illustration that the fault isolation module should be modelled using a timed discrete-event models since the fault signals generated by the fault detection module can be considered as a discrete-event that occurs at a certain time instant.

(g) Procedure to model the fault isolation module using a timed discrete-event approach when monitored system is modelled applying an interval observer approach.

(h) Proposition of a new fault diagnosis method derived from the results obtained in the *Part II* of this PhD thesis. This method can be seen as an evolution of the proposed by (Puig et al, 2005b).

The main conclusion of this chapter is that modelling the fault isolation module using a timed discrete-event approach allows enhancing the performance of this module regarding its accurateness. This result derives from the timed discrete-event nature of the fault signals generated by the fault detection module. Besides, it must be noticed that this aspect does not depends whether the monitored system is modelled analytically or qualitatively.

11.3 Further work

When all the required tasks were carried out in order to achieve the planned objectives, some new important aspects regarding passive robust fault diagnosis based on intervals observers appeared which were kept out of the scope of this PhD thesis. However, they were listed as a further work since the analysis of these points may enhance the performance of the interval observer regarding the whole fault diagnosis process. This set of new tasks, which were kept as a further work, is:

(a) Disturbance and noise influence on the performance of the fault detection module and the effect of the observer gain on it.

(b) Observer gain design procedure to avoid some of the fault detection drawbacks related to the analytical model approaches (*Table 2.1*): *i.e* avoiding the wrapping effect minimizing the noise effect.

(c) A proper extension of the concept minimum detectable fault in a multiple fault scenario.

(d) Design procedure of the elements of the observer gain matrix which have not been set to avoid the wrapping effect in order to counteract the possible negative influence of obviating this effect.

(e) A proper definition of the minimum isolable fault and its benefits when considered in the fault diagnosis stage.

Design procedure to enhance the fault isolation result using the observer gain matrix as a tuning parameter in order to add more fault distinguishability.

Appendices

Appendix A

In this section, it is demonstrated that the residual relation given by Eq. (3.31) is satisfied when the interval observer (Eq.(3.7)) is stable and both its state-space matrix $\boldsymbol{A}$ and its observation gain matrix $\boldsymbol{L}$ are positive, assuming the observability of the system (Eq. (3.1)) for all $\tilde{\boldsymbol{\theta}} \in \boldsymbol{\Theta}$. Besides, the observer gain is assumed to satisfy the following relation: $\boldsymbol{0} \le \boldsymbol{L_o} \le \boldsymbol{L_p}$, understood element by element. According to these assumptions, it is satisfied:

(a) $0 \le (\boldsymbol{LC})_{ij} \le a_{ij}$ being a_{ij} and $(\boldsymbol{LC})_{ij}$ the elements placed in the i^{th}-row and j^{th}-column of matrices $\boldsymbol{A}$ and $\boldsymbol{LC}$, respectively and where $i, j = 1,...,nx$

(b) $0 \le (\boldsymbol{L_o})_{ij} \le (\boldsymbol{L_p})_{ij}$ being $(\boldsymbol{L})_{ij}$ and $(\boldsymbol{L_p})_{ij}$ the elements placed in the i^{th}-row and j^{th}-column of the observation gain matrix $\boldsymbol{L}$ and its value when a predictor model is used, respectively and where $i = 1,...,nx$ and $j = 1,...,ny$

(c) $\left\|\boldsymbol{A} - \boldsymbol{LC}\right\| < 1$

According to Eq. (3.29) of *Section 3.2.3*,

$$\boldsymbol{r}(k) + \boldsymbol{H}_r(q^{-1}, \boldsymbol{\theta})\boldsymbol{r}(k) = \boldsymbol{r}(k)_{\boldsymbol{L=0}} \tag{12.1}$$

where the transfer function $\boldsymbol{H}_r(q^{-1}, \boldsymbol{\theta})$ is given by Eq.(3.27) and, as mentioned in *Section 3.2.3*, the term $\boldsymbol{r}(k)_{\boldsymbol{L=0}}$ corresponds to the residual generated by the simulation approach. Then, Eq. (12.1) can be re-written as follows using the *matrix inversion lemma*

$$\boldsymbol{r}(k) = \left(\boldsymbol{I} - \boldsymbol{C}(\boldsymbol{\theta})\left(q\boldsymbol{I} - \boldsymbol{A}_0(\boldsymbol{\theta})\right)^{-1}\boldsymbol{L}\right)\boldsymbol{r}(k)_{\boldsymbol{L=0}} = \boldsymbol{r}(k)_{\boldsymbol{L=0}} - \boldsymbol{C}(\boldsymbol{\theta})\sum_{j=0}^{k-1}\boldsymbol{A}_0(\boldsymbol{\theta})^{k-j-1}\boldsymbol{L}\boldsymbol{r}(j)_{\boldsymbol{L=0}} \tag{12.2}$$

Particularizing Eq. (12.2) for the residual interval upper bound ($\overline{\boldsymbol{r}}(k) = \overline{\boldsymbol{r}}(k)_{\boldsymbol{L=0}} - \boldsymbol{C}(\boldsymbol{\theta})\sum_{j=0}^{k-1}\boldsymbol{A}_0(\boldsymbol{\theta})^{k-j-1}\boldsymbol{L}\overline{\boldsymbol{r}}(j)_{\boldsymbol{L=0}}$ which satisfies the relation $\overline{\boldsymbol{r}}(k) > 0$ [18] in a non-faulty scenario and noticing that the term $\boldsymbol{C}(\boldsymbol{\theta})\sum_{j=0}^{k-1}\boldsymbol{A}_0(\boldsymbol{\theta})^{k-j-1}\boldsymbol{L}\overline{\boldsymbol{r}}(j)_{\boldsymbol{L=0}}$ is a function of the matrix $\boldsymbol{L}$, every component related to the residual upper bound $\overline{\boldsymbol{r}}(k)$ achieves its maximum value in the range $\boldsymbol{0} \le \boldsymbol{LC} \le \boldsymbol{A}$ for $\boldsymbol{L} = \boldsymbol{0}$ (that is, when the observer eigenvalues are equal to the ones related to the monitored system). On the other hand, in the predictor case ($\boldsymbol{L} = \boldsymbol{L}_p$) this term can be approximated taking into account that $\boldsymbol{A}_o(\boldsymbol{\theta})^k = \boldsymbol{0}$ for $k > nx$ since in this case all the observer eigenvalues are placed at the origin. In consequence, every component related to the residual $\overline{\boldsymbol{r}}(k)$ achieves its minimum value. Finally, considering a

[18] $\overline{\boldsymbol{r}}(k) > \boldsymbol{0}$ should be understood component by component, that is: $\overline{r}_i(k) > 0 \quad i = 1,\cdots,ny$

value of the observer gain ($\boldsymbol{L} = \boldsymbol{L}_o$) which is between the two previous extreme cases, the expression $\boldsymbol{0} \le \boldsymbol{A} - \boldsymbol{LC} \le \boldsymbol{A}$ allows establishing the following relation for whatever time instant $k>0$

$$\overline{r}_i(k)_{\boldsymbol{L}_p} \le \overline{r}_i(k)_{\boldsymbol{L}_o} \le \overline{r}_i(k)_{\boldsymbol{L}=\boldsymbol{0}} \quad i = 1, \cdots, ny \tag{12.3}$$

Conversely, for the case of the residual interval lower bound which satisfies the relation $\underline{\boldsymbol{r}}(k) < 0$ in a non-faulty scenario, a similar expression can be obtained using an analogous reasoning:

$$\underline{r}_i(k)_{\boldsymbol{L}=\boldsymbol{L}_p} \ge \underline{r}_i(k)_{\boldsymbol{L}=\boldsymbol{L}_o} \ge \underline{r}_i(k)_{\boldsymbol{L}=\boldsymbol{0}} \quad i = 1, \cdots, ny \tag{12.4}$$

As a result of Eq. (12.3) and Eq. (12.4), the following relation is obtained

$$\left[r_i(k)_{\boldsymbol{L}=\boldsymbol{L}_p} \right] \subseteq \left[r_i(k)_{\boldsymbol{L}=\boldsymbol{L}_o} \right] \subseteq \left[r_i(k)_{\boldsymbol{L}=\boldsymbol{0}} \right] \quad i = 1, \cdots, ny \tag{12.5}$$

completing the proof.

Appendix B

This section illustrates the required condition so that the residual relation given by Eq. (3.31) can be satisfied in steady-state. Although it is not strictly necessary, as hypothesis, it will be assumed all the elements of matrix $\boldsymbol{A}$ are positive and the observer gain matrix $\boldsymbol{L}$ satisfies the relation $\boldsymbol{0} \le \boldsymbol{L_o} \le \boldsymbol{L_p}$, understood element by element.

According to Eq. (3.29) of *Section 3.2.3*, the residual fullfils the following relation:

$$\left(\boldsymbol{I} + \boldsymbol{C}(\boldsymbol{\theta}) \left(q\boldsymbol{I} - \boldsymbol{A}(\boldsymbol{\theta}) \right)^{-1} \boldsymbol{L} \right) \boldsymbol{r}(k) = \boldsymbol{r}(k)_{\boldsymbol{L}=\boldsymbol{0}} \tag{12.6}$$

where, the term $\boldsymbol{r}(k)_{\boldsymbol{L}=\boldsymbol{0}}$ corresponds to the residual generated by the simulation approach. Then, Eq. (12.6) can be expressed in steady-state as

$$\left(\boldsymbol{I} + \boldsymbol{C}(\boldsymbol{\theta}) \left(\boldsymbol{I} - \boldsymbol{A}(\boldsymbol{\theta}) \right)^{-1} \boldsymbol{L} \right) \boldsymbol{r}(\infty) = \boldsymbol{r}(\infty)_{\boldsymbol{L}=\boldsymbol{0}} \tag{12.7}$$

Thus, applying the *contractivity property* (see *Definition 2* in *Section 2.3.2.5.2*) of a linear system, the relation

$$\left[\boldsymbol{r}(\infty) \right] \subseteq \left[\boldsymbol{r}(\infty)_{\boldsymbol{L}=\boldsymbol{0}} \right] \tag{12.8}$$

is satisfied when

$$\left\| \left(\boldsymbol{I} + \boldsymbol{C}(\boldsymbol{\theta}) \left(\boldsymbol{I} - \boldsymbol{A}(\boldsymbol{\theta}) \right)^{-1} \boldsymbol{L} \right) \right\| \ge 1 \tag{12.9}$$

Then, given that $\boldsymbol{A}$ and $\boldsymbol{C}$ are constant matrices and $\boldsymbol{L}$ satifies the relation $\boldsymbol{0} \le \boldsymbol{L_o} \le \boldsymbol{L_p}$, the following residual relation can be written

$$\left[r_i(\infty)_{\boldsymbol{L}=\boldsymbol{L}_p} \right] \subseteq \left[r_i(\infty)_{\boldsymbol{L}=\boldsymbol{L}_o} \right] \subseteq \left[r_i(\infty)_{\boldsymbol{L}=\boldsymbol{0}} \right] \quad i = 1, \cdots, ny \tag{12.10}$$

Eq. (12.9) confirms that the elements of matrices $\boldsymbol{A}$, $\boldsymbol{C}$ and $\boldsymbol{L}$ do not have to be positive.

Appendix C

In this section, it is demonstrated that the steady-state of the residual sensitivity to a input fault,$\boldsymbol{S}_{fu}$, (Eq.(3.49)) satisfies the relation (3.53) when the interval observer fullfils $0 \le \boldsymbol{LC} \le \boldsymbol{A}$ and $\boldsymbol{\theta} \le \boldsymbol{L}_{\boldsymbol{o}} \le \boldsymbol{L}_{\boldsymbol{p}}$, neglecting the direct-input matrix $\boldsymbol{D}$ ($\boldsymbol{D} \approx \boldsymbol{\theta}$). Thus, Eq. (3.49) can be written as:

$$\boldsymbol{s}_{fu}(\infty) = \lim_{q \to 1} \boldsymbol{S}_{fu}(q^{-1}, \boldsymbol{\theta}) == -\Big(\boldsymbol{C}(\boldsymbol{\theta})\big(\boldsymbol{I} + \boldsymbol{LC}(\boldsymbol{\theta}) - \boldsymbol{A}(\boldsymbol{\theta})\big)^{-1} \boldsymbol{B}(\boldsymbol{\theta})\Big) \boldsymbol{F}_u(\boldsymbol{\theta}) \tag{12.11}$$

According to procedure applied in *Section 3.3.3*, Eq. (12.11) can be seen as the steady-state value of $\boldsymbol{S}_{fu}$ for an abrupt fault modelled as a unit-step function (Gertler, 1998). Then, considering that this fault occurs at time instant $k=0$ and propagating $\boldsymbol{S}_{fu}$ from this time instant until $k=\infty$, Eq. (12.11) can be written as:

$$\boldsymbol{s}_{fu}(\infty) = -\boldsymbol{C}(\boldsymbol{\theta}) \left[\sum_{j=0}^{k-1} \big(\boldsymbol{A}(\boldsymbol{\theta}) - \boldsymbol{LC}(\boldsymbol{\theta})\big)^{k-j-1} \boldsymbol{B}(\boldsymbol{\theta}) \boldsymbol{F}_u(\boldsymbol{\theta}) \right]_{k \to \infty} \tag{12.12}$$

Since the estability of the interval observer is assumed and it satisfies $0 \le \boldsymbol{LC} \le \boldsymbol{A}$ and $\boldsymbol{\theta} \le \boldsymbol{L}_{\boldsymbol{o}} \le \boldsymbol{L}_{\boldsymbol{p}}$, the following relation can be written:

$$0 \le \big\| \boldsymbol{A}(\boldsymbol{\theta}) - \boldsymbol{LC}(\boldsymbol{\theta}) \big\| \le \big\| \boldsymbol{A}(\boldsymbol{\theta}) \big\| \le 1 \tag{12.13}$$

In consequence, the steady-state of $\boldsymbol{S}_{fu}$ (Eq. (12.11)) will satisfy the relation given by Eq. (3.53). This is

$$\left| s_{f_{i,j}}(\infty, \boldsymbol{\theta})_{\boldsymbol{L}=\boldsymbol{L}_{\boldsymbol{p}}} \right| \le \left| s_{f_{i,j}}(\infty, \boldsymbol{\theta})_{\boldsymbol{L}=\boldsymbol{L}_{\boldsymbol{o}}} \right| \le \left| s_{f_{i,j}}(\infty, \boldsymbol{\theta})_{\boldsymbol{L}=\boldsymbol{\theta}} \right| \quad i = 1, \cdots, ny \quad j = 1, \cdots, nu \tag{12.14}$$

Bibliography

Adrot, O. Maquin, D., Ragot, J (2000) *"Bounding Approaches to Fault Detection of Uncertain Dynamic Systems"*. IFAC SafeProcess'00. Hungary. September, 2000.

Adrot, O., Flaus, J.M. (2003) "Trajectory Computation of Dynamic Uncertain Systems". In Proceedings of Conference on Decision and Control, CDC'03. Hawaii. USA. 2003.

Alonso, C. J., Pulido, J.B., Rodríguez, J.J., Llamas, C.. (2000) "Diagnosis of dynamic systems: a framework to integrate fault modes and learned domain knowledge". In Current trends in qualitative reasoning and applications. 2000 Edition. Pages 33-47. Edición Digital @tres. June, 2000. Spain.

Armengol, J., Vehi, J., Travé-Massuyès, L., Sainz, M.A. (2000)*"Interval Model-Based Fault Detection using Multiple Sliding Windows"*. IFAC SAFEPROCESS'00. Hungary. September, 2000.

Armengol, J., Vehí, J., Travé-Massuyès, L., Sainz, M.A. "Application of multiple sliding time windows to fault detection based on interval models" Workshop on Principles of Diagnosis DX'01, pp. 9-16. San Sicario, Italy, 2001.

Ayoubi, M..(1994) "*Fault diagnosis with dynamic neural structures and application to a turbocharger.*" Proc. IFAC Symp. Fault Detection Supervision and Safety for Technical Processes, SAFEPROCESS, Espoo, Finland, Vol. 2, pp. 618-623.

Bartys, M. (2002). "Specification of Actuators Intended to Use for Benchmark Definition, DAMADICS" Internal Report, http:// diag.mchtr.pw.edu.pl/damadics.

Basseville, M. and Benvenista, A. (1986) (eds) " *Detection of Abrupt Changes in Signals and Dynamics Systems* " LNCIS 77, Springer-Verlag, Berlin.

Basseville, M. (1988) " *Detecting changes in signals and systems – a survey* " Automatica 24(3): 309-326.

Basseville, M. & Nikirov , I.V. (1993) " *Detection of abrupt changes: theory and applications*. " Prentice Hall. 1993

Bazaraa, M.S., Sherali, H.D. & Shetty, C.M. (1993) "Nonlinear Programming". John Wiley & Sons. New York. 1993.

Beard, R. V. *"Failure Accommodation in Linear Through Self Reorganizing* (1971)*"* PhD Thesis, MIT, Mass., USA.

Blanke, M., Kinnaert, M., Lunze, J., Staroswiecki, M. (2003) "Diagnosis and fault-tolerant control". Springer-Verlag Berlin Heidelberg.

Cembrano, G. et al. (2002). "Global Control of the Barcelona Sewerage System for Environment Protection". In Proceedings of IFAC World Congress, Barcelona.

Chang, I. C., Yu, C. C. and Liou, C. T. (1994) *"Model-based approach for fault diagnosis: Part I Principles of deep model algorithm (DMA)"* Ind. Eng. Chem. Res., 33:1542-1555, 1994.

Chantler, M.J., Daus, S., Vikatos, T. and Coghill, G.M. (1996) "The use of quantitative dynamic models and dependency recording engines". In Proc. of the Seventh International Workshop on Principles of Diagnosis (DX-96). Pp. 59-68. Val Morin, Quebec, Canada.

Chen, J. and Zhang, H. Y. (1990) *"Parity vector approach for detcting failures in dynamic systems"* Int. J. Sys. Sci 21(4): 756-770.

Chen and G. Provan (1997) Modeling and diagnosis of timed discrete event systems: a factory automation example," in Proceedings of the American Control Conference, June, pp. 31-36,

Chen J. & Patton, R.J. (1999)*"Robust Model-Based Fault Diagnosis for Dynamic Systems*". Kluwer Academic Publishers. 1999.

Chilali, M., Gahinet, P. and Apkarian, P. "Robust Pole Placement in LMI Regions" IEEE Trans. Automatic Control, vol. 41, no. 3, pp. 436-442, 1996.

Chow, E. Y. and Willsky, A. S. (1980) "*Issues in the development of a general algorithm for reliable failure detection"*, Proc. of the 19th Conf. on Decission and Control, Albuquerque, NM.

Chow, E. Y. and Willsky, A. S. (1984) "*Analytical redundancy and the design of robust detection systems"*, IEEE Trans. Automat. Contr. AC-29(7): 603-614.

Clark R.N. (1989) "State estimation for instrument fault detection." In Patton RJ, Frank PM, Clark RN (eds). *Fault diagnosis in dynamic systems, theory and application*. Prentice Hall, Englewood Cliffs, NJ, 1989.

Combastel, C., Gentil, S., Rognon, J.P. (2003) *"Toward a better integration of residual generation and diagnostic decision"* IFAC SafeProcess 2003, Washington DC. USA

Console, L., Picardi, C., Thesider, D. (2001) "Temporal Decision Trees or the lazy ECU vindicated". IJCAI-INT Joint Conf. on Artificial Intelligence, 545-550, Seattle.

Cordier, M.O. C. Dousson. 2000 « Alarm driven monitoring based on chronicles«. IFAC SAFEPROCESS'00. p. 286-291. Budapest, Hungary.

Cordier, M., P. Dague, M. Dumas, F. Levy, J. Montmain, M. Staroswiecki, and L. Travé-Massuyès, (2000) "A comparative analysis of AI and control theory approaches to model-based diagnosis". 14th European Conference on Artificial Intelligence (ECAI 2000), Berlin, Germany.

Cordier, M., P. Dague, Levy, J. Montmain, M. Staroswiecki, and L. Travé-Massuyès, (2004) "*Conflicts versus analytical redundancy relations: a comparative analysis of the model-based diagnosis approach from the artificial intelligence and automatic control perspectives*". IEEE Trans. On Systems, Man, and Cybernetics. Part B: Cybernetics, 34(5): 2163-2177, 2004.

Cugueró, P., Puig, V., Saludes, J., Escobet, T. (2002) *"A Class of Uncertain Linear Interval Models for which a Set Based Robust Simulation can be Reduced to Few Pointwise Simulations"*. In Proceedings of Conference on Decision and Control 2002 (CDC'02). Las Vegas. USA. 2002.

de Kleer, J. (2003) "Fundamentals of Model-based Diagnosis". 14th International Workshop on Principles of Diagnosis, DX 2003.

Daigle, M., Koutsoukus, X., Biswas, G. (2007) "A Discrete Event Approach to Diagnosis of Continuous Systems" Workshop on Principles of Diagnosis DX'07. Nashville, TN, USA.

Ding X., Frank P.M. (1991) *"Frequency domain approach and threshold selector for robust model-based fault detection and isolation"*. Proc IFAC/IMACS Symp. SAFEPROCESS '91, Baden-Baden, 307-312.

Dvorak, D. and B. Kuipers. (1992) "Model-based monitoring of dynamic systems". Readings in Model Based Diagnosis. pp 249-254. 1992.

El Ghauoui, L., Calafiore, G. (2000) "Identification of ARX models with time-varying bounded parameters: a semidefinite programming approach". IFAC Symposium on System Identification. Santa Barbara. California. USA.

Emami-Naemi A, M.M. Akhter & S.M. Rock. . (1988) *"Effect of model uncertainty on failure detection: the threshold selection"*. *IEEE Transactions on Automatic Control*, AC-33, pp. 1106-1115. 1988

Fagarasan, I., Ploix, S., Gentil, S. (2004) "Causal fault detection and isolation based on a set-membership approach" Automatica, pp. 2099-2110, 2004.

Frank, P.M., Ding, X. (1994) "Frequency Domain Approach to Optimally Robust Residual Generation and Evaluation for Model-based Fault Diagnosis". Automatica, Vol. 30, No. 5, pp. 789-804.

Frank, P. M. and Keller, L. (1981) *"Sensitiviy descriminating observer design for instrument failure detection"* IEEE Trans. Aero. and Electron. Syst. AES-16: 460-467.

Frank, P. M. and Wünnenberg, J. (1989) *"Robust fault diagnosis using unknown input schmes"* in R. J. Patton, P. M. Frank and R. N. Clark (eds), Fault Diagnosis in Dynamic Systems: Theory and Application. Prentice Hall, chapter 3, pp. 47-98.

Frank, P. M. (1990) *"Fault diagnosis in dynamic system using analytical and knowledge based redundancy – a survey and some new results",* Automatica 26(3): 459-474.

Frank, P.M. (1991) *"Enhancement of robustness in observer-based fault detection"*. *IFAC Symposium SAFEPROCESS'91*, Baden-Baden, Vol. 2, 275-287.

Frank, P.M. (1996) *"Analytical and qualitative model-based fault diagnosis- a survey and some new results",* European J. of Contr. 2(1): 6-28.

Frank, P. M. and Ding, X. (1997) *"Survey of robust residual generation and evaluation methods in observer-based fault detection systems",* J. of Process Control 7(6): 403-424.

Favre, C. (1994) *"Fly-by-wire for commercial aircraft: the Airbus experience"* Int. J. Contr. 59(1): 139-157.

Gertler J.J. (1988) "*Survey of model-based failure detection and isolation in complex plants*" IEEE Contr. Syst. Ag. 8(6): 3-11

Gertler J.J. (1997) "*Fault detection and isolation using parity relations*" Contr. Eng. Practice 5(5): 653-661

Gertler J.J. (1998) "*Fault Detection and Diagnosis in Engineering Systems*." Marcel Dekker. 1998

Gouzé, J.L., Rapaport, A, Hadj-Sadok, M.Z. (2000) *"Interval observers for uncertain biological systems"*. Ecological Modelling, No. 133, pp. 45-56, 2000.

Hamelin, F., Sauter, D. (2000) "Robust fault detection in uncertain dynamic systems". Automatica, Volume 36, Issue 11, November, Pages 1747-1754.

Hamelin, F., Hassan, N., Sauter, D. (2001) "*Fault detection method of uncertain systems using interval model*". In Proceedings of European Control Conference 2001, ECC'01. Portugal.

Hamscher, W. , Console. L., Kleer, J. (1992) "Readings in Model based Diagnosis". Morgan Kaufmann Pub., San Mateo, 1992.

Hansen, E. (1992) *"Global Optimization using Interval Analysis"*. Marcel Dekker.1992

Himmelblau D. (1978): "Fault Detection and Diagnosis in Chemical and Petrochemical Processes". Amsterdam: Elsevier.

Horak, D.T. & Guidance, J. (1988) *"Failure detection in dynamic systems with modelling errors"*. *Control and Dynamics*, 11 (6), 508-516.

Hoskins, J.C., Himmelblau, D. M. (1988): "Artificial neural network models of knowledge representation in chemical engineering".- Comput. Chem. Eng., Vol. 12, Nº 9/10, pp 882-890.

Ingimundarson, A., J.M. Bravo, V. Puig and T. Alamo (2005). Robust fault diagnosis using parallelotope-based set-membership consistency tests. In: ECC-CDC'05. Sevilla,Spain.

Isermann, R. (1984) *"Process fault detection based on modelling and estimation methods: A survey"* Automatica 20(4): 387-404.

Isermann, R., Balle, P. (1996): "Terminology in the field of supervision, fault detection and fault diagnosis".- IFAC Committee SAFEPROCESS, presented during Symp. SAFEPROCESS, Hull, England.

Isermann, R. (1997) *"Supervision, fault-detction and fault-diagnosis methods – an introduction"* Contr. Eng. Practice 5(5): 639-652.

Isermann, R. (2005) *"Model-based fault-detection and diagnosis – status and applications"* Annual Reviews in Control 29 (2005) 71–85. Elsevier Ltd.

Isermann, R. (2006) "*Fault-Diagnosis Systems - An Introduction from Fault Detection to Fault Tolerance*" Springer Verlag

Jacques, P., Hamelin, F., Aubrun, C. (2003) "Optimal fault detection in a closed-loop framwork: a joint approach". IFAC SAFEPROCESS '03, Washington DC. USA.

Johansson, A., Bask, M., Norlander, T. (2006). "Dynamic threshold generators for robust fault detection in linear systems with parameter uncertainty". Automatica, Volume 42, Issue 7, July, Pages 1095-1106.

Jones, H. L. (1973) *"Failure Detection in Linear Systems"* PhD Thesis, MIT, Mass., USA.

Kolev, L.V. (1993) "Interval Methods for Circuit Analysis". Singapore. World Scientific. 1993.

Korbicz J., Patan K. and Obuchowicz A. (1999) *"Dynamic neural networks for process modelling in fault detection and isolation systems.*"- Int. J. Appl. Math. and Comput. Sci., Vol. 9, Nº 3, pp. 519-546.

Kościelny, J.M. (1995) "Fault isolation in industrial processes by the dynamic table of states method". Automatica 31(5), pp. 747-753.

Kościelny, J.M, Zakroczymski, K (2000) "Fault isolation method based on time sequences of symptom appearance". In Proccedings of IFAC SAFEPROCESS 2000, Budapest. Hungary.

Kościelny, J.M. (2001) "Diagnostics of Automated Industrial Processes.- Warsaw: Akademicka Oficyna Wydawnicza.

Kościelny, J.M., Korbicz, J., Kowalczuk, Z., Cholewa, W. (2004). "Fault Diagnosis". Springer-Verlag,

Kościelny, J.M., Korbicz, J., Kowalczuk, Z., Cholewa, W. (2004a). "Fault Diagnosis". Springer-Verlag, Chapter 2.

Kościelny, J.M., Korbicz, J., Kowalczuk, Z., Cholewa, W. (2004b). "Fault Diagnosis". Springer-Verlag, Chapter 3.

Kościelny, J.M., Korbicz, J., Kowalczuk, Z., Cholewa, W. (2004c). "Fault Diagnosis". Springer-Verlag, Chapter 18.

Kramer, M. A., Leonard, J. A. (1990): "Diagnosis using backpropagation neural networks. Analysis and criticism".- Comp. Chem. Eng., Vol. 14, Nº 12, pp 1323-1338.

Krysander, M., Aslund, J., Nyberg, M. (2008). "An efficient algorithm for finding minimal over-constrained sub-systems for model-based diagnosis". IEEE Transactions on Systems, Man, and Cybernetics – Part A: Systems and Humans, 30(1), pp. 197-206.

Kühn, W. (1998) *"Rigorously computed orbits of dynamical systems without the wrsapping effect"* Computing 61, 47-67. 1998.

Kuipers, B. (1994) *"Qualitative reasoning – Modelling and Simulation with Incomplete Knowledge",* MIT Press . Cambridge, M.A.

Leicht, R., Shen, Q., Conghil, G., Chantler, M. and Slater, A. (1994) " *Qualitative model-based diagnosis of dynamic systems*", Colloquim of the Institution of Measurement and Control.

Ljung, L., (1987) " *System identification: Theory for the user"*, Prentice-Hall, 1987.

Lohner, R.J. (1987) "Enclosing the Solution of Ordinary Initial and Boundary Value Problems", in Kaucher, E., Kulisch, U. & Ullrich, Ch. (eds.): Computer arithmetic: Scientific Computation and Programming Languages. B.G. Teubner, pages 255-286. Stuttgart. 1987.

Loiez, E., Taillibert, P. (1997). "Polynomial temporal band sequences for analog diagnosis". In Proc. of IJCAI-97. Pgs. 474-479. Nagoya, Japan.

Lunze, J. (1994) "*Qualitative modelling of linear dynamical systems with quantized state measurements"*, Automatica 30(3): 417-431.

Lunze, J. (2000). "Diagnosis of Quantised Systems". Proc. 4th IFAC Symp. Fault Detection, Supervision and Safety for Technical Processes, SAFEPROCESS, Budapest, Hungary, Vol. 1, pp. 60-65.

Lunze, J., Supavatanakul, P., Puig, V., Quevedo, J. (2006). "Diagnosis of timed automata: Theory and application to the DAMADICS actuator benchmark problem. Control Engineering Practice 14, pp. 609-619.

Maquin D. and Ragot J. (2000). "Diagnostic des systèmes linéaires".Hermes Science Publications.

Mehra, R. K. And Peschon, J. (1971) *"An innovations approach to fault detction and diagnosis in dynamic systems"* Automatica 7: 637-640.

Meseguer, J., Puig, V., Escobet, T. (2006a) "Observer gain effect in linear observer-based fault detection" IFAC SAFEPROCESS'06.

Meseguer, J., Puig, V., Escobet, T. (2006b) "Observer gain effect in linear interval observer-based fault detection" IFAC SAFEPROCESS'06.

Meseguer, J., Puig, V., Escobet, T., Quevedo, J. (2006c) "Observer gain effect in linear interval observer-based fault isolation" International Workshop on Principles of Diagnosis DX'06.

Meseguer, J., Puig, V., Escobet, T., Quevedo, J. (2007a) "Sensor Fault Diagnosis using Linear Interval Observers" Workshop on Principles of Diagnosis DX'07. Nashville, TN, USA.

Meseguer, J., Puig, V., Escobet, T. (2007b). "Observer Gain Effect in Linear Interval Observer-based Fault Detection" CDC'07 . New Orleans. USA.

Meseguer, J., Puig, V., Escobet, T., Tornil, S. (2007c) "Approximating Fault Detection Linear Interval Observers Using *l*-Order Interval Predictors" Proceedings of European Control Conference 2007 (ECC'07). Kos, Greece.

Meseguer, J., Puig, V., Escobet, T. (2008a) "Robust Fault Detection Linear Interval Observers Avoiding the Wrapping Effect". IFAC World Congress 2008, Seul, Korea.

Meseguer, J., Puig, V., Escobet, T. (2008b) “Fault Diagnosis using a Timed Discrete Event Approach based on Interval Observers”. IFAC World Congress 2008, Seul, Korea.

Meseguer, J., Puig, V., Escobet, T. (2008c). “Observer Gain Effect in Linear Interval Observer-based Fault Detection” Journal of Process Control (JPROCONT-D-07-00232).

Meseguer, J., Puig, V., Escobet, T. (2008d) “Fault Diagnosis using a Timed Discrete Event Approach based on Interval Observers”. Submitted to IEEE SMC Transactions - Part A.

Meseguer, J., Puig, V., Escobet, T. (2009) . “Fault Isolation Module Implementation using a Timed Discrete-Event Approach”. IFAC SAFEPROCESS 2009, Barcelona, Spain.

Milanese, M., Norton, J., Piet-Lahanier, H., Walter, E. (eds) (1996). “Bounding Approaches to System Identification”. Plenum Press. New York. 1996.

Mironovski, L. A. (1979) *“Functional diagnosis of linear dynamic system – a survey”* Automn Remote Control 40: 1198-1205.

Mironovski, L. A. (1980) *“Functional diagnosis of dynamic system – a survey”* Automn Remote Control 41: 1122-1143.

Moore, R.E. (1966) *“Interval analysis”*. Prentice Hall. 1966.

Moore R. E. (1979) *“Methods and applications of interval analysis”*. SIAM. Philadelphia, Pennsylvania, 1979.

Mosterman, P.J., Kapadia, R. and Biswas, G. (1995). “Using Bond Graphs for Diagnosis of Dynamic Physical Systems”. Proc. &yh Int. Workshop Principle of Diagnosis, Goslar, Germany, pp. 81-85.

Mosterman, P.J. (1997) "Hybrid dynamic systems: a hybrid bond graph modeling paradigm and its applications in diagnosis", PhD Thesis. Vanderbilt University, Tennessee, USA.

Mosterman, P., Biswas, G. (1999) “Diagnosis of continuous valued systems in transient operating regions”. IEEE T.on Systems, Man, and Cybernetics, vol. 29, nº6, pp. 554-565.

Ng, H.T. (1990) “Model-based, multiple fault diagnosis of time-varying, continuous physical devices”. 6th Conference on Artificial Intelligence Applications, Santa Barbara, USA, pp. 9-15.

Nedialkov, N.S., Jackson, K.R. (2001) “A New Perspective on the Wrapping Effect in Interval Methdos for Initial Value Problems for Ordinary Differential Equationhs”, in Kulisch, U., Lohner, R.J. & Facius, A. (eds.): Pespectives on Enclosure Methods. Springer Verlarg. 2001.

Nickel, K.. (1985) “How to fight the wrapping effect”. In K. Nickel ed. “Interval Analysis 1985”. Lecture Notes in Computer Science, No. 212, pp. 121-132. Springer-Verlag. 1985.

Nyberg, M. (1999) *“Model based fault diagnosis. Methods, theory and automotive engine applications”* PhD Thesis, Department of Electrical Engineering, Linköping University, 1999.

Patton, R. J. and Kangethe, S. M. (1989) *“Robust fault diagnosis using eigen-structure assignment of observers”* in R. J. Patton, P. M. Frank and R. N. Clark (eds), Fault Diagnosis in Dynamic Systems, Theory an Application, Prentice Hall, chapter 4, pp. 99-154.

Patton, R.J. and Chen J. (1991). “A review of parity space approaches to fault diagnosis.” Proc. IFAC Symp. Fault Detection, Supervision and Safety for Thecnical Processes, SAFEPROCESS, Baden-Baden, Germany, Vol. 1, pp. 65-81, pp. 239-255.

Patton, R.J. (1994) *“Robust model-based fault diagnosis: the state of the art”* SAFEPROCESS, 1994.

Patton, R. J., Chen, J. (1996) “*Robust fault detection and isolation (FDI) systems, in C. T. Leondes (ed.), Dynamics and Control (Vol. 74): Techniques in Discrete and Continuous Robust Systems”,* Academic Press, pp. 171-224.

Patton, R. J., Chen, J. (1997) “*Observer-based fault detection and solation: robustness and applications*”, Contr. Eng. Practice 5(5): 671-682.

Patton, R. J., Chen, J. (1998) *“Proceedings of IFAC Symposium on Fault Detection Supervision and Safety fot Technical Processes – SAFEPROSS'97”*, Pergamon. ISBN 0-08-0423817.

Patton, R.J., P.M. Frank, R.N. Clark. (2000) “Issues of fault diagnosis for dynamics systems”. Springer Verlag.

Pawlak, Z. (1983) “Information Systems. Theoretical Foundation. – Warsaw: Wydawnictwa Naukowo-Technicze, WNT.

Pau, L. F. (1981): “Failure Diagnosis and Performance Monitoring” New York: Marcel Dekker, Inc.

Peng, Y., Youssouf, A., Arte, P., Kinnaert, M. (1997) “A Complete Procedure for Residual Generation and Evaluation with Application to a Heat Exchanger” IEEE Transactions on Control Systems Technology, Volume: 5 , Issue: 6 , Dec. 1997 Pages: 542 – 555.

Petti, T., Klein, J., Dhurjati, P.S. (1990) *“Diagnostic model processor: using deep knowledge for process fault diagnosis”*. AIChE Journal, Vol 36, no. 4,pp. 565-575.

Ploix, S., Adrot, O., Ragot, J. (1999). “Parameter Uncertainty Computation in Static Linear Models”. 38th IEEE Conference on Decision and Control. Phoenix. Arizona. USA. 1999.

Ploix, S., Adrot, O., Ragot, J (2000) *“Bounding Approaches to the Diagnosis of Uncertain Static Systems”*. IFAC SafeProcess, 2000. Budapest. Hungary.

Ploix, S., Adrot, O. (2006). “Parity relations for linear uncertain dynamic systems”. Automatica, Volume 42, Issue 9, September 2006, Pages 1553-1562.

Puig, V., Saludes, J., Quevedo, J. (1999) *“A new algorithm for adaptive threshold generation in robust fault detection based on a sliding window and global optimisation"*. In Proceedings of European Control Conference 1999, ECC'99. Germany, September.

Puig, V., Quevedo, J., Tornil, S. (2000) *"Robust Fault Detection: Active versus Passive Approaches"* IFAC SAFEPROCESS'00. Hungary. September, 2000.

Puig, V., Cugueró, P., Quevedo, J. (2001) "Worst-case estimation and simulation of uncertain discrete-time systems using zonotopes". In Proceedings of European Control Conference 2001, ECC'01. Portugal, September. 2001.

Puig, V., Quevedo, J., Escobet, T., De las Heras, S. (2002a) "Robust Fault Detection Approaches using Interval Models". IFAC World Congress (b'02). Barcelona. Spain. 2002.

Puig, V., Cugueró P., J., Quevedo, J., Escobet, T. (2002b) "Time-invariant approach to worst-case simulation and observation of discrete-time uncertain systems". In Proceedings of Conference on Decision and Control 2002 (CDC'02). Las Vegas. USA.2002.

Puig, V., Quevedo, J., Escobet, T., Stancu, A. (2003a) *"Passive Robust Fault Detection using Linear Interval Observers"*. IFAC Safe Process, 2003. Washington. USA.

Puig, V., Saludes, J., Quevedo, J. (2003b) "*Worst-Case Simulation of Discrete Linear Time-Invariant Interval Dynamic Systems"*. Reliable Computing, 9(4), pp. 251-290.

Puig, V;Escobet ;T Quevedo, J. (2004a) *"Grup COS: Recerca en control i supervisió al departament ESAII de la UPC"*. En: *Recerca en automàtica, visió i robòtica*. Eds. Antoni Grau; Vicenç Puig, p. 67-79. ISBN/ISSN: 84-7653-844-8

Puig, V; Quevedo, J, Escobet T; Morcego, B, Ocampo, C. (2004b). "Control tolerante a fallos (parte II): mecanismos de tolerancia y sistema supervisor", Revista Iberoamericana de Automática e Informática Industrial RIAI, 2, 2004, 5-21.

Puig, V; Quevedo, J, Escobet T; Pulido, B. (2004c) *" On the integration of Fault Detection and Isolation in Model Based Fault Diagnosis"*. DX'04

Puig, V., Stancu, A., Quevedo, J. (2005a) "*Set versus Trajectory based Approaches to Interval Observation*". Conference on Decision and Control & European Control Conference (CDC-ECC'05). Sevilla. Spain.

Puig, V., Schmid, F., Quevedo, J., Pulido, B. (2005b) "A New Fault Diagnosis Algorithm that *Improves the Integration of Fault Detection and Isolation"*. Conference on Decision and Control & European Control Conference (CDC-ECC'05). Sevilla. Spain.

Puig, V., Stancu, A., Quevedo, J. (2005c) "Simulation of Uncertain Dynamics Systems Described *by Interval Models: a Survey". IFAC World Congress (IFAC'05), Prague. Tzech Republic.*

Puig, V., Mrugalski, M., Ingimundarson, A., Quevedo, J., Witczak, M. and Korbicz, J. (2005d). "*A gmdh neural network based approach to passive robust fault detection using a constraints satisfaction backward test*". In: IFAC World Congress. Prague, Tzech Republic.

Puig, V., Stancu, A., Escobet, T., Nejjari, F., Quevedo, J., Patton, R.J. (2006a). "Passive robust fault detection using interval observers: Application to the DAMADICS benchmark problem" Control Engineering Practice, Volume 14, Issue 6, Pages 621-633.

Puig, V., Quevedo, J., Escobet, T., Meseguer, J. (2006b). "Toward a better integration of passive robust interval-based FDI algorithms". IFAC SAFEPROCESS'06. Beijing. China.

Pulido, B., C. Alonso, F. Acebes. (2001) "Lessons learned from diagnosing dynamic systems using possible conflicts and quantitative models". In Lecture Notes in Artificial Intelligence. International Conference on Industrial and Engineering Applications of Artificial Intelligence and Expert Systems, IEA/AIE 01. Budapest, Hungary. June, 2001 (corrected version of the article in DX, 2001).

Pulido, B., C. Alonso. (2002) "Possible conflicts, ARRs, and conflicts". In Proc. of the 13th International Workshop on Principles of Diagnosis, DX02. Semmering, Austria. Pages 122-128. May, 2002.

Pulido, B., Gonzales, C., (2004). "Possible conflicts: a compilation technique for consistency based diagnosis". IEEE Transaction on Systems, Man, and Cybernetics – Part B: Cybernetics, 34 (5), 2192–2206.

Pulido, B., V. Puig, T. Escobet, and J. Quevedo. (2005) "A new fault localization algorithm that improves the integration between fault detection and localization in dynamic systems". Workshop on Principles of Diagnosis DX'05. Monterey, California, USA.

Quevedo, J., Puig, V., Nejjari, F., Escobet, T. , Aguilar, J., Pulido, B. (2003) "An improvement of model based fault isolation based on a dynamic signature matrix for delayed systems". Workshop on Advanced Control and Diagnosis, Duisburg.

Rapaport, A., Gouze, J.L., (2003) "Parallelotopic and practical observers for nonlinear uncertain systems", Internatonal Journal of Control, Vol. 76, pp. 237-251, 2003.

Reiter, R.A. (1987) "Theory of Diagnosis from First Principles". Artificial Intelligence, Vol. 32, pp. 57-95.

Rinner, B., Weiss, U. (2004) "On-line monitoring by dynamically refining imprecise models" IEEE Trans. On SMC, Part B. Vol. 34, No. 4. Pg. 1811-1822. Special Section on Diagnosis of Complex Systems: Bridging the methodologies of the FDI and DX communities. August.

Sainz, M.A., Armengol, J. Vehí, J. (2002). "Fault detection and isolation of the three-tank system using the modal interval analysis". Journal of Process Control, Volume 12, Issue 2, February, Pages: 325-338.

Sampath, M., R. Sengupta, S. Lafortune, K. Sinnamohideen, and D. Teneketzis, (1996). "Failure diagnosis using discrete-event models, IEEE Transactions on Control Systems Technology, vol. 4, no. 2, pp. 105-124.

Sorsa, T., Koivo, H. N. (1993): "Application of artificial neural networks in process fault diagnosis".- Automatica, Vol. 29, Nº 4, pp 843-849.

Staroswiecki, M., P. Declerk, (1989) "Analytical redundancy in non linear interconnected systems by means of structural analysis". IFAC Advanced Information Processing in Automatic Control (AIPAC-89), Nancy, France.

Syfert, M., Kościelny, J.M. (2001): "Fuzzy neural network based diagnostic system. Application for three tank system"- Proc European Control Conference, ECC, Porto, Portugal, pp. 1631-1636.

Tibken, B., Hofer, E.P. "A New Simulation Tool for Uncertain Discrete Time Systems". In Proceedings of European Control Conference 1993 (ECC'93). Holland, September. 1993.

Thoma, J.U. and Bouamama B.O. (2000). "Modelling and Symulation in Thermal and Chemical Engineering, Bond Graph Approach" Berlin: Springer Verlag.

Tadeusiewicz, R., Flasinski, M. (1991) "Pattern Recognition". Warsaw: Polish Scientific Publisher.

Theilliol, D., Sauter, D., Vela Valdes, L.G (1997). Integration of Qualitative and Quantitative Methods for Fault Detection Isolation. Proceedings of IFAC Safeprocess'97, Hull, UK.

Travé-Massuyes L., R. Milne. (1997) *"TIGER: Gas Turbine condition monitoring using qualitative model based diagnosis"*. IEEE Expert Intelligent Systems and Applications, May-June, 1997.

Travé-Massuyès, L., Escobet, T., Olive, X., 2006. "Diagnosability analysis based on component supported analytical redundancy relations. IEEE on Systems, Man, and Cybernetics – Part A: Systems and Humans, 36 (6), 1146–1160.

Tzafestas, S. G. and Watanabe, K. (1990) "*Modern approaches to system/sensor fault detection and diagnosis"* Journal A 31(4): 42-57.

Venkatasubrarnanian, V., Rengaswamy, R. and Kavuri, S. (2003a) "*A review of process fault detection and diagnosis. Part I: Quantitative model based-methods*". Computers and Chemical Engineering 27 (2003) 293/311. Published by Elsevier Science Ltd.

Venkatasubrarnanian, V., Rengaswamy, R. and Kavuri, S. (2003b) "*A review of process fault detection and diagnosis. Part II: Qualitative models and search strategies*". Computers and Chemical Engineering 27 (2003) 293/311. Published by Elsevier Science Ltd.

Ulerich, N. H., & Powers, G. A. (1988). Online hazard aversion and fault diagnosis in chemical processes: the digraph/fault tree method. IEEE Transactions on Reliability 37 (2), 171/177

Viswanadham, N. and Srichander, R. (1987) *"Dault detection using unknown input observers"* Control-Theory and Advanced Technology 3(2): 91-101.

Willsky, A. S. and Jones, H. L. (1976) *"A generalized likelihood ratio approach to the detection and estimation of jumps in linear systems"* IEEE Trans. Automat. Contr. AC-21: 108-121.